FRAME

FORECASTING AND ASSESSING EUROPE'S STRATEGIC RAW MATERIALS NEEDS

DELIVERABLE D3.3

Producing a predictivity map outlining the CRM exploration potential areas and the major prospective minerals belts

This project has received funding from the European Union's Horizon 2020 research and innovation programme under grant agreement No 731166

GeoERA RAW MATERIALS

Deliverable D3.3

Producing a predictivity map outlining the CRM exploration potential areas and the major prospective minerals belts

Project:	Forecasting and Assessing Europe's Strategic Raw Materials needs
Acronym:	FRAME
Grant Agreement:	731166
Funding Scheme:	Horizon 2020
Webpage:	www.frame.lneg.pt
Work Package:	WP3"Critical and Strategic Raw Materials Map of Europe"
Work Package Leader:	Martiya Sadeghi, Geological Survey of Sweden (SGU)
Deliverable Title:	Producing a predictivity map outlining the CRM exploration potential areas and the major prospective minerals belts
Deliverable Number:	3.3
Deliverable Leader:	Geological Survey of Sweden (SGU)
Involved beneficiaries:	SGU, LNEG, BRGM, CGS, GSI, HGI-CGS, HSGME, IGME, MBFSZ, GeoInform-GIU, IGR, GeoZS, NGU, MINDeSEA Teams
Dissemination level:	Report
Version:	V.6
Status:	Final
Authors:	Martiya Sadeghi, Guillaume Bertrand, Nikolaos Arvanitidis, Daniel de Oliveira, Håvard Gautneb, Eric Gloaguen, Tuomo Törmänen, Helge Reginiussen, Sophie Decree, Aurete Pereira, Lídia Quental, Edward Lynch, Eoin McGrath, Pedro Delgado Arenas, Susana María Timón Sánchez, Klemen Teran, Marian Munteanu, Zoltán Horváth, Erik Jonsson, Rute Salgueiro, Kálmán Török, Gábor Kovács, Csaba Vígh, Javier González, Egidio Marino, Luis Somoza, Teresa Medialdea , Iker Blasco, Thomas Kuhn, Pedro Ferreira, Vitor Magalhaes, Boris Malyuk
Reviewed by:	FRAME WPs leader, MINDeSEA leader, FRAME PL
Approved by:	Daniel de Oliveira
Date:	2020-11-15

This project has received funding from the European Union's Horizon 2020 research and innovation programme under grant agreement No 731166

Contents

This project has received funding from the European Union's Horizon 2020 research and innovation programme under grant agreement No 731166

This project has received funding from the European Union's Horizon 2020 research and innovation programme under grant agreement No 731166

This project has received funding from the European Union's Horizon 2020
research and innovation programme under grant agreement No 731166

Disclaimer

This project has received funding from the European Union's Horizon 2020 research and innovation programme under grant agreement No 731166

1 Introduction

The prime aim of work package (WP) 3 in the FRAME project is to produce a map of strategic and critical raw materials (SCRM) for Europe, including the so-called energy and conflict minerals. In cooperation with other FRAME WPs, there was a consensus on the methodology used for the identification and selection process of the SCRM to be included in the metallogenic map (Arvanitidis, et al., 2019), linked mainly to information collected from existing databases , such as the ones of ProMine, Minerals4EU (M4EU) and European Geological Data Infrastructure (EGDI).

In this report we present a general overview of the main metallogenetic provinces in Europe and, in more detail, we present the metallogenetic maps and their description for rare earth elements, graphite, cobalt, lithium, phosphor, niobium and tantalum with the contribution from the other FRAME work packages (WP4, WP5 and WP6) and the Mineral Resource Expert Group (MREG) on landbased cobalt and phosphor metallogenic areas in the European sea with the contribution from the MINDeSEA project. The digital version on the metallogenetic areas have been prepared and delivered in D3.2. The Methodology and some example of prospectivity maps are presented in this report while all final prospectivity maps for selected CRM commodities will be presented in report D3.5.

EuroGeosurveys' Mineral Resources Expert Group (MREG) presented an updated map on critical raw materials in 2017, (Bertrand et al., 2018) (Figure1), based on the ProMine mineral deposit database. The mineral resource information, including data sharing and networking by European Geological Surveys, is crucial and the main focus in FRAME's WP3 is to update the CRM and strategic raw materials data setsand also to introduce pan European metallogenetic belts on selected commodities, including Critical Energy and conflict minerals.

This project has received funding from the European Union's Horizon 2020 research and innovation programme under grant agreement No 731166

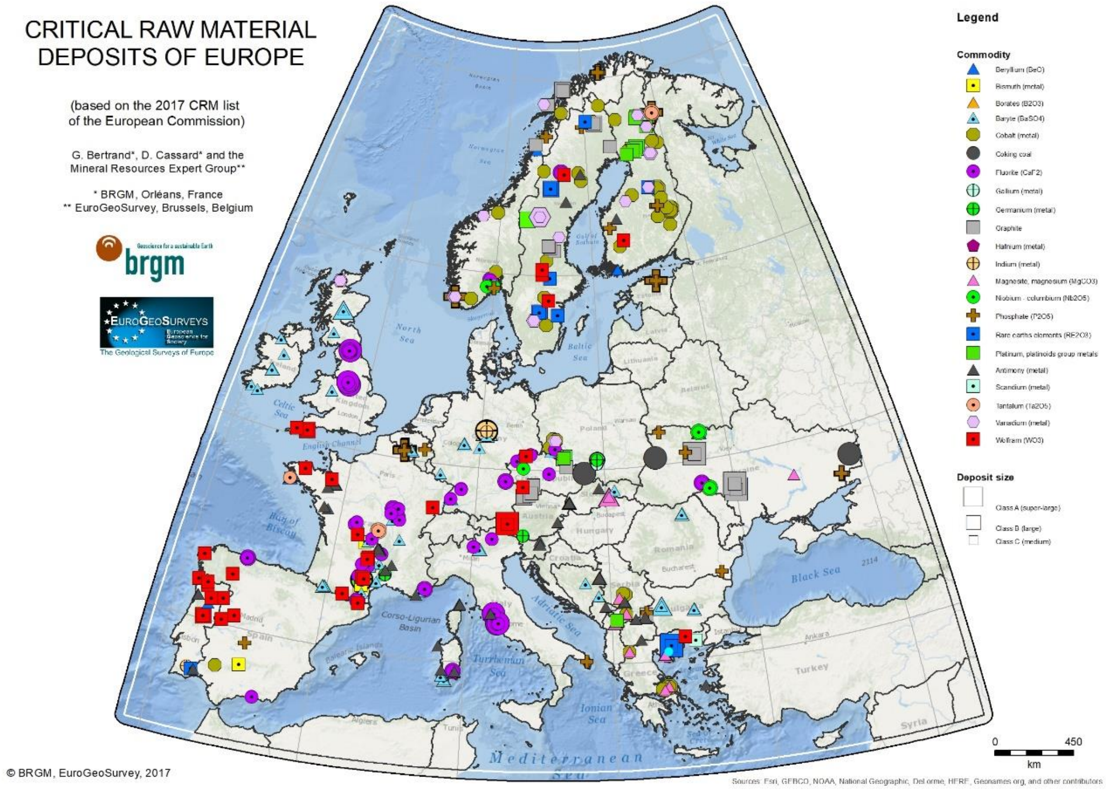

Figure 1. An overview of main Critical Raw Material (CRM) deposits (source: Bertrand et al., 2018)

2 Predictivity map

2.1 Introduction

In the past, economic geologists used a light table to simply overlay different thematic maps to examine spatial relationships and analogue data integration between important multi-disciplinary criteria to guide exploration and produce mineral potential and other relevant maps. Nowadays, it is possible to collect and store the data and information in digital formats and to use different GIS and statistical approaches to deliver maps showing favourable areas referring to a specific commodity. Carranza (2017) describes mineral potential mapping (MPM- also termed mineral potential modelling) as quantifying and mapping of the likelihood that mineral deposits may be found by exploration in a study area.

This project has received funding from the European Union's Horizon 2020 research and innovation programme under grant agreement No 731166

An objective of WP3 in the FRAME project is to produce predictive assessments – in the form of prospectivity maps (predictivity maps) - of CRM based on GIS exploration tools at the continental scale, in order to identify high potential mineral provinces and mining districts.

The basic purpose of prospectivity mapping is to assess the spatial distribution of the favorability of occurrence of a non-random phenomenon (assuming that a phenomenon cannot be predicted if it is purely random). In the case of mineral prospectivity mapping, the phenomenon is the occurrence of a mineralization. Many mineral prospectivity mapping methods exist. They can be grouped in two categories:

- The "expert guided" methods rely on the existing knowledge of experts, in the form of e.g. exploration guides or metallotects. These guides are searched to discover analogs and hopefully new mineralization. This is more or less how mineral exploration was empirically conducted by economic geologists in the past centuries. The development of computers and databases during the last decades allowed to automatically process larger volumes of data and thus improve the accuracy and reliability of the methods.
- The "data driven" methods rely more on the processing of data to deduce "knowledge" ("learning" from input datasets) that is then used to identify the areas that are favourable to discover new mineralization. Date driven methods largely progressed in the past decades with the tremendous development of computing capacities and databases.

When it comes to mineral prospectivity mapping at continental scale (which is the goal of this work), encompassing huge geographic coverage, numerous geological environments and large volumes of data, data driven methods are well appropriate. In this work, we have used a data driven approach – the CBA (for Cell Based Association) – that has been recently developed by BRGM (Tourlière et al., 2015). Preliminary result on prospectivity mapping are presented and published in different events (e.g. Bertrand et al., 2020, Sadeghi et al., 2020a and Sadeghi et al., 2020b)

2.1.1 Cell based association (CBA)

Most data driven mineral prospectivity mapping methods are based on unequivocal relationships between points (e.g., known deposits) and the cartographic entities that contain them (pixels or polygons associated with, for instance, geological information).

This project has received funding from the European Union's Horizon 2020 research and innovation programme under grant agreement No 731166

The knowledge "learned" by the process will be solely based on this unequivocal relationship. For instance, a deposit will unequivocally be linked to the lithology polygons that contains it, without considering surrounding lithologies. This "shortcut" may lead to several issues that could significantly bias the results.

The first issue resides in the uncertainties in polygon contours and point location. Cartographic objects are drawn with a certain error in their location that could be significant, especially at continental scale. That may result in a wrong association between a point (deposit) and a polygon (lithology). In addition, geological maps display surficial formation that could cover large areas but are not related to mineralization (Quaternary covers, for instance).

The second issue resides in the fact that the surface of polygons is often considered a relevant parameter for weighting. That is the case for instance in the Weight of Evidence method (Bonham-Carter et al., 1988, 1989; Agterberg et al., 1990) where surfaces of lithological formations are used to calculate density of deposits. This may lead to artefacts because geology is in 3D and the surface extension of a formation is not necessarily related to its overall importance.

The third issue resides in the spatial distribution of points that is often not considered in data driven mineral prospectivity methods. That may lead to the inappropriate generalization of a local feature to a whole formation. For instance, skarn deposits are not located in a whole carbonate formation, but along its contact with intruding magmatic bodies.

To solve these issues, we believe that considering the geological environment around known deposits and "learn" from this information to assess the favorability is more appropriate than considering solely the "point-polygon" unequivocal link. The CBA method has been developed with this underlying base principle.

2.1.1.1 Description of the CBA method

The application of the CBA method relies on a succession of relatively simple steps of data processing and calculation. The basic needs in terms of data to apply the method are 1) a set of known deposits containing the targeted commodity in the area of study (learning set) and 2) a map of relevant geological features. In the present study, we have used

This project has received funding from the European Union's Horizon 2020 research and innovation programme under grant agreement No 731166

datasets of deposits produced by work packages 4, 5 and 6 of the FRAME project, and the 1 to 1.5 million geological map of Europe compiled by BRGM (Billa et al., 2008).

The first step of the CBA method is to superimpose a regular grid ("cells") over the area of study (Figure 2). The size of the cells is an important parameter that is directly connected to the scale of the input map. If they are too small, most of them will intersect only one lithology polygon, if they are too large, they will intersect "too many" (if not all) lithology polygons. The cell size needs to be carefully chosen to allow sufficient lithological association variability in all the cells.

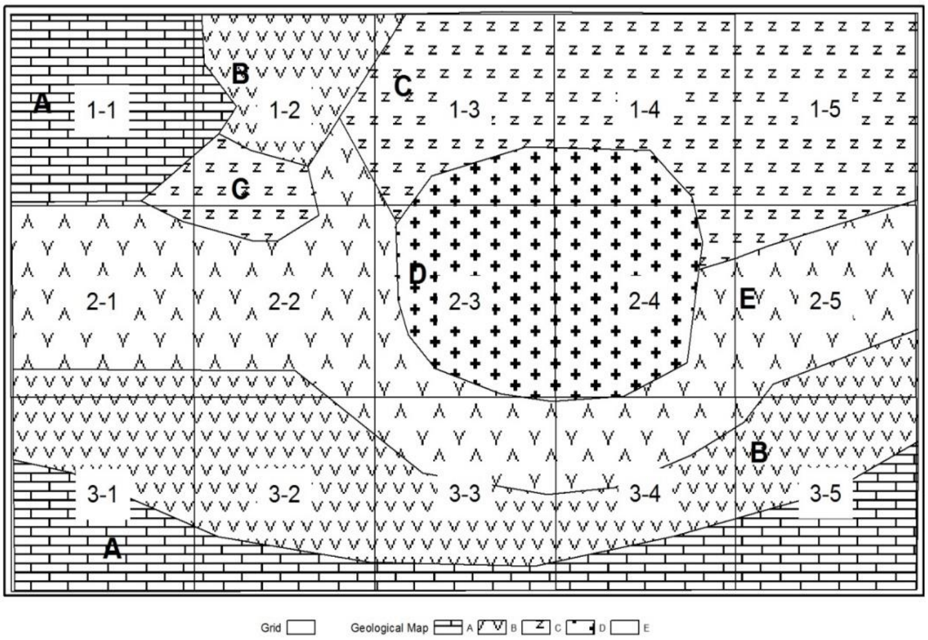

Figure 2. The first step of the CBA method is to superimpose a regular grid over the area of study.

In the second step, an attribute table is built from the intersection between the grid and the map polygons. This attribute table codes the presence (1) or absence (0) of each lithology in each cell of the grid. It then provides a "lithological spectrum" that describes the lithological associations in all cells of the grid. Note that the surface of the intersection between lithological polygons and cells is not considered, because it is likely meaningless in 2D (as geology is 3D).

This project has received funding from the European Union's Horizon 2020
research and innovation programme under grant agreement No 731166

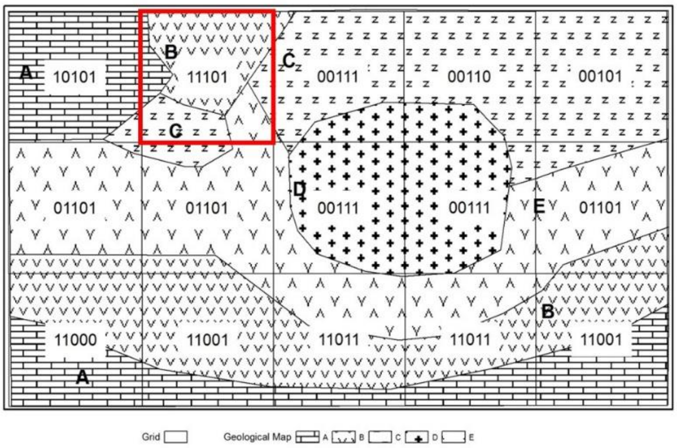

Cell#	Lithological spectrum				
	A	B	C	D	E
1-1	1	0	1	0	1
1-2	1	1	1	0	1
1-3	0	0	1	1	1
1.-4	0	0	1	1	0
1-5	0	0	1	0	1
2-1	0	1	1	0	1
2-2	0	1	1	0	1
2-3	0	0	1	1	1
2-4	0	0	1	1	1
2-5	0	1	1	0	1
3-1	1	1	0	0	0
3-2	1	1	0	0	1
3-3	1	1	0	1	1
3-4	1	1	0	1	1
3-5	1	1	0	0	1

Figure 3. Each cell of the grid (left) is coded in an attribute table (right) for the presence (1) or absence (0) of each lithology.

In a third step, we identify the lithological associations related to known deposits. To do so, a buffer is drawn around each deposit, which surface is equal to those of cells. Lithological associations in all buffers are coded similarly to grid cells. At the end of this process, we have built two attribute tables to describe lithological associations: one for the cells of the grid and one for the buffers around known deposits. The lithological associations in buffers are associated with deposits and are then considered favourable (Figure 3). The following step is to compare lithological associations of grid cells and buffers. A simple way is to consider as favourable all associations in grid cells that are exactly similar to favourable associations in deposit buffers. For instance, in Figure 4, the two green cells in the upper middle of the figure could be considered favourable because they have exactly the same association found in deposit 2 buffer. Another way to compare lithological associations in grid cells and buffers is to group them, using algorithms such as AHC (ascending hierarchical classification). A third way is to score all cells of the grid on their similarity with favourable associations in the buffers. This last yields a continuous range of values for all cells of the grid, allowing a more precise assessment of their relative favourability.

This project has received funding from the European Union's Horizon 2020 research and innovation programme under grant agreement No 731166

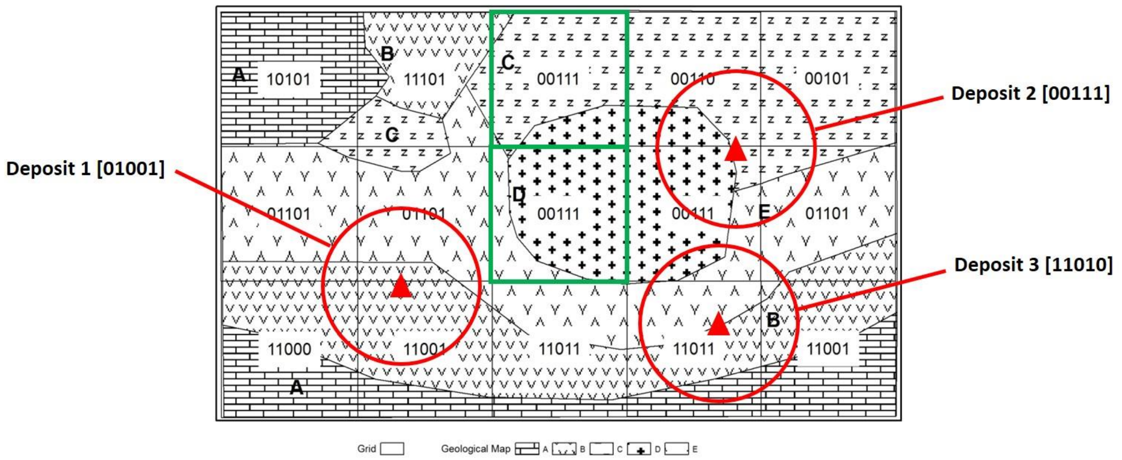

Figure 4. lithological associations in cells and deposit buffers are compared to identify favourable cells.

2.1.1.2 Specific developments

In the present work, we have chosen to score (rank) all the cells of the grid on the similarity of their lithological associations with those contained in the deposit buffers. To do so, we use a frequency ratio (FR) that is calculated according to the following formula:

$$FR = \frac{\text{frequency of lithology n in all deposit buffers}}{\text{frequency of lithology n in all cells of the grid}}$$

FR shows if a lithology is preferably associated with known deposits (FR>1) or not (FR≤1).

There are certainly many ways to combine frequency ratios to calculate the score of each cell. In this work, we have tested five of them that are:

- The sum of FR of all lithologies present in the cell;
- The product of FR of all lithologies present in the cell;
- The sum of « favourable » lithologies (FR>1) present in the cell;
- The product of « favourable » lithologies (FR>1) present in the cell;
- The simple sum of the frequency in deposit buffers of all lithologies present in the cell.

For each commodity (i.e. dataset) in the scope of the project, these five scoring approaches were statistically tested, in order to assess their performance and identify the most accurate. To do so, we performed the followings tasks for each dataset:

This project has received funding from the European Union's Horizon 2020 research and innovation programme under grant agreement No 731166

- 100 CBA prospectivity test maps were calculated;
- For each one of them, 50% of the dataset (randomly selected) was used as training set and the remaining 50% was used as controlling set;
- For each test map, a ROC (Receiver Operating characteristic) curve was calculated with the controlling set and its performance was measured with the AUC (Area Under Curve) indicator;
- For each scoring method, an average AUC value and standard deviation were calculated, that allowed to measure its performance per dataset.

For each dataset, scoring methods were evaluated on their average AUC value. The results of these statistical tests for the lithium, cobalt and natural graphite datasets are synthetized in the Figure 5 below. They show that the "simple product of FR" scoring technique is largely underperforming for all 3 datasets. This result is not really a surprise as the product of all frequency ratios is likely to produce a high variability of results, which could hamper accuracy and reliability. It also shows that the "simple sum of frequencies in deposit buffers" scoring technique is slightly underperforming for all 3 datasets. Finally, the statistical test results show that the "simple sum of FR", the "sum of favourable FR" and the "product of favourable FR" scoring techniques provide results of quite similar accuracy, with slightly better results for the "simple sum of FR" scoring technique for all 3 datasets. Therefore, we have used this scoring technique for the CBA prospectivity maps of lithium, cobalt and natural graphite.

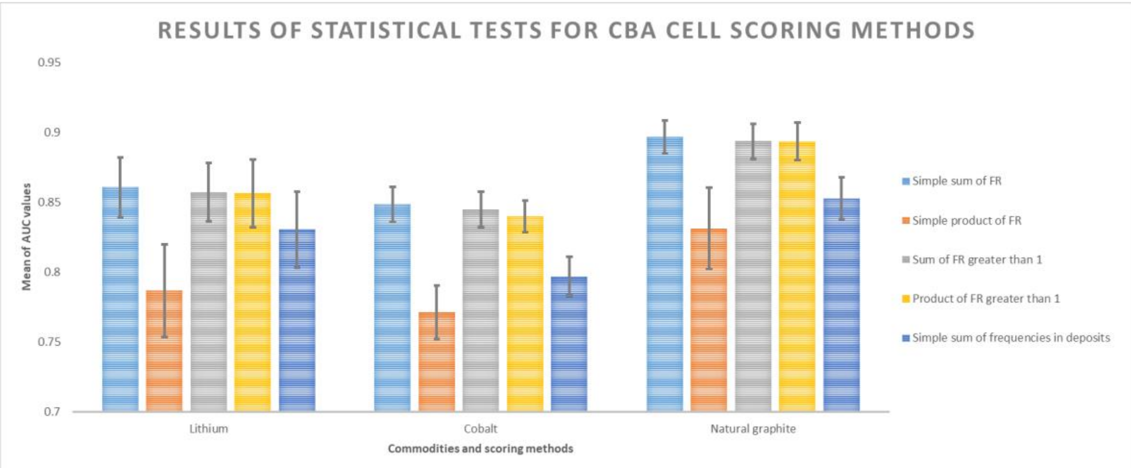

This project has received funding from the European Union's Horizon 2020 research and innovation programme under grant agreement No 731166

Figure 5. Results of the statistical tests of CBA cell scoring methods for the Li, Co and natural graphite datasets.

2.1.2 Fuzzy weights of evidence

Fuzzy weight of evidence (Fuzzy-WofE) is the fuzzy analog of the ordinary WofE method (more details on methodology can be read from Porwal et al., 2003 and Porwal et al., 2006 and references therein). This method provides a better theoretical framework for handling the complexity of modeling multi-class data in a flexible and consistent way.

In brief, the followed method estimates the fuzzy favorability membership value for each of the jth class in the ith lithology related variable, using the knowledge-based logistic membership function (Porwal et al., 2003):

$$\mu A{\sim}xij = \frac{1}{1 + e^{-a(xij-b)}}$$

where b is the inflexion point (values between 0 and 100), α is the slope of the function and xij the overall class score of the jth class in the ith lithology related variable.

The overall class score is calculated by the following equation:

$$Xij = Wj * Wi$$

where wj is the class weight of the jth class in the ith lithology related variable and wi is the weight of the ith lithology related variable.

The fuzzy values were estimated through a fuzzy simple additive weighting method (FSAW) that captures the knowledge of a group of experts according to the method proposed by Chou et al. (2008).

Generated fuzzy predictor patterns are based on (a) knowledge-based fuzzy membership values and (b) data-based conditional probabilities applied to a comparison of the results.

This project has received funding from the European Union's Horizon 2020 research and innovation programme under grant agreement No 731166

2.2 Exmples of prospectivity (Favourability) maps

The CBA prospectivity maps were calculated with the deposit datasets compiled by WP 4 (phosphate), 5 (lithium, cobalt and natural graphite) and 6 (niobium and tantalum) of the FRAME project and the final maps and description will be presented in deliverable report **D3.5.** The 1 to 1.5 million geological map (1/1,500,000) compiled by BRGM (Billa et al., 2008) and a regular grid of 10 by 10 km cell size. 10 by 10 km may seem rather coarse, and it certainly is, but it is in the order of size of an exploration permit, and it was a good compromise between "geological reality" and "computing constrains". Note that the CBA prospectivity maps do not include Greenland, although it is a highly strategic region for mineral exploration. The reason is that the input 1 to 1.5 million geological map of Europe does not cover Greenland. However, the fuzzy weight of evidence approache, in the present work, uses different data sources and includes Greenland.

To ease the reading of the prospectivity maps, favourability scores have been color coded in five classes, going from "very low" to "very high" favorability. Note that it is a relative classification. Note also that the visual result significantly depends on the method used to classify the scores.

Finally, note that only the geology (lithology) was used to characterize the associations in grid cells and deposit buffers. No geochemical or geophysical datasets were used because no such dataset was available at the scale of the whole European continent. Anyway, further developments of the present work could be done to refine the CBA prospectivity mapping at regional scale, in favourable areas, with additional pertinent datasets.

The CBA favourability map for lithium (Figure 6) was built with the database of energy critical elements deposits compiled by the WP5 of the FRAME project. This database contains 595 deposits and occurrences containing lithium. CBA scores were calculated with the "simple sum of frequency ratios" scoring technique. They were grouped in 5 classes, from "very low favourability" to "very high favourability" using the Jenks natural breaks classification.

This project has received funding from the European Union's Horizon 2020
research and innovation programme under grant agreement No 731166

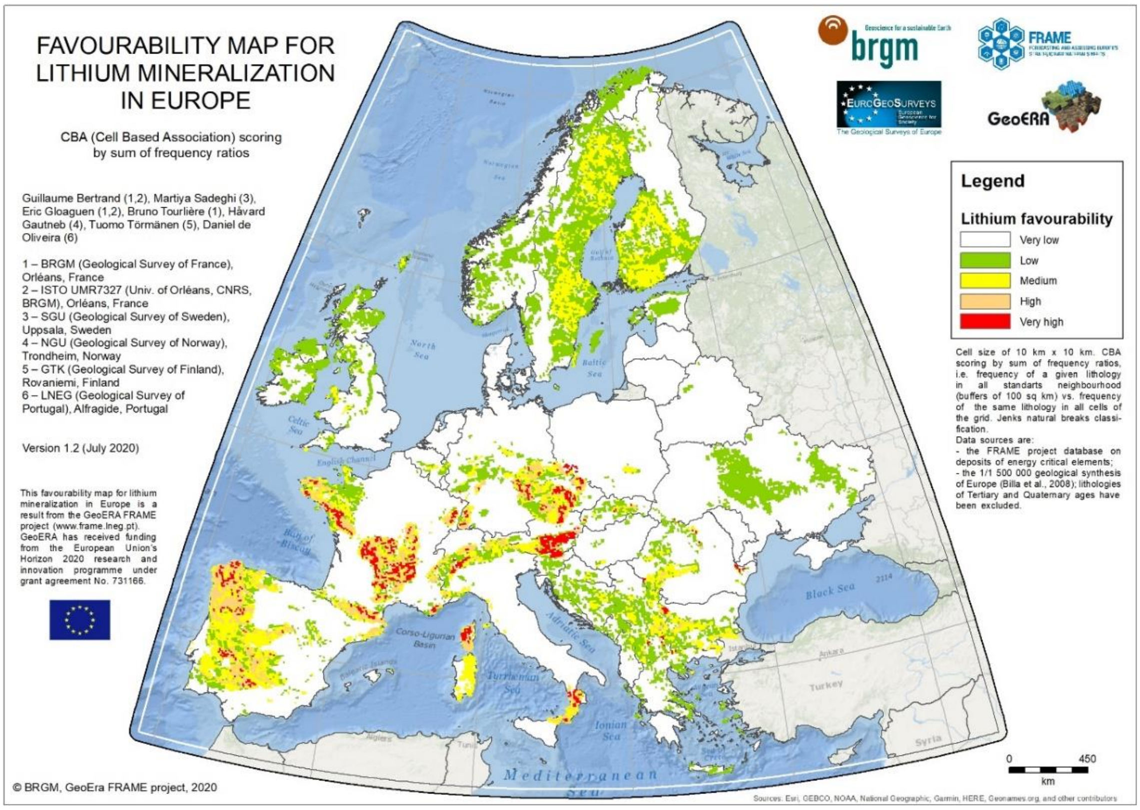

Figure 6. CBA favourability map for lithium in Europe.

The Fuzzy-WofE method has applied for the conflict minerals containing tantalum (Ta). Figure 7 shows the prospectivity map for Tantalum using this method (Sadeghi et al., 2020b). The results of our prospectivity mapping highlight several Ta mineral potential areas related to evolved granite to leucogranite bodies mostly in Scandinavia, Spain, France and Portugal (e.g Morille-Martinamor district, Fontão and Penouta where previous exploration activities on those elements were carried out in past). The late Neoproterozoic to early Cambrian Schist-Greywacke Complex (SGC) of the Variscan belt, in Central Iberian Zone, is also indicated as favourable area for Nb and Ta. Pegmatites in the Campo Mineiro De Lagares in the CIZ are another area of interest. Pegmatites in central Iberian zone is another area of interest, as is the case for Campo Mineiro De Lagares. The late Neoproterozoic to early Cambrian Schist-Greywacke Complex (SGC) of the Variscan belt, in Central Iberian Zone, is also indicated as favourable area for Ta. In Sweden, the pegmatites of the Varuträskt area, close to Skellefteå, dated to c. 1.8-1.77 Ga, are clearly highlighted in the prospectivity maps. The areas related to Fennoscandian

This project has received funding from the European Union's Horizon 2020 research and innovation programme under grant agreement No 731166

carbonatites appear also to be strongly favourable as Nb and Ta mineral potential targets. In the northern, central and southern parts of Sweden, high to moderately favourable areas are related to numerous individual granitic pegmatite dykes of Proterozoic age.

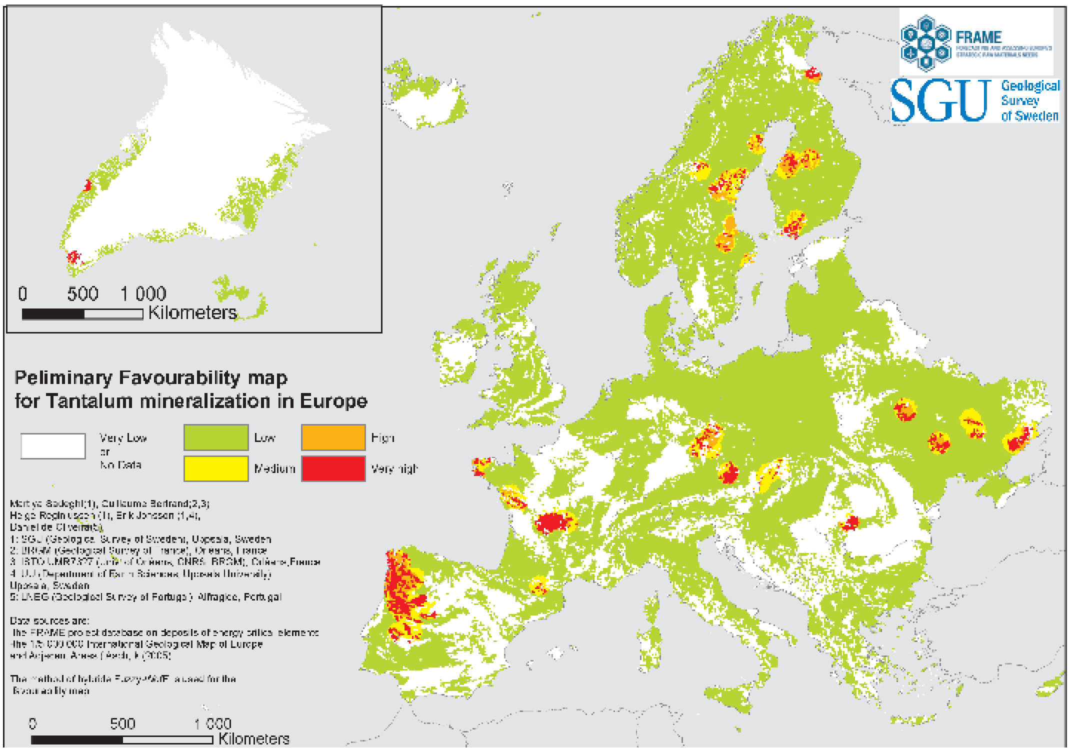

Figure 7. An example of favorability maps using hybrid fuzzy weights of evidence (Tantalum mineralization in Europe) produced in the FRAME project.

2.3 Summary

In conclusion, there is not a “best” method to produce a favourability map, and each data- or knowledge-driven method has its advantages and limitations, the most important being the quality and quantity of input data which is critical to prospectivity mapping. We believe that, to produce a valuable and applicable favourability or prospectivity map, it is critical to have a set of multidisciplinary harmonized data sets. At European scale, probably the best way is to start with data gathering on mineral deposits

This project has received funding from the European Union's Horizon 2020 research and innovation programme under grant agreement No 731166

in a harmonized way, which is a main task for FRAME project (harmonized geological dataset that also includes Greenland with same resolution and accuracy). The favourability maps presented herein and derived from these datasets enable identifying permissive and prospective areas, at continental scale, that reflect the geological data and knowledge applied. In further steps, the highest mineral potential will be highlighted taking also into account data and knowledge updates related to mineral systems at regional scale, economic geology approaches, till and lithogeochemical data, and airborne geophysics measurements.

Then the prospectivity mapping at district and local scale will identify target areas of advanced exploration potential. Ultimately, potential assessment of those areas will consider knowledge and data updates addressing deposit scale exploration efforts including alteration, mineralogy, ground geophysics and detail geochemical sampling. This methodology represents different development stages, scales and progress of economic geology surveys which could be a tool to improve effectiveness and efficiency of future investments in exploration. Improved understanding and support for a balance management of competitive land-usage interests is an additional benefit.

This project has received funding from the European Union's Horizon 2020 research and innovation programme under grant agreement No 731166

3 Overview of the Metallogenetic provinces in Europe

The geological evolution of European terrains provided favourable conditions for the formation of a variety of mineral deposits in time and space. Distribution of metallogenic provinces strongly correlates with tectonic setting and evolution, and the largest metallogenic provinces are shown in Figure 8. These include the Fennoscandian Shield, Caledonian province, Variscan province, Alpine province and Greenland comprising the Gardar and north Atlantic igneous province.

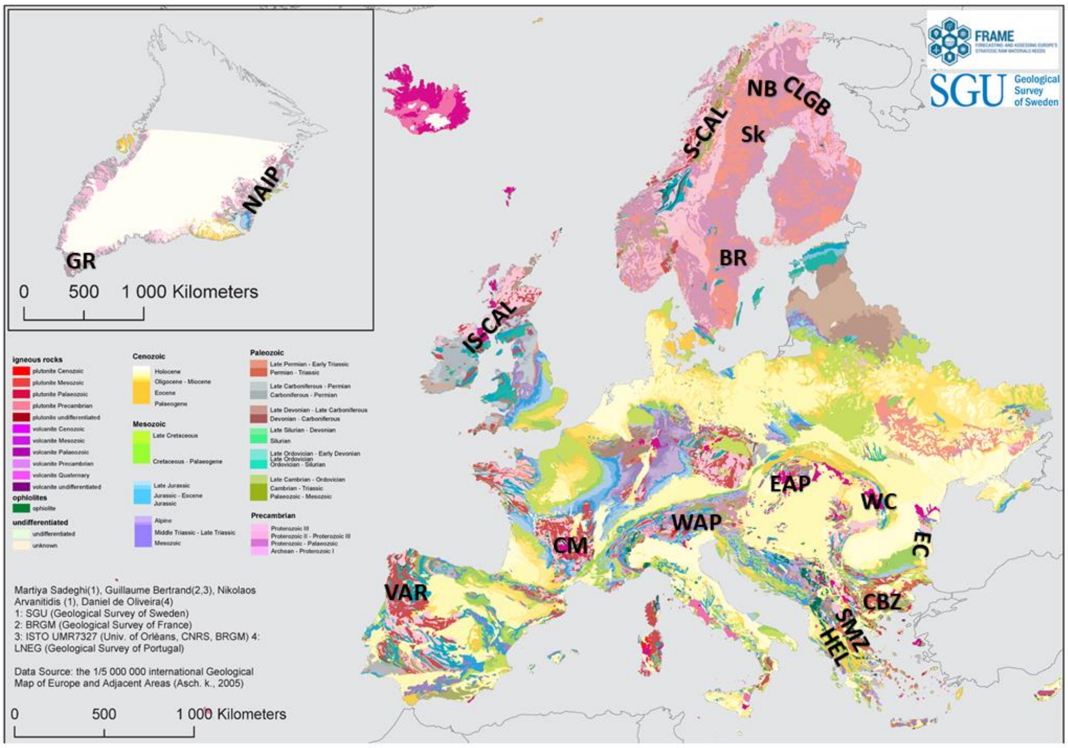

Figure 8. an overview on geological map of Europe and Greenland modified after Asch (2005) and the main metallogenetic areas in Europe. GLGB: central Lappland greenstone belt; NB: Norrbotten; Sk:Skellefte; BR: Bergslagen; S-CAL: Scandinavian Caledonides; IS-CAL: Ireland-Scotland Caledonides; EAP: Eastern Alpine province; WAP: Western Alpine province; WC: Western Carpathian; EC: Eastern Carpathian; CB: Carpathian-Balkan Zone; SMZ: Serbian-Macedonian Zone;

This project has received funding from the European Union's Horizon 2020 research and innovation programme under grant agreement No 731166

HEL: Hellenides; CE: Central massif; VAR:Variscan metallogenic province; Gr: Gardar province; NAIP: North Atlantic Igneous Province.

3.1 Fennoscandian shield

The Precambrian geological history and metallogeny of this province were summarized by Weihed et al. (2005). Fennoscandia is the most important metal mineralization district of Europe. Metallogenic areas within Fennoscandian are geographically rather distributed, although variable in age and importance (Lahtinen et al., 2012). The FODD database and metallogenic map over Scandinavian outlines several important metallogenic and geotectonic events (Figure 9).

The oldest rocks in Fennoscandian are Archean rocks that host several critical metals, for example granitoids rocks with 2.9-2.7 Ga in Lobash and Mätäsvaara representing Mo porphyry and 2.7 Ga granite and pegmatite hosting orogenic gold contain Au, Li, Be (e.g. in Pampalo). A Paleoproterozoic cratonic to rifting stage affected the Archean continents at 2.50-2.44 Ga, producing mafic layered intrusion that contain Cr, PGE, Ni, V, Ti (e.g. Kemi deposit, Mustavaara). 2.4-2.0 Ga Cratonic rifting contain Ni, Co, V in black shale hosted and SEDEX deposits (e.g. Talvivaara). 2.1-2.05 Ga rifting produced mafic and ultramafic intrusion, VMS and alkaline intrusion contain Ni, PGE, V, Ti, REE, Nb (e.g. Kevitsa, Viscaria). Rifting process at 2.0 Ga produced magmatic Ni-Cu such as Pechenga.

Paleoprotrozoic subduction-related 1.93-1.88 Ga arcs hosting several VMS deposit epithermal deposits, IOCG (e.g. Pyhäsalmi, Falu mine, Garpenberg, Boliden, Zinkgruvan, Kristineberg) with critical metals such as P in addition to base metals. Paleoproterozoic collision during 1.91 Ga-1.79 Ga produced orogenic gold and mafic -ultramafic intrusion with potential for Au, Ni and Co (e.g. Kittilä, Björkdal, Pahtohavare). Paleoproterozoic late to post collisional 1.88 -1.62 Ga magmatism produced mafic intrusion, pegmatites and carbonatite with potential for Ti-V, Li, Nb-Ta-Be, REE- and Ni. (e.g. Koivusaarenneva, Korsnäs, Rodsand, Espedalen). 1.6-1.14 Ga cratonic, in continental margin hosted Co-Ni related to mafic -ultramafic intrusion (e.g. Skuterud). 1.14-0.97 Ga collisional host mafic and felsic intrusion contain Mo, Ni (e.g. Knaben, Flåt) and finally, 960-920 Ma post collisional host mafic intrusion contain Ti-V (e.g. Tellnes).

Neoproterozoic rifting and passive margin tectonics host VMS and carbonatite deposits (e.g. Fen and Mojfjell) with potential for critical commodities such as REE, Nb, P, and V. Phanerozoic passive margin, island arc and ophiolites contain V, Mo, Ni, PGE

This project has received funding from the European Union's Horizon 2020 research and innovation programme under grant agreement No 731166

mineralization, VMS-style base metal and black shale-related mineralization (e.g. Stekenjokk, Lokken, Joma, Myrviken). Finally, an intraorogenic phase started 435-440 Ma continues with mafic and ultramafic intrusion hosting base metal and Ni. 430-390 Ma collisional orogeny with sandstone hosted and orogenic gold bearing critical elements such as Ti and Au (e.g. Laisvall) and during the post collisional 400-360 Ma, REE, Nb, Zr hosted in the alkaline intrusion, and ultramafic alkaline and carbonatite (e.g. Kovdor, Sokli) and finally during the 300-240 Ma rifting so called Oslo rift; Mo and Ag in the porphyry and hydrothermal vein getting developped (e.g. Nordli, Kongsberg).

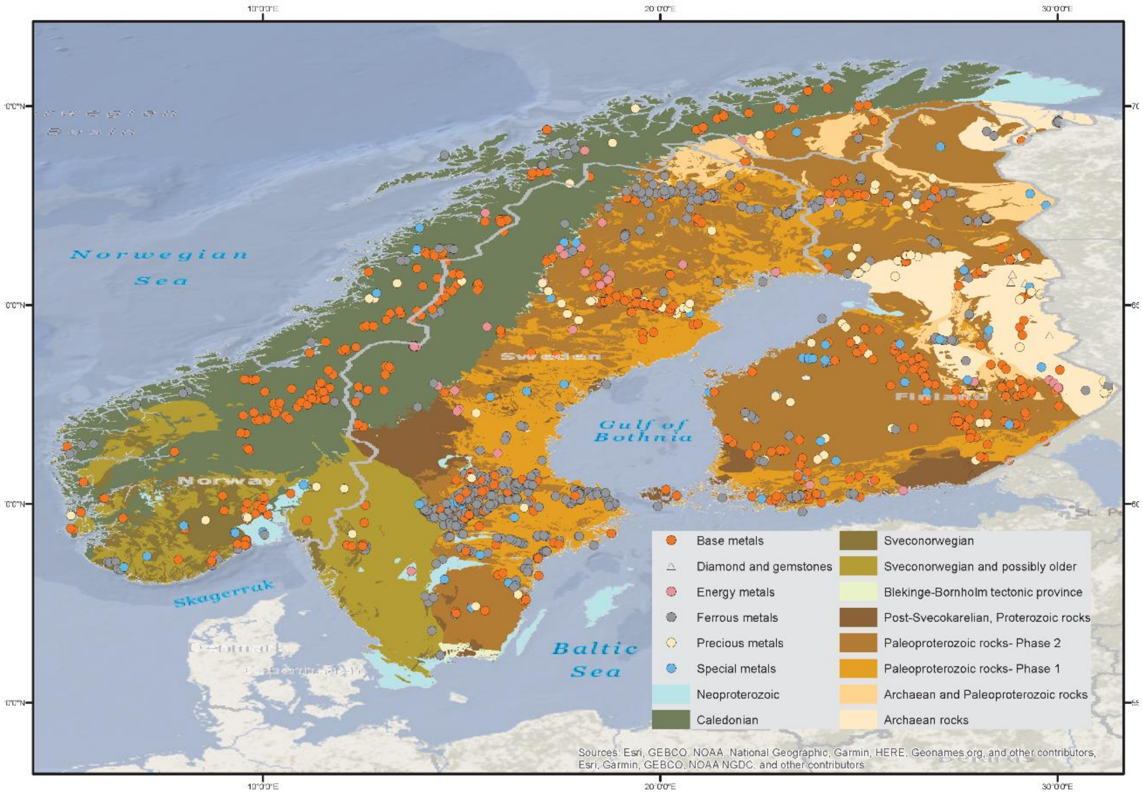

Figure 9. General view on the Fennoscandian shield (European part) and main mineralizations. (Source of deposit: Fennoscandian ore deposit database (FODD) – Eilu et al. 2012).

In this report we summarize a selection of the key metallogenetic provinces in the Fennoscandian shield

This project has received funding from the European Union's Horizon 2020 research and innovation programme under grant agreement No 731166

3.1.1 The Skellefte District (Sweden)

The bedrock in the Skellefte district was formed or reworked by Svecokarelian orogenic processes (from about 1.96 to 1.75 Ga). This time interval includes subduction-related processes, collision, and extension-related collapse of the thickened crust. The peak of Svecokarelian deformation and metamorphism occurred between 1.85 and 1.80 Ga (Stephens et al. 1997), but earlier phases of deformation at 1.89 – 1.87 Ga have been reported by Skyttä et al. (2012a, b).

The Svecokarelian orogen comprises Svecokarelian intrusive rocks, formed by orogenic processes and Svecofennian supracrustal rocks, i.e. early orogenic sedimentary and volcanic rocks, the latter hosting the VMS deposits of the Skellefte district. Major shear zones trending north-south and WNW-ESE are linked to changes in metamorphic grade (Skyttä et al., 2020) and also played a role in controlling the present location of VMS deposits in this province (Carranza and Sadeghi, 2012).

The Skellefte metallogenic area is defined by the presence of different rocks hosting different types of mineral deposits. The Skellefte group hosts a large number of VMS deposits which historically is the most important economic deposit type in the area (Kathol and Weihed, 2005). The Jörn GI metagranitoids (Figure 10) host non-economic porphyry copper mineralization. Volcanic rocks of the Arvidsjaur Group and coeval intrusive rocks of the Perthite monzonite suite dominate the bedrock in the area north of the Skellefte district. The replacement copper- zinc (Cu ± Zn) ores of the Adak mining camp, the Storliden mine, and the Svartliden prospect are all probably related to the early evolution of a juvenile continental arc. These deposits share several characteristics with VMS deposits but are characterized by stringer zone Cu mineralization instead of massive sulphide deposits. A few deposits, interpreted to have been formed by epithermal processes (i.e. the Boliden ore, Bergman Weihed et al. 1996), are known in the Skellefte district (epithermal gold). These deposits may have been formed under subaerial or shallow-water conditions.

Regional-scale mapping of the prospectivity for volcanogenic massive sulphides (VMS) deposits and estimation of undiscovered VMS endowment in the Skellefte district was carried out by Carranza and Sadeghi (2010) and they obtained estimates of 709 Kt of undiscovered ***Cu*** endowment, 3190 Kt of undiscovered ***Zn*** endowment, 95 Mt of undiscovered ***ore tonnage***, and 48 undiscovered VMS deposits.

This project has received funding from the European Union's Horizon 2020 research and innovation programme under grant agreement No 731166

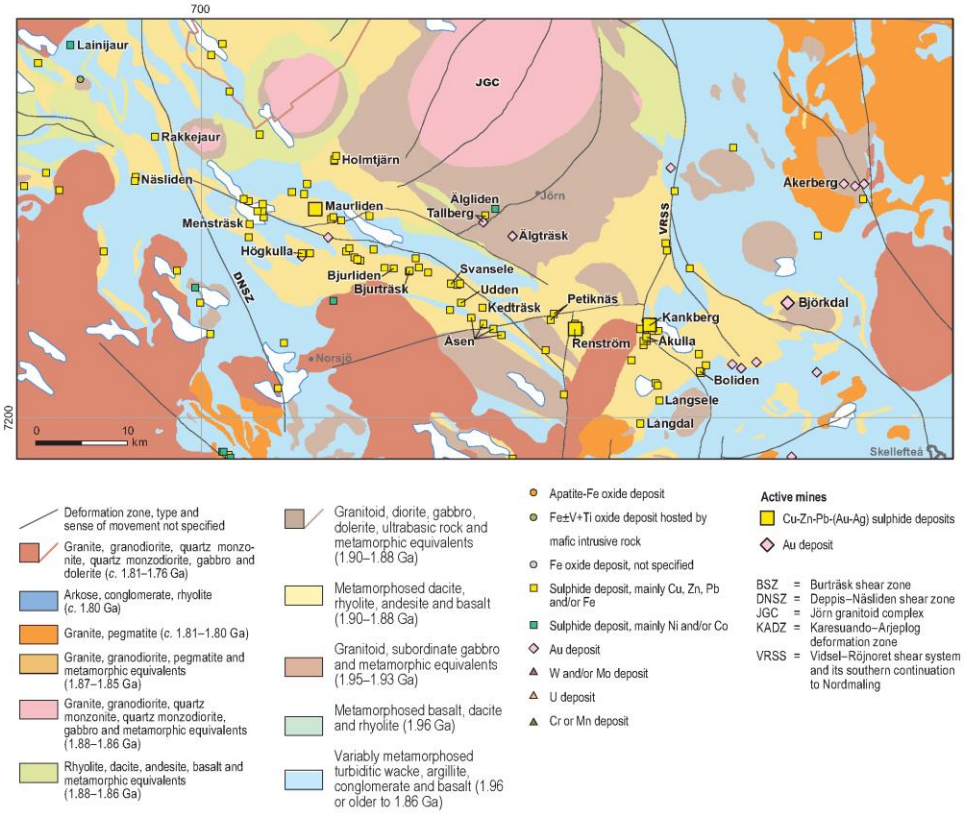

Figure 10. Detailed view of the metallic mineral deposits in the Skellefte district (modified from Skyttä et al, 2020)

3.1.2 The Norrbotten District (Sweden)

Two lithotectonic units (the Norrbotten and Överkalix units) occur inside the Paleoproterozoic (2.0–1.8 Ga) Svecokarelian orogen in northernmost Sweden. Archean (2.8–2.6 Ga and possibly older) basement, are the oldest rocks in this province. Siliciclastic sedimentary rocks, predominantly intermediate to felsic volcanic rocks, and both spatially and temporally linked intrusive rock suites, deposited and emplaced at 1.9–1.8 Ga, form the syn-orogenic component (Bergman and Weihed ,2020). Metallogeny of the Northern Norbotten ore province has been recently published by Martinsson et al. (2016), while geology and mineralization in Norrbotten was described by Bergman et al. (2001). Iron oxide-apatite (IOA) mineralization, including the two worldlargest underground Fe ore mines (Kiruna and Malmberget), skarn-related Fe oxide, base metal sulphide, and epigenetic Cu–Au and Au deposits occur in the Norrbotten lithotectonic unit.

This project has received funding from the European Union's Horizon 2020 research and innovation programme under grant agreement No 731166

The Northern Norrbotten Ore Province in northernmost Sweden includes the type localities for Kiruna-type IOA deposits and has been the focus for intense exploration and research related to Fe oxide-Cu-Au mineralization during the last few decades. Several different types of Fe-oxide and Cu-Au ± Fe oxide mineralization occur in the region and include: stratiform/stratabound Cu ± Zn ± Pb ± Fe oxide type, iron formations (including BIF's), Kiruna-type IOA mineralization, and epigenetic Cu ± Au mineralization. Generally, the formation of Fe oxide ± Cu ± Au mineralization is directly or indirectly dated between ~2.1 and 1.75 Ga (Martinsson et al., 2016)

In summary, The Norrbotten lithotectonic unit contains one of Sweden's major mining districts with two underground mines (Kiruna and Malmberget), dominated by Fe and Cu–Au metallic mineral resources hosted by Paleoproterozoic rocks (Figure 11). The metallic mineral resources in the Norrbotten and Överkalix lithotectonic units (Figure11) are classified and summarized by Billström et al. (2011) as follow:

1. Kiruna-typeFe oxide-apatite deposits hosted by Paleoproterozoic (1.9 Ga), syn-orogenic volcanic rocks (Svecofennian lithostratigraphic sequence), with a focus on the largest deposit at Kiirunavaara, immediately south of the town of Kiruna in the Norrbotten lithotectonic unit.
2. skarn-related Fe oxide deposits, attention being addressed here to the Sahavaara deposit close to Kaunisvaara, in the northeastern part of the Norrbotten lithotectonic unit (Figure 11).
3. stratiform–stratabound base metal sulphide deposits hosted by volcaniclastic rocks in the early Paleoproterozoic (2.5–2.0 Ga) pre-orogenic rocks (Karelian lithostratigraphic sequence), the focus being placed here on the Viscaria Cu–Fe and Huornaisenvouma Zn–Pb–Ag–Cu deposits (Figure 11); and
4. epigenetic Cu–Au and Au deposits, attention below being placed on the Pahtohavare and Aitik deposits in the Kiruna and Gällivare areas, respectively, hosted by different rock successions inside the Norrbotten lithotectonic unit (Figure 11).

Other types of mineralization, including minor Fe–Ti–V deposits in mafic intrusive rocks of different ages and some molybdenite deposits in felsic intrusive rocks, occur in the Norrbotten and Överkalix lithotectonic units. More information can be found in Bergman et al. (2001), Hallberg et al. (2012), Martinsson et al. (2016) and the Fennoscandian Ore Deposit Database at http://en.gtk.fi/mineral_resources/exploration.html.

This project has received funding from the European Union's Horizon 2020 research and innovation programme under grant agreement No 731166

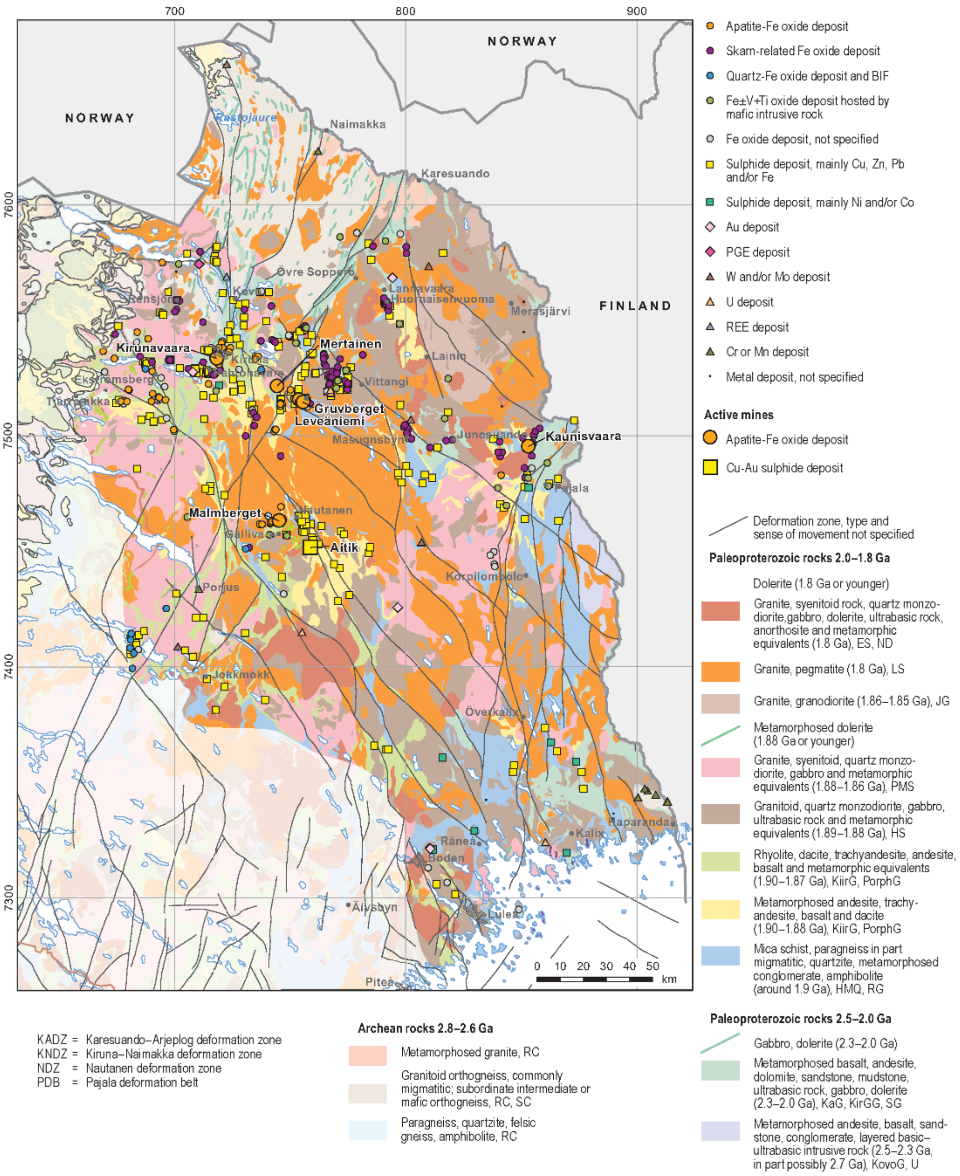

Figure 11. Spatial distribution of different types of metallic mineral deposits in the Norrbotten and Överkalix lithotectonic units classified by commodity. Currently operating mines are shown with larger symbols. Data extracted from the Geological Survey of Sweden's mineral resource database. (modified from Bergman and Weihed, 2020)

3.1.3 The Bergslagen District (Sweden)

Felsic volcanic rocks (c. 1.91–1.89 Ga) and interlayered limestone, hosting Zn–Pb–Ag ± Cu ± Au ± Fe sulphide and Fe oxide deposits, characterize the Bergslagen lithotectonic unit,

This project has received funding from the European Union's Horizon 2020 research and innovation programme under grant agreement No 731166

Svecokarelian orogen, south-central Sweden. Three sulphide mines are currently in operation. Siliciclastic sedimentary rocks stratigraphically envelop this volcanic succession, and all the rocks are intruded by a dominant calc-alkaline, c. 1.91–1.87 Ga plutonic suite. More alkali–calcic magmatic activity, combined with the emplacement of anatectic granite and pegmatite, overlapped and succeeded the polyphase metamorphism and migmatization events at c. 1.87–1.83 Ga and c. 1.82–1.75 Ga, respectively. The younger granites are genetically linked partly to W skarn deposits and locally host Mo mineralization (Stephens and Jonsson, 2020).

The Bergslagen lithotectonic unit is characterized by several thousand metallic mineral occurrences of variable composition, dominated by Zn–Pb–Ag ± Cu ± Au ± Fe sulphide and various types of Fe oxide deposits, the latter including skarn hosted deposits, banded iron formations (BIFs) and Kiruna type Fe oxide-apatite deposits. Skarn W and some minor granite-hosted Mo sulphide deposits are also present. This metallogenic province is commonly referred to as the Bergslagen ore (or mining) district.

The Zn–Pb–Ag ± Cu ± Au ± Fe sulphide and Fe oxide deposits are spatially and temporally associated with this early major magmatic phase. The emplacement of granite, granodiorite, syenitoid rock and subordinate quartz monzodiorite, gabbro and ultramafic rocks (the GSDG intrusive rock association), combined with the deposition of volcanic rocks, occurred during subsequent phases of magmatic activity at c. 1.87–1.84 Ga and c. 1.81– 1.78 Ga (Figure 12). However, granite plutons sensu stricto – locally associated with pegmatite, containing high contents of U and/or Th and lacking coeval mafic or ultramafic counterparts – are volumetrically the most prominent magmatic component formed after c. 1.87 Ga (Figure 12; granite and pegmatite (GP) intrusive rock association) (Stephens and Jonsson, 2020). In particular, granite and pegmatite plutons emplaced at c. 1.82–1.75 Ga are associated with some of the W skarn and Mo sulphide deposits.

The metallic mineral resources in the Bergslagen ore district are presented by Stephens and Jonsson (2020), making use of a division proposed by Allen et al. (1996) and Stephens et al. (2009):

1. stratabound, volcanic-associated, limestone–skarn hosted, Zn–Pb–Ag–(Cu–Au) ± Fe sulphide deposits (SVALS-type);
2. stratiform ash–siltstone-hosted Zn–Pb–Ag ± Cu sulphide deposits (SAS-type);
3. skarn- or carbonate-hosted Fe and Fe–Mn oxide deposits, including both syngenetic and contact metasomatic varieties;
4. REEs in skarn-hosted Fe oxide deposits and pegmatites;
5. quartz-rich Fe oxide deposits, including BIF facies;
6. Kiruna-type, apatite–Fe oxide deposits;

This project has received funding from the European Union's Horizon 2020 research and innovation programme under grant agreement No 731166

7. W skarn deposits;
8. granite-hosted Mo sulphide deposits; and
9. orthomagmatic Ni–Cu sulphide deposits.

Allen et al. (1996) and Stephens et al. (2009) provide more detailed geological information on individual deposits. More details on such deposits can also be found in Stephens et al. (2009), Sadeghi (2019) on REE, Jonsson et al (2019) on REE and CRM.

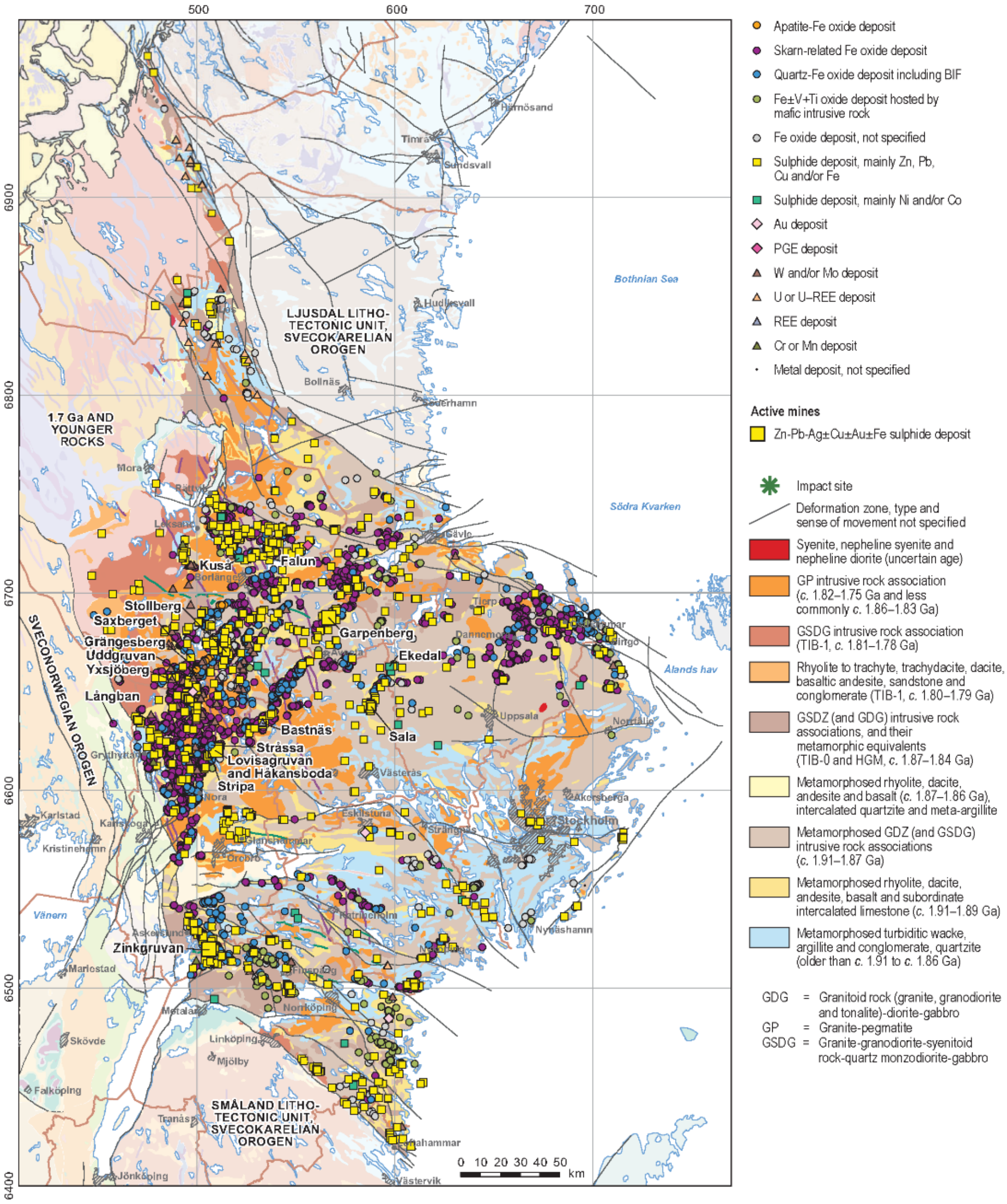

Figure 12. Spatial distribution of metallic mineral deposits in the Bergslagen lithotectonic unit and surrounding areas, classified based on commodity. The three currently operating mines are shown

This project has received funding from the European Union's Horizon 2020 research and innovation programme under grant agreement No 731166

GeoERA RAW MATERIALS

with larger symbols. Data extracted from the mineral resource database at the Geological Survey of Sweden. (Figure modified from Stephens and Jonsson, 2020)

3.1.4 The Vihanti-Pyhäsalmi area (Finland)

The Vihanti-Pyhäsalmi district is located at the border zone between the Archaean craton in the northeast and the Paleoproterozoic Svecofennian domain in central Finland. It is part of the Savo belt and contains one operating and four past mines and several uneconomic VHMS (Volcanic Hosted Massive Sulphide) deposits. Regional, semi-regional and mine scale 3D models of the Vihanti-Pyhäsalmi area were built during the ProMine project (Laine et al., 2015). VHMS mineralization in this area forms a linear ore belt (Eilu et al, 2013) and this belt formed in an intra-arc extensional setting at c. 1.92 Ga (Lahtinen et al., 2012). The Savo belt is the NW part of the Raahe-Ladoga zone also known as the Main Sulphide Ore Belt in Finland or the Raahe-Ladoga Shear Complex (Kärki et al. 2012) (Figure 13). In terms of exploration criteria in this area, spatial association of VHMS deposit with lower Pyhäsalmi group or the overlaying Vihanti group and also co-genetic subvolcanic intrusions are extremely important for exploration on this area.

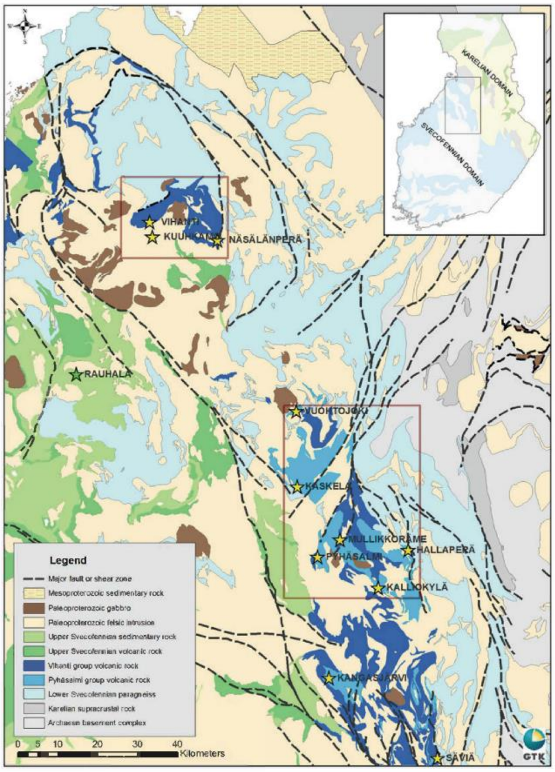

This project has received funding from the European Union's Horizon 2020 research and innovation programme under grant agreement No 731166

Figure 13. General view of the Vihanti and Pyhäsalmi areas and the semi-regional 3D modelling build up in the ProMine project (red) and the most important Zn-Cu deposits (stars). The main structural features are presented by black lines. (map from Laine et al., 2015)

3.1.5 Central Lapland Greenstone Belt (Finland)

The Central Lapland greenstone belt is dominated by Paleoproterozoic rocks formed at c.2450 Ma comprising mantle plume-related komatiitic to rhyolitic lavas on the Archean cratonic basement (Hanski, 2015). These activities are associated with large layer mafic intrusion. These rocks hosting stratiform Cr and Fe-Ti-V deposits, PGE-enriched reefs, and Ni-Cu-PGE contact and offset mineralization. During a 300-400 Ma period, a succession of quartzite-dolomite and basalt took place and was followed by komatiitic to picritic volcanism. Mafic magmas intermittently formed layered sill-like intrusions within the sediments, most notably at -~2220 Ma and ~2050 Ma. At a later stage, when deep-water, pelitic continental margin sediments were deposited, intruding mafic magma produced Ni-Cu deposits (2050 Ma) in relatively small magma chambers. This prolonged extensional regime was interrupted by a collisional event, which led to thrusting of a ~2000 Ma slab of ancient oceanic lithosphere (the Kittilä Group) onto older cratonic rocks. This took place at ~1920 Ma, as deduced from felsic dikes and granodioritic plutons of this age within the Kittilä Group. Roughly simultaneously, a juvenile calc-alkaline arc complex was formed farther north (western part of the Inari area) and was shortly followed by the up thrust of the Lapland granulite belt.

The supracrustal rock sequence in central Lapland was completed with the deposition of molasse-like, coarse- clastic sediments in a fore-arc basin soon after -1880 Ma synorogenic felsic plutonism and associated minor volcanism.

Summarizing, the supracrustal units of the central Lapland Greenstone belt can be divided into ; the Karelian 2.44–2.0 Ga rift-related metamorphosed volcano-sedimentary sequence deposited on the Archean basement and the 1.89–1.77 Ga Svecofennian sequence dominated by clastic metasedimentary units (Lehtonen et al., 1998; Hanski et al., 2001; Hanski and Huhma, 2005). Niiranen et al, (2015) stated, based on the modeling of gold in this area, still there is potential to be undiscovered gold large deposit in the part (Figure 14). Rasilainen et al., (2017) published a series of mineral resource assessment in Finland and in Figure 15 Shown the main metallogenic area for Au, PGE, Co-Cu-pd-Zn, and Ni in the entire Finland. More details can be found in Rasilainen et al. (2017) and reference therein.

This project has received funding from the European Union's Horizon 2020 research and innovation programme under grant agreement No 731166

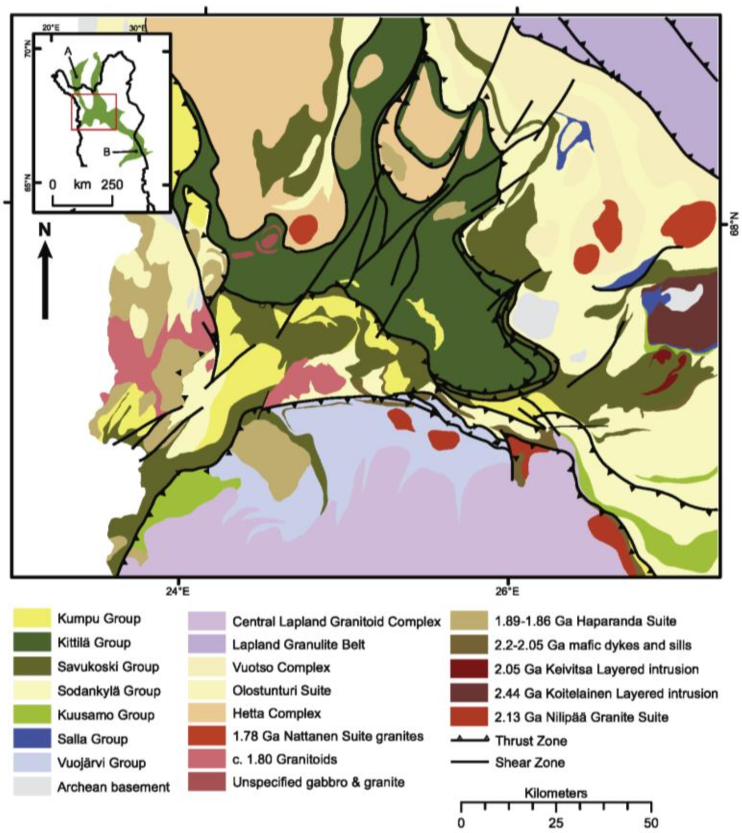

Figure 14. Location of central Lapland Greenstone Belt (CLGB) and the main lithology- (modified from Niiranen et al., 2015)

This project has received funding from the European Union's Horizon 2020
research and innovation programme under grant agreement No 731166

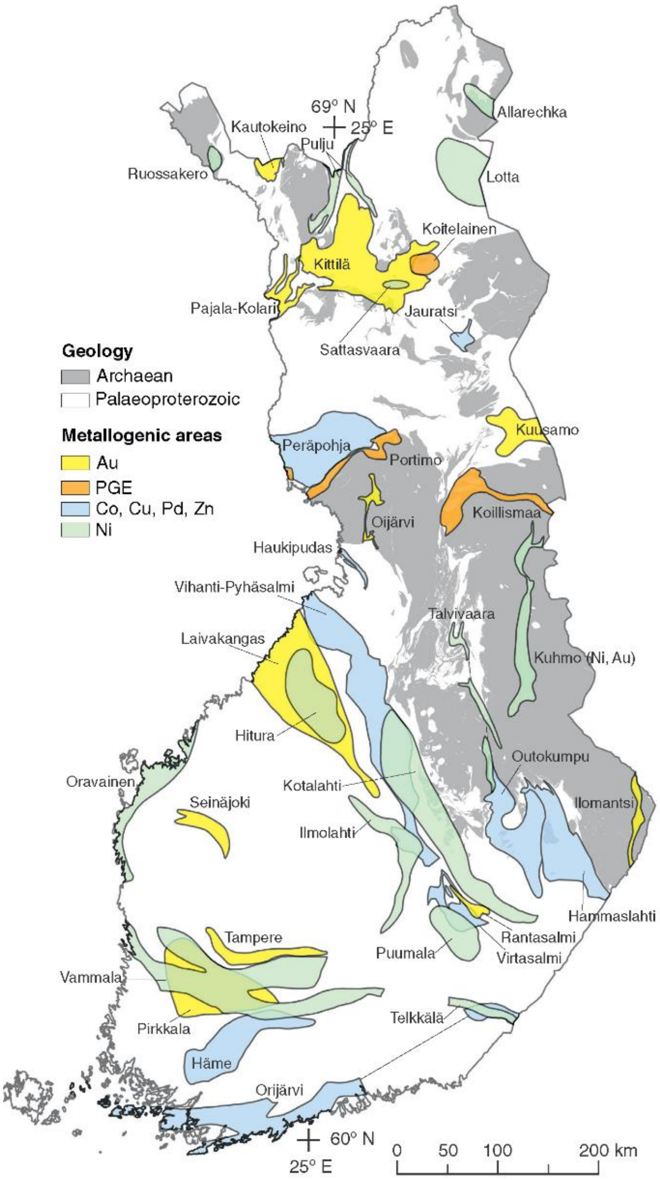

Figure 15. Metallogenic areas dominated by PGE, Ni, Cu, Zn and Au deposits in Finland (Eilu et al., 2009, 2012). Note that (1) metallogenic areas for gold and nickel overlap at Kuhmo and (2) the Talvivaara area comprises three separate subareas. (Figure from Rasilainen et al., 2017)

This project has received funding from the European Union's Horizon 2020 research and innovation programme under grant agreement No 731166

3.2 Caledonides province (northwest Europe and Greenland)

The Caledonides: Metallogeny and Critical and Strategic metal potential

3.2.1 The Caledonian Orogeny

The Caledonides trend north-eastwards through Ireland, Scotland, Scandinavia, and eastern Greenland, tracing the suture of the Iapetus Ocean. The Caledonian Orogeny evolved over >200 Myrs from the early- to mid-Palaeozoic, resulting in the collision of the Laurentia, Baltica , Avalonia , Dashwoods, Ganderia, Meguma, Carolinia and Suwanee palaeocontinents during the closure of the Iapetus Ocean (Figure 16). Phases of arc-arc, arc-continent and continent-continent collision occurred leading to crustal deformation and thrust faulting, arc-related magmatism, and Barrovian-style metamorphism. The Caledonides were subsequently subject to post collisional collapse, high-K calc-alkaline magmatism, and later erosion and exhumation leading to the exposure of rocks from a range of palaeodepths (Roberts, 2003).

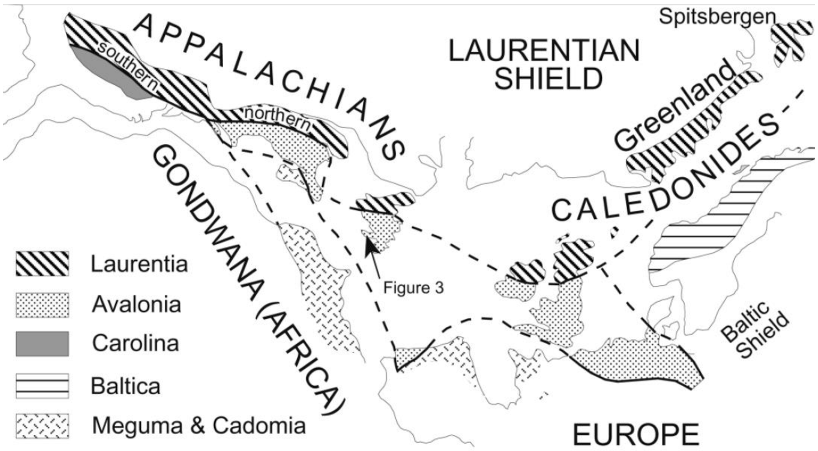

Figure 16. Outline of the Caledonian and Appalachian mountain ranges, tracing the suture of the Iapetus Ocean, after McNamara et al. (2001).

Caledonian deformation and magmatism led to orogenic and stratabound mineralization styles within Pre-Caledonian basement rocks. Orthomagmatic mineralization formed through early stage primitive magmatism and later ophiolite exhumation, whereas magmatic and magmatic-hydrothermal deposits associated with more evolved calc-alkaline to alkaline magmas formed during the mid- to latter-stages of convergence.

This project has received funding from the European Union's Horizon 2020 research and innovation programme under grant agreement No 731166

Distinct stratabound mineralization styles formed throughout the orogeny including Volcanogenic Massive Sulphide (VMS) and Irish type deposits whilst late-stage orogenic collapse and extension yielded a range of polymetallic veins that host diverse mineralization.

3.2.1.1 Ireland

The Iapetus suture runs Northwest through central Ireland from Limerick to Drogheda. Thrusting and deformation associated with the Caledonian orogeny run sub-parallel to this structure. Ireland is divided into several basins and mineral provinces: The North-western Basement Province, the Mayo-Curlew, Central Ireland, and Munster Basins and the Longford-Down and Leinster Massifs.

Palaeozoic Orogenic Au deposits

Proterozoic basement rocks of the North-western Basement Province and within the Mayo-Curlew basin host orogenic Au deposits that formed as mineralised quartz veins and shear zones during the latter stages of the Caledonian Orogeny (e.g. Curraghinalt and Cregganbaum; Rice et al., 2016). The Au was likely scavenged from a Proterozoic basement source however, Te enrichment in the Wicklow and Wexford deposits suggest a possible magmatic influence (Standish et al., 2014).

Ordovician VMS deposits

A phase of VMS mineralization is recognised within intermediate to felsic calc-alkaline magmas of the Upper Ordovician, including the Avoca Cu-(Pb-Zn) deposit of the Leinster Massif and the Charlestown Cu-(Zn-Pb-Ag) deposit, Co. Mayo (Hollis et al., 2014).

Granite-hosted and porphyry-style mineralization

Large S-type batholiths were emplaced across Ireland during the late stages of the Caledonian Orogeny in the late Silurian to early Devonian. The Galway Granite and Newry Igneous Complex both exhibit weak Mo-(Cu) porphyry and skarn style mineralization whereas the Leinster Granite exhibits spodumene and muscovite pegmatites, anomalously enriched in Li, W, Cs, Nb and Ta (Chew and Stillman, 2009; Barros and Menuge, 2016). Au and Pt stream sediment anomalies were identified proximal to the Leinster Granite by the ongoing Tellus survey.

Irish-type Zn-Pb deposits

This project has received funding from the European Union's Horizon 2020 research and innovation programme under grant agreement No 731166

"Irish type" carbonate-hosted Zn-Pb deposits (e.g. Navan) occur within the Central Ireland and Munster Basins. The occur along NE-trending Caledonian faults and are hosted within Carboniferous carbonate rocks of the late Courceyan substage, but were likely formed during the Chadian (Hitzman, 1995; Johnston et al., 1996).

Carbonatite-hosted Rare Earth Elements (REEs)

The Carboniferous Cahermore carbonatite of the Beara Peninsula, southwest Ireland represents one of the few known carbonatite intrusives of the southern Caledonides and exhibits moderate light REEs, Co, Cr and Ni enrichment (Brady and Moore, 2012).

3.2.1.2 Scandinavia

The Scandinavian Caledonides encompass the entirety of Norway and parts of western Sweden. They are defined by a series of NNE-trending nappes containing allocthonous material from the Laurentian plate that are bound by Baltic basement to the east and west (Grenne et al. 1999).

Sediment-Hosted deposits

Basement rocks of the Uppermost Allocthon of western Norway host a range of sediment hosted deposits including stratabound polymetallic and dolomite-hosted stratiform Fe (+Mn) deposits; graphite-rich metasedimentary deposits are also distributed throughout the Holandsfjord, Senja and Lofoten-Vesterålen regions (Grenne et al., 1999; Gautneb, 2015).

The Organic Carbon, U, V, Mo, Ni and REE enriched Alum Shales formed through anoxic sedimentation along the Baltic coastal margin during the mid- to late Cambrian; they are widely distributed across northern Europe, but are of economic interest in the Billingen-Fallbygden area, southern Sweden (Grenne et al., 1999).

Prior to Caledonian orogenic collapse, sandstone-hosted Pb-Zn±(Ag-Cu-F-Ba) sulphide deposits were deposited within Neoproterozoic to early Cambrian sediments of the orogenic foreland of Sweden and Norway. A lesser group of dolomite-hosted Zn-(Pb) Mississippi Valley Type deposits formed in the Sagelvvatn area of northern Norway during this time (Grenne et al., 1999).

VMS stratabound deposits

Cu-Zn-(Pb) VMS deposits are hosted within Cambrian to Silurian age Ultramafic and basaltic lavas of the Gula Complex and Støren Group of Trondheim, central Norway as well as the Fundsjø and Stekenjokk volcanic units. Several large early Ordovician VMS deposits including the Lokken Cu-Zn-(Pb-Ag-Au) deposit formed within supra-subduction

This project has received funding from the European Union's Horizon 2020 research and innovation programme under grant agreement No 731166

zone ophiolites of the Karmøy-Bømlo-Bergen area, the western Grong District, Leka island and the Lyngen peninsula. Lesser Zn-Pb and Cu-Zn VMS deposits occur in the early- to mid-Ordovician of southwest Norway and the late Ordovician of the Røros, Meråker, Sulitjelma and Birtavarre-Vaddas districts respectively (Grenne et al., 1999).

Carbonatite-hosted REEs

Carbonatites of latest Precambrian to Early Cambrian occur within the Seiland Igneous Province of northern Norway and the Fen Complex southwest of Oslo. Whilst the Fen complex has been mined for Fe, Nb, P, Mn and Th, these carbonatites are also a potential economic source of REEs, containing up to 1.6 wt% total REEs in regions (Marien et al., 2017).

Orthomagmatic hosted PGMs (± Chromite) and base metal deposits

Layered gabbros of the latest Precambrian Seiland Igneous Province host Fe-Ti-(V) mineralization as ilmenomagnetite and ilmenite disseminations and localised concentrations of Ni, Cu and PGMs, whereas ultramafic and mafic magmas of the Gula and Råna Complexes exhibit disseminated Ni-Cu sulphide mineralization (e.g. Bruvann). Caledonian ophiolites of the Seve Nappes and the early Ordovician supra-subduction zone ophiolites both exhibit chromite (± PGM) cumulate layers, whereas massive sulphide Cu-Ni-PGM mineralization occurs in the upper ophiolite section of the Gjersvik Group, central Norway (Grenne et al., 1999).

Granite-hosted and porphyry-style mineralization

Shoshonitic to high-K calc-alkaline plutons and associated porphyry-style Cu-Mo mineralization were emplaced in the mid-Ordovician including Follafoss and Møklevatn in central Norway (Grenne et al., 1999). Sub-economic molybdenite-bearing pegmatites were emplaced at Malvika during the culmination of arc-style convergence in the Late Ordovician to Early Silurian and exhibit skarn-style W enrichment (James et al., 1993).

Polymetallic vein mineralization

Polymetallic vein deposits variably containing Ag, Au, Cu, Zn, Pb, Sb, As, Bi, U, W, F and Be formed in several settings in the late stages of the Caledonian orogeny. These include within Late Ordovician to Early Silurian granite batholiths, in basement structural domes and shear zones, in deformed pegmatites between Rana and Ofoten, and associated with Caledonian foreland thrust faults (Grenne et al., 1999).

This project has received funding from the European Union's Horizon 2020
research and innovation programme under grant agreement No 731166

3.2.1.3 Eastern Greenland

The Caledonides are traced NNE across the northeastern margin of Greenland from Scoresby Sund in the south to Kronprins Christian Land in the north. In this region they are predominantly composed of folded and thrusted portions of the Laurentian crustal margin. The extensive glacial and geological cover and relatively low levels of exploration in these regions make this region is highly prospective for future exploration however several significant resources are already known.

3.2.2 Pre-Caledonian basement mineralization

Orthomagmatic Ni-Cu, Au and PGE mineralization occurs either as disseminated sulphides or as PGE-bearing chromitite layers within mafic and ultramafic rocks of the Vestfjord and Liverpool Land regions. Magnetite, and hematite-ilmenite layers occur in association with basaltic magmas in the Gletscherland area, containing significant Fe and Ti mineralization as well as traces of V. Archean and lower Proterozoic gneisses and migmatites bearing U and Au mineralization are observed at the Flyverfjord complex and in the Frænkel Land region associated with the Lower Proterozoic Hagar migmatite sheet. Paleoproterozoic skarn mineralization bearing REEs, Ag, W, Cr and V at Dickinson Fjord and Ni, Cu and Ag mineralization at Charcot Land (Stendal and Frei, 2008; Kolb et al., 2016).

Neoproterozoic stratabound Cu

Stratabound copper occurrences occur within the Neoproterozoic Eleonore Bay Supergroup at eight stratigraphic levels. Mineralization is hosted within quartzite and shales and may be traced over 275 km. Although mineralization is dominated by interstitial chalcopyrite in sandstone, shales either host chalcocite-(bornite) or pyrite-chalcopyrite occurring within coarser-grained laminae and as veins (Stendal and Frei, 2008).

Granite-associated W-Sb-As mineralization

“Skarnoid” scheelite mineralization occurs within metasedimentary rocks proximal to granite and granodioritic intrusions at various localities across central East Greenland from Milne Land to Andrees Land. Arsenopyrite-bearing and scheelite-bearing vein systems occur at the base of the Eleonore Bay Supergroup in association with granites and pegmatites. Carbonate-hosted scheelite and stibnite mineralization occurs along an extensional fault system within the Neoproterozoic to Middle-Ordovician Yomer Ø Group, lower intervals within this sequence also exhibit pyrite, sphalerite, galena, chalcopyrite, arsenopyrite and gold mineralization (Stendal and Frei, 2008).

This project has received funding from the European Union's Horizon 2020 research and innovation programme under grant agreement No 731166

3.2.3 Late Caledonian polymetallic vein mineralization

Variably base metal, As, Bi, Sb, Ag, Au and U enriched veins occur regionally in association with N-S trending faults of the eastern fault zone in central East Greenland. Mineralization exploited the fault zone as a pathway, facilitating the upwelling of metal enriched basinal brines. Veins range in size from centimetres to meters in thickness and in some instances, may be traced over >1.5 km (Stendal and Frei, 2008).

3.3 Variscan province

The Variscan orogen or Variscan belt formed in the late Paleozoic by the collision between the continents of Gondwana and Laurussia during the Variscan (Hercynian) Orogeny. This belt was divided into three main segments, which are the Appalachians, Variscides, and Urals (Matte, 1991, 2002). The Variscan or Variscides orogen extends from Morocco, the Iberian Peninsula, and Central Europe. In the latter zone, it is limited to the NE by the Tornquist or Trans-European Fault zone which stretches from the Baltic coast of Poland to the Carpathians. The southern limit is the Alpine Front (inset in Figure 17).

This continental collision caused the development of a polyphase orogeny, from the Early Devonian to the Early Permian, and comprising three major stages of metallogenesis. The first stage of the Variscan orogeny (Early Devonian-Early Carboniferous) corresponds to the closure of the Rheic Ocean followed by continental subduction and it is during this stage that the sediment-hosted Pb-Zn and volcanogenic massive sulfide deposits (VHMS) were deposited. The second stage corresponds to the Variscan continental collision. The third stage (Pennsylvanian to Lower Permian) is a syn- to post-orogenic collapse marked by normal faults, development of granulite metamorphism of the lower crust, and emplacement of granites. Most of the magmatic-hydrothermal rare-metal mineralizations and hydrothermal metal-rich sulfide mineralizations are associated with the emplacement of peraluminous granites and rare-metal granites of this stage (Marignac and Cuney, 1999).

In the Iberian Peninsula, the Variscan orogen appears throughout the NW, named the Iberian Massif, which in turn is divided into several areas with different structural and stratigraphic characteristics. The different areas comprise the Cantabrian (CZ), Western Asturian-Leonese (WALZ), Central Iberian (CIZ), Galicia-Trás-Os-Montes (GTMZ), Ossa-Morena (OMZ) and South Portuguese (SPZ) zones (Figure 17). A brief description of the metallogeny of each area with a focus on CRM is shown below.

The eastern part of the CZ is well-known by the variety of small-sized mineral occurrences of Pb-Zn-Ba-Hg, F-Ba, Cu-Co-Ni, Hg-Ba, Sn-As, Fe-Mn, As-Sb-Fe which are usually in Carboniferous carbonates, either related to the Permian-basement unconformity or

This project has received funding from the European Union's Horizon 2020 research and innovation programme under grant agreement No 731166

inside fractures or folds caused by the Late Variscan orogeny (Luque et al., 1990). There is also a Carboniferous Mn-Fe sedimentary deposit, with small hydrothermal Mn nodules deposited in a deep-marine environment, which probably was the source bed for most of the epithermal deposits of Permian age in the CZ (Martínez García et al., 2004).
The WALZ offers a wide variety of mineralization, although often of small size. The metal elements present are Fe, Pb, Zn, Cu, Ag, Au, Mo, Sb, Mn, W, U, Hg, As, and Co, and the most important nonmetallic minerals are barite and magnesite (Luque and Ruiz, 1990).

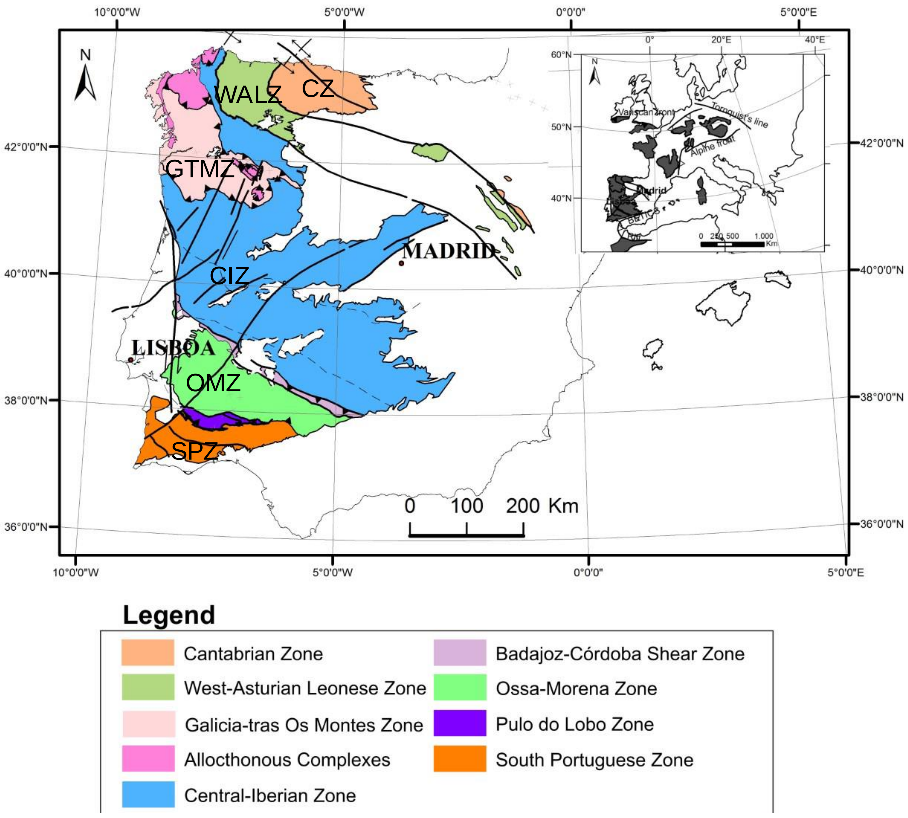

Figure 17. Location of Variscan orogen and zones in the Variscan belt in the Iberian Peninsula. Zone boundaries modified after Julivert et al. (1974), Quesada (1991) and Martínez-Catalán et al. (2014).

The CIZ is the largest area and a major metallogenic province of the Iberian Massif. The main metallogenic features that characterize the ore deposits of this zone are described according to their geological setting and their relationship with the tectonomagmatic events (Gumiel and Arribas, 1990). Thus, there are important exhalative Sb-Hg prospects

This project has received funding from the European Union's Horizon 2020 research and innovation programme under grant agreement No 731166

related to preorogenic volcanism such as the stratabound Sb deposit of San Antonio or the Almadén deposit that represents the biggest Hg concentration in the world. A large and diverse group of Sn, W, U, P, Li, Pb, Zn, Cu, Sb, and Au mineralization related genetically to the collisional granitoids intruded during the Variscan Orogeny. Some deposits originated from ore-forming fluids produced during the emplacement of the granitoids, whereas others were formed as the result of the remobilization of preexisting Sedex deposits. Most of the W-Sn deposits related to syn- and late-kinematic granites of alkali trend, appear as scheelite, wolframite, cassiterite, and sulphide rich-veins and stockworks traverse the granites and metasedimentary host rocks, or as greisen-type deposits. There are also important U deposits, intragranitic veins, and some pegmatites, which also may contain Be, Nb, Ta, Li, and REE-rich minerals. Some of the main Sn- and -Li-rich deposits in the Iberian Massif are located in the CIZ and, of a lesser extent, in the GTMZ to the northwest. Sn-Li mineralization occurs principally in aplite-pegmatite bodies and hydrothermal veins with quartz and phosphates. The Li-rich minerals include spodumene, petalite, and Li-rich micas (lepidolite) and the phosphates amblygonite-montebrasite. An important type of Sn-Nb-Ta-rich mineralization occurs as disseminations in the apical or marginal areas of small and fine-grained leucogranite bodies. Typical mineralization consists of Ta-rich cassiterite, columbite group minerals, microlite, tapiolite, and lepidolite.

The OMZ extends across the Portugal-Spain borderline, defining a 120 x 240 km2 belt with NW-SE orientation. It displays a great variety of types of mineralization and a large number of ore deposits and showings (>650), including Fe, Pb-Zn, Cu, Au, Ag, Sb, Ni, Mn, W, Hg, barite, variscite, U and coal. They formed by very different processes during the Cadomian and the Variscan orogeny (Tornos et al., 2004). Cadomian mineralization, include volcanic-hosted massive sulphides, barite, and Zn-Pb Sedex deposits and porphyry copper-like mineralization. The Variscan Orogeny led to the formation of syn-metamorphic and peri-granitic base metal-bearing veins, small volcanic-hosted polymetallic massive sulphide deposits, iron oxide replacements, and skarns, magnetite and Cu-Ni magmatic ore bodies and Sn-W veins. The Aguablanca ore deposit represents the unique example to date of an economic Ni-Cu-(PGE) magmatic sulphide deposit related to mafic-ultramafic magmatism in southern Europe. Finally, Late Variscan hydrothermal activity is responsible for the formation of Pb-Zn and Cu-dominated lodes, Hg replacements, and U-rich veins.

One of the domains of the SPZ, the Iberian Pyrite Belt (IPB), is a metallogenic province in SW Portugal and Spain hosting the largest concentration of massive sulphide deposits

This project has received funding from the European Union's Horizon 2020 research and innovation programme under grant agreement No 731166

worldwide. The IPB is a 250 km long and 20-70 km wide belt that includes eight huge VHMS deposits, e.g. Rio Tinto (500 Mt), in Spain, and Neves Corvo (>300 Mt), in Portugal (Inverno et al., 2015). The average grade of all VHMS deposits in the IPB is 45% S, 40% Fe, 1.3% Cu, 2.0 % Zn, 0.7% Pb, 26 g/t Ag and 0.5 g/t Au. Metals such as Sn, Cd, Co, Hg, Bi, Se, etc., are present in concentrations ranging from tens to hundreds of ppm. The massive ore minerals are pyrite, sphalerite, chalcopyrite, galena (and cassiterite at Neves Corvo) and they are also present with quartz-chlorite-sericite-carbonate in the stockwork ore. The VHMS deposits in IPB are exhalative or formed by shallow subsurface replacement of either muds/shales or coherent felsic volcanic rocks. Hundreds of small Mn deposits are also related to the felsic volcanism (Tornos, 2006).

3.4 Alpine -Balkan-Carpathian-Dinaride province

3.4.1 Eastern Apline province

The Alpine mountain range, which extends over the area eastwards of the line Bodensee Lake (Switzerland) - Milan (Italy) to the city of Maribor (Slovenia) and Vienna (Austria) as its easternmost borders, is based on different geological and structural characteristics, divided into Eastern and Southern Alps. The boundary between them is Periadriatic fault system - PAF (also called Periadriatic lineament), which extends from Ivrea in the west towards Bolzano, Brunico, Gailtal, Karavanke Mountains Velenje, Varaždin and further into the Panonian Basin in the east. Eastern Alps occupy the area north of the PAF, the same tectonic position as in the West Carpathians, while the area south of the PAF belongs to the Southern Alps, where tectonic blocks were overthrust towards south during the Alpine orogenesis

Nappe systems are the main structural feature of Eastern Alps. Most of the Eastern Alps is composed of Austroalpine structural units which represent nappe systems of rocks developed on Adria microplate. They were overthrust towards the north on Pennnic nappes which are composed of rocks formed in Alpine Tethys ocean (Penninic realm). The lowermost structural units are rocks of European tectonic plate margin and foreland defining Subpenninc and Helvetic nappes. Detailed structure end tectonic evolution of Eastern Alps is described in Grad et al. (2009), Schmid et al. (2004, 2013, 2020) and Schuster et al. (2013).

Morphology and structural units of the Eastern Alps were induced by Alpine orogeny from Early Cretaceous onwards, when an extensional tectonic regime evolved into a compressive one, causing subduction of Pennine ocean crust under Austroalpine,

This project has received funding from the European Union's Horizon 2020 research and innovation programme under grant agreement No 731166

followed by a continental collision with orogenic climax in Eocene. These two events caused two metamorphism peaks, first during the Cretaceous ("eoalpine" phase) and the second one during Eocene-Oligocene ("neoalpine" phase) (Pohl and Belocky, 1999). The peak of metamorphism in Oligocene was followed by collapse of Eastern Alps together with opening of Pannonian basin on the east, which resulted in formation of shear zones and faults. A tonalitic magma was intruded along the PAF, forming "Periadriatic intrusive bodies".

Among the most characteristic ore deposit types in the Eastern Alps are carbonate hosted Mississippi Valley Type Pb-Zn ore deposits, polymetallic SEDEX ore deposits, metasomatic siderite ore deposits, and hydrothermal vein type Au deposits.

3.4.1.1 Subpenninc and Lower Penninc units of Taueren window

Metamorphic rocks of the Subpenninic tectonic unit exposed in Tauren tectonic window in western part of Austria contain numerous quartz veins and lenses with Au, Ag and As mineralization. Arsenopyrite, pyrite and native gold are the main ore minerals, while mineralization contains also elevated levels of Bi, Pb and Sb. Gastein is probably the most widely known Au deposits in the Taueren window and is part of Rauris-Gastein Au metallogenic belt. In the Taueren window, Au mineralization can also be found in Schellgaden-Oberdorf, Rotgülden-Schurfspitze, Pöllatal-Maltatal and Hirzbach-Schiedalpe-Kloben melogenic belts (Weber, 1997). Mineralization postdates the Neoalpine metamorphic phase and are connected with retrograde metamorphism in Miocene, which caused increased fluid flow (Pohl and Belocky, 1999).

Another important ore deposit type found in the Tauren window are stratabound W ore deposits such is Felbertal – Mittersill for instance. They are hosted by metamorphosed clastic sediments and submarine lavas of lower Paleozoic age with scheelite as main ore mineral (Holzner and Stumpfl, 1980). Formation of mineralization was considered as syngenetic, but discovery of strong connection of high grade W ores with nearby gneiss representing metamorphosed metagranitoid of Carboniferous age in Mittersill, show that mineralization can be considered as poly-metamorphosed granite related stockwork type W deposit (Raith and Schmidt, 2010). Metallogenic associations related to Variscan granites in the Subpenninc and Lower Penninc units of Tauern window fit into igneous felsic group – Sn, W, Ta, Nb (Mo, Li, Be, B, In, F).

This project has received funding from the European Union's Horizon 2020 research and innovation programme under grant agreement No 731166

Rocks exposed in the Tauern window host also several polymetallic (Cu-Pb-Sb-Zn) stratiform and vein type ore deposits. Cu-U deposits in quartzites, gneisses and phyllites deposited during metamorphic remobilization are also known at Rauristal (Weber, 1997).

The Subpenninc and the Lower Penninc rocks are exposed also in Rechnitz tectonic window, where an Sb-vein deposit Schlaing was formed in neoalpine phase (Schroll and Pak, 1983), while other connect it with the postorogenic Miocene andesite vulcanism.

3.4.1.2 Austroalpine unit

The Austroalpine tectonic unit is composed of a series of nappe systems which differ from each other in lithological composition as well as in degree of metamorphosis they underwent. Austroalpine tectonic unit is traditionally divided on Upper and Lower Austroalpine nappes (Webber, 1997).

The Lower Austroalpine nappes such as Semmering-Wechsel, Radstadt and Err-Bernina nappes have only limited outcrops. These nappes are structurally the lowest unit of the Austroalpine nappes.

The Upper Austroalpine nappes consist of carbonate sediment rocks of Northern Calcareous Alps nappes, and low-grade metamorphic rocks of Greywacke zone nappe and Silvretta-Seckau nappes. They are overlaid by eoalpine high-pressure metamorphic rocks belt represented by the Koralpe-Wölz nappes which was formed during intercontinental subduction of middle and lower crust during Cretaceous (Schmid et al., 2020). Structurally uppermost parts of Upper Austroalpine are Ötztal-Bundschuh and Drauzug-Gurktal nappes composed of the low-grade metamorphic rocks (Schmid et al., 2020).

3.4.1.3 Lower Austroalpine Unit

Rocks of the Lower Austroalpine nappes contain several Fe, U, baryte and polymetallic Cu-Pb-Zn ore fields (Weber, 1997). Fe mineralization at Semmering is formed as layers and lenses of siderite and hematite between Triassic quartzite and dolomite rocks. Veins and lenses in quartzite host also U mineralization at Rädestadt Tauern, and Semmering U ore fields. On Semmering area discordant fault bound baryte veins and lenses are also very frequent. They are hosted by quartzite and dolomite and were formed from fluids released during the Cretaceous eoalpine metamorphic phase (Pohl and Belocky, 1999).

3.4.1.4 Upper Austroalpine unit – Grauwacke zone and Silvretta-Seckau nappes

Paleozoic rocks of Grauwacke zone at the base of Northern Calcareous Alps host significant, even world class ore deposits of Fe and magnesite. Fe ore deposits are concentrated especially in the eastern part of Grauwacke zone. The biggest and the most

This project has received funding from the European Union's Horizon 2020 research and innovation programme under grant agreement No 731166

renowned Fe ore deposit is Erzberg, where massive siderite ore forms irregular stratabound ore bodies in Devonian limestones. Siderite mineralization is enveloped by fine grained ankerite. Some of the researchers proposed marine synsedimentary SEDEX origin of mineralization due to the stratiform nature of some parts of ore deposit and age difference between siderite and ankerite Holzer and Stumpfl (1980) and Prochaska (2016). However, recent research shows that Erzberg ore was formed by hydrothermal-metasomatic process induced by hypersaline hydrothermal fluids released either by eoalpine metamorphic phase in the Creatceous (Pohl and Belocky, 1999) or during the Upper Triassic by increased heat flow due to the rifting process combined with dewatering of sedimentary basins due to the increased load of platform carbonates (Prochaska, 2016).

According to the Prochaska (2016) magnesite mineralization has similar characteristics as the Fe mineralization in Grauwacke zone and was formed during the same process. Epigenetic nature of stratiform and stratabound magnesite formation in Veitsch area was confirmed by Azim Zadeh et al. (2015), only that they identify its formation in the early Permian. The main areas of magnesite/talc occurrences are the areas of Veitsch, Dienten and Hochfilzen.

Metamorphic rocks of the Veitsch nappe contains also significant amounts of graphite hosted by graphite slates of Upper Carboniferous.

The western part of Grauwacke zone is rich with polymetallic Cu, pyrite, Pb and Zn mineralization. Schwaz-Brixlegg area contain stratabound, vein and breccia hosted ore deposits rich in sulfosalts minerals (Arlt and Diamond, 1998). Epigenetic Cu ores were fund also on area of Röhrerbühel-Kitzbühel, Hohe-Salve-Einheit, Leoganag, Jochenberg-Einheit, Mitterberg-Mühlbach-Larzenbach, Zell and See-Radstad-Mandling district. Their formation can relate to hypersaline fluids released during Cretaceous eoalpine metamorphic phase as well as neoalpine metamorphic event in Eocen-Oligocen (Raith and Schmidt, 2010). They regularly contain increased Ag, Hg and Sb levels as well as U and Co-Ni minerals (Weber, 1997). At Kitzbühel area were discovered also baryte concordant and discordant ore lenses.

3.4.1.5 Upper Austroalpine unit – Northern Calcareous Alps nappes

For nappes, which compose Northern Calcareous Alps are characteristic stratiform synsedimentary SEDEX and early diagenetic ore deposits of Fe and Mn. Iron ores were formed in the Permian, Lower and Middle Triassic, while Mn mineralization is connected with the Jurassic (Lias) extension of the area.

This project has received funding from the European Union's Horizon 2020 research and innovation programme under grant agreement No 731166

Similar to the Grauwacke zone, epigenetic Cu sulphosalts with elevated levels of Ag, Zn, Hg, Mn and Pb ores can be found in Northern Calcareous Alps nappes (Montafon and Arlberg for instance). Middle and Upper Triassic carbonate rocks of Northern Calcareous Alps frequently contain also stratabound Pb-Zn ores, which is hosted by the same lithological sequence as Bleiberg Pb-Zn mine which is representative of Mississippi Valley Type Pb-Zn ore deposits. Moreover, also isotopic composition corresponds between them, so they can be considered as carbonate hosted Mississippi Valley type deposits. Ore contain elevated values of Ag, Bi, Cd, Cu, Ga, Ge, Hg (Weber, 1997).

Northern Calcareous Alps contain also sedimentary U mineralization in Permian clastic rocks and large number of evaporite significant evaporite (halite) deposits. Such deposits can also contain phosphate minerals.

Rocks of Cretaceous Gossau beds, which were formed in small basins within Northern Calcareous Alps contain accumulations of bauxite on contacts with underlying lithological units.

3.4.1.6 Eoalpine high pressure zone

High-grade metamorphic rocks of eoalpine high pressure belt is on area of Weinebene and Wölzer Taueren intersected by spodumene-bearing LCT pegmatites, which beside Li minerals contain also Be, Nb, Ta and Sn carrying minerals (Göd, 1989, Gourcerol et al., 2019 and Webber, 1997). They are related to an extensional regime in the Permian.

Very common are also neoalpine post-Eocene quartz Au-bearing veins, which also contain Ag, As, Co, Cu, Pb and Sb. They can be found at Pusterwald, Kliening-Kothgraben and Flatschach-Knittelfeld (Weber, 1997).

The largest part of the ore deposits in the eoalpine high pressure belt belongs to Fe ore deposits which can be either siderite or hematite. (Pohl and Belocky, 1999) consider that were ore deposits such as Hüttenberg and Waldenstein formed by the hydrothermal fluids released during neoalpine metamorphosis. Some of the ore deposits, however, can have Paleozoic SEDEX origin were but were metamorphosed during Alpine orogeny (Weber, 1997).

The eoalpine high pressure zone contains also several polymetallic Ag-Cu-Fe-Zn-Pb with increased levels of Ga, Ge and In. Mineralization is discordant and epigenetic. Among the more important areas of polymetallic mineralization is Schladmnig. Furthermore, mineralization of Hg, Sb and W are also known in eoalpine high pressure belt.

Within Innsbruck quartzphylite the most important role plays the magnesite ore body Tux. Magnesite was formed during metamorphic and overthrusting processes (Moretani

This project has received funding from the European Union's Horizon 2020 research and innovation programme under grant agreement No 731166

et al., 1982). Along the magnesite occurrences, As, Sb and W mineralization can be also found in Innsbruck quartzphylites.

3.4.1.7 Upper Austroalpine unit – Ötztal-Bundschuh and Drauzug-Gurktal nappes

The structurally highest nappes of Austroalpine units are the most characteristic carbonate hosted Mississippi Valley Type ore deposits hosted by Middle to Upper Triassic (Anisian to Carnian) carbonate rocks and polymetallic Cu-Pb-Zn SEDEX type ore deposits hosted by deep-water clastic sediments of Paleozoic age.

SEDEX mineralization is especially frequent in "Paleozoic of Graz" where is hosted by Devonian black shales which alternates with diabase, tuffs, carbonate phyllites and marbles. Sphalerite is the main ore mineral, followed with Ag-bearing galena, baryte and fluorite (Weber, 1983). Zonation typical for SEDEX deposits, where stratiform sulphides form the central part of ore body, surrounded by baryte and iron oxides on the margin, was detected.

Carbonate hosted Mississippi Valley type Pb-Zn ore deposits along PAF, partly belong to the Drauzug structural unit in Austria/Slovenia and partly to the South alpine nappes in Italia. They are epigenetic and stratabound to specific stratigraphic levels in Anisian, Ladinian or Carnian limestones. Common features of mineralized horizons are increased level of organic matter, prograding dolomitization and presence of layer with lower permeability in hanging wall (most commonly black shales) which could act as a screen. Ore was formed also in paleokarst caverns, breccias developed by metasomatic replacement of limestone and discordant veins along faults and fractures which were mineralized by remobilization of existing ore (Dolenec et al., 1983). The source of the metals was laterally migrating low temperature hydrothermal fluids. An increased presence of organic matter in certain horizons enabled bacterial activity which released H2S into pore waters. Mixing of hydrothermal fluids and pore waters enabled sulphide formation (Herlec et al., 2010). In some cases, the ore formation was syngenetic or early diagenetic (Topla, Slovenia for instance), where hydrothermal fluids flowed into the tidal plains, forming stratiform mineralization in carbonates. The most know ore deposits from this group are Bleiberg (Austria), Mežica (Slovenia) and Raibl and Salafossa (Italy). Since the majority of Mississippi Valley Type ore deposits are formed along the PAF, it could have an impact on ore genesis. Pb-Zn ores have simple mineral assemblages (galena, sphalerite, pyrite, marcasite), are characterized by colloidal type of mineral growth (especially sphalerite) and contain elevated levels of As, Cd, Ge, Mo and Tl (Weber, 1997).

This project has received funding from the European Union's Horizon 2020 research and innovation programme under grant agreement No 731166

3.4.2 Western Carpathians in the Alpine-Carpathian-Dinaride region

The arch structure of the Carpathian Range with the Pannonian Basin in its centre evolved by the escape and rotation of two microplates (referred to as Alcapa and Tisia blocks) during their movement towards the East European Craton. The two microplates contact at the SW-NE striking Mid-Hungarian Mobile Belt (Csontos & Nagymarosy 1998), a continuation of the Periadriatic Seam of the Alps, mostly covered by Neogene basin sediments (based on CHMP2030 report). The Alcapa-based ranges striking from SW–NE to W–E are named Western Carpathians, the Tisia-based ranges in Ukraine and Romania are the Eastern and Southern Carpathians. In the outer part of the arch an uplifted collisional zone was formed with nappe systems, flysch and molasse basins, while the inner part is a mosaic of variably uplifted and subsided terranes during the Cenozoic. Inside the arch, the Pannonian Basin was formed mostly in the Neogene extensional regime and has a high geothermal potential (Horváth et al. 2015).

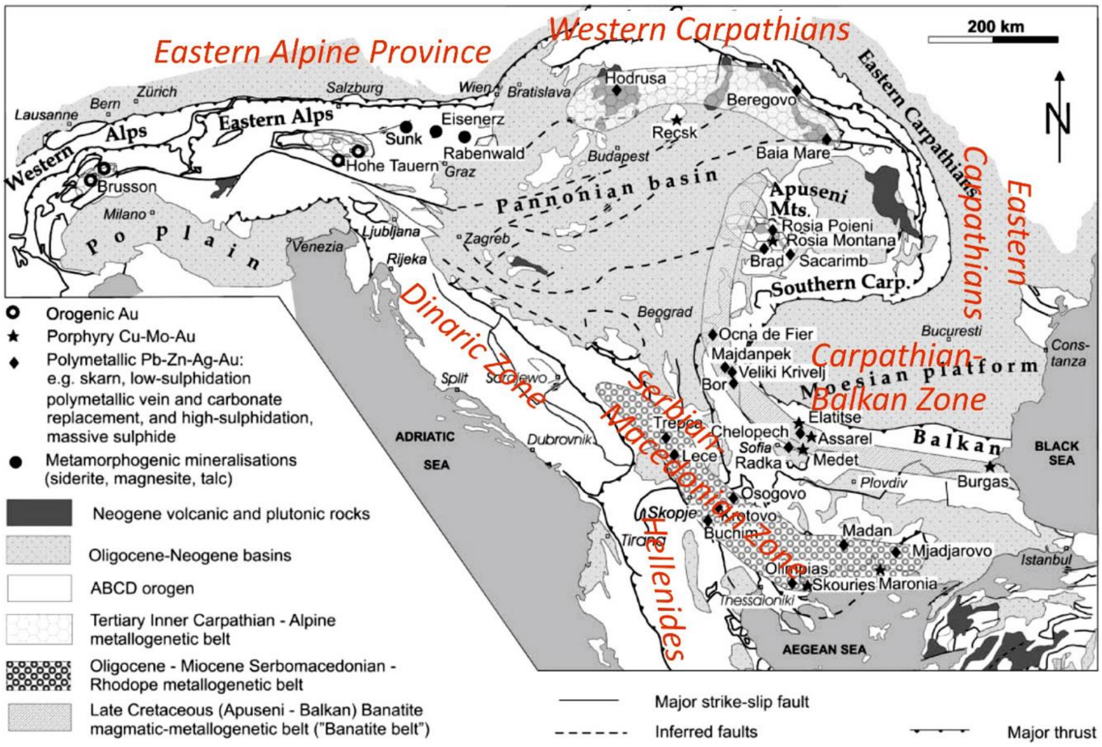

This project has received funding from the European Union's Horizon 2020 research and innovation programme under grant agreement No 731166

GeoERA RAW MATERIALS

Figure 18. Metallogenic provinces within the Alpine-Balkan Carpathian-Dinaride region (Melcher et al. 2017)

The Pre-Cenozoic, partly metamorphic, sequences host several inherited, reworked, and also newly formed ore deposits. MVT Pb-Zn ores, minor stratiform Fe occurrences, and basic volcanism-related VMS deposits occur in the Rodna Mts and the Rebra Paleozoic, Eastern Carpathians. Kuroko-type VMS deposit occurs at Tulghes (Eastern Transylvania, Romania). Lahn-Dill type Fe deposits and rhyolitic volcanism-related base metal sulphide veins are typical in the Poiana Rusca Mts. in the South (Kräutner 1996). Stratabound (metasomatic), often black shale-hosted and vein type siderite, barite and base metal sulphide mineralizations are most abundant in the Paleozoic of the Slovakian Ore Mountains, but also present in metasomatised Triassic carbonates in NE Hungary (e.g. Rudabánya). The granite bodies of this region are also associated with Sn-W-Mo and U-REE-Au lodes. U-Mo-Cu and magnetite deposits of the Slovakian Ore Mts, Sb-Au and W-Au deposits in the Low Tatra and the Small Carpathian Mts. are further important mineralizations in the Western Carpathian region (Grecula et al. 1996). Stratiform Mn mineralizations occur in several localities hosted by Toarcian and by Oligocene black shales (Rojkovič et al. 2008), the Úrkút Mn deposit (Hungary) also bears phosphate-rich lenses with REE accumulation (Grasselly & Pantó 1988).

This project has received funding from the European Union's Horizon 2020 research and innovation programme under grant agreement No 731166

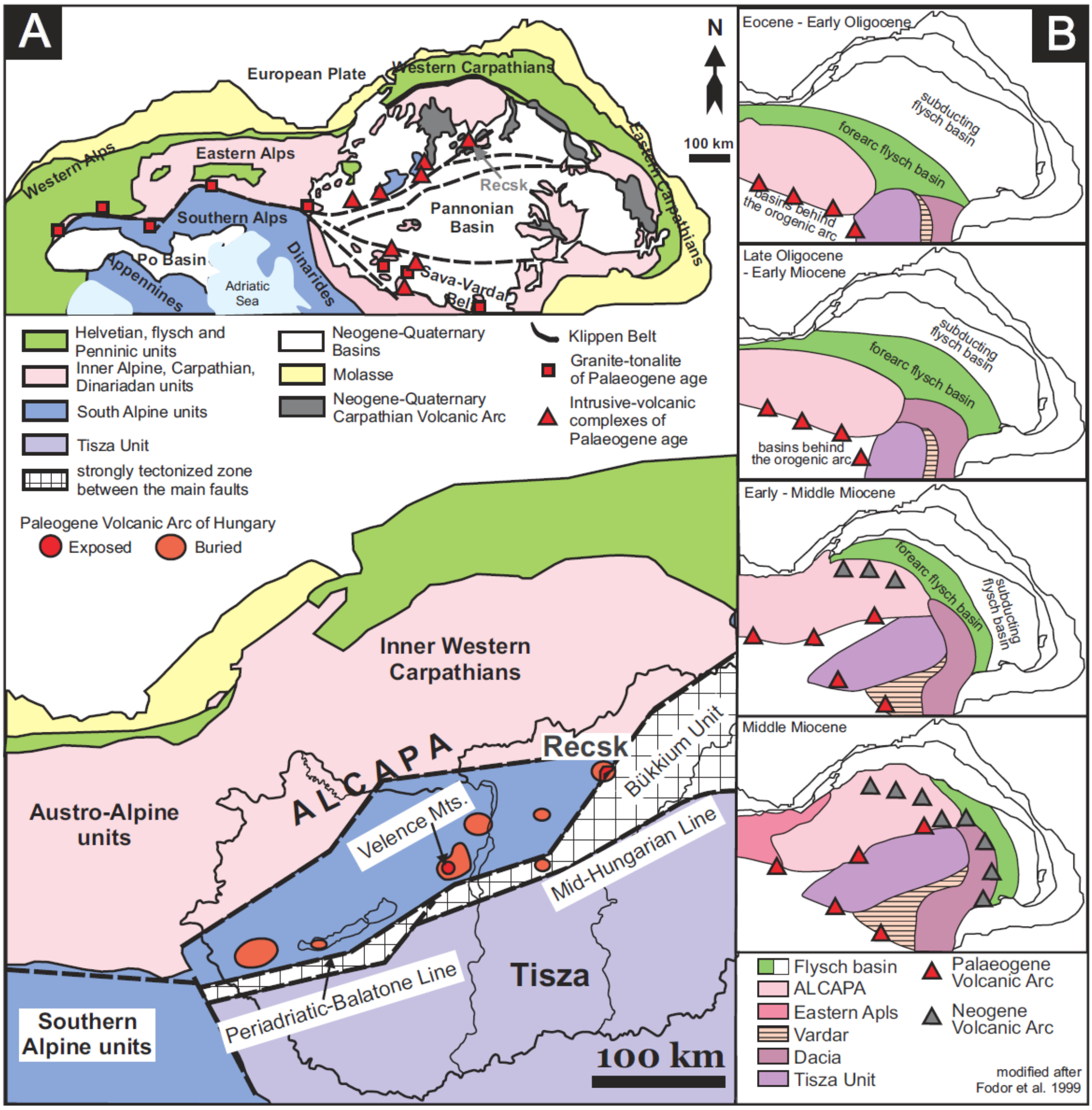

Figure 19. Location and formation of Paleogene and Neogene volcanism in the Alp-Carpathian region. (Takács et al., 2017).

The Oligocene–Miocene magmatic suite forms the Inner Carpathian Volcanic Chain south of the main ranges of the Western Carpathians (Slovakia and Hungary), the volcanic mountains of the Eastern Carpathians, and the Apuseni Mts. (Romania) in a post-

This project has received funding from the European Union's Horizon 2020 research and innovation programme under grant agreement No 731166

collisional extension regime. All of these are dominantly andesitic, but dacites and, mainly from the Miocene, rhyolites are also voluminous. These volcanic-subvolcanic formations host several types of ore deposits of economic value. Beyond these, some alkaline, mostly basic volcanic suites are also present in the region, but with no ore deposits of importance.

Late Paleogene volcanism in the vicinity of the Mid-Hungarian Mobile Belt, active as dextral strike-slip zone at this time, produced several minor volcanic bodies and attached polymetallic sulphide mineralizations, of which the Recsk porphyry Cu-Au with attached skarn and epithermal ores is the most significant (e.g. Baksa et al., 1980). In the Miocene Inner Carpathian Volcanic Chain, the deposits of the Štiavnické Mts in Central Slovakia (precious metal mining district) and the vicinity of Baia Mare can be mentioned as most prominent, although all volcanic edifices host at least vein type epithermal deposits (Neubauer et al., 2005).

It is important to notice that several volcanic structures continue in buried position under thick Late Miocene–Quaternary sediments of the Great Hungarian Plain in the Northeast, downthrown by fault zones of the Mid-Hungarian Mobile Belt (Harangi, 2001; Harangi & Lukács, 2019).

3.4.2.1 Brief descriptions of some selected deposits

Here we provide relevant information on some Hungarian deposits that are related to the Western Carpathian Province.

Polymetallic and precious ores:

Contact and hydrothermal metasomatic ores: Recsk, Szabadbattyán.
Porphyric copper ore: Recsk.
Hydrotermal ores: Pátka (Velence Hills), Nagybörzsöny (Börzsöny Hills), Gyöngyösoroszi, Parádsasvár (Mátra Hills), Recsk-Lahóca (Between the Mátra and Bükk Hills), Telkibánya, Rudabányácska (Eperjes-Tokaj Hills).
Polymetallic ores in granite intrusions: Pátka, Szűzvár (Velence Hills).
Volcanic eruption centers: Velence Hills, Northeastern Mátra Hills, Lahóca, Nagybörzsöny, Mátra Hills.

This project has received funding from the European Union's Horizon 2020 research and innovation programme under grant agreement No 731166

As potential ore indications post-volcanic geisirites: Füzérradvány, Gyöngyössolymos, Asztag-kő, Gyöngyösoroszi.

Regarding bauxites the most important deposits are located to former industrial bauxite mining sites: Nyirád, Halimba, Iharkút, Fenyőfő, Alsópere, Bakonyoszlop, Iszkaszentgyörgy, Gánt and Nagyegyháza in the Transdanubian Central Range (Central Hungary).

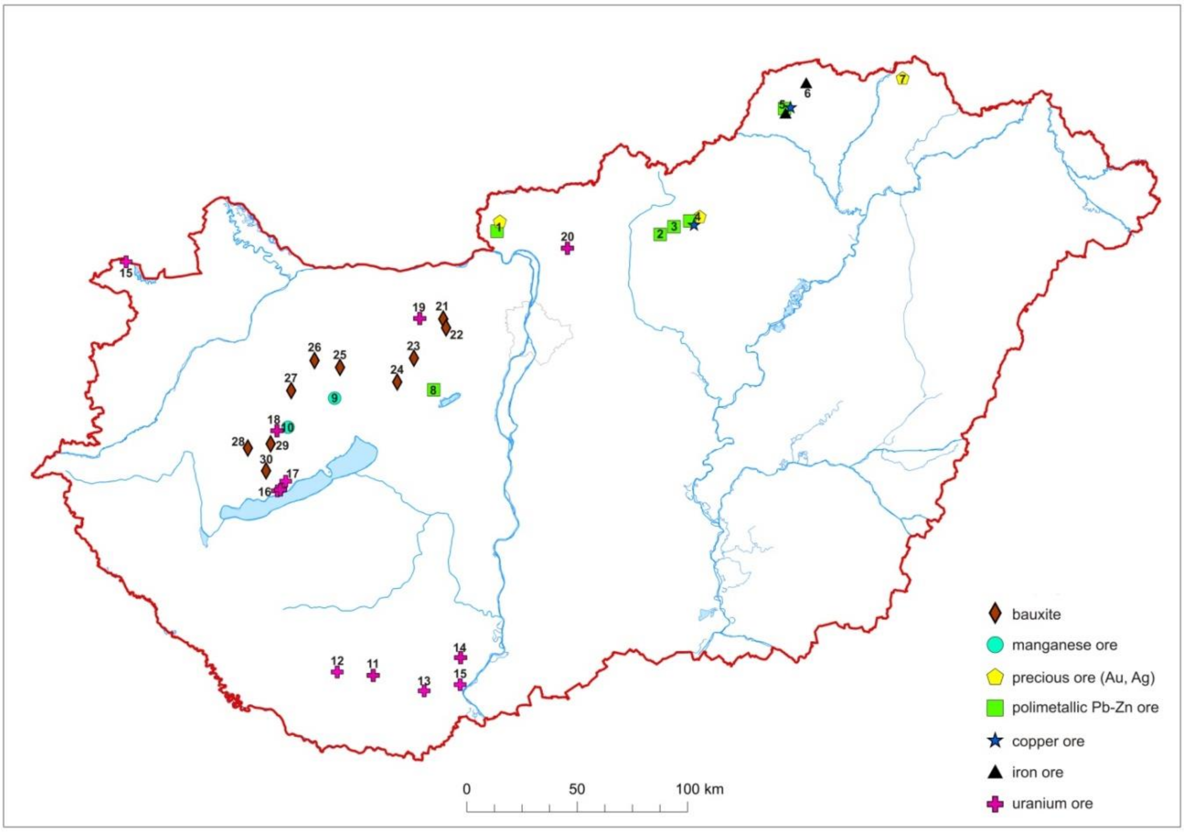

Figure 20. Prognostic map of ores and radioactive mineral resources in Hungary. Copper, polymetallic Pb-Zn and precious ore resources: Nagybörzsöny (1), Parádsasvár (2), Gyöngyösoroszi (3), Recsk (4), Telkibánya (7), Pátka (8). Iron ore: Rudabánya (5), Martonyi (6). Manganese ore: Eplény (9), Úrkút (10). Radioactive mineral (U,Th) resources: Western Mecsek (11), Dinnyeberki (12), Máriakéménd (13), Bátaszék-Leperdpuszta (14), Somberek (15), Sopron-Fertőrákos (16), Balatonrendes (17), Köveskál (18), Ajka Coal Basin(19), Tatabánya Coal Basin (20), Csővár (21).

This project has received funding from the European Union's Horizon 2020 research and innovation programme under grant agreement No 731166

Bauxite resources: Csabdi (22), Óbarok (23), Gánt (24), Iszkaszentgyörgy (25), Bakonyoszlop (26), Fenyőfő (27), Iharkút (28), Nyírád (29), Halimba (30), Hegyesd (31).

Recsk

The mineralization in the Recsk area is a Paleogene intrusive-volcanic complex hosted porphyry Cu-(Mo-Au), with associated Cu-Zn skarn, shallow epithermal Cu-Au-Ag and Au-Ag-Pb-Zn ores (Lahóca deposit) and carbonate-hosted Pb-Zn ores at depth (Recsk Deep deposit).

Börzsöny

The Börzsöny area is characterized by a Miocene neutral volcanic-intrusive complex with a porphyry copper mineralization in the deep zones, and a disseminated or vein type polymetallic Cu-Pb-Zn-(Au-)Ag-Bi-Co ore associated with a low sulphidation epithermal Au mineralization.

Gyöngyösoroszi

Epithermal vein-type Pb-Zn mineralizations in Miocene andesite both in Gyöngyösoroszi and Parádsasvár. The shallow parts of the mineralization contain some gold and silver in Gyöngyösoroszi, while the Parádsasvár mineralization contains additional Cu and minor Cd. These ore deposits from Börzsöny to the Tokaj Hills have already been largely mined.

Rudabánya

Metasomatic Fe mineralization (limonite, siderite, ankerite) in Triassic carbonates with minor associated Pb and Cu ores. The main mineralization is found in Rudabánya, with some other minor ones in the surroundings (e.g. Martonyi). High Carlin gold potential was found in the Rudabánya Iron Ore Formation by Korpás et al. 1999 and by Földessy et al. 1999.

Transdanubian Central Range

Paleogene neutral volcanism related deep porphyry copper mineralization and associated polymetallic Pb-Zn (fluorite) mineralization (Pátka and Szűzvár) in the granite of the Velence Hills together with metasomatic Pb mineralization in Paleozoic carbonates near Szabadbattyán. High Carlin gold potential was found in the Polgárdi Limestone and Úrkút Manganese Ore Formation.

This project has received funding from the European Union's Horizon 2020 research and innovation programme under grant agreement No 731166

Tokaj-Zemplén Hills

Mineralizations of the Tokaj Mountains comprise two types. The first one is epithermal Au-Ag and/or polymetallic mineralizations (Telkibánya, Rudabányácska), and the second one is a shallow As, Hg (Sb, Tl) mineralization related to hot water springs and bound to silicified, clayey limnic sediments (Sárospatak, Regéc).

3.4.2.2 Relevant research projects earlier in Hungary and recently in the MBFSZ

Trace element content of Hungarian bauxites was summarized by Szantner et al. (1986). The most important trace element of industrial importance is gallium (Ga). Bauxite is one of the main sources for this important critical element, and during the existence of the alumina industry in the last century, Hungary was a significant provider of this element in Europe. Hungarian bauxites contained 30-104 ppm Ga_2O_3. Along with the Ga, Ti (1.7-3.3 m/m %), Zr (290-1600 ppm as ZrO2), and V (530-3400 ppm as V2O5) are worth mentioning, although these elements were never exploited and now they are found in the red mud waste except for the Ga.

Trace element study of Hungarian ores with special emphasis on critical elements is an ongoing research topic in the Mining and Geological Survey of Hungary. The first pilot research, that of the Nagybörzsöny occurrence has been finished recently. Two types of mineralizations occur in this region. The first is characterized by arsenopyrite, pyrite, pyrrhotite, chalcopyrite, galena, sphalerite with native gold and bismuth and Bi-bearing sulfosalts. The other one contains sphalerite, galena, pyrite and chalcopyrite. We analyzed archive and newly collected samples as well. We focused on the trace element content of the ores; thus, the samples were processed with AR in a closed bomb and analyzed with ICP OES and ICP MS. Some samples show somewhat higher concentrations of Sb, In, Bi, but majority of the samples do not show particular enrichment. Co, Ga, Ge, V, W and platinum group elements show generally low concentrations although the latter ones may show somewhat elevated concentration values in one or two samples.

Studies at the University of Miskolc have also contributed to the better understanding of distribution of critical elements in some of the rocks and ores as well as mining wastes in Hungary (http://kritikuselemek.uni-miskolc.hu/?p=criticel_monografia_sorozat).

This project has received funding from the European Union's Horizon 2020 research and innovation programme under grant agreement No 731166

3.4.3 Eastern Carpathian province

The Eastern Carpathians are made up, from the East to the West, of: (1) a flysch belt, thrust over the East European Craton, (2) a Caledonian (Avalonian) crustal fragment containing metamorphic basement and sedimentary cover (mostly Mesozoic), known traditionally as the Crystalline-Mesozoic Zone (CMZ) and (3) a Miocene-Quaternary volcanic chain (mostly andesitic). The ore deposits in the Eastern Carpathians are related with the CMZ and the Miocene volcanic chain.

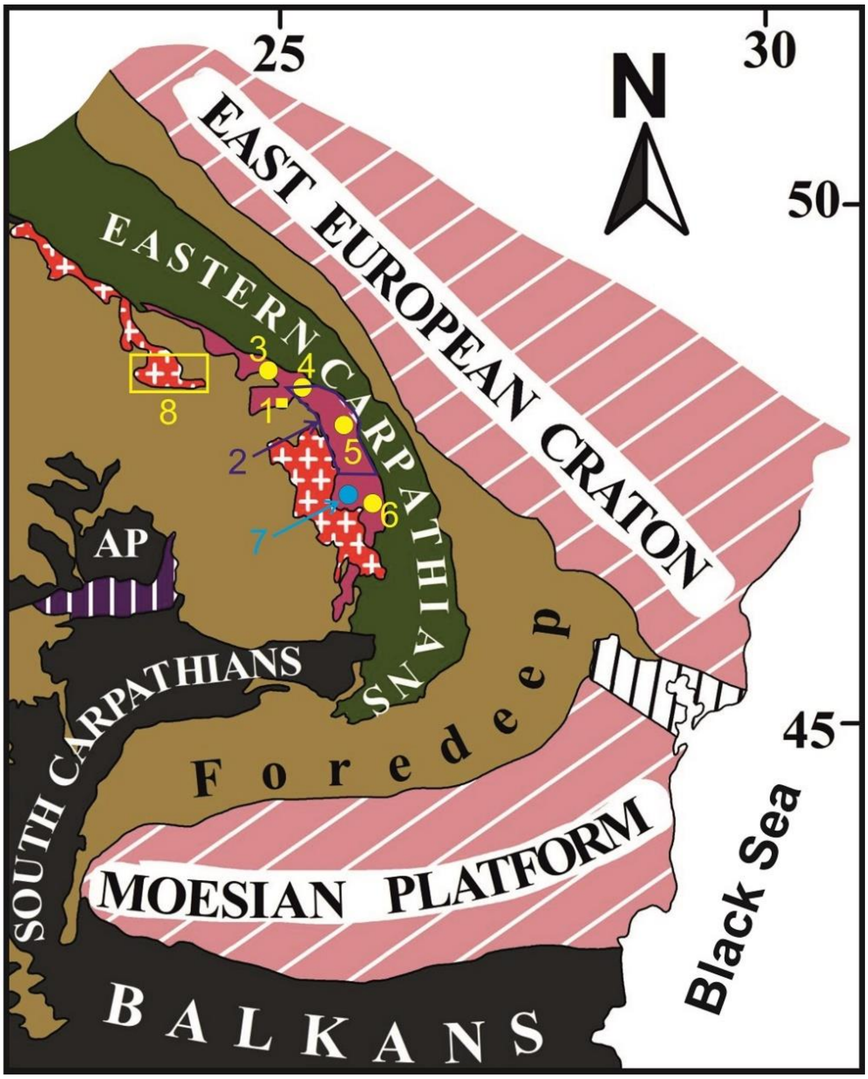

Figure 21. Location of the main ore deposits in the Eastern Carpathians. AP = Apuseni Mountains. 1 = Pb-Zn deposits (Mississippi Valley-type); 2 = location of the manganese ± barite mineralization (area detailed in Figure 22); 3 = Baia Borşa-Burloaia metallo-genetic field; 4 = Fundul Moldovei

This project has received funding from the European Union's Horizon 2020 research and innovation programme under grant agreement No 731166

metallogenetic field; 5 = Leşul Ursului metallogenetic field; 6 = Bălan metallogenetic field; 7 = Jolotca and Aurora mineralization; 8 = the Miocene epithermal provin-ce of the Eastern Carpathians (detailed in Figure 23).

The CMZ has a metamorphic basement with complicated tectonics including pre-Alpine (Caledonian) and Alpine (Aptian-Albian) thrust nappes. The Late Proterozoic Rebra Group, metamorphosed under the amphibolite facies P-T conditions (staurolite-kyanite), hosts the Mississippi Valley-type Pb-Zn deposits from Valea Blaznei and Guşet (Rodna Mts.), in dolomitic rocks (point 1 in Figure 21). The ore consists of lenses and layers with pyrite, sphalerite, galena, chalcopyrite, magnetite, bournonite, proustite-pyrargirite and baryte. Valea Blaznei was mined till 1980s, with the extraction of ca. 5 Mt with an average grade of ca. 1.5% Pb and 3.3% Zn. The remained resource is estimated at 15 Mt with an average grade of 2% Zn and 1% Pb (data from Vodă, 2002).

The Tulgheş Group, part of an Ordovician volcanic arc complex metamorphosed under greenschist facies P-T conditions, contains manganese and base metal (VMS) deposits.

The manganese deposits are low grade (25-30% Mn), occur in the Tg2 Formation of the Tulgheş Group and form lenses to layers within graphite-rich cherts or carbonate schists. The ore is carbonate-dominated (rhodochrosite, kutnohorite, Mn-calcite), with varied contributions of silicates (tephroite, spessartine, rhodonite, pyroxmangite, dannemorite, stilpnomelane), sulfide (pyrite, alabandite, chalcopyrite) and oxides (hübnerite, jacobsite, psilomelane, manganite, pyrolusite, birnessite, wad). The oxidation zones have been mined as iron ore in the 1800s and the early 1900s.

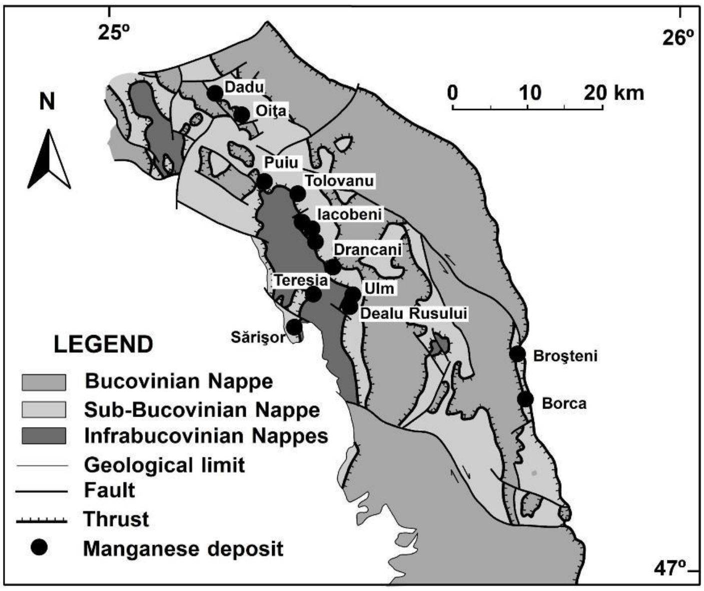

This project has received funding from the European Union's Horizon 2020 research and innovation programme under grant agreement No 731166

GeoERA RAW MATERIALS

Figure 22. Spatial distribution of the Mn deposits in the Eastern Carpathians (area 2 in Figure 21). Note the concentration of all economic Mn mineralization in the Sub-Bucovinian Nappe.

All the economic Mn deposits are in the Sub-Bucovinian Alpine Nappe: Iacobeni, Oiţa, Colacu, Dadu, Dealul Rusului, Tolovanu, Teresia, Sărişor (Figure 22). Beside the main components (Mn, Fe, SiO2), the ore has some P, Co, REE, which were not considered as commodities. In the present, the only Mn mine under operation is Ulm open pit. The extracted reserve is ca. 9.5 Mt at 27.5% Mn and 12.5% Fe. It is estimated that 22 Mt at 24% Mn and 11% Fe are still in the deposits (Vodă, 2002).

The graphite-rich cherts of the Tg2 Formation of the Tulgheş Group also contain barite lenses at Holdiţa, (ca 0.45 Mt at 50% BaSO4) were mined and 0.8 Mt at 0.45% BaSO4 remained (Vodă, 2002).

The Tg3 Formation of the Tulgheş Group from the Bucovinian nappe of the CMZ hosts Kuroko-type VMS deposits related to Ordovician volcanics (mostly rhyolitic) and chlorite schists. The most important metallogenetic fields of this type are (from north to south) Baia Borşa-Burloaia (pyrite, Zn, Pb, Cu, point 3 in Figure 21), Fundul Moldovei (Cu-Zn-Pb, point 4 in Figure 21), Leşul Ursului (Cu-Zn-Pb, point 5 in Figure 21) and Bălan (Cu, point 6 in Figure 21). Bi, Sb, Ag, Au, Ga, V, Co, In, Ba occur in the ore of these deposits as trace elements (Borcoş et al., 1984). Beside pyrite, chalcopyrite, sphalerite and galena, the ore minerals include tetrahedrite, bournonite, arsenopyrite, jamesonite, cassiterite, galenobismuthite, bismuthinite, native bismuth, native gold, native silver (Borcoş et al., 1984). The extracted reserves of polymetllic ore from all VMS deposits of Tulgheş Group considered together is 76 Mt of polymetallic ore at 1.5% Pb, 2.5% Zn and 0.5% Cu and 55 Mt Cu ore at 0.7% Cu. The remaining reserves are 75 Mt ore at 1.64% Zn, 2.7% Zn and 0.44 Cu (Vodă, 2002). Mănăila deposit is the only one of this type still in operation, with 4.6 Mt at 0.97% Cu, 0.32% Pb, 0.68% Zn, 25.8 g/t Ag and 0.23 g/t Au in open pit (Vast Resources, 2020).

The Mesozoic metallogenesis in the CMZ produced the hydrothermal barite deposit at Ostra (exhausted), hydrothermal iron ore (siderite, hematite, barite) at Delniţa and uranium mineralization at Crucea-Botoşana and Tulgheş.

The Triassic Ditrău alkaline intrusive complex generated the magmatic-hydrothermal mineralization at Jolotca and Aurora (point 7 in Figure 21), containing Mo, Zn, Pb, Cu and REE. Jolotca also contains Au, Ag, Bi, Te, Y, Nb, while Aurora contains fluorine. The ore

This project has received funding from the European Union's Horizon 2020 research and innovation programme under grant agreement No 731166

minerals include molybdenite, pyrite, sphalerite, galena, parisite, bastnäsite, monazite and orthite.

The Miocene metallogenetic province is concentrated in the Baia Mare metallogenetic district, in the north-western part of the Miocene-Quaternary volcanic chain of the Eastern Carpathians, where several deposits have been mined since medieval times (ca. 1300), the main mining fields being Ilba, Nistru, Săsar, Herja, Baia Sprie, Şuior and Cavnic.

The ore is of low- to intermediate sulfidation epithermal type (veins, breccia pipes and impregnations), containing base metal ore (Cu-Pb-Zn) with Au-Ag enrichment in the shallow parts of the deposits. The deposits in the Baia Mare district are spatially related to the E-W trending Dragoş Vodă fault system and the associated secondary fractures (Figure 23). The data on the occurrence of the mineralization, commodities and ore mineralogy are based on Borcoş et al. (1984). The resource and grade data are from Kouzmanov et al. (2005).

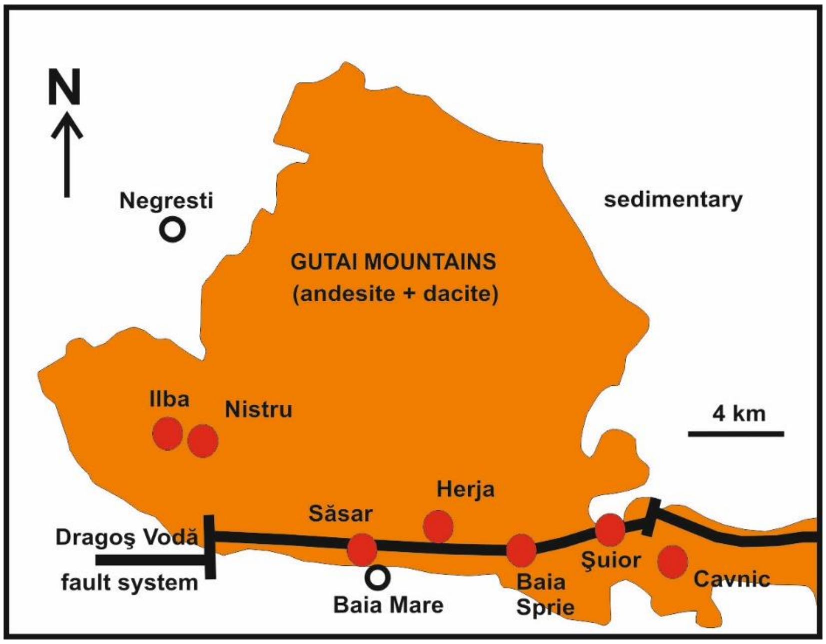

Figure 23. Geographic distribution of the main mining fields in Baia Mare metallogenetic district (area 8 in Figure 21).

The **Ilba** mining field contains veins and impregnations with Pb, Zn and Cu ± Au, Ag as main commodities. As, Mn, Cd, Co, Sb, Bi, Ga ± Te, Se and In occur as trace elements. Ore

This project has received funding from the European Union's Horizon 2020 research and innovation programme under grant agreement No 731166

minerals are pyrite, sphalerite, wurtzite, chalcopyrite, tetrahedrite, hematite, galena, bournonite, pyrrhotite. Resources: 0.3 Mt at 0.6% Cu, 11 g/t Ag, 0.3 g/t Au.

The **Nistru** mining field contains Pb, Zn and Cu ± Au, Ag as main commodities and subordinated As, Mn, Cd, Co, Sb, Bi ± Te, Se, In, Ge. Veins and impregnations. Ore minerals: pyrite, sphalerite, wurtzite, chalcopyrite, galena, tetrahedrite, hematite, magnetite bournonite, pyrrhotite, pyrargyrite. Resources: 1.5 Mt at 1.5% Zn, 0.8% Pb, 28 g/t Ag, 0.6 g/t Au.

The **Săsar** (+ Valea Roşie + Dealul Crucii) mining field consists of vein groups, ramified upward ± passing to breccias. The ore is dominantly Au+Ag, with subordinated Pb, Zn, Cu, Sb. Ore mineralogy: pyrite, sphalerite, galena, native gold, native silver, chalcopyrite, proustite, pyrargyrite, tetrahedrite, jamesonite, acanthite, stibnite, arsenopyrite, marcasite, bournonite, plumosite, stefanite, füllopite. Resources: 0.15 Mt at 3.25% Zn, 1.2% Pb, 18 g/t Ag, 1.5 g/t Au. Dealul Crucii is the type locality of the mineral fulöppite (Pb3Sb8S15).

The **Herja** mining field contains veins of Pb-Zn ore with subordinated Cu, Au, Ag, Sb, Bi, Ga, In, W, Sn, Te, Co, Ni. The ore is made up of sphalerite, pyrite, chalcopyrite, galena, pyrrhotite, arsenopyrite, stibnite, berthierite, semseyite, fizelyite. Resources: 1 Mt at 5.2% Zn, 3.5% Pb, 47 g/t Ag, 0.4 g/t Au. Herja is the type locality of the mineral fizelyite (Pb14Ag5Sb21S48).

The **Baia Sprie** (Felsőbànya, in Hungarian) mining field (Pb, Zn, Cu, Au, Ag) contains veins and impregnations. Subordinated elements: As, Cd, Sb, Bi, Ga, Tl, Co, W.The Principal vein is 5,250 m long, more than 1,000 m in depth, and up to 22 m thick (Lang, 1979; Grancea et al., 2002). Ore mineralogy includes more than 70 species, among which the most widespread are pyrite, chalcopyrite, sphalerite, galena, hematite, magnetite, pyrrhotite, wolframite, scheelite, tetrahedrite and stibnite. Resources: 4.3 Mt at 1.2% Zn, 1.0% Pb, 0.6 % Cu, 29 g/t Ag, 0.4 g/t Au.

Baia Sprie is type locality for the minerals andorite PbAgSb3S6, dietrichite (Zn,Fe2+,Mn)Al2(SO4)4·22(H2O), felsőbànyaite Al4(SO4)(OH)10·5(H2O), klebelsbergite Sb3+4O4(OH)2(SO4), monsmedite H8K2Tl2(SO4)8·11(H2O), semseyite Pb9Sb8S21 and szmikite MnSO4·(H2O).

The **Şuior** mining field contains Au, Ag, Pb, Zn and Cu, with subordinated As, Sb, Cd, Ga. Breccia pile with sulfide impregnations at shallow levels, veins of sulfide ore at depth. Ore mineral assemblages include pyrite, sphalerite, wurtzite, arsenopyrite, chalcopyrite,

This project has received funding from the European Union's Horizon 2020 research and innovation programme under grant agreement No 731166

tetrahedrite, galena, boulangerite, marcasite, native gold, native silver. Resources: 9.3 Mt at 2.3% Zn, 1.4% Pb, 36 g/t Ag, 3 g/t Au.

Cavnic mining field (Pb, Zn, Cu, Au, Ag). Other commodities: As, Sb, Cd, Ga, Bi, In, Ga, Tl, Ge, Se, Te. Sulfide veins and impregnations. Ore minerals: pyrite, galena, sphalerite, chalcopyrite, tetrahedrite, hematite goethite, native gold, bournonite, stibnite realgar, orpiment, cinnabar. Resources: 5.9 Mt at 2% Zn, 1.5% Pb, 27 g/t Ag, 0.4 g/t Au.

Cavnic is the type locality of rhodochrosite (MnCO3).

3.4.4 Carpathian-Balkan zone

The Carpathian-Balkan Zone comprises the Apuseni Mountains, the Southern Carpathians and the Balkans (with the Srednogorie Zone). The most prominent metallogenetic province in this zone is the Banatite Magmatic and Metallogenetic Belt (BMMB), also named as the Apuseni-Banat-Timok-Srednogorie (ABTS) Belt, which extends > 1,500 km in length and 30 km to 70 km in width (Figure 24). The metallogenesis of the BMMB is related to Late Cretaceous intrusions (mostly diorite, granodiorite and granite) associated, most probably, with the closure of Vardar Ocean (e.g., Ciobanu et al., 2002; Sutphin et al., 2013). The ore deposits in the BMMB are mostly of metasomatic (skarn), porphyry copper and epithermal types (± VMS features). According to Cook et al. (2009), "the BMMB has a pronounced Bi-Te signature, recognizable in styles of mineralization ranging from skarns to porphyry and epithermal types." The geographic distribution of all types of ore deposits in the BMMB is given in Ciobanu et al. (2002), (Figure 24).

The skarn-type deposits with (past) mining activity are **Băişoara** – Fe+Zn+Pb+B, **Băiţa Bihor** – Cu+Mo+Zn+Pb+Au+Bi+W+B, (Apuseni Mountains), **Ruschiţa** – Zn+Pb, **Ocna de Fier** – Fe+Cu+Zn+Pb+B, **Dognecea** – Zn+Pb+Cu+Ag, **Oraviţa-Ciclova** – Cu+Zn+Pb+Au+Mo+W, **Sasca Montană** – Cu+Zn+Pb+Au+Mo and **Moldova Nouă** – Cu+Au+Mo (in Banat, Southern Carpathians), **Krumovo** – Fe; Burdtzeto – Fe+Cu, **Propada** – Cu+Fe, **Mladenovo** – Cu+Fe and **Velikovets** - Fe (eastern Srednogorie). Out of these, only **Băiţa Bihor** is still in operation, the other ones being closed before the year 2000.

Băiţa Bihor contains many orebodies with varied commodities: Cu, Pb, Zn, Mo, Bi, W, B, Au, Ag but also with trace amount of Cd, Ni, Co and Te (Borcoş et al., 1984). It has reserves of ca 3 Mt at 0.56% Cu, 1% Zn, 0.46% Pb, 0.09% Mo and 0.064% Bi (Ciobanu et al., 2002).

This project has received funding from the European Union's Horizon 2020 research and innovation programme under grant agreement No 731166

Ore minerals include chalcopyrite, sphalerite, galena, bornite, molybdenite, scheelite, ludwigite, szaibelyite, kotoite, fluoborite; the Bi signature is proven by the occurrence of bismuthinite, native Bi, wittichenite, emplectite, cosalite, lillianite, hodrushite, aikinite (Borcoş et al., 1984; Tămaş and Andrii, 2020).

Several skarn prospects, such as **Tincova** – Fe+Zn+Pb+Bi+W (Romania) and **Kučajna** – Zn+Pb+Cu+Ag (Serbia), were indicated by Ciobanu et al. (2002)..

Sutphin et al. (2013) mentioned 15 porphyry copper deposits in the BMMB: Moldova Nouă (Romania), Majdanpek, Bor, Borska Reka, Veliki Krivelj, Cerovo, Dumitru Potok, Valja Strz (Serbia), Elatsite, Assarel, Medet, Vlaykov Vruh, Karlievo, Tsar Assen and Prohorovo (Bulgaria) and a further 10 prospects. The largest porphyry copper deposits in the BMMB are (data from Sutphin et al., 2013): **Moldova Nouă** – 500 Mt at 0.35% Cu (Banat), **Majdanpek** – 1,000 Mt at 0.6% Cu, 0.005% Mo, 0.35 g/t Au, 1 g/t Ag, and Bor (with Borska Reka and Veliki Krivelj) – 2,141 Mt at 0.64% Cu, 0.002% Mo, 0.24 g/t Au, 0.5 g/t Ag (Timok); **Elatsite** – 350 Mt at 0.39% Cu, 0.26 g/t Au, 0.2 g/t Ag and **Assarel** (with Orlovo Gnezdo) – 390 Mt at 0.43% Cu and 0.19 g/t Au (Panagyurishte District of the central Srednogorie zone).

Among the epithermal deposits, the largest is **Chelopech** (in operation) – 60 Mt at 1.24% Cu and 3.38 g/t Au, followed by **Radka** (closed) Cu+Au (10 Mt) and **Elshitsa** (closed) – Cu+Au+Ag (ca. 10 Mt at 1.03% Cu), all in the Panagyurishte District of the central Srednogorie zone (data from Ciobanu et al., 2002).

The SEDEX-type deposit **Kremikovtsi** (Srednogorie zone, Bulgaria) contains Fe-Mn ore and barite (Ciobanu et al., 2002; Mladenova et al., 2004).

Another metallogenetic province with large-scale deposits is the Miocene (14-7 Ma) magmatic province in the southern part of the **Apuseni Mountains** (Metaliferi Mountains). The ore is related to the volcanic and intrusive rocks emplaced along transtensional fractures generated by the rotation of the Tisza block (Roşu et al., 2004). The ore deposits are distributed along four main NW-SE-trending alignments: (1) Brad-Săcărâmb, (2) Almaş-Stănija, (3) Roşia Montană-Bucium and (4) Baia de Arieş. An additional metallogenetic area related to this province occurs south of the Golden Quadrilateral, including Deva porphyry copper deposit. The mineralization occurs in veins (Au-Ag±Te and base metal), epithermal breccia pipes and replacement bodies, and in

This project has received funding from the European Union's Horizon 2020 research and innovation programme under grant agreement No 731166

subjacent porphyry Cu-type systems within an area of ca. 900 km2 known as the Golden Quadrilateral (Figure 24).

Most epithermal deposits (e.g., Baia de Arieş, Larga, Haneş, Almaşu Mare, Bucium, Musariu, Brădişor, Ruda-Barza, Băiţa-Crăciuneşti, Săcărâmb) are closed. A Te-Bi signature was remarked for Musariu (Ciobanu et al., 2004). Among the epithermal deposits in the Golden Quadrilateral, resources were estimated for **Roşia Montană**, with 400.4 Mt at 1.3 g/t Au, 6 g/t Ag, **Rodu-Frasin**, with 35.2 Mt at 1.12 g/t Au and 3 g/t Ag, and **Certej**, with 61.1 Mt at 1.79 g/t Au and 10 g/t Ag (Kouzmanov et al., 2005).

The porphyry copper deposits in the Metaliferi Mountains are classified as: Cu-Mo(-Au) (Deva, Roşia Poieni), Cu-Au (Valea Morii, Bolcana, Rovina, Voia, Tălagiu, Larga, Trâmpoiele, Valea Tisei, Bucium-Tarniţa) and Au-Cu (Colnic, Cireşata). The largest deposits are **Roşia Poieni** (in operation), with 431 Mt at 0.55% Cu and 0.25 g/t Au; **Rovina Valley Group** (Rovina, Colnic and Cireşata intrusions), with 396 Mt at 0.16% Cu and 0.55 g/t Au (EUROSUN, 2020); **Bucium-Tarniţa**, with 335 Mt at 0.50% Cu and 0.36 g/t Au; **Tălagiu**, with 150 Mt at 0.35% Cu and 0.60 g/t Au; **Bolcana** (with Măgura), with 90 Mt at 0.30% Cu and 0.03 g/t Au; **Deva**, with 20 Mt at 0.70% Cu and 0.5 g/t Au. Data from Sutphin et al. (2013), except for Rovina Valley Group.

This project has received funding from the European Union's Horizon 2020 research and innovation programme under grant agreement No 731166

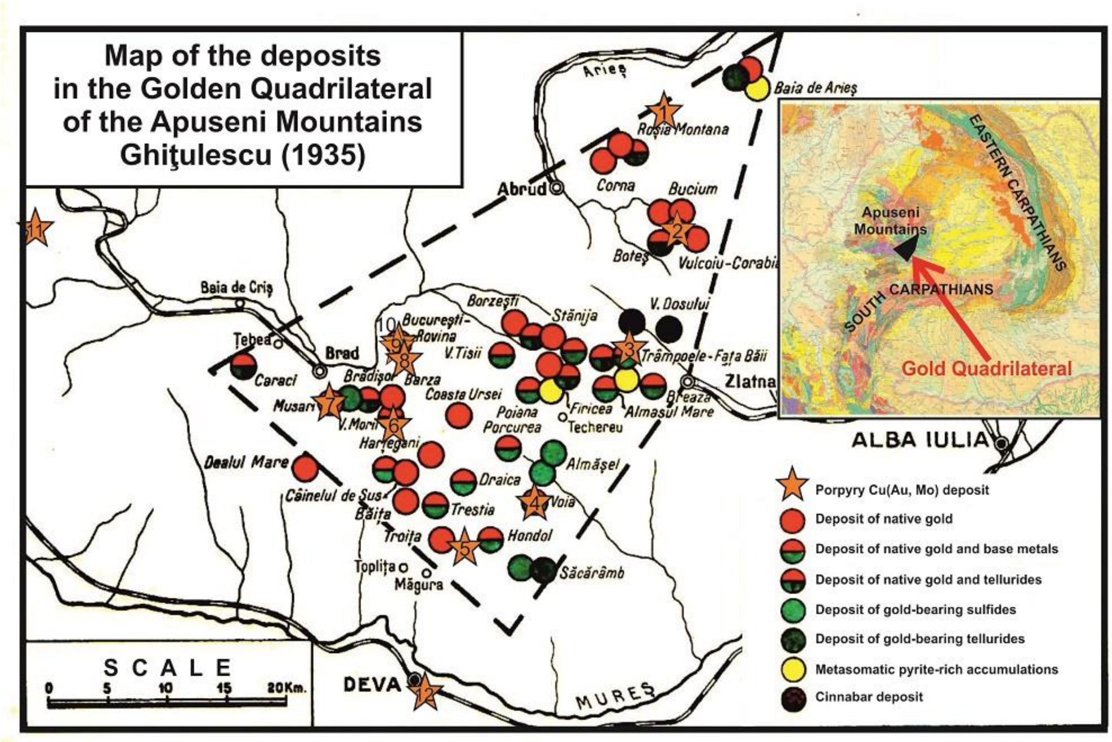

Figure 24. Spatial distribution of the ore deposits in the Golden Quadrilateral of the Apuseni Mountains. Porphyry-Cu deposits: 1-Roşia Poieni; 2-Bucium-Tarniţa; 4-Voia; 5-Bolcana; 6-Valea Arsului; 7-Musariu; 8-Cireşata; 9-Colnic; 10-Rovina; 11- Tălagiu; 12-Deva. Out of the epithermal deposits in the Apuseni Mountains, **Zlatna** is type locality of native tellurium, **Baia de Arieş** is type locality of the minerals sylvanite $(Au,Ag)_2Te_4$, while **Săcărâmb** is type locality of krautite - $MnAs^{+5}O_3(OH)_2\cdot(H_2O)$, krennerite - $AuTe_2$, muthmannite - $AgAuTe_2$, nagyagite - $AuPb(Sb,Bi)Te_{2\text{-}3}S_6$, petzite - Ag_3AuTe_2, stutzite - $Ag_{5\text{-}x}Te_3$,(x=0.24-0.36) tellurite - TeO_2.

Some shear zone type Au deposits occur in the Variscan successions from the central and western part of the Balkan Mountains (Bulgaria and Serbia). Although none of these deposits is in operation, it is of note the ore mineral assemblage, including W, Sb and Bi minerals: scheelite, tetrahedrite, boulangerite, bournonite, pyrargyrite, proustite, owyheeite, native Bi, bismuthinite, pekoite, aikinite, friedrichite and Co-rich pyrite (Mladenova et al., 2004).

The Southern Carpathian also contain occurrences and deposits of graphite, beryllium, lithium and Co-Ni (+ Cu) sulfides.

Graphite (flakes) occurs in Parâng and Căpăţânii Mountains and was mined at Negovanu-Olteţ, Ungurelaş, Râbari-Olteţ and Cătălinu-Galbenu, in the regionally metamorphosed

This project has received funding from the European Union's Horizon 2020 research and innovation programme under grant agreement No 731166

rocks of the Danubian realm, in a graphite-carbonate formation. All the grafite mines in the Southern Carpathians are closed.

Beryl occurs in pegmatites of metamorphic segregation in the Getic Nappe, more abundant at Teregova (Semenic Mts), Piatra Albă-Goaţa and Conţu (Lotru Mts), Vidruţa and Despina (Latoriţa Mts.).

Lithium (spodumene, lepidolite) is known in pegmatites of metamorphic segregation in the Getic Nappe, at Conţu (Lotru Mts.).

Occurrences of **cobalt**-containing mineralization are known in the South Carpathians at Valea Vâlsanului-Brădet, Tiţianu-Dealul Negru and Urdele, as magmatic Ni-Cu-Co sulfide concentrations in the Proterozoic basement, and at Valea lui Neguleţ and Bădeanca-Dăniş (Leaota Mts.), as five elements vein type ore. Ore mineralogy includes pyrite, maucherite, nickeline, smaltite-safflorite, tetrahedrite, chalcopyrite, sphalerite, galena.

3.4.5 Serbo-Macedonian metallogenic zone

The geology of Serbo-Macedonian zone (SMZ) has potential to host several different type of deposits Among the Non-Energy Metallic Minerals, base and precious metals, in particular zinc, lead, copper, gold, and silver are becoming an increasingly important and rapidly growing target for the mining industry. For example, in the north-eastern part of Greece, where most of the potential resources and feasible deposits are hosted, polymetallic gold deposits occur in a wide range of genetic types, comprising magmatic porphyry copper type deposits, hypothermal/mesothermal manto-type polymetallic sulphides and epithermal gold systems.

The SMZ is part of the Carpathian-Balkan or the Hellenic-Balkan belt, which was formed along the southern margin of the Eurasian plate during Mesozoic-Cenozoic time. Structural data has indicated that the Rhodope and Serbo-Macedonian zones or massifs (Jones et. al. 1992; Dinter and Royden, 1993) are products of Alpine convergence between Africa and Europe during Cretaceous to Tertiary time, which led to the formation of a metamorphic core complex and silicic to intermediate magmatism (Burchfiel, 1980; Ivanov, 1989; Burg et al., 1990, 1995, 1996; Jones et al., 1992; Ricou et al., 1998; Lips et al., 2000).

In the Rhodope zone, Alpine convergence resulted in a north-dipping subduction zone, which gave rise to Late Cretaceous calc-alkaline magmatism with related porphyry Cu-Au and high sulphidation epithermal Au-Cu mineralization in the Srednogorie zone in

This project has received funding from the European Union's Horizon 2020 research and innovation programme under grant agreement No 731166

Bulgaria (Moritz et al., 2003; Von Quadt et al., 2003). During the Tertiary, plate convergence moved southward. Throughout the Rhodope zone, the latest stages of extension are indicated by the development of late Eocene to Oligocene sedimentary basins followed up by late Eocene to Oligocene – early Miocene calc-alkaline to shoshonitic volcanic-plutonic suites. The resulting arc extends across the Greek-Bulgarian border and hosts epithermal gold systems of high exploration and exploitation potential. The deposits were formed during the post-collisional orogenic collapse and related crustal extension (Marchev P. et al., 2005).

In regional scale three metallogenetic zones of the Hellenic-Balkan belt (Arvanitidis et al, 2015) are evolved (Figure 25):

Sredna Gora metallogenetic zone with porphyry copper and epithermal gold deposits related to Late Cretaceous magmatic activity. **Rhodope** metallogenetic zone with epithermal gold deposits and porphyry copper molybdenum deposits related to Tertiary magmatic activity , and **Serbo-Macedonian** metallogenetic zone with porphyry copper – gold deposits and carbonate-replacement manto Pb-Zn-Ag-Au deposits related to Tertiary magmatic activity (Arvanitidis, 1993, 2010; Arvanitidis et al, 2012, Arvanitidis et al, 2015) (Figure26). Minable carbonate-replacement polymineralic ore deposits are the Olympias deposit in Halkidiki, northern Greece, and the Lece, Trepca, Sasa and Zletovo deposits in Serbia. Potential porphyry Cu-Au ore deposits of particular importance are the Skouries deposits in Halkidiki, northern Greece, Bukovik-Kadiica and Bucim in North Macedonia and Bor in Serbia.

Eastern Halkidiki peninsula (SMZ)

The eastern part of Halkidiki peninsula in northern hosts mineral system that are typical for the of Serbo-Macedonian metallogenic zone. The SMZ geology in that area consists of gneisses, mica schists, amphibolites and marbles that are part of two major lithostratigraphic units of Paleozoic age, known as the Kerdylia and Vertiskos formations (Figure 26). The Olympias, Madem Lakkos and Mavres Petres carbonate-replacement manto-type polymetallic sulphide deposits belong geotectonically to the Kerdylia formation whereas the Skouries porphyry copper-gold deposit is part of the Vertiskos formation. The Kerdylia formation to the east comprises biotite gneiss interbedded with hornblende gneiss, amphibolite and marble, probably derived from an original volcano-sedimentary sequence (Kockel et al., 1971). The Vertiskos formation to the west overlying the Kerdylia formation consists mainly of two-mica gneiss, in places containing garnet-, tourmaline- and sillimanite-bearing quartz-feldspar gneiss and ortho-amphibolite. Metamorphosed mafic and ultramafic rocks occur frequently near the contact with the

This project has received funding from the European Union's Horizon 2020 research and innovation programme under grant agreement No 731166

Kerdylia formation. Rare marbles are considered to be tectonically emplaced slices of Mesozoic carbonate rocks (Arvanitidis, 1993). The contact between the Kerdylia and Vertiskos formations is partly gradational, but largely deformed and displaced by the major Stratoni-Varvara fault zone.

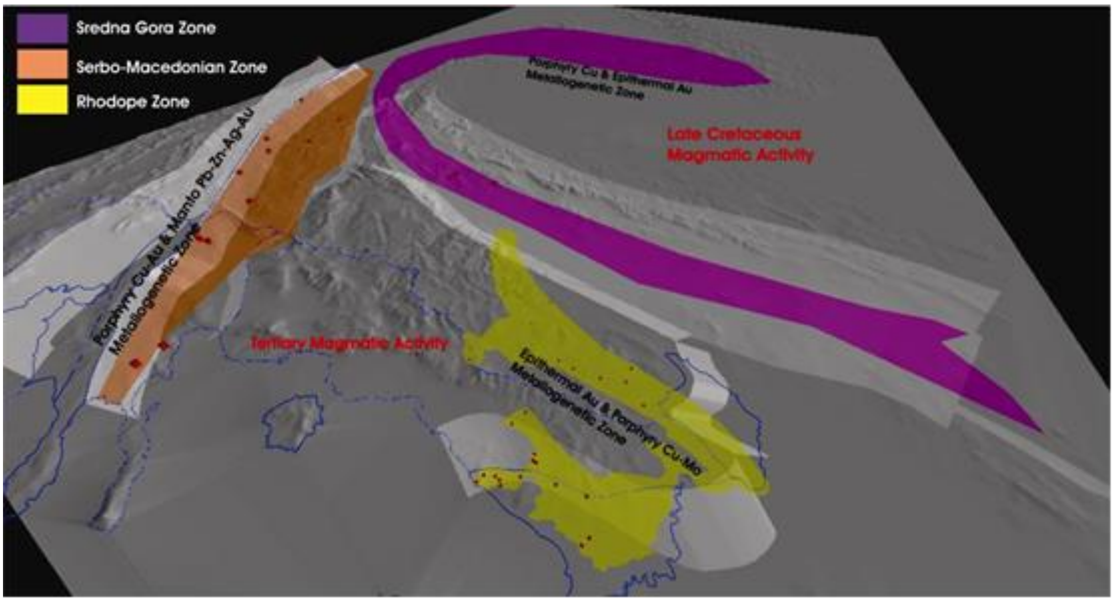

Figure 25. Major mineral systems related to SMZ, Rhodope and Sredna Gora zones (Source: X-mine project)

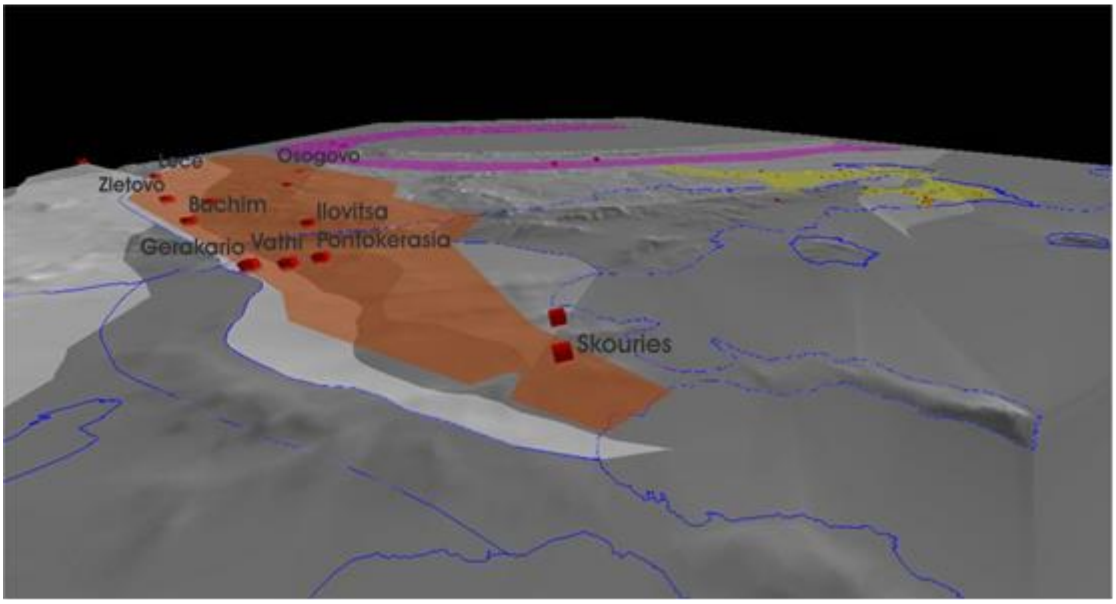

This project has received funding from the European Union's Horizon 2020 research and innovation programme under grant agreement No 731166

Figure 26. Major porphyry Cu-Au deposits in the Serbo-Macedonian zone (Source: X-mine project)

The Olympias deposit is a polymetallic (Pb, Zn, Ag, Au) massive sulphide carbonate-replacement ore body hosted by Kerdylia marbles (Kalogeropoulos et al, 1989). The depositional mechanism and structural setting of the ore bodies are genetically related to fault-controlled mineralizing fluids ascending and interacting with reactive carbonate rocks interbedded within crystalline basement of the Kerdylia formation. Two main deposits have been identified, the West and East deposits. The structure of the deposit and the fault-controlled setting of the orebodies show clearly the stratabound replacement mantos at the contact and inside the marbles. A deeper-seated extension of the west ore body is indicated and makes a potential target to further underground surveys and exploration drilling.

This project has received funding from the European Union's Horizon 2020 research and innovation programme under grant agreement No 731166

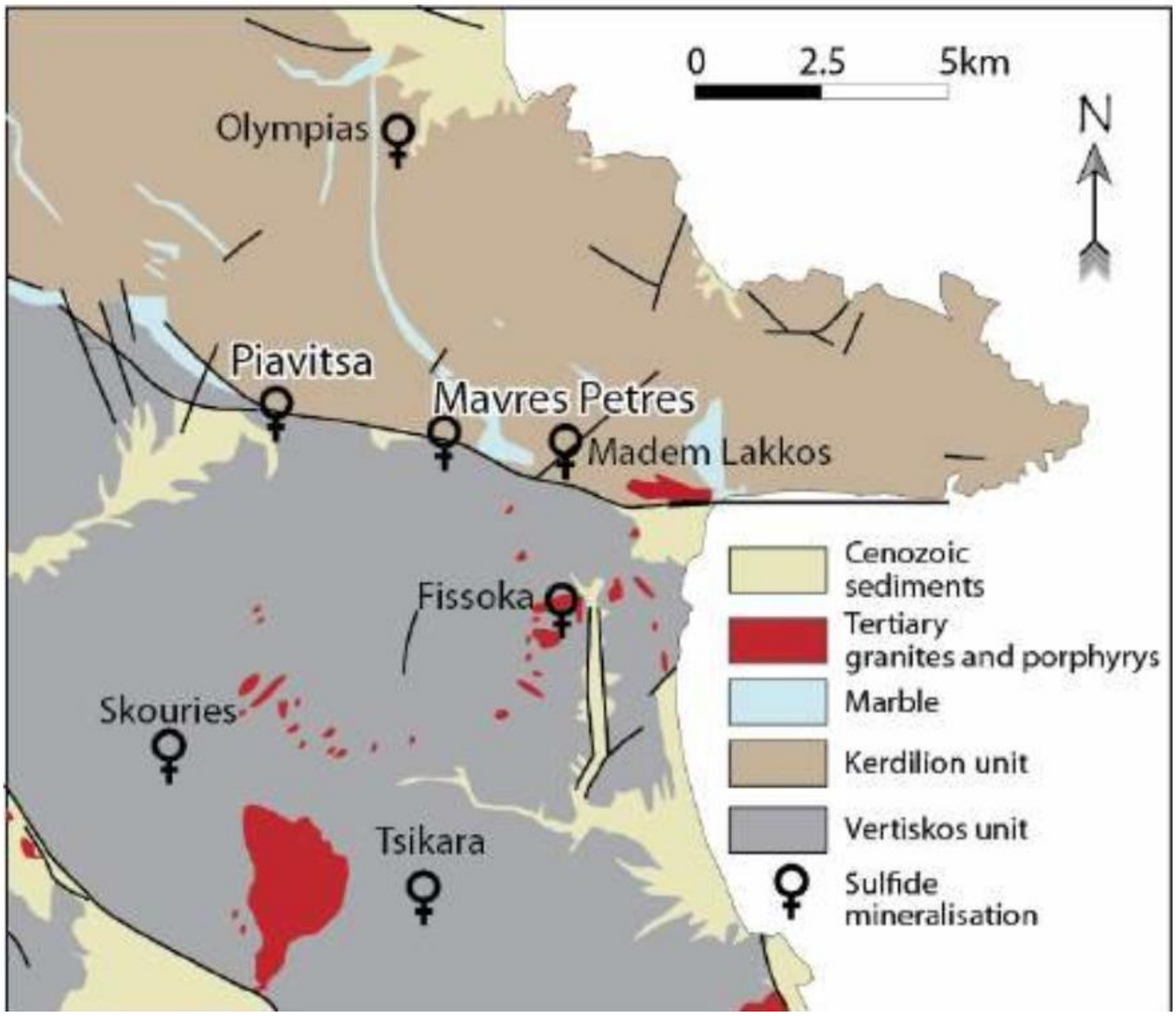

Figure 27. Simplified geological map of the Kassandra mining district. Cu-Au porphyry deposits occur at Skouries, Fisoka and Tsikara, while manto-type carbonate replacement deposits are represented by the Ag-Pb-Zn mineralizations at Mavres Petres, Madem Lakkos, the Au-Ag-Pb-Zn Olympias deposit and the Piavitsa prospect, which is also associated with Au-rich veins.

Madem Lakkos and Mavres Petres are, like Olympias massive stratabound replacement deposits hosted by Kerdylia formation marbles and developed along cross-cutting fault zones. The geological setting comprises also the major Stratoni-Varvara thrust fault bringing the Kerdylia marble interbedded, biotite gneiss and Vertiskos amphibolite in contact tectonically. The E-W trending Stratoni-Varvara fault also displays a semi-regional control on the extension of the polymetallic mineralization and the location of the Madem Lakkos, Mavres Petres, Piavitsa and Varvara ore deposits.

This project has received funding from the European Union's Horizon 2020 research and innovation programme under grant agreement No 731166

The Skouries ore deposit (Eliopoulos et al, 1991) is part of the NW trending SMZ porphyry copper belt (Figure 27) extending through North Macedonia to Serbia and Romania. The Skouries porphyry intrusion consists of a series of rhyodacitic, dioritic to andesitic dykes and stocks emplaced into Vertiskos amphibolitic basement rocks in association with ultrabasic lithologies. It forms a pipe-like, mineralized subvolcanic body with surface dimensions of 180 m N-S and 200 m E-W and a vertical extent of at least 700 m (Frei, 1995).

Western Thrace (Rhodope zone)

The Rhodope zone (Figure25) in Thrace comprises complex metamorphic rocks of inferred Paleozoic age, such as gneisses and amphibolites, structurally overlain by lower grade metamorphic sequences belonging to the Mesozoic Circum-Rhodope zone. This zone consists of metasedimentary and meta-volcanosedimentary series (Pomoni and Papadopoulos, 1986). The underlying metasedimentary series comprises carbonate rocks (calc-schist, marble, dolomitic marble) and the overlying meta-volcanosedimentary series consists predominantly of greenschists (chlorite-epidote-talc-actinolite bearing). The Circum Rhodope zone has been folded, metamorphosed and thrusted onto Rhodope metamorphic basement during Alpine orogenesis in late Cretaceous time.

The epithermal gold deposits in the Thrace region are related to the post-collisional extension during late Eocene–Oligocene. A number of structurally controlled rift-basins along the southern and eastern margins of the Rhodope zone were formed during this crustal extension. The basins are characterized by deposition of Early Eocene sediments (molasses, limestones) followed by late-Eocene–early Oligocene volcanosedimentary series with calc-alkaline to shoshonitic volcanic rocks (Innocenti et.al., 1984; Fitikas et al., 1980) (Figure 28). The Saint Demetrios and Perama Hill deposits are related to Oligocene volcanic arc magmatism. This arc extends across the Greek-Bulgarian border hosting epithermal systems of high exploration and exploitation potential.

This project has received funding from the European Union's Horizon 2020 research and innovation programme under grant agreement No 731166

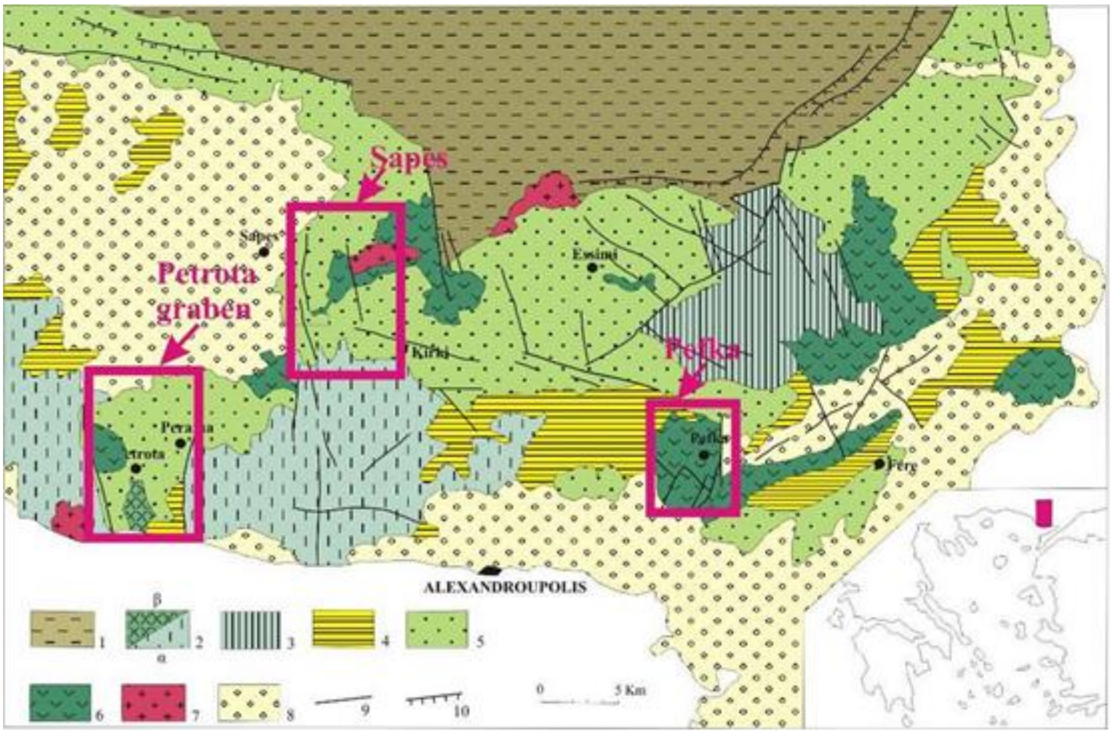

Figure 28. Geological sketch map of Western Thrace (Papadopoulos P. modified by Michael C.). 1) Rhodopean basement, 2) Circum-Rhodope zone – Makri unit (upper Triassic – upper Jurassic age), Phyllite series, Mafic rocks (gabbro-diorites), 3) Circum-Rhodope zone - Melia unit (Lower Cretaceous–upper Cretaceous age), Flysch - ophiolite, 4) Eocene sedimentary deposits, 5) Eocene – Oligocene volcano-sedimentary deposits, 6) Oligocene volcanics, 7) Oligocene intrusive rocks, 8) Neogene and Quaternary sediments, 9) Faults, 10) Overthrust.

The Perama Hill epithermal gold deposit is located in the eastern part of the Petrota graben (Figure 28) consisting of subaqueous pyroxene andesitic flows, debris-flows and hyaloclastites, resting on turbiditic series (Lescuyer et. al., 2003). The Perama sandstones, which host the gold mineralization, are coeval with subaerial felsic eruption in the western part of the graben constituting pyroclastic flows, accretionary lapilli tuff, quartz porphyry domes and dacite flows (Lescuyer et. al., 2003). The metamorphic basement close to the deposit is part of the Circum Rhodope zone (Mesozoic age) and consists of greenschists and calcschists. Silicified fracture zones and hydrothermal breccias occur at the contact between Mesozoic greenschists-calcschists and Perama sandstones. Silicification and advanced argillic alteration (kaolinite-illite) are the main alteration styles of the epithermal gold mineralization in Perama Hill.

This project has received funding from the European Union's Horizon 2020 research and innovation programme under grant agreement No 731166

The Sapes/Aghios Demetrios epithermal gold deposit comprises strongly altered andesitic agglomerates, tuffs, lavas and volcanic breccias. The paragenetic distribution of the mineral assemblages distinguishes four main and two overlapping alteration zones in the area (Michael et al., 1989; Michael, 1995; Michael, 2005; Velinov et al., 1999). The main alteration zones are: Silicification (hydrothermal eruption vent breccias), advanced argillic alteration (subzones of alunite, diaspore, argillic alteration and pyrophyllite), propylitic alteration, potassic alteration (southern part of the Tertiary basin). The overlapping alteration zones are: sericitic alteration (Aghios Demetrios deposit) and adularia-rich alteration (southern part of the Tertiary basin). The hydrothermal eruption vent breccias are the favourable structural setting for the gold mineralization in the Aghios Demetrios deposit. The younger north-eastern faults caused displacement of the wall rocks.

In general, the SMZ metallogenic zone, is part of the southernmost part of the Carpathian-Balkan metallogenetic belt, which is very often named as Hellenic-Balkan belt. As mentioned, the Carpathian-Balkan metallogenetic belt was formed along the southern margin of the Eurasian plate during Mesozoic-Cenozoic time. Three metallogenetic zones are found in the Hellenic-Balkan belt (Figure 29):

1) The Sredna Gora metallogenetic zone with porphyry copper and epithermal gold deposits related to Late Cretaceous magmatic activity,

2) the Rhodope metallogenetic zone with epithermal gold deposits and porphyry copper-molybdenum deposits related to Tertiary magmatic activity and

3) the Serbo-Macedonian metallogenetic zone with porphyry copper – gold and manto Pb-Zn-Ag-Au deposits related to Tertiary magmatic activity.

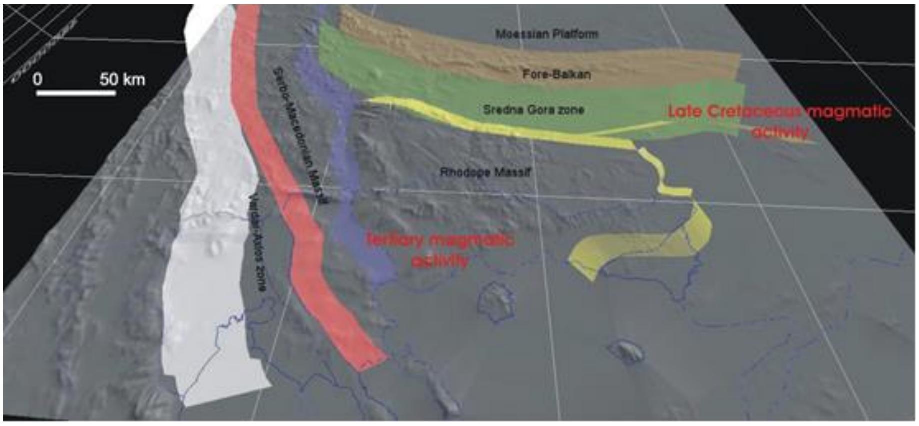

This project has received funding from the European Union's Horizon 2020 research and innovation programme under grant agreement No 731166

GeoERA RAW MATERIALS

Figure 29. Hellenic-Balkan belt metallogenic zones dated from Late Cretaceous to Neogene. (Source: X-mine project)

This project has received funding from the European Union's Horizon 2020 research and innovation programme under grant agreement No 731166

4 Metallogenic map based on CRM commodities on land

4.1 Rare Earth elements

4.1.1 Introduction

The demand for rare earth elements (REE) has grown enormously in recent times as they are essential for many new technologies. World mine production based on mineral commodity summaries 2020 (UGSS, 2020) is 190 000 and 210 000 tons in 2018 and 2019, respectively. The total reserves are reported to about 120 000 000 tons. World resources of REE are relatively abundant in the Earth's crust, but mineable concentrations are less common than for most other ores. (Table 1, Figure 30)

Table 1. World Mine Production and Reserves: Reserves for Canada, Greenland, Tanzania, and South Africa were previously included with "Other countries." (source USGS, 2020)

	2018	2019	
United States	18,000	26,000	1,400,000
Australia	21,000	21,000	3,300,000
Brazil	1,100	1,000	22,000,000
Burma (Myanmar)	19,000	22,000	NA
Burundi	630	600	NA
Canada	—	—	830,000
China	[10]120,000	[10]132,000	44,000,000
Greenland	—	—	1,500,000
India	2,900	3,000	6,900,000
Madagascar	2,000	2,000	NA
Russia	2,700	2,700	12,000,000
South Africa	—	—	790,000
Tanzania	—	—	890,000
Thailand	1,000	1,800	NA
Vietnam	920	900	22,000,000
Other countries	60	—	310,000
World total (rounded)	190,000	210,000	120,000,000

Based on Figure 30, China owns 38 percent of the world's reserves; Vietnam, Brazil, Russia, and India have substantial deposits. Europe, including Greenland, has a high potential of voluminous deposits but most of them are not sufficiently advanced that reserves can be reported. Still, presently over 63 % of the REE used globally are produced in China.

This project has received funding from the European Union's Horizon 2020 research and innovation programme under grant agreement No 731166

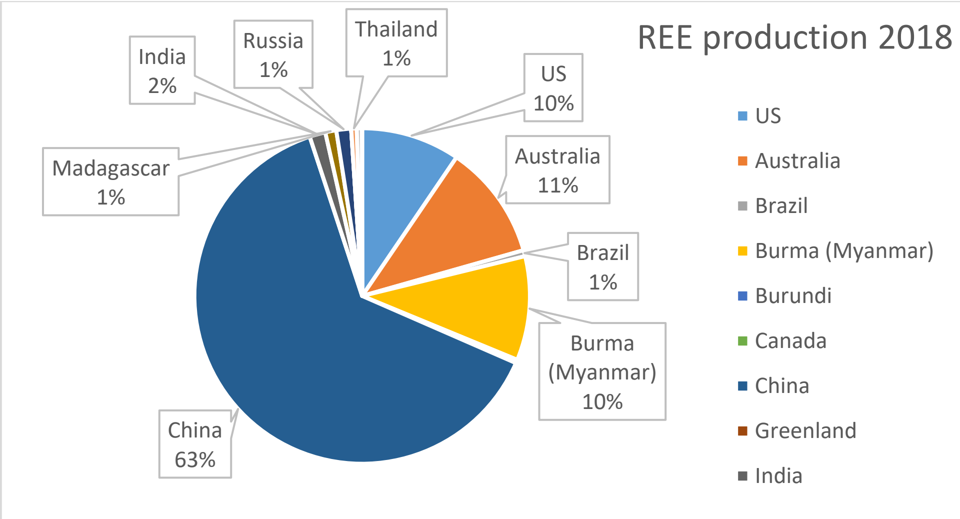

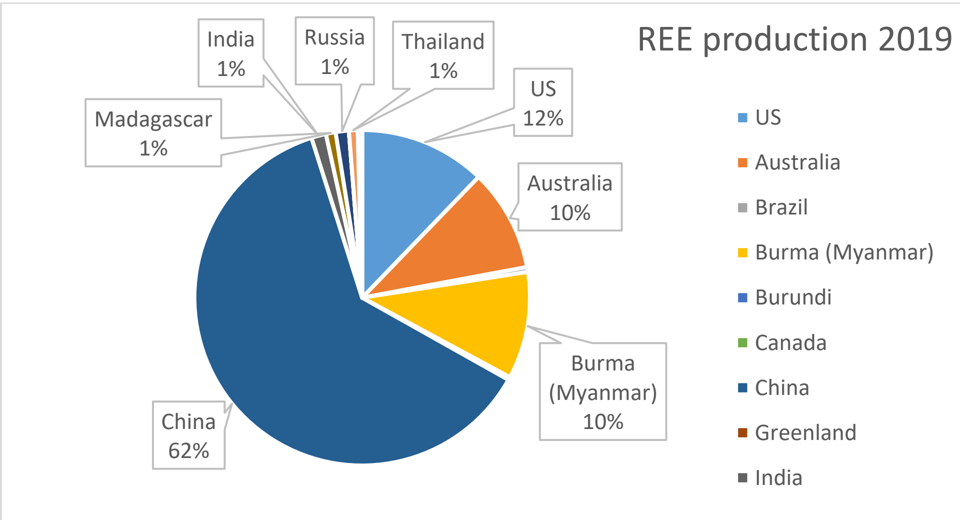

This project has received funding from the European Union's Horizon 2020
research and innovation programme under grant agreement No 731166

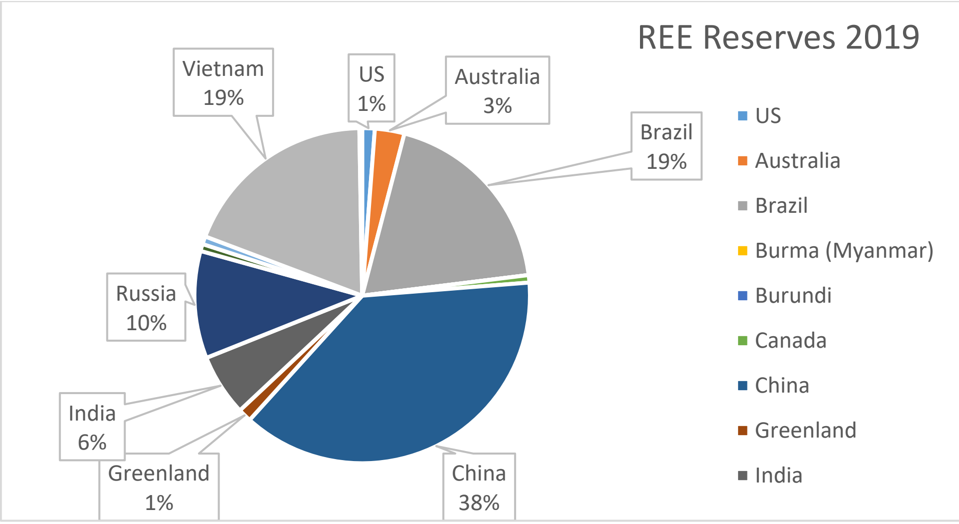

Figure 30. Rare earth element world production by country for the year 2018, 2019 and Reserves. Data Source USGS (2020).

There are many different types of REE mineral deposits/occurrences in Europe; these have been found in a variety of geological environments and are of a wide range of ages. However, REE occurrences can be fundamentally divided into primary and secondary types. Most of the primary types are related to igneous processes in continental rift/extensional settings. The secondary types are formed when enrichments develop through sedimentary processes such as erosion and accumulation of heavy minerals, weathering and soil development.

The aim of this part of the report is to give an overall and general view of REE deposit distribution in Europe and briefly present the metallogenic area on REE and this version of the metallogenic area is a revised version on what Goodenough et al. (2016) are presented. The classification on REE will be based on genetic classification

4.1.2 REE mineralization types in Europe

There are many different types of REE mineral deposits in Europe, including both Light Rare Earth Elements (LREE) and Heavy Rare Earth Elements (HREE) (Goodenough et al., 2016). Sweden hosts a large number of known REE occurrences and numerous REE-bearing minerals were originally discovered in Swedish mines and deposits, including Bastnäs and Ytterby in the Bergslagen province (Figure 31) (e.g. Jonsson 2014; Sadeghi,

This project has received funding from the European Union's Horizon 2020 research and innovation programme under grant agreement No 731166

2019; Sadeghi et al., 2020c). Greenland is endowed with several large REE mineral deposits, in various geological settings. The largest deposits are hosted by peralkaline intrusions related to the Gardar Province in South Greenland, encompassing the deposits at Kvanefjeld, Kringlerne, and Motzfeldt Sø. REE mineral deposits are also associated with carbonatites at the margins of the North Atlantic Craton in west Greenland. (Sørensen et al. 2011). Finland hosts a few sub-economic to economic REE deposits mostly associated with intrusions of alkaline rocks (e.g. Sokli carbonatite and Iivaara ijolite complexes). (Sarapää et al. 2013), located in the central part of Fennoscandian shield. Norway hosts a variety of REE mineral occurrences, including primary and secondary deposits, typically associated with alkaline igneous and carbonatite magmatic systems (e.g. Fen, Kodal, and others) (Andersen 1986, Ihlen et al. 2014). In southern and central Europe, the extensional and rift systems are less deeply eroded, and potential REE deposits are likely to be buried. Carbonatites in Mesozoic to Cenozoic rifts of Central Europe may well be prospective for REE, whilst secondary deposits associated with alkaline magmatism are of interest in the Mediterranean countries. (Figure 31). A prospectivity map realized by Bertrand et al. (2017) for REE, using the DBQ (DataBase Querying) method shows favourable prospective areas in Europe (Figure 32). As alkaline/peralkaline intrusions is by far the most enriched metallogenic family, this prospectivity map closely mimics their spatial distribution in Europe, highlighting potentially favourable areas, such as the Svidnya-Seslavtsi region in Bulgaria, for instance. In addition, it shows favourable areas related to other metallogenic families, such as IOCG deposits in the northern Svecofennian belt (northern Sweden), placers in French Britany and Normandy, pegmatites in southern Austria or the Iberian massif (northern Portugal), or numerous bauxite occurrences in the Delfi region (Greece).

This project has received funding from the European Union's Horizon 2020 research and innovation programme under grant agreement No 731166

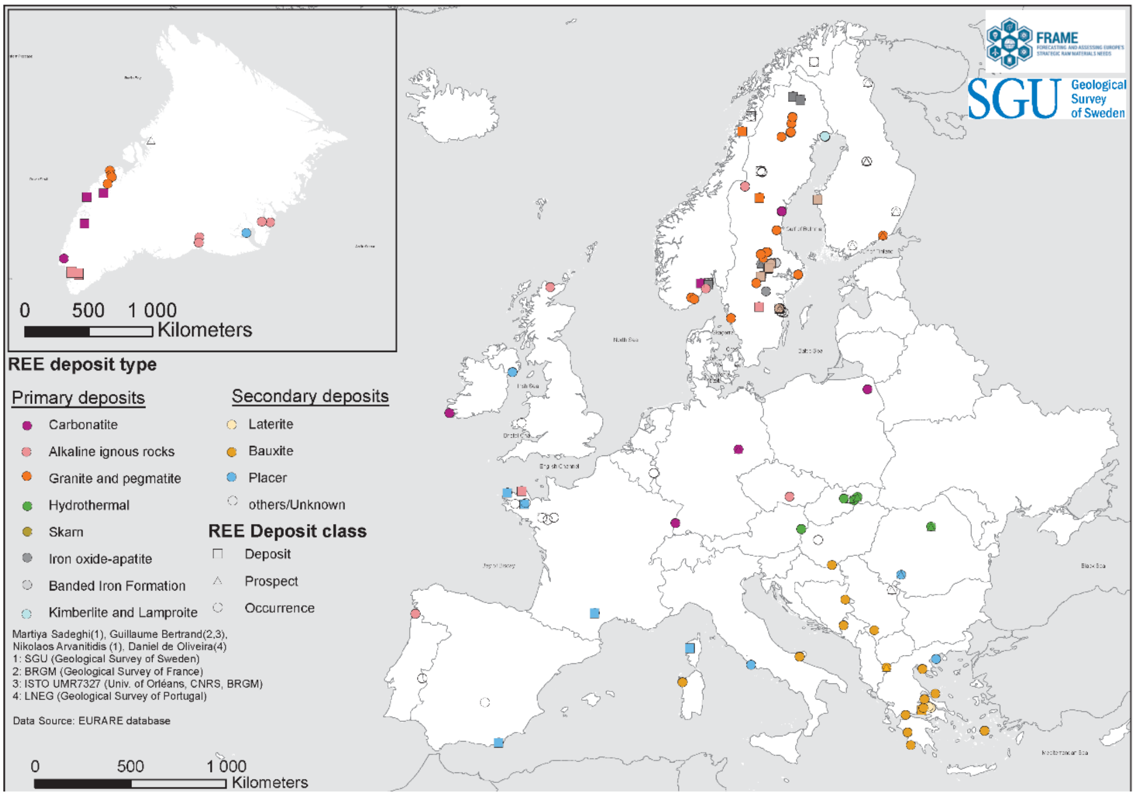

Figure 31. Map showing the main REE mineral occurrences and deposit types in Europe (revised). Data source: EURARE

This project has received funding from the European Union's Horizon 2020 research and innovation programme under grant agreement No 731166

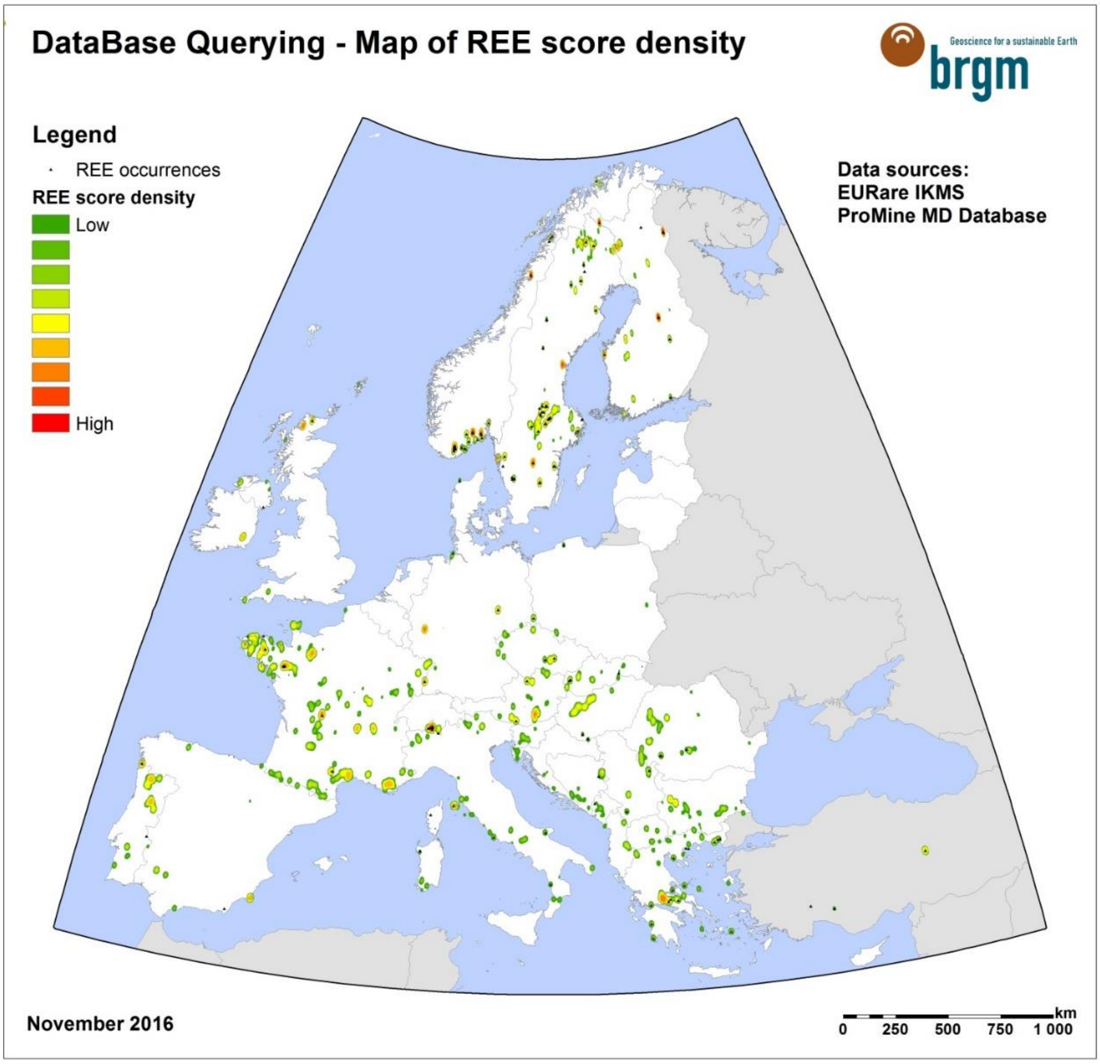

Figure 32. Prospectivity map of kernel density of REE scores in Europe, calculated with the DataBase Querying method (Bertrand et al., 2017)

4.1.3 REE metallogenic provinces

A simplified metallogenetic map of REE (Figure 33) has been prepared based on these previous works. This map shows overall distribution and potential of REE mineral exploration targets based on the different genetic types' classification. The carbonatite and alkaline igneous rocks are presented separately, because of the significant potential of tonnage and grade they commonly host. The secondary REE mineral resources are presented as a separate target area related to bauxite, laterite and placer deposits.

This project has received funding from the European Union's Horizon 2020 research and innovation programme under grant agreement No 731166

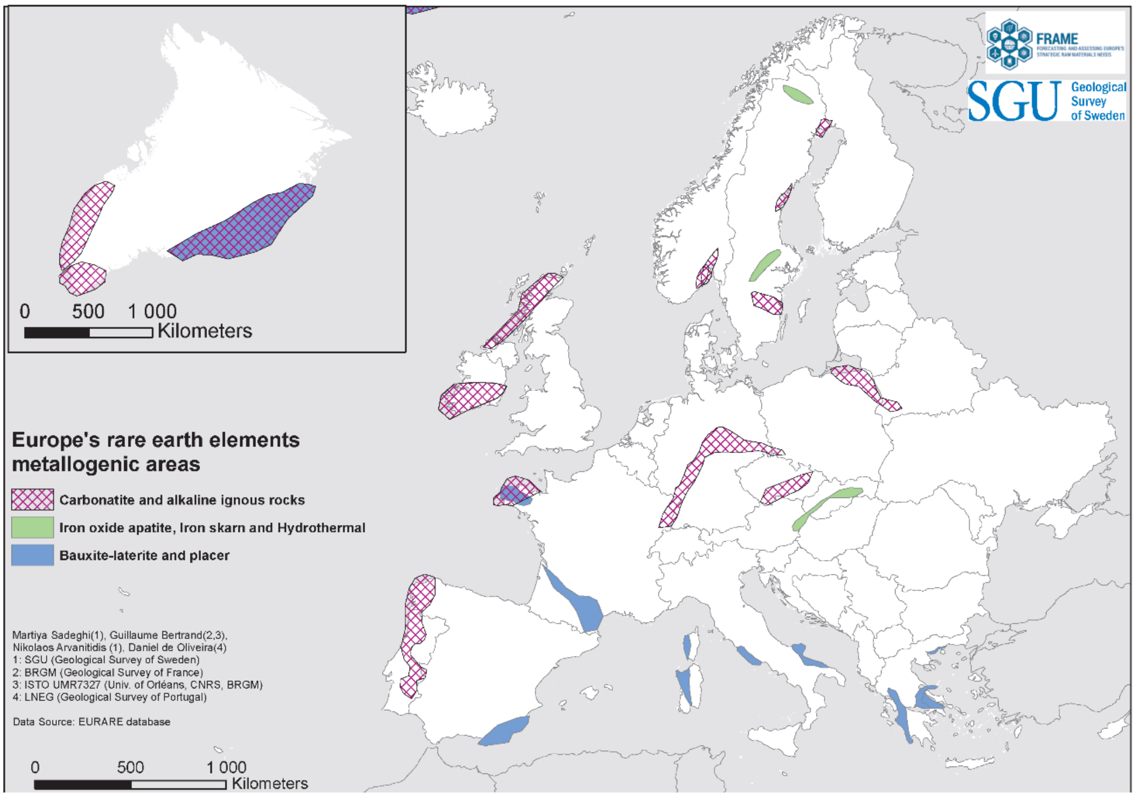

Figure 33. Map showing major REE metallogenetic areas and related exploration potential in Europe (Revised version).

4.1.3.1 Metallogenic area for REE asscoaited with alkaline rocks

The most important primary deposits with high grade and tonnage are typically associated with alkaline-peralkaline igneous rocks and carbonatites formed in extensional intracontinental rifts (Chakhmouradian and Zaitsev, 2012; Goodeough et al., 2016). Europe is characterized by numerous deep, intracontinental extensional zones and rifts which contain alkaline igneous rocks. These vary in age from the Paleo- and Mesoproterozoic of the Fennoscandian shield, via the Mesoproterozoic Gardar Province in SW Greenland to the Cenozoic rifts around the Mediterranean. REE occurrences of potential economic interest are commonly associated with peralkaline syenitic intrusions in these igneous provinces (Figure 34). The Norra Kärr deposit consists of a c. 1.5 Ga old, small, complex intrusion of agpaitic rocks located east of lake Vättern in southern Sweden (cf. Jonsson 2013 and references therein). The Norra Kärr alkaline complex consists of four main rock types, traditionally named grennaite, kaxtorpite, lakarpite and pulaskite.

This project has received funding from the European Union's Horizon 2020 research and innovation programme under grant agreement No 731166

Grennaite is essentially an often porphyritic, relatively fine-grained (but locally coarse and pegmatitic) catapleiite and eudialyte-bearing nepheline syenite. The other rocks are varieties of nepheline syenite with different texture and mineralogy. The pegmatitic grennaite contains abundant eudialyte, which may contain up to 9 wt.% TREO (Jonsson, 2013). According to recent data from the present concession holder, Tasman Metals Ltd, the deposits contain REE, Zr, Nb, Y and Hf of economic relevance. The resource is estimated at 60.5 Mt averaging 0.54% total rare earth oxide with 53% of that being heavy rare earth oxides. Other examples of syenitic intrusions in Sweden with possible potential for REE include the Permian Särna nepheline syenite intrusives in western central Sweden, comprising cancrinite-bearing nepheline syenites, which possibly formed in relation to the Oslo rift (Lundqvist 1997, Bylund and Patchett 1977, Magnusson 1923)

The Meso-proterozoic Gardar province in South Greenland is an intracratonic rift province containing a variety of volcanic and plutonic igneous rocks of alkaline and peralkaline affinity. Of the intrusions in the province the economically most important for REE are the Ilimaussaq intrusion (1160 Ma), and the Igaliko Nepheline Syenite Complex (1273 Ma) (Upton et al., 2003), hosting the Kvanefjeld and Kringlerne REE deposits, and the Motzfeldt Sø REE deposit respectively.

The Ilímaussaq intrusion was largely emplaced during block subsidence and formed by three pulses, of which the third formed a layered series of nepheline syenite, enriched in the elements REE, U, Th, Nb, Ta, Be, Zr, and F. The Ilimaussaq intrusion hosts two World Class REE deposits (i) Kvanefjeld, an intermediate series sandwiched between roof and floor series, which consist mainly of lujavrites, and (ii) Kringlerne, where the bottom cumulates of kakortokite outcrop (Karup-Møller & Rose-Hansen 2013).

The Kvanefjeld multi-element deposit is an accumulation of various igneous rocks from the central part of the Ilimaussaq intrusion. The bulk of the REE and the U is associated with lujavrite rocks containing disseminated steenstrupine, sphalerite and villiaumite (NaF). Indicated JORC compliant resource is 437 Mt containing 6.6 Mt TREO (0.24 Mt HREO), 350 Mlbs U3O8, and 1.4 Mt Zn.

The Kringlerne multi-element deposit is hosted in agpaitic kakortokite and consists of a total of 29 exposed cyclic layers with a total thickness of about 200 m, made up by arfvedsonite-dominated kakortokite, eudialyte-dominated kakortokite, and a nepheline-feldspar-dominated kakortokite, respectively. Eudialyte, the main ore mineral, is enriched in REE-Zr-Nb-Ta (Karup-Møller & Rose-Hansen 2013). The indicated resource (JORC-compliant) is 1,400 Mt plus at 0.65 % TREO. The proposed mining technique is open pit

This project has received funding from the European Union's Horizon 2020 research and innovation programme under grant agreement No 731166

near the fjord, hauling the ore to a nearby beneficiation plant, producing three products: (i) eudialyte concentrate (REE, Nb, Zr); (ii) feldspar concentrate, and (iii) arfvedsonite concentrate, all to be shipped for further processing and/or use outside Greenland.

The Motzfeldt Sø REE deposit is part of the Motzfeldt Centre, which in turn is one intrusion of the Igaliko Nepheline Syenite Complex, and shows significant Ta-Nb enriched zones related to altered syenite, minor pegmatite and diorite dykes, and high grade REE intersections related to the pegmatite intrusives at depth (Tukiainen,1988).

Relatively few alkaline igneous intrusions outside the Nordic countries have known potential REE resources. One such example is the Cnoc nan Cuilean intrusion of the Loch Loyal Syenite Complex in north-west Scotland. This Silurian-age syenitic intrusion contains mafic syenites and syenodiorites that are rich in the LREE-bearing mineral allanite. Part of the intrusion contains hydrothermally altered zones containing biotite-magnetite veins that are rich in allanite and apatite and contain up to 2% TREO (Walters et al., 2013) The extent of these veins is not known and no estimate of the REE resource has been made.

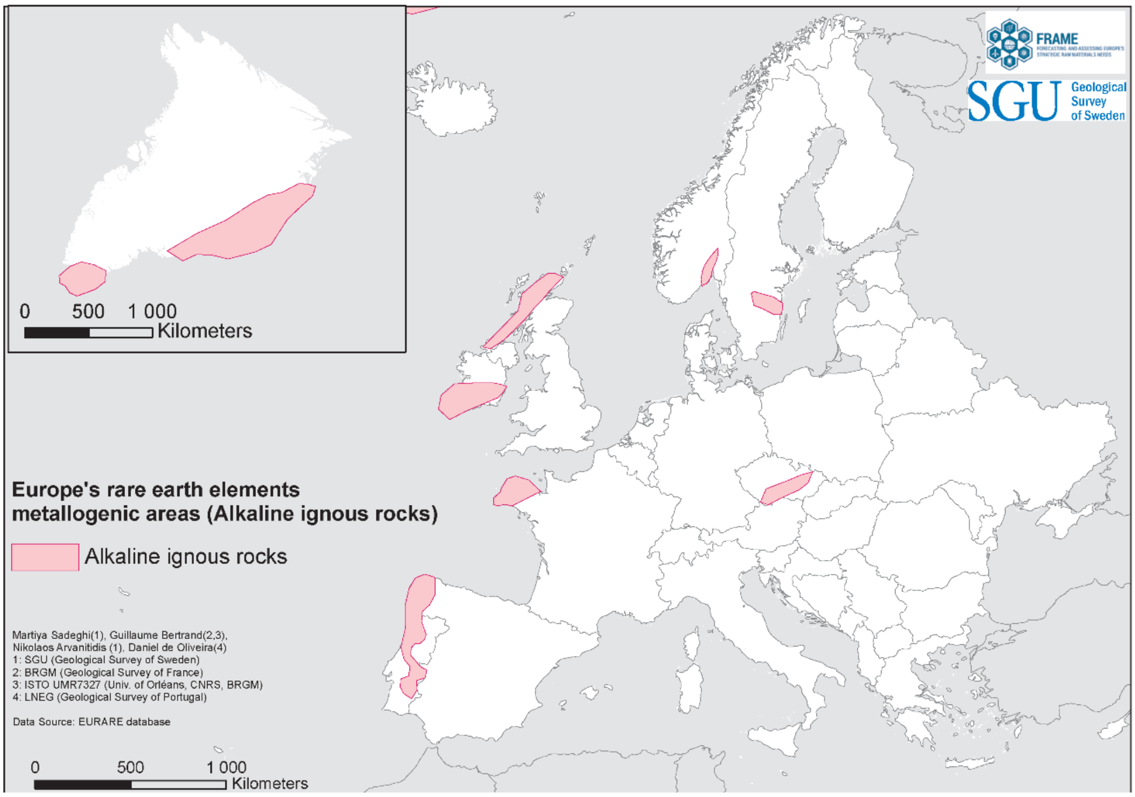

This project has received funding from the European Union's Horizon 2020 research and innovation programme under grant agreement No 731166

Figure 34. overview map of Europe showing the approximate extent of the key REE metallogenic belts related to REE associated with alkaline igneous rocks.

4.1.3.2 Metallogenic area for REE associated with carbonatite rocks

Carbonatites are igneous carbonate rocks in which the modal percentage of carbonate exceeds 50% (IUGS, Le Maitre, 2002). Carbonatites often occur in continental extensional or rift settings, in several cases in association with alkaline to peralkaline syenitic rocks.

The origin of carbonatite magmas, whether they formed from liquid immiscibility with silicate melts, or as directly mantle-derived small-degree partial melts, continues to be debated. Important ore minerals for REE in carbonatites is typically carbonates/fluorocarbonates (e.g. ancylite, bastnäsite, parasite, synchysite) and phosphates (e.g. apatite, florencite, monazite), although significant concentrations may also be found in oxides and silicates.

High concentrations of REEs value in whole rock, and some enrichments of LREE, have been identified in sövite (calcite carbonatite) from the Alnö alkaline complex in Sweden, which includes both silicic (syenitic) and carbonatitic rocks. Known or potentially REE-bearing minerals within the Alnö complex include apatite, monazite, synchysite, aeschynite, fersmite, brockite, (perovskite, pyrochlore), titanite, zirkonolite, wöhlerite and Ti-andradite. (Kresten et al., 1981). North of Alnö proper, several intrusions have been identified by the geological survey of Sweden north of the village Söråker, and some of them show elevated REE concentrations in carbonatite. Similar, but smaller dykes occur in the Kalix area, close to the Finnish border in northeasternmost Sweden. They contain leucoxene, apatite and perovskite, among other minerals (Figure 35)

Greenland is endowed with a number of carbonatite-associated REE deposits formed between the Archaean and Jurassic, most notably the Sarfartoq Carbonatite Complex, Qaqarssuk carbonatite, Tikiusaaq carbonatite and Niaqornakassak. . The most important of those, in terms of REE resources, are Sarfartoq, Qaqarssuk and Tikiussaq. These three carbonatites are located in southern West Greenland in the Archaean basement of the North Atlantic Craton.

The Sarfartoq carbonatite intrusion is located on a Precambrian thrust zone and intruded c. 600 Ma ago during the opening of the Iapetus Ocean. The host rock consists of orthogneiss with schlieren of amphibolite. The complex has an ellipsoidal shape and covers about 90 km², of which 10 km² are intrusive carbonatites. The core of the complex

This project has received funding from the European Union's Horizon 2020 research and innovation programme under grant agreement No 731166

consists of rauhaugite with schlieren of sövite and beforsite dykes, surrounded by a Na-type fenite zone with aegirine- and pyrochlore-bearing rocks. The carbonatite contains REE-bearing minerals in veinlets of dolomite, and in shear zones with thorium, uranium, K-feldspar alteration, and limonitisation (Secher & Larsen, 1980). The most common REE-minerals are synchysite and zhonghuacerite, (http://www.hudsonresources.com/). These minerals are relatively enriched in LREE, most notably Ce, La and Nd.

The Qaqarssuk carbonatite complex consists of carbonatite ring-dykes that are elliptical to semi-rectangular in shape and intruded into the Archaean basement 173 Ma ago (Larsen et al., 1983). The carbonatite covers an area of 15 km² and is surrounded by fenitised basement. The ring-dykes consist of sövite, olivine-sövite, and dolomite carbonatite. They are cut by late-stage sövite veins, REE-carbonatite veins, ferrocarbonatite and lamprophyre dykes (Knudsen & Buchardt, 1991) and these late veins represent the main REE resource at Qaqarssuk. The sövites contain increasing amounts of silicate minerals and inclusions of fenitised basement when moving away from the centre of the complex. The fenites are composed of albite, alkali amphibole, and alkali pyroxene (Knudsen & Buchardt, 1991). The major REE minerals in the complex are ancylite, burbankite, huanghoite and qaqarssukite.

The carbonatite complex of Tikiusaaq was discovered in 2005 (Steenfelt et al., 2006). The presence of the carbonatite was predicted by a study of regional stream sediment geochemistry and aeromagnetic data. The complex consists of a central intrusive carbonatite surrounded by a fenite zone with carbonatite and aillikite dykes. Both magmas have common origin within carbonated upper mantle (Tappe et al., 2009). The carbonatite intruded 165-150 Ma ago associated with the opening of the Labrador Sea. Apart from REEs, the carbonatite complex hosts phosphor, niobium and tantalum. The highest grade REEs are associated with a thorium anomaly.

The Sokli intrusion in Finland consists of a carbonatite core surrounded by carbonatite and a wide fenite aureole. The Sokli intrusion is part of the Kola alkaline province, which consists of nearly thirty Devonian, ca. 360-380 Ma alkaline intrusions of various sizes (Kramm et al., 1993). The Sokli intrusion hosts an unexploited phosphate ore deposit, in addition to which it is enriched in Nb, Ta, Zr, REE and U (Korsakova et al., 2012). REE-bearing minerals include Sr-REE-apatite, monazite, ancylite, bastnäsite, strontianite, barite and "brabantite". The main REE-rich carbonate minerals recognised in the Jammi carbonatite veins at Sokli are ancylite and bastnäsite. They are strongly enriched in LREE,

This project has received funding from the European Union's Horizon 2020 research and innovation programme under grant agreement No 731166

P, F, Sr and Ba. Apatite occurs as large and elongated grains closely associated with monazite.

The Fen Complex, an early Cambrian intrusive complex of alkaline rocks and carbonatites, is situated in Nome municipality, Telemark County, Norway, in the vicinity of the late Palaeozoic Oslo Rift (Brøgger,1921; Bergstøl and Svinndal,1960; Andersen, 1988, Meert et al. 1998; Dahlgren, 2004). There are several different igneous rocks within the complex, including basic rocks, lamphrophyric rocks and carbonatitic rocks. Of these, the carbonatitic rocks are specifically interesting for REEs. Hematite-ankerite carbonatite is generally highly enriched in thorium (0.1 to 1.0 wt.% Th) and REEs (0.3 to 2.0 wt.% TREE) (Svinndal, 1970; Lie and Østergaard, 2011a, 2011b). The REE mineralization mainly consists of monazite, bastnäsite, synchysite and parisite (Andersen, 1986; Lie & Østergaard 2011a).

Carbonatites occur in many of the younger extensional zones and intra-continental rift systems in Southern Europe, but few are exposed. One carbonatite that has been assessed for its REE potential is the buried Delitzsch carbonatite complex, containing the Storkwitz deposit, which lies within a Cretaceous rift zone in Germany. It is under exploration by Seltenerden Storkwitz AG. JORC compliant resource estimates show an indicated resource of 2.02 million tonnes of ore at a grade of 0.49%, and an inferred resource of 2.4 million tonnes of ore at a grade of 0.42%. The ore is LREE-dominated, and also rich in Nb.

This project has received funding from the European Union's Horizon 2020 research and innovation programme under grant agreement No 731166

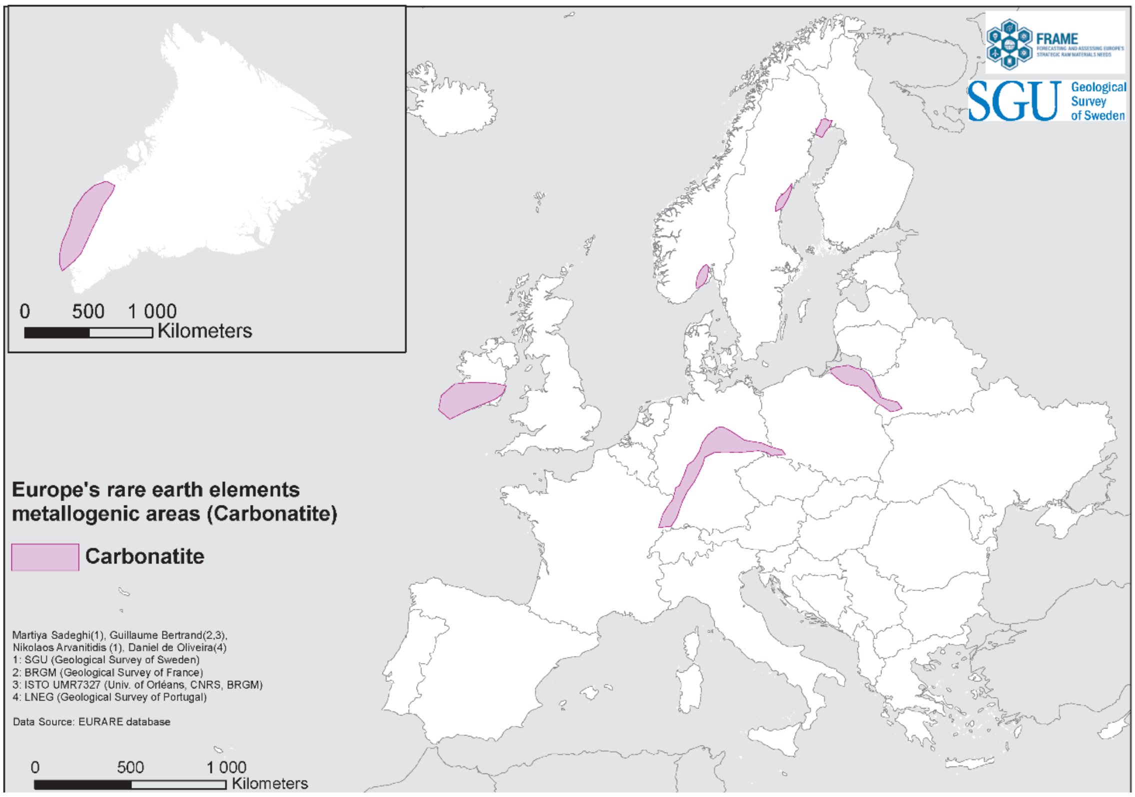

Figure 35. overview map of Europe showing the approximate extent of the key REE metallogenic belts related to REE associated with carbonatite rocks.

4.1.3.3 Metallogenic area for REE associated with Iron oxide-apatite and Iron skarn mineralization

Magnetite-(hematite)-apatite ores of the Kiruna type comprise the biggest iron mines in Europe today. Typically, these genetically debated deposits (cf. Parak, 1975, Hitzman et al. 1992; Jonsson et al. 2013; and references therein) are hosted by felsic to intermediate metavolcanic rocks of ages between c. 1.90-1.87 Ga. They generally exhibit anomalously high concentrations of REEs, which are hosted by primary fluorapatite and commonly also later-formed phases, mainly monazite-(Ce) and allanite-(Ce) (e.g. Harlov et al., 2002; Jonsson et al., 2010; Majka et al. 2013). Total REE contents in this fluorapatite may reach up to weight-percent levels. Important examples of this deposit type include Kiirunavaara and Malmberget (Bergman et al., 2001) in northernmost Sweden, and Grängesberg-

This project has received funding from the European Union's Horizon 2020 research and innovation programme under grant agreement No 731166

Blötberget-Idkerberget in Bergslagen, south central Sweden (Figure 33). (Sadeghi, 2019; Jonsson et al., 2019 and references therein).

In the Olserum area, in the vicinity of the palaeoplacer localities mentioned below (in the Västervik region), are additionally several vein or schlieren-hosted, REE-rich mineralizations associated with iron oxides (Gustafsson, 1992). These presently relatively unstudied deposits are apparently epigenetic, contain abundant monazite-(Ce) and xenotime-(Y) in addition to apatite, biotite and magnetite, and exhibit a relatively high proportion of HREE Another example is the Kodal deposit located in the Paleozoic alkaline province of the Oslo rift in southern Norway, which forms a Fe-Ti-oxide-rich pyroxenite dyke (e.g. Ihlen et al., 2014).

The Bastnäs-type deposits (Geijer, 1961) are located in the Palaeoproterozoic Bergslagen ore province of south-central Sweden, where they form a discontinuous, narrow belt of approximately 100 km length, the so-called REE-line (Jonsson & Högdahl 2013). These deposits occur in what is interpreted as skarn-altered carbonate horizons within c. 1.89-1.87 Ga felsic metavolcanic units (cf. Andersson et al. 2013; Jonsson & Högdahl, 2013, Andersson, 2004). LREE-enriched deposits are located mainly in the Riddarhyttan-Bastnäs area, and deposits showing enrichment in LREE and Y+HREE are mainly located in the Norberg district (Holtstam & Andersson, 2007). Typical host minerals comprise cerite, törnebohmite and allanites (sensu lato), as well as REE-fluorocarbonates such as bastnäsite (cf. Jonsson, 2013; Holtstam & Andersson, 2007; Andersson, 2004). A large number of these minerals have their type localities among the Bastnäs-type deposits.

4.1.3.4 Metallogenic area for REE asscoaited with granite and granitic pegmatite

This type of mineralization occurs in several granite intrusions and numerous granitic pegmatite fields in the crystalline bedrock of the Fennoscandian shield. These intrusive rocks range in age from around 1.82 to c. 1.0 Ga, during the successive growth of the Fennoscandian crust (Romer & Smeds, 1994, 1996, 1997). Additionally, the potential for new discoveries is reasonably high. The highest contents of REE are found in some pegmatite-hosted oxides, phosphates and silicates (e.g. samarskite and euxenite-type minerals, monazite and xenotime, yttrialite-fluorthalenite, fergusonite, gadolinite, yttrotantalite.. The most important granitic pegmatites and granitoids with potential for REE mineralization are, Tåresåive (highest contents of REEtot = 94,900 ppm) in northern Sweden (Norrbotten lithotectonic unit), Näverån in Central Sweden (close to the Caledonides), as well as granitoids in Bergslagen (e.g., Ytterby; highest contents of

This project has received funding from the European Union's Horizon 2020 research and innovation programme under grant agreement No 731166

REEtot = 30,624 ppm), and granite in the southwestern part of Sweden, (e.g., Balltorp; highest contents of REEtot = 8800 ppm), more details can be found in Sadeghi , 2019 and Sadeghi et al., 2020c)

Allanite-bearing pegmatites are common and have variable LREE/HREE ratios. one example of this type of deposit is the granitic REE-rich pegmatite at Gloserhei in the Froland community in southern Norway, which is famous for its large allanite crystals, weighing up to 5 tons. This pegmatite is part of the Sveconorwegian South Norwegian Pegmatite Belt which extends from Kragerø in the NE to Kristiansand in the SW. The pegmatite is enriched in Y, REE, U, Th, and Zr. The Høgtuva Be-REE-U-Sn-mineralization and Tysfjord granite in central Norway are two examples of potential granite-hosted deposits. Both mineralizations are related to Proterozoic metamorphized granites of the Trans-Scandinavian Igneous Belt (TIB). The mineralized gneiss at Høgtuva is enriched in Be (0.12 wt.%), U (149 ppm), LREE (La+Ce+Sm = 687 ppm), HREE (Eu+Tb+Yb+Lu = 237 ppm), Th (278 ppm), F, Li, Nb (293 ppm), Y (644 ppm), Zr (7733 ppm) and Sn (94 ppm) (Wilberg and Lindahl, 1991; Wilberg, 1989). Several hydrothermal deposits in granite breccias or felsic gneiss occur in Greece and contain anomalous values of REEs. Examples of these occurrences are, Samothrace Island and Esochi – N. in Greece and the REE bearing minerals are allanite, monazite, xenotime, apatite and zircon (Eliopoulos et al., 2014.).

4.1.3.5 Metallogenic area for REE asscoaited with laterite/Bauxite

Bauxite deposits occur along the northern shore of the Mediterranean Sea, from Spain to Turkey, encompassing Greece, parts of southern France, Vlasenica, Bosnia - Herzegovina; Mortaş, Hungary, Italy (Bárdossy, 1982; Özlü, 1983).Many of these bauxites, which formed by intense lateritic weathering of residual clays, are currently mined for aluminium, and the red mud waste from bauxite processing represents a potential REE resource (Deady et al., 2014). For example, bauxite deposits in the Parnassos-Ghiona geotectonic zone in central Greece. (i.e. Prossorema and Frussia (Steni Arachovis) are situated on Upper Jurassic limestones and contain REE bearing minerals such as detrital rabdophane-Ce, florencite-Ce, churchite and xenotime (Laskou and Andreou, 2003)). Similar detrital REE minerals are also accumulated in the Hungarian bauxite deposits (Bardossy et al., 1976). ΣREE content reaches values as high as 2319 ppm and show a wide variation in their chemical composition especially in LREE contents. The concentration of REE in bauxite deposits is controlled by their initial

This project has received funding from the European Union's Horizon 2020 research and innovation programme under grant agreement No 731166

content in the parent rocks, by diagenetic or epigenetic modifications, by the influence of circulating waters and underlying barriers of limestone (Laskou and Andreou, 2003). Greece is the only EU country with extensive but low-grade nickel laterites. The Greek laterites are unique in the world in that they are sedimentary and have originated by transport and sedimentation of laterite-derived material, generated by weathering of ultramafic rocks, on karstic Triassic –Jurassic limestones or on ultramafic ophiolitic rocks (Valeton et al., 1987; Eliopoulos and Economou-Eliopoulos, 2000). The multistage transportation and re-deposition of the laterite ore is well documented by the presence of a conglomerate composed mostly of rounded-elongated saprolite and silicified saprolite. The post-sedimentary redistribution of metals resulting in changes of the mineralogical composition of laterites is demonstrated by the presence of asbolane and Mn, Co, Ni-rich zones in the lowest parts of the Aghios Ioannis (Nissi)). Nissi is characterised by both nickel and bauxitic laterites with very high values, up to 6440 ppm ΣREE, along with an enrichment in Mn, Ni and Co within the lowermost part of laterite and footwall limestone of the Nissi deposit. Such an enrichment in both light and heavy REE and the presence of authigenic REE minerals bastnaesite, hydroxylcarbonate-(Nd) and hydroxylcarbonate-(La) are consistent with a download mobilization of REE and concentration at the footwall limestone like in the majority of karstic bauxite deposits with authigenic REE minerals (Maksimovic and Panto, 1991).Another important laterite deposit in Greece is located in Lokrida (Marmeiko). The deposit is hosted by Upper Jurassic-Lower Cretaceous limestone and contains bastnäsite and monazite as REE-bearing minerals. Among the main factors controlling the REE content in laterites are the composition of the rock source, the duration of the lateritisation process, the size of the ore bodies, the distance of the transportation, the pH and Eh conditions (Economou-Eliopoulos et al., 1997).

4.1.3.6 Metallogenic area for REE asscoaited with placers

An example of a placer deposit is found in Vale de Cavalos in Portugal, where an Ordovician sedimentary succession includes quartzites that are rich in the REE-bearing minerals monazite and zircon. The Aksu Diamas region in Turkey hosts alkaline volcaniclastic rocks of Cenozoic age that locally have significant concentrations of heavy minerals hosted in placer deposits (e.g. in the Çanakli prospect, which is under exploration by AMR Mineral Metal Inc.). Placers of grey monazite nodules are also found in France, mainly in Brittany (Donnot et al., 1973), formed from low-grade metamorphosed black shales of Dinantian- (Châteauneuf-du-Faou, Corlay) or

This project has received funding from the European Union's Horizon 2020
research and innovation programme under grant agreement No 731166

Ordovician age (le Grand-Fougeray, Châteaubriand), or even from Upper Precambrian series (Brioverian), along the edge of Ordovician series (Craon). Similar layers of shales with monazite nodules and associated placers (but of lesser interest) are also known in the southern Massif Central, in the Ardennes and in the French Pyrennees (Arize massif) (Lacomme et al., 1993). In the Västervik region in southeastern Sweden, several occurrences of U-rich, REE-bearing minerals have been identified in quartzite-dominated Palaeoproterozoic metasedimentary successions (e.g. Gustafsson, 1992). These are interpreted to represent paleoplacer-type original concentrations of heavy mineral sands.

In East-Greenland the Jurassic placer deposit on Milne Land represents another potential source for REEs. The deposit lies within the Mesozoic basins in central East Greenland that formed during the opening of the North Atlantic Ocean (Larsen et al., 2003). The placer consists of heavy mineral-rich arkosic sandstones and breccias, which are rich in zircon, monazite, Ti-minerals and garnet. The units form the lowermost 20 m of the Charcot Bugt Formation, which rest unconformably on a Proterozoic migmatitic granite. The best outcrops are found on Hill 800, where these sedimentary rocks are 40-50 m thick and are found over an area of more than 500 m in diameter (Larsen et al., 2003; Schatzlmaier et al., 1972). Another important source of REE are the black sands in the Nea Peramos and Strymonikos Gulf derived from the plutonic rocks of the area mainly the Kavala pluton. Analysed samples show elevated values of La, Ce, Nd. Y and Pr. Mineralogical studies determined the following REE minerals monazite, allanite, titanite, uraninite, zircon, and apatite.

4.2 Phosphate

4.2.1 Introduction

Phosphorus is essential for living plants and animals. It is mostly found as apatite and is principally used to produce fertilizers (82% of the production). Phosphorus is therefore needed to satisfy the growing demand for food related to the growth of the world population. An increase of about 2% per year in the global market is expected (European Commission, 2015).

The European countries are net importers of phosphate, with an average of 4,000,000 tonnes of natural phosphate-rich material imported per year (European Commission, 2015). Phosphorus was consequently added to the list of Critical Raw Materials for the

This project has received funding from the European Union's Horizon 2020 research and innovation programme under grant agreement No 731166

EU in 2014. Europe also imports other by-products that can be potentially (and quite easily) recovered from phosphate mineralization, namely the Rare Earth Elements (REE), Fluorspar (F) and Vanadium (V).

Phosphorus is mostly exploited from sedimentary phosphate deposits. North Africa, China, the Middle East, South Africa, the USA and Russia are the main producers of this resource, the reserves of which are above 1,300,000 Mt for each of these countries. Reserves reach 50,000,000 for the Moroccan deposits (European Commission, 2015). Other sources of phosphates comprise igneous apatite deposits (major deposits in Finland, Russia, South-Africa, and Brazil; European Commission, 2015) and deposits occurring on the continental shelf of the Atlantic, Pacific and Indian Oceans (Cook and Shergold, 1986).

4.2.2 Phosphate mineralization types in Europe

In Europe, phosphate deposits and occurrences are abundant and widely distributed (Figures 36 and 37). They are igneous or sedimentary in origin and their age varies from the Archean to the Pleistocene (Figure 36). Various sub-types of igneous-related phosphate deposits occur (defined according to Inspire; Figure 38) and are detailed in the section ". Igneous-related types" here below.

This project has received funding from the European Union's Horizon 2020 research and innovation programme under grant agreement No 731166

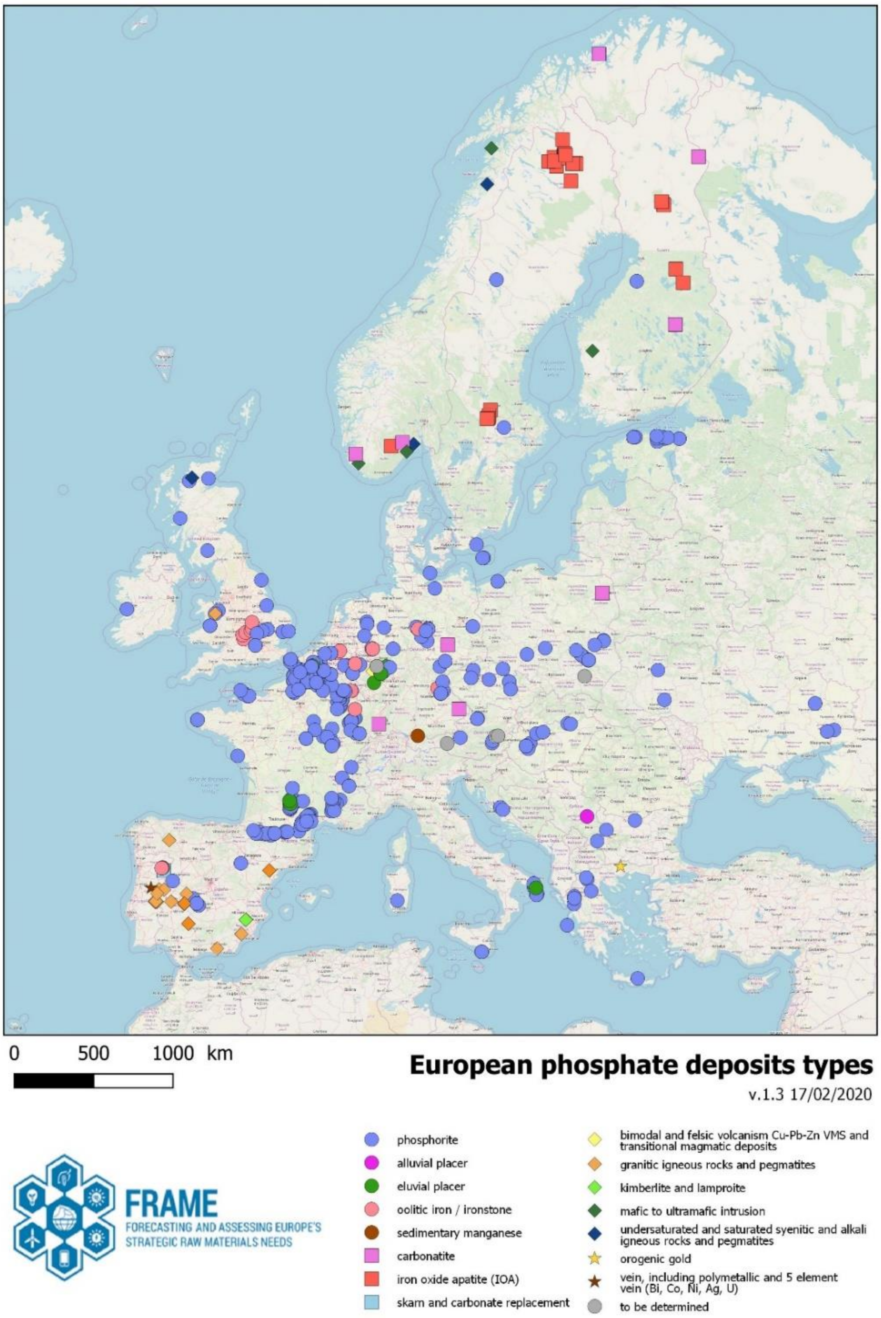

This project has received funding from the European Union's Horizon 2020 research and innovation programme under grant agreement No 731166

Figure 36. Map illustrating the mineral deposit type of phosphate mineralization in Europe. Report "Deliverable D4.2" of the FRAME project-WP4.

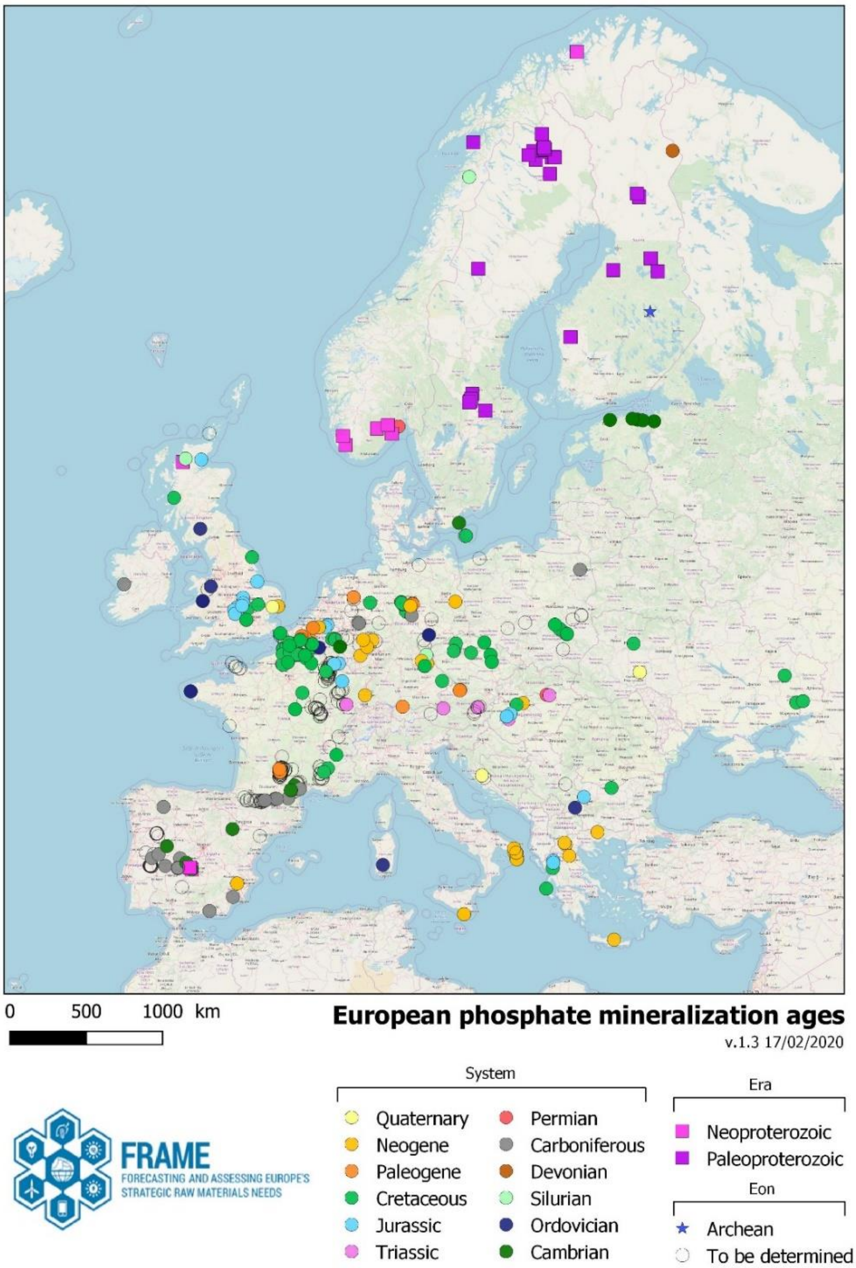

This project has received funding from the European Union's Horizon 2020 research and innovation programme under grant agreement No 731166

Figure 37. Map illustrating the phosphate mineralization in Europe according to their age (System/Period for Phanerozoic mineralization, Era for Proterozoic mineralization, and Eon for Archean mineralization). Report "Deliverable D4.2" of the FRAME project-WP4.

4.2.2.1 Igneous-related types

Carbonatite

In Finland, the Devonian Sokli carbonatite complex hosts a large apatite deposit, the reserves of which are estimated at 190 million tonnes (Ahokas, 2015). The highest modal values of apatite are observed in phoscorite (up to 50%) (O'Brien and Hyvönen, 2015). The Siilinjarvi phosphate deposit is associated with a carbonatitic complex dated at ~2610 Ma (GTK unpublished report in O'Brien et al., 2015). Ore reserves of 234 Mt at an average grade of 4 wt% P2O5 are estimated (O'Brien et al. 2015). In Norway, the Neoproterozoic Fen carbonatite complex is known for its Nb and REY mineralization, though it also hosts apatite-rich facies (containing up to 29% apatite; Ihlen et al., 2014). The Seiland Igneous Province (Norway) comprise Neoproterozoic to Cambrian alkaline complexes, among which the Lillebukt Complex that presents an interest for its phosphate content (Ihlen et al., 2014). In Sweden, the Neoproterozoic Alnö carbonatite contains ~2 million tonnes at a grade varying from 2 to 6% P_2O_5. Other small occurrences of phosphate associated with carbonatites are known in Italy and Germany (Figure 38)

Unsaturated and saturated syenitic and alkali granitic igneous rocks and pegmatites

The Misværdal Complex (Norway) is a Silurian alkaline complex comprizing mostly pyroxenites that are the main carriers of apatite. Resources could reach 30 Mt at 4.1% P2O5 (Ihlen et al., 2014). The Loch Borralan and Loch Loyal Silurian intrusions (Scotland, UK) host apatite-rich facies that present a potential regarding phosphate (Notholt and Highley, 1981; Walters et al., 2013). Other alkaline complexes containing apatite at a near-economic grade are found in Italy (Stoppa et al., 2016).

Kimberlite and lamproite

The most known lamproite in Europe is present in Spain, at Jumilla. There, Miocene jumillites host an apatite mineralization (Venturelli et al., 1991).

Mafic to ultramafic intrusion

This project has received funding from the European Union's Horizon 2020 research and innovation programme under grant agreement No 731166

In Norway, the Neoproterozoic Rogaland Anorthosite Province constitutes one of the most promising targets regarding phosphate exploitation, with resources being above 300 Mt at a grade reaching 8.0-10.2% of apatite for the individual cumulate zones (Ihlen et al., 2014). The Paleoproterozoic Lofoten-Vesteralen Mangerite Complex (LVMC, Norway) – where nelsonite ore (containing between 2.75 and 4.23% P_2O_5) is present as thick veins and breccias - constitutes another interesting area regarding its potential for P (Ihlen et al., 2014). In southern Norway, the Kodal deposit is found in the Permian Larvik Complex (Oslo Igneous Province). It is made of pyroxenitic ore lenses rich in apatite, with resources of 70 Mt, grading at 4.9% P_2O_5 (Ihlen et al., 2014). In Finland, the Paleoproterozoic Kauhajärvi gabbro and appinite at Vanttaus are intrusions enriched in apatite that could present an interest for future phosphate exploration (Kärkkäinen and Appelqvist, 1999; Sarapää et al., 2013).

Iron oxide apatite (IOA)

Most of the iron oxide apatite deposits in Europe are found in Sweden, with (i) the major mining areas in the northern Norrbotten district that have reserves and resources estimated at 2372 Mt of iron oxide-apatite ore (Figure 38) (Hallberg et al., 2016). This Paleoproterozoic mineralization comprises mostly magnetite-hematite-apatite and associated calcite, actinolite and diopside (Frietsch and Perdahl, 1995), and (ii) the Bergslagen district, with the Grängesberg mine that has estimated resources of 148 Mt (Hallberg et al., 2006). In Norway, the Nissedal area is known for occurrences of magnetite–hematite-apatite deposits. The Mesoproterozoic Søftestad deposit presents remaining resources of ~0.5 Mt, with ~55% Fe and 3.9% P_2O_5 (Ihlen et al. 2014, and references therein).

Metasomatic replacement/ hydrothermal veins

The most important European apatite deposits of a hydrothermal origin – and (at least spatially) associated with granite – are the post-Variscan quartz-apatite veins occurring in the southern Central Iberian Zone (mining district of Logrosan and Belvis-Navamoral; Vindel et al., 2014). This was one of the most important phosphate sources in Europe from the 1850s to the Second World War (Vindel et al., 2014). In the Bamble-Lillesand Block (Norway), the paragneiss at Rossavika hosts pseudo-carbonatitic lenses and veins

This project has received funding from the European Union's Horizon 2020 research and innovation programme under grant agreement No 731166

enriched in apatite. The grade of the lenses varies between 7.63 and 21.34 wt.% P_2O_5 (Ihlen et al., 2014). In Sweden, the REE-P mineralization occurring at Olserum, Djupedal and Bersummen is present as veins and vein zones hosted in metasedimentary rocks. It is thought to be deposited from high temperature hydrothermal fluids, in connection with the granite (Andersson et al., 2019).

4.2.2.2 Sedimentary phosphorites

Three main episodes of phosphogenesis are known during the Lower Paleozoic, the Upper Cretaceous, and the Tertiary. They led to the formation of deposits of major importance.

Lower Paleozoic phosphorites constitute most of the phosphorites in Europe, testifying for the presence of a phosphogenic province within the Avalon and the Baltic Platforms. Such deposits are commonly associated with glauconitic sediments or black shales (Notholt and Brasier, 1986). At Fontanarejo (Spain), early Cambrian phospharenite and phospharenorudite constitute resources of about 2,000,000 tonnes (Notholt et al., 1989). In Serbia, Ordovician metamorphosed phosphatic sandstone presents 95 million tonnes grading at ~10% P_2O_5 (Torbica and Lapčević, 2012). Ordovician sandstone containing phosphatic shells accounts for deposits of 750-800 million tonnes of P_2O_5 in northern Estonia (Raudsep, 1997).

An important sedimentary phosphate unit of Upper Cretaceous age is known throughout the Paris and Mons Basins (France and Belgium), where it forms economic deposits of phosphatic chalk. These deposits reveal a significant phosphogenic episode that occurred during Cretaceous time on the NE margins of the Anglo-Paris Basin (Jarvis, 1992) and result in the formation of numerous phosphorite occurrences/deposits. In the Mons and Paris Basins, phosphatic chalk, enriched pockets of residual phosphates, and phosphatic channels infills lead to total resources of 600-900 million tonnes at 8-10.5% P_2O_5 in the Mons Basin (Robaszynski, 1989), and 12-15 million tonnes at 7-14% P_2O_5 in the Paris Basin (Monchiardini, 1989). The Taplow Cretaceous phosphate chalk (UK) has reserves estimated at 500,000 tonnes (only for its SW side). In addition, reserves of other 246,000 tonnes can be found in Cenomanian condensed phosphatic glauconitic marl of the Cambridge Greensand (UK; Notholt et al., 1979). In Germany (Lower Saxony), the Lengede-Broitstedt deposit presents a grade of about 4% P_2O_5 (Notholt et al., 1979). Cretaceous phosphatic beds associated with iron ore in the Oberpfälz district (Germany) represent reserves of at least 30,000 tonnes at 20% P_2O_5 (Notholt et al., 1979). In Greece

This project has received funding from the European Union's Horizon 2020 research and innovation programme under grant agreement No 731166

(Drymonas deposit), phosphatized limestone horizons of Cretaceous age has reserves of about 7 Mt at ~25% P_2O_5 (Tzifas et al., 2014).

The Cenozoic constitutes another major period of phosphogenesis leading to the formation of many deposits and occurrences in Europe (Arthur and Jenkyns, 1981). The largest are known in the area of Salento (Italy), where Miocene phosphate-rich limestones account for at least 60 million tonnes grading at 7-8 % P_2O_5. Additional 10 million tonnes of Upper Pliocene (?) nodular phosphate-rich rocks at a grade in the range 10.5-20.5 % P_2O_5 are present in the same area (Notholt et al., 1979). Oligo-Miocene phosphatic nodule-rich formations in Sicily have resources of 7 million tonnes at about 15% P_2O_5 (Donnalucata district; Notholt et al., 1979; Cultrone et al., 2008). In Germany, phosphorite deposits associated with Lower Tertiary Fe and Mn oxide ores in the Lahn district account for 750,000 tonnes at a grade above 20% P_2O_5 (Notholt et al., 1979).

Beside the deposits formed during these three main phosphogenic episodes, it is worth mentioning a few others economically interesting mineralizations. Among these, the Proterozoic Lampinsaari deposit (Finland), made of a lenticular bed of apatite-bearing dolomite, skarn and apatite-rich gneiss, accounts for 39 million tonnes at a grade of 2.6% P_2O_5 (Notholt and Brasier 1986; Notholt et al., 1989). Devono-Carboniferous phosphorites being potentially interesting from an economic point of view are present in Ireland, France, Spain, UK, Romania and Germany (Notholt et al., 1979, 1989). In the County Clare (Ireland), Upper Carboniferous condensed sequences of phosphate rocks have estimated resources of 1.25 million tonnes at 20-25% P_2O_5 (Notholt et al., 1979). The north Pyrenean fault zone (France) and the area of the Rhenish Schiefergebirge and Harz Mountains constitute other targets regarding their potential in phosphate mineralization (Notholt et al., 1979).

This project has received funding from the European Union's Horizon 2020
research and innovation programme under grant agreement No 731166

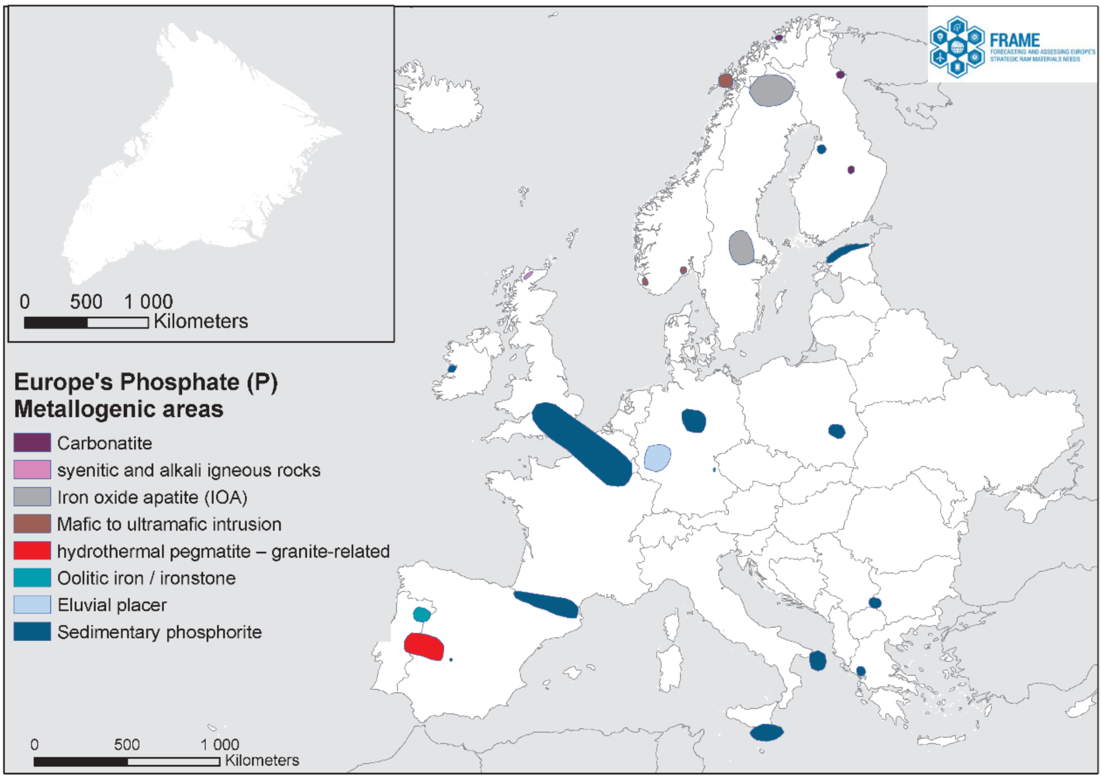

Figure 38. Overview map of Europe showing the approximate extent of the key phosphate metallogenic belts

4.3 Metallogeny of Niobium-Tantalum in Europe

European Nb-Ta occurrences, and specifically those enriched in tantalum, are mainly associated with evolved granites and granitic pegmatites, and to a lesser degree, from hydrothermal systems associated with granitic intrusions. Granitic pegmatites of the rare element type carrying variable proportions of niobium and in particular, tantalum, as well as similarly mineralized granites are known from the Palaeoproterozoic bedrock of the Fennoscandian Shield and several younger granites and granitic pegmatite suites in Europe (e.g. the Variscan belt of the Iberian Peninsula, the Massif Central of France and the Bohemian massif). Specifically, peraluminous granites together with granitic pegmatites of the more fractionated LCT-family (enriched in lithium, cesium and tantalum) are of primary relevance in these areas (Figs. 39 and 40)

This project has received funding from the European Union's Horizon 2020 research and innovation programme under grant agreement No 731166

Niobium is also hosted by (mainly) pyrochlore-group minerals in carbonatitic as well as syenitic rocks, which have a more restricted distribution, and are typically concentrated in smaller, localized intrusions or massifs. As in the case with REE-mineralization hosted by such rocks, the most important European deposits are characteristically associated with alkaline–peralkaline, *mostly* plutonic rocks and carbonatites that have formed in intracontinental rift-settings during extensional episodes (e.g. Goodenough et al. 2016, and references therein).

Secondary deposits (placers) also occur, but, as far as is known, these have a significantly more restricted distribution than the primary deposit types.

4.3.1 Metallogenic areas for Nb-Ta associated with granites and granitic pegmatites

In the **Iberian Peninsula** the primary Nb-Ta mineralizations are genetically associated with peraluminous granites and granitic pegmatite fields in different geological settings, belonging to the Variscan Galicia-Centro Iberian Pegmatitic Province, encompassing the Central-Iberian Zone (CIZ) and the Galicia Trás-Os-Montes Zone (GTMZ; e.g. Roda et al. 2016). The secondary mineralizations are represented by placers in close association with primary mineralizations in Portugal. Both mineralization types represent occurrences or deposits, of which several were exploited for Sn, Ta-Nb, and/or W in the past, and some being recent exploration and mining targets (e.g. Alves and Leal Gomes, 2015; Roda et al., 2016). Niobium-tantalum-rich mineralization in the Iberian Variscan Massif is associated with peraluminous rare-metal granites (RMG), with granitic pegmatites belonging to the LCT family, but also includes LCT-NYF hybrid suites, as well as quartz-rich hydrothermal veins. Nb-Ta mineralization associated with RMG occurs as disseminations in the apical or marginal volumes of small, fine-grained leucogranite bodies. Typical mineralization consists of tantalum-rich cassiterite, columbite-type minerals, microlite minerals, tapiolite (sensu lato) etc. Some of the most representative examples are Argemela hill-top, in Portugal (Charoy and Noronha 1996; Michaud 2019) and Ponte Segade (Canosa et al. 2012), Golpejas (Arribas et al. 1982), El Trasquilón (García Guinea and Martínez Frías,1992), Navasfrías (Llorens 2011) and Penouta (Llorens et al. 2017; López-Moro et al. 2017; Alfonso et al., 2018), in Spain. The Penouta deposit, exploited by Pacific Strategic Minerals S.L., is the only operating Ta mine in Europe and constitutes an important contributor to meet European Ta demand. The reserve is estimated at 13 Mt

This project has received funding from the European Union's Horizon 2020 research and innovation programme under grant agreement No 731166

averaging 750 ppm Sn and 90 ppm Ta. The Golpejas deposit was mined from 1950 to 1986, mainly to extract cassiterite. In 1964, Minera del Duero S.A. carried out exploration, feasibility studies and drilling campaigns, which yielded grades of 1500 g/t Sn and 70 g/t combined Nb-Ta and mined the ore until 1981. The recent requests for permits by mining companies to explore and potentially exploit this type of deposit, formerly exploited for Sn, Ta-Nb and/or W, show the potential economic relevance of Nb-Ta in this region. The LCT-type granitic pegmatites are generally small dykes or irregular bodies characterized by coarse and variable grain-size. They are concentrically but irregularly zoned, typically showing a thin border zone, a wall zone, an intermediate zone, an albite zone, and a massive quartz core. Ta mineralization is mostly concentrated to the intermediate and albite zones and consists of minerals of the columbite, ixiolite and microlite types. Mineralization carrying other metals may also be present, including Be (as beryl), Cs (as pollucite), Li (as spodumene, petalite and lepidolite) and Sn (as cassiterite). LCT-type pegmatites occur in aureoles surrounding the roofs of their parental granite intrusions, and the mineralized and most fractionated pegmatites are typically found the farthest away from the granite. Pegmatitic bodies showing these features are common in the Iberian Variscan Massif, most of which are Li-rich pegmatites and/or with Nb-Ta oxides. Examples of Li pegmatites with Nb-Ta oxides are Tres Arroyos (Garate-Olave et al., 2017), Las Navas (Gallego Garrido, 1992), La Canalita (Llorens, 2011) in Spain, and Campo Mineiro De Lagares and Serra da Arga mining region (Roda-Robles et al. 2014; Leal-Gomes, 2016) in Portugal. The Serra de Arga mining region in the GTMZ is one of the most representative examples of this mineralization type in Portugal, featuring a wide variety of paragenetically different rare element pegmatite bodies, represented by both endo-granitic dykes and exo-granitic ones in metasedimentary host rocks (Pereira and Leal Gomes, 2014; Alves and Leal Gomes, 2015; Leal Gomes, 2016; SIORMINP, 2002). This mining region overall exhibits a wide range of metalliferous ores (Au, Ag, Sn, Nb-Ta, W, Zn and Li) and associated exploration potential (Alves and Leal Gomes, 2015). Notably, it has yielded some of the richest Ta_2O_5 concentrates (up to 43% Ta_2O_5; Leal Gomes, 2016). Identified Nb-Ta minerals include (*sensu lato*) tantalite, tapiolite, ixiolite, columbite and tantalian rutile (Leal Gomes, 2016; SIORMINP, 2002). The Campo Mineiro de Lagares and Nossa Senhora da Assunção mining fields (Sátão-Aguiar da Beira, Viseu) are other good examples of this mineralization type in Portugal, outcropping in an area of polyphase Variscan deformation of the CIZ (Alves et al., 2010). In this region, the richest so far encountered Ta_2O_5 concentrates were previously reported (up to 61% Ta_2O_5; Leal Gomes,

This project has received funding from the European Union's Horizon 2020 research and innovation programme under grant agreement No 731166

2016). Identified Nb-Ta minerals include (*sensu lato*) columbite, tantalite, pyrochlore-group minerals and ixiolite (Leal Gomes, 2016).

The Beauvoir granite in **France** is a peraluminous rare-metal granite located in the Echassières complex within the French Massif Central. Another rare metal granite in the northern part of the French Massif Central containing Nb-Ta is the Montebras granite, known for its associated LCT-type granitic pegmatites. The Tréguennec deposit in the Armorican Massif is estimated to contain 1300 tonnes of Nb and 1600 tonnes of Ta (BRGM database).

Czech Republic – Germany. Nb and Ta bearing minerals within the Erzgebirge region are almost exclusively related to the strongly fractionated A-type granites and accompanying Sn-W-Li greisen mineralization. In the Nakolice and Šejby areas, leucogranites of the Central Moldanubian Plutonic Complex are intersected by pegmatite dykes containing Nb-Ta minerals. Nb and Ta minerals occurs in **Slovakia** in the Western Carpathians as accessory minerals in granitic pegmatites related to peraluminous S-type granites of Variscan age (Uher et al., 2010). LCT pegmatites containing Nb-Ta minerals occur in the East Carlow Deformation Zone, southeast **Ireland** at the margin between the Late Caledonian S-type Leinster granite and Ordovician metasediments and metavolcanics (Barros, 2017, Kaeter and Menuge, 2017a, b).

Ukraine hosts several granitic pegmatite-associated Nb-Ta mineralizations including the Blakyni Skeli and Kruta balka in the central and western part of the Priazovskyi crystalline massif, south-eastern part of the Ukrainian shield. Nb-Ta bearing LCT pegmatites occur at Dilyanka Dobra (Stankuvatsky, Nadiya) located in Dobrovelychkivskyi district of Kirovohrad region. A tantaliferous pegmatite swarm occur at Komendantivske in the Poltava region. Several Lithium bearing pegmatites containing Ta has been identified at Lypnyazki in the central part of the Ukrainian Shield.

The Proterozoic bedrock of **Sweden and Finland** contains a very large number of known granitic pegmatites, of which many have been quarried for one or several commodities over time; mainly quartz and feldspar, but also micas as well as several more uncommon or rare minerals and metals. These granitic pegmatites occur both singularly as well as in groupings and chemically/mineralogically zoned fields (e.g. Sundius, 1951; Brotzen, 1959; Smeds,1990). The most important regions with variably Nb-Ta and Li-mineralised LCT-type granitic pegmatites in the Swedish part of the Fennoscandian shield are the eastern

This project has received funding from the European Union's Horizon 2020 research and innovation programme under grant agreement No 731166

part of the Skellefte district in northern Sweden, the Västernorrland area in central Sweden, and the eastern Bergslagen province with the Stockholm area in southeast central Sweden (cf. Smeds, 1990). All major LCT-pegmatite fields in Sweden are located within low to medium-grade metamorphosed Svecofennian c. 1.9 Ga meta(volcano-)sedimentary successions, and associated with parental late-Svecokarelian, c. 1.8 Ga S-type granites such as the Stockholm, Härnö and Skellefte granite suites (e.g. Smeds, 1990; Romer & Smeds, 1997, and references therein). This is well demonstrated by the abundance of LCT pegmatites in greywacke-type metasedimentary rocks in the Bothnian basin of north central and northern Sweden, as well as in the southern Stockholm area. Characteristic host minerals are dominated by (*sensu lato*) columbite-tantalite and microlite-pyrochlore, as well as Nb-Ta-enriched cassiterite. Tantalum is a main commodity in the Rosendal complex pegmatite and associated, nearby deposits in the western part of the Uusima supracrustal belt in SW Finland (Kemiö metallogenic area). The area comprises late-orogenic granitic pegmatites with a significant potential for feldspar, quartz, tantalum and beryllium. Feldspar and quartz and minor volumes of beryl and columbite-tantalite have previously been extracted from the Kemiö pegmatites. The Emmes-Kaustinen area in Ostrobothnia hosts (1.79 Ga) LCT-pegmatites of the albite-spodumene subgroup. The pegmatites crosscut the Svecokarelian 1.95–1.88 Ga supracrustal rocks composed of greywackes and mica schists (Eilu, 2012; and references therein). Late-orogenic Svecokarelian (ca. 1.8 Ga) LCT type pegmatites containing Li and Be minerals and Fe-Mn phosphates, as well as different columbite-type minerals occur immediately to the south of the Tampere schist belt in central SW Finland in the Eräjärvi metallogenic area (Eilu, 2012; and references therein).

4.3.2 Metallogenic areas for Nb-Ta associated with alkaline rocks

The Gardar alkaline igneous province of southern **Greenland**, and alkaline rocks of the Paleogene alkaline province in East Greenland are prospective tracts for Nb, and to a lesser extent, Ta. Of the former, the very large agpaitic nepheline syenite complexes at e.g. Illimaussaq have mainly been targeted for their contents of REE, but very significant average grades of 0.2 % Nb have been reported (cf. Thrane et al., 2014). Another prospective area in Greenland is the Caledonian belt in northern East Greenland (Steensgard et al., 2016). The Katajakangas and Kontioaho Nb-REE deposits are located in Otanmäki, central **Finland**, within gneissic, 2.06-2.04 Ga alkaline granitoids (Kärenlampi

This project has received funding from the European Union's Horizon 2020 research and innovation programme under grant agreement No 731166

et al. 2020, and references therein). In Northeast **Poland**, alkaline c. 0.35 Ga gabbroic to syenitic massifs intrude the crystalline basement (Demaiffe et al., 2013); of these, the Elk syenitic intrusion hosts Nb-Ta minerals. The c. 0.23 Ga Ditrău alkaline massif in **Romania** (e.g. Dallmayer et al., 1997) is the most significant Nb-Ta and REE mineralized area in the Eastern Carpathians. A significant Nb-Ta mineralization occurs within gneiss near Grădiștea de Munte in the southern Carpathians. Alkaline rocks containing Nb-Ta mineralizations occur at Tsentralnyi located in the Donetsk region in the southeastern part of **Ukraine**.

4.3.3 Metallogenic areas for Nb-Ta associated with carbonatites

Several carbonatite complexes with exploration potential occur in western **Greenland**. These include the Sarfartoq carbonatite complex as well as the Qaqarssuk, Tikiusaaq and Grønnedal-Ika complexes (Steensgard et al., 2016). Notably, the early Phanerozoic Fen carbonatite complex in Telemark, on the margin of the Permian Oslo Paleorift, southern **Norway** hosts the Fen REE-Nb deposit, which includes the Søve Nb deposit at Ulefoss which was mined during 1953-1965 (e.g. Ihlen et al., 2014). **Swedish** carbonatites include Alnö and Åkersjön, both in central Sweden. The Sokli P-Fe-Nb-(Ta) deposit in northeastern **Finland** is hosted by the c. 0.38 Ga Sokli carbonatite complex (Rukhlov & Bell, 2010), which forms part of the Kola Alkaline Province (KAP). In **Germany**, the Storkwitz intrusive carbonatite complex hosts a marginally economic REE-Nb mineralization (Niegisch et al. 2020). The subeconomic Kaiserstuhl (15-18 Ma) carbonatite complex in South West Germany is situated in the Upper Rhinegraben rift of the Central European Magmatic Province (Schleicher et al., 1991; Wilson and Downes, 2006). The Novopoltavske deposit in Zaporizhia region in **Ukraine** is located within a complex of alkaline rocks and carbonatites in the Azov block of the Ukrainian Shield.

4.3.4 Metallogenetic area for Nb-Ta associated with placers

In **Portugal**, examples of Nb-Ta-enriched placers, most commonly associated with primary mineralizations, were identified in Eiradas, Escusa, Mãos, Meixedo and Santa Cristina (Serra De Arga mining region), Almendra mine, Quinta da Levada and Marinhol (Guarda mining region) (e.g. Leal Gomes 2016; SIORMINP 2002; Vieira 2010), and in Chaves, Montalegre (and Boticas) (Vila Real mining region; Ramos, 2010). Overall, (*sensu lato*) columbite – tantalite minerals and Nb-Ta enriched cassiterite were the main ore minerals reported from these Portuguese placers (SIORMINP, 2002). Nb and Ta are also found in placer deposits (Nakolice and Šejby) sourrounding the leucogranites in the

This project has received funding from the European Union's Horizon 2020 research and innovation programme under grant agreement No 731166

Central Moldanubian Plutonic Complex in the **Czech Republic**. Furthermore, Nb-Ta minerals have been identified in recent alluvial placers beneath the Bratislava massif, at Limbach in **Slovakia** (Uher and Žitňan, 2007). The large Malyshevske zircon-rutile-ilmenite placers in the Dnipropetrovsk region of **Ukraine** contain Nb-Ta.

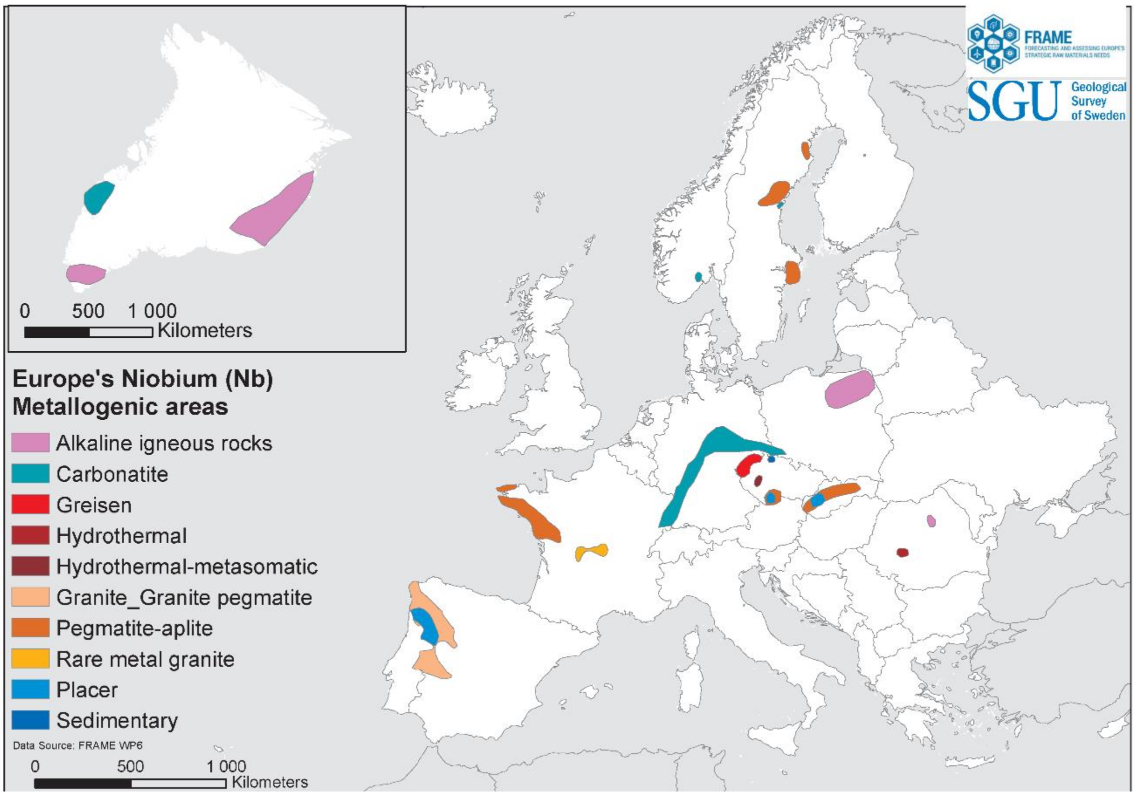

This project has received funding from the European Union's Horizon 2020 research and innovation programme under grant agreement No 731166

Figure 39. Overview map of Europe showing the approximate extent of the key Niobium metallogenic belts

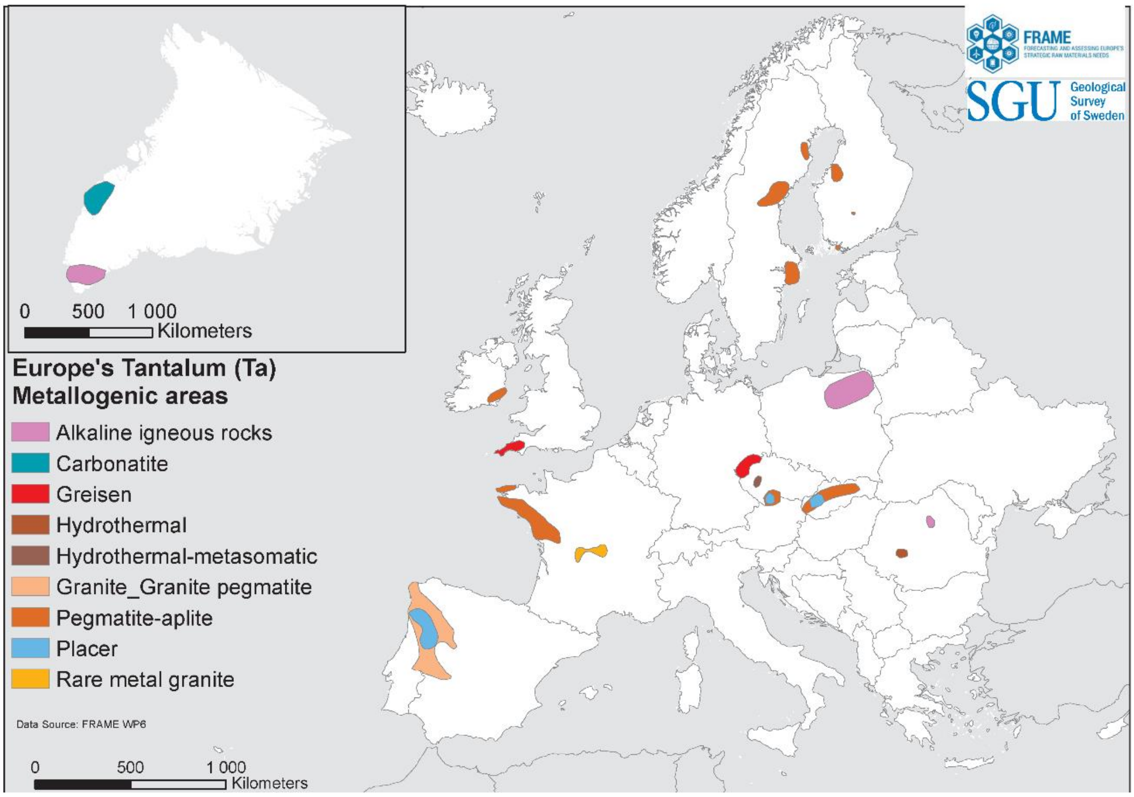

Figure 40. Overview map of Europe showing the approximate extent of the key Tantalum metallogenic belts

4.4 Energy Critical elements (natural graphite, lithium, cobalt)

The WP 5 in the FRAME project has a separate deliverable report entitled “provide mineral potential and prospectivity maps of key mineral provinces in Europe with deposits of, or potential for, energy critical elements in collaboration with WP3”. To avoiding repetition, comprehensive information on energy critical elements refer to the Deliverable D5.1.

In this report the distribution of graphite, lithium and cobalt mineralization in Europe is presented.

This project has received funding from the European Union's Horizon 2020 research and innovation programme under grant agreement No 731166

4.4.1 Keys mineral provinces (Lithium)

Taking into account the results of both mineral prospectivity and the distribution of lithium deposits and occurrences, **25 metallogenic provinces have been defined**. **Magmatic and magmatic-hydrothermal lithium mineralization** form numerous provinces that are mainly associated with two important orogenies: the Svecofennian and the Variscan. **Sedimentary-hydrothermal provinces** are hosted in more recent terranes (Cambrian to Neogene): 1) in some area (Li-bearing Fe-Mn deposits) of the Palaeozoic and Mesozoic sedimentary platforms affected by fluid circulation; 2) in the Neogene accretionary belts that are affected by extensional tectonic setting and arid climate during the Miocene (eg Jadar deposit, Pannonian basin); 3) in Mesozoic-Paleogene bauxites developed on the Pelagonian metamorphic massif (e.g. Hungary, Greece) (Figure 41).

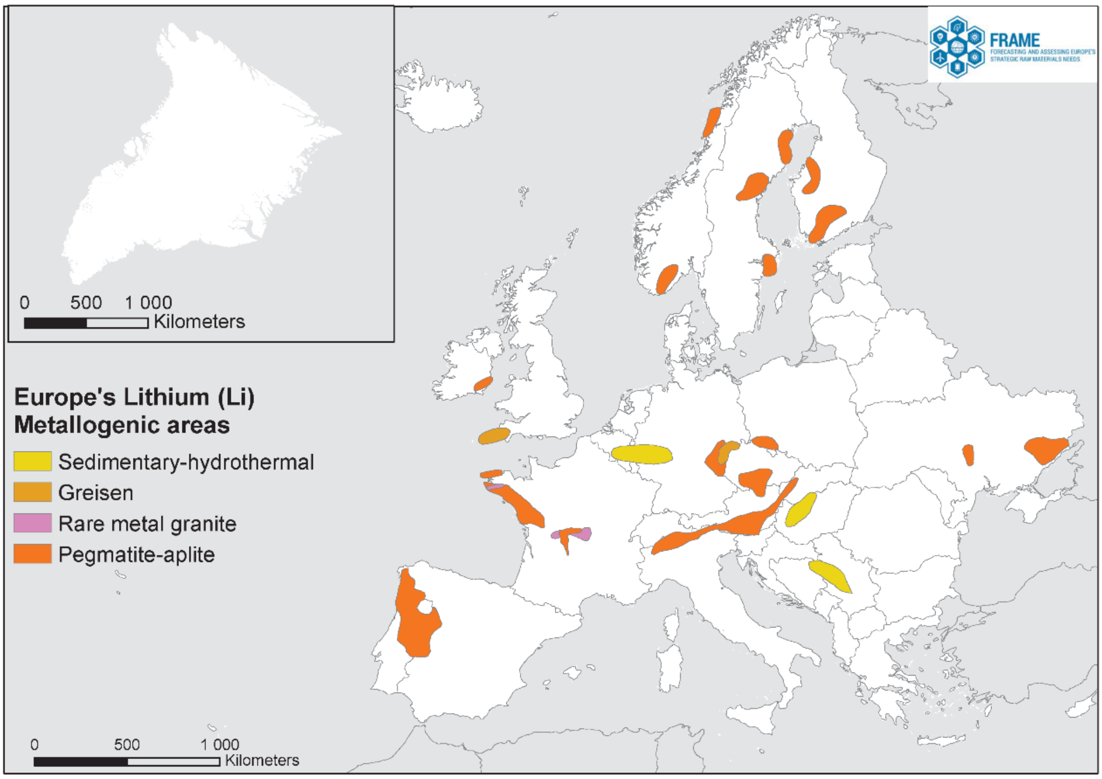

Figure 41. Main metallogenic provinces for lithium in Europe according the genetic type

Numerous **Li-rich pegmatites** are observed in several pegmatites field throughout Europe. In central Ukraine, several field of spodumene and petalite-bearing pegmatites

This project has received funding from the European Union's Horizon 2020 research and innovation programme under grant agreement No 731166

are known in the Archean basement, in the **Shpolyansko-Tashlykskiy province** (e.g. ***Nadiya*** deposit 728,896t Li_2O) and in the east of Ukraine, in the **Shevchenkivske province** (e.g. ***Shevchenkovskoe*** deposit 69,960 t Li_2O). In Finland and Sweden, prospective lithium-rich pegmatites are associated to the Svecofennian orogen (1.92-1.77 Ga). Most of them are emplaced close to dome or dome-like migmatitic areas affecting metasedimentary belts. Migmatitic areas are also intruded by numerous anatectic granites. Some typical examples are the **Kaustinen province** (e.g. ***Rapasaari deposit*** 49,632*t Li_2O)* and in the south of Finland, the **Somero-Tammela province** (e.g. ***Hirvikallio*** deposit *2,685 t Li_2O).* To the west in central Sweden, the Bothnian basin made of sedimentary and volcanic rocks (1.91-1.86 Ga) host the ***Skellefteå*** province (e.g. ***Varuträsk*** deposit) and the **Västernorrland province** (***Järkvissle***, ***Orrvik***). In the south of Sweden, the **Stockholm province** host the smallest potential. (***Utö*** archipelago). Another very prospective target is represented by **Variscan pegmatites**. The most important Variscan lithium-bearing pegmatite province is **the Galicia – Central-Iberian province** (Portugal and Spain) composed of more than 20 major Li-pegmatite fields (e.g. ***Barroso*** *241,000 t Li_2O*, ***Sepeda,*** *103,000 t Li_2O*, ***Alvarrões***, 51,069t Li_2O) and at the Spain-Portugal boundary, the ***Almendra-Fregeneda*** pegmatite field. In France, the most prospective areas for pegmatites are the **Ambazac-Creuse-Millevaches** province (***Chedeville*** pegmatites, Raimbault, 1998), the **South Brittany province** (***Saint-Sébastien-sur-Loire***) and the **Leon province** (e.g. ***Santec***). In the Bohemian Massif, lithium-bearing pegmatite fields are mainly represented by three provinces, the **Sudetes**, the **Saxo-Thuringian** and the **Moldanubian provinces**. In United Kingdom, the main Lithium-rich pegmatite-aplite is the ***Meldon*** aplite (45,500.16 t Li_2O) located in the **Cornwall province**. In Romania, Spodumene-albite subtype pegmatites are known in the ***Conţu-Negovanu*** pegmatite field (South Carpathians) In Austria, pegmatites are not Variscan but Lower Permian in age. The **Austroalpine province** (e.g. ***Weinebene*** spodumene deposit, *109,800 t Li_2O*) is composed of thousand pegmatites on an extend of 400km, from the north of Torino up to the south of Vienna.

Lithium-rich high-phosphorus rare element granites are scarce in Europe. Despite their small size (<1 km^3) they are the host of large, disseminated mineralization. Some amblygonite-quartz veins are sometimes associated with those granites. In France, the most important target for lithium-rich granites is the **rare element belt** that includes 4 rare-element granites and rhyolite, (e.g. ***Beauvoir*** granite 375,300t Li_2O). To the west, in the Armorican massif, the **Audierne bay province** include several dykes of Li-rich high-

This project has received funding from the European Union's Horizon 2020 research and innovation programme under grant agreement No 731166

phosphorus rare element granite (e.g. ***Tréguennec-Prat-ar-Hastel*** dyke, 66,300 t Li_2O). In Iberia (Spain and Portugal) several Isolated amblygonite-quartz veins, amblygonite-lepidolite-bearing rare-element granite are also known in the CIZ (e.g. ***Argemela*** deposit in Portugal, 49,950 t Li_2O and the ***San José – Valdeflorez*** deposit, 683,200t Li_2O in Spain). In United Kingdom, the ***Saint Austell*** granite contains a large volume of disseminated Li-bearing micas (Zinnwaldite, Lepidolite) with resources estimated to 2,921,631.77 t Li_2O.

The most important **lithium-rich greisens** are located within lithium-poor low-phosphorous rare element granites in the **Erzgebirge province** at the Czech-Germany boundary. Numerous greisens are known in this area, the most emblematic being the ***Cinovec*** greisen with Li resources estimated to 2,921,631t Li_2O and the ***Zinnwald*** greisen with Li resources estimated to 124,959.69 t Li_2O. In United Kingdom, the main greisen mineralization is located in the **Cornwall province**. The ***Tregonning-Godolphin*** and ***Cligga-Head*** granites represent small but significant volumes of metasomatised granite with lithium hosted by lepidolite.

Some European mineralization are related to **exogenous processes** (fluid circulation, supergene weathering, alterite remobilization by erosion, etc). Among the various type of lithium mineralization associated to these processes, the main known lithium mineralization in Europe are the Jadar-type, some Li-bearing Mn-Fe- mineralization (lithiophorite) and some Li-bearing bauxites. Li-rich hectorite mineralization seems to be absent in Europe. In Serbia, the ***Jadar*** deposit (resources of 2,524,020t Li_2O) is the most important deposit of the **Jadar province.** This deposit is characterized by several 1.5 to 35m-thick lenses of jadarite (Lithium borosilicate) interbedded within a Miocene lacustrine serie close to a basement where granites and spodumene pegmatites occur suggesting local lithium enrichment in the basement. Other occurrences in the Miocene lacustrine sediments are mainly Li-bearing montmorillonite. In Europe, bauxite deposits occur from Spain to Turkey, including parts of southern France, Hungary, Italy, Greece and the Balkans. Despite this large number of occurrences, the lithium content of European bauxite remains poorly constrained apart from the **West Hungary bauxite province**. Thus, Li-bearing minerals in bauxite deposits are known in Cretaceous bauxites from Hungary (e.g. ***Halimba*** mining district) and in Jurassic to Cretaceous bauxites from Greece.

In Europe, Lithiophorite-bearing Fe-Mn deposits are of 2 types, Fe-Mn reddish siliciclastic rocks and Mn-Fe lenses or layers. In these Fe-Mn rich rocks, the presence of lithioporite

This project has received funding from the European Union's Horizon 2020 research and innovation programme under grant agreement No 731166

is secondary, related to fluid circulation. Despite the presence of lithiophorite, the amount to lithium is generally low. A first group of deposits in Scotland, Wales (e.g., ***Drosgol Mine***), England (***Clews Gill***), in the **Ardennes province** (Belgium: ***Ottré***, ***Beez***; Germany: ***Harz***) is Cambrian to Early Ordovician in age. The second group is mainly found in Hungary (***Eplény*** and ***Urkut*** Mn deposits) and deposits are Jurassic in age.

4.4.2 Key mineral provinces graphite

Even if graphite is a quite common mineral in meta-sedimentary rocks in many places in Europe, it is rare to find enrichments that are economical interesting. Presently mining is taking places only in three European countries (Austria, Norway and Ukraine) and the present consumption of graphite is about 85.000 t/a of which about 90% is imported (European Commission, 2020)

Graphite is formed when volatiles like CO_2, CH_3 and H_2O are released from organic matter during metamorphism. Chemical reduction leads to the formation of carbon and graphite. If this is deposited syn-genetically in the rock the result is flake graphite deposit, if however, the carbonaceous material is deposited epigentically in veins the results is vein type graphite deposits. (Buseck and Beyssac, 2014). The industry classifies graphite deposits into three types; 1-flake, 2-vein and 3-amorphous graphite. The latter is usually not amorphous but micro crystalline, with grain size of graphite crystals less than 1 micrometer (Beyssac and Rumble, 2014).

Compared to lithium, cobalt or most other mineral commodities, there are relatively few studies of graphite occurrences. Graphite mines are most commonly private enterprises, and data on resources and reserves ore often confidential. The information available related to geology and resources are therefore very variable for graphite occurrences in Europe.

World mining data (Reichl and Schatz, 2019) show that presently graphite is produced in Austria, Germany Norway and Ukraine.

From the groupings of occurrences shown on Figure 42. 30 provinces are shown, a large number of the occurrences have the genetic type unclassified due to the mentioned low number of studies available.

Roughly the following main area with graphite mineralization is present:

a. The Fenneoscandian shield area, of Norway, Sweden and Finland
b. The Ukrainian shield

This project has received funding from the European Union's Horizon 2020 research and innovation programme under grant agreement No 731166

c. Central Austria and Bavaria

d. The Iberian peninsula of Spain and Portugal

The graphite occurrences of the **Fennoscandian shield** are all of Proterozoic age and occur in high metamorphic grade metasedimentary rocks. Norway, Sweden and Finland there are more than 50 occurrences registered in each country. The most famous or largest deposits in each country is the Skaland graphite deposits on Islands of Senja in Norway, the Nunasvarra deposit of northern Sweden and the Pipumäki occurrence of Central Finland. Official grade or tonnage from, Nunasvarra is 25.6 % graphite and 12.3 Mt, from Piipumäki 6.4% graphite and in northern Norway 28 different occurrences have an aggregate estimated tonnage of 241.6 mt and average graphite content of 9.3% (Lynch *et al.,* 2016; Lynch *et al.,* 2018; Gautneb *et al.,* 2020; Palosaari *et al.,* 2020).

The graphite occurrences of the **Ukraine** are all located on the Ukrainien shield which is broken up by faults into several blocks which comprises arcehan to proterozoic rocks of metasedimentary gneisses amfibolites and various mafic to acid igneous rocks. The most important graphite occurrence in Ukraine is the Zavalyevskiy deposit, which is also the only in current production. Our database contains 35 occurrences and deposits registered in Ukraine that have aggregated resources 1615 Mt with an average graphite content of 5.1%.

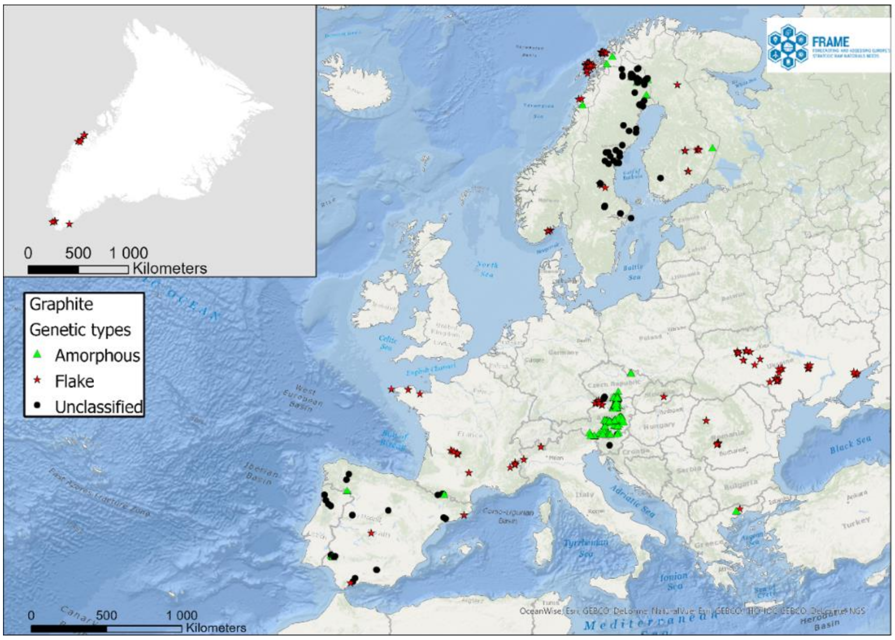

This project has received funding from the European Union's Horizon 2020 research and innovation programme under grant agreement No 731166

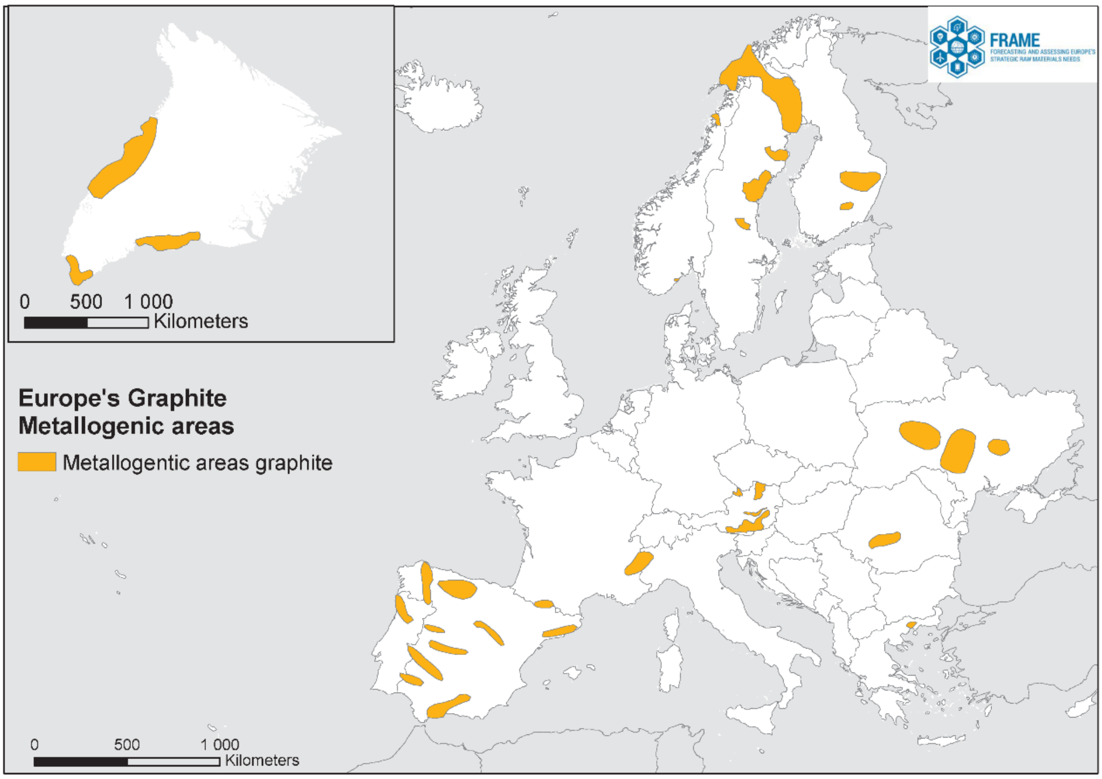

Figure 42. Genetic type of graphite occurrences and the main metallogenetic provinces of graphite in Europe.

In **Greenland** there are 7 occurrences in our database, they are described by (Stensgaard *et al.,* 2017). They are all located in Archean or Proterozoic rocks. They are all flake graphite occurrences and the resources is determined for some of them and with tonnages in the range from 1 to 5 mt and graphite content in the range from 5 to 25%.

In **Spain** there is scattered occurrences all over the Iberian Peninsula, very few studies are published. In the Aracena mountains in southern Spain graphite occurrences are described from the Neoproterozoic rocks containing meta sedimentary gneisses, amfibolites and granulites. Graphite occur strata bound with typical 10 -30% graphite, but can reach up to 50%. A number of mines where in production around 1910 (Rodas *et al.,* 2000).

This project has received funding from the European Union's Horizon 2020 research and innovation programme under grant agreement No 731166

In **Austria** there are 4 provinces with graphite occurrences in north east the **Dosendorf** graphite province (Figure 42). The graphite occurs in a series of paragneisses, amphibolites and marbles that are of Proterozoic age. Metamorphic conditions have been up to 700-800 °C and 8-11 Kbar (Müller *et al.,* 2016). Carbon content of the graphite bearing rocks can be very high up to 60% with a median of 38%. (Schedl *et al.,* 2016). At about 30 different sites, graphite where mined from 1995 until the last closed in 1994 (Hofbauer, 1995).

The north western province the **Moldanubikum (Bavarikum)** graphite province. These occurrences occur in the Kropfmühl- Herzogsdorf comples and comprises graphite schist comparable to the Krompfmühl area in Germany. Graphite content are reported to reach up to 48% (Holzer, 1964). Graphite was produced periodically until 1963.

In the **Veitsch nappe (Kaisersberg)** there are about 50 occurrences which for a large part contain microcrystalline (amorphous) graphite) and semi graphite (Rantitsch *et al.,* 2004). Metamorphic conditions have reached upper green schist facies. Carbon content can reach up to 90% locally. In this province the only graphite mine in operation Austria (Kaisersberg) is located producing about 420 t/a of graphite.

In **Drau-Mur (Sothern Styria area)** the area is dived into 2 different tectonic units. Host rocks are believed to be of Palaeozoic ages that was metamorphosed up to 500-600°C and 6-10 Kbar. Graphite occurs in several layers reaching thicknesses up to about 1 meter. Graphite has been mined periodically in this area at a couple of deposits, Last mining activity was in 1916 (Ucik, 1992; Schuster *et al.,* 2006)

4.4.3 Key mineral provinces for Cobalt

Cobalt occurs as relatively common trace to minor constituent in many types deposit types of different commodities. In Europe, the most common deposit types are orthomagmatic Ni-Cu-Co deposits, volcanogenic Cu-Zn-sulfide deposits (VMS), Iron Oxide-Cu-Au deposits (IOCG), 5-element and other vein-type deposits, sediment-hosted Cu deposits, lateritic Ni-Co deposits and metasediment-hosted Cu-Au-Co deposits (e.g. Horn et al., 2020). Generally, the Co content of the se deposits vary from less than 100 ppm (0.01 %) to a few thousands of ppm. Most of the cobalt bearing deposits and occurrences are clustered in Nordic countries (Finland, Sweden and Norway), with more scattered deposits occurring in southern and central Europe. Several lateritic deposits are clustered in the Balkans, Greece and Ukraine, but cobalt is generally not extracted from these deposits. Currently cobalt is produced only from three mines in Finland in Europe. The Eu consumption of cobalt ores, concentrates and intermediates is ~14 000 t of which

This project has received funding from the European Union's Horizon 2020 research and innovation programme under grant agreement No 731166

14% comes from within the EU (Finland) and the rest is exported mainly from DRC (European Commission, 2020)

As a minor constituent, cobalt is often not included in mineral resource and reserve estimates. Where available, data indicate significant resources mainly in Finland, Norway and the Balkans. Largest resources occur in the black schist hosted Talvivaara (Sotkamo) Zn-Ni-Cu-Co mine in Finland (~290 000 t) and in the lateritic Mokra Gora Ni-Co deposit in Serbia (360 000 t) (Horn et al., 2020)

Based on the clusters of occurrences shown on Figure 43. 34 provinces were delineated. Broadly, the following main cobalt metallogenic zones are:

a) The Fennoscandian shield: Norway, Sweden and Finland
b) Greenland
c) The Balkans and Greece
d) SW and central Europe

Most of the cobalt occurrences of the **Fennoscandian shield** are Proterozoic in age, ranging from Archean to Early Proterozoic in Finland, Early Proterozoic in Sweden (Paleozoic in the Calonides in westernmost Sweden) to Meso-Neoproterozoic to Paleozoic in Norway. All three countries contain a high number of Co-bearing occurrences with Finland having 123, Norway 85 and Sweden 63. In Finland, past production of cobalt came from the Kotalahti and Vammala belts (orthomagmatic Ni-Cu-Co deposits) and from the Outolumpu area Cu-Zn-Ni-Co VMS deposits. Very little Co-production data is available from the Ni-Cu-Co deposits but the Outokumpu area mines (5) produced 75 000 t of Co. Current mine production comes from Kevitsa Ni-Cu-Co-Au-PGE deposit; 450-550 t per year, Kylylahti Cu-Zn-Ni-Co deposit; 450 t per year, and Sotkamo (Talvivaara) Ni-Zn-Cu-Co deposit; estimated to be 500 t per year. In Norway, most significant Co deposits are magmatic Ni-Cu-Co deposits and Co-containing VMS deposits in southern and central Norway (e.g. S-Norway, Joma-Lokken, and Sulithjelma areas). Historic Co-production has come from e.g. Ertelien Ni-Cu mine (1789 t) and the Skuterud Cu-Co mine, from southern Norway (Sandstad et al., 2012). In Sweden, most of the known Co-deposits are magmatic Ni-Cu-Co deposits in the Skellefte and Bergslagen areas with historic Co production from Bergslagen area deposits and, e.g. Gladhammar in southern Sweden (Hallberg et al., 2012).

This project has received funding from the European Union's Horizon 2020 research and innovation programme under grant agreement No 731166

The bulk of Co-occurrence in **Greenland** are located in western Greenland, in the Archean Maniitsoq Norite belt, which contains some 65 orthomagmatic Ni-Cu-Co+PGE occurrences (North American Nickel, 2015; Stensgaard et al., 2017).

The **Balkans and Greece** host some 27 lateritic Ni-Co deposits and occurrences. Some deposit in Greece, Albania, Kosovo and North Makedonia have been mined for nickel but not for Co. However, they contain locally significant Co-resources, especially the Mokra Gora deposit in Serbia (Horn et al., 2020). Further lateritic Ni-Co deposits occurr in Ukraine.

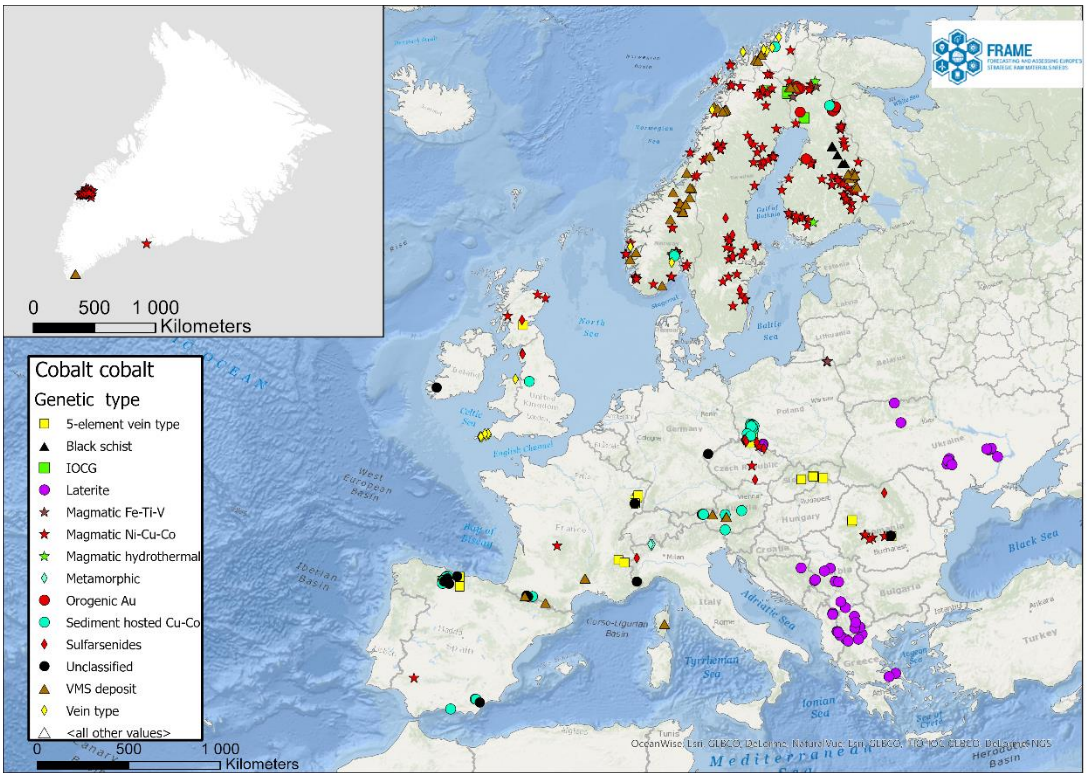

This project has received funding from the European Union's Horizon 2020 research and innovation programme under grant agreement No 731166

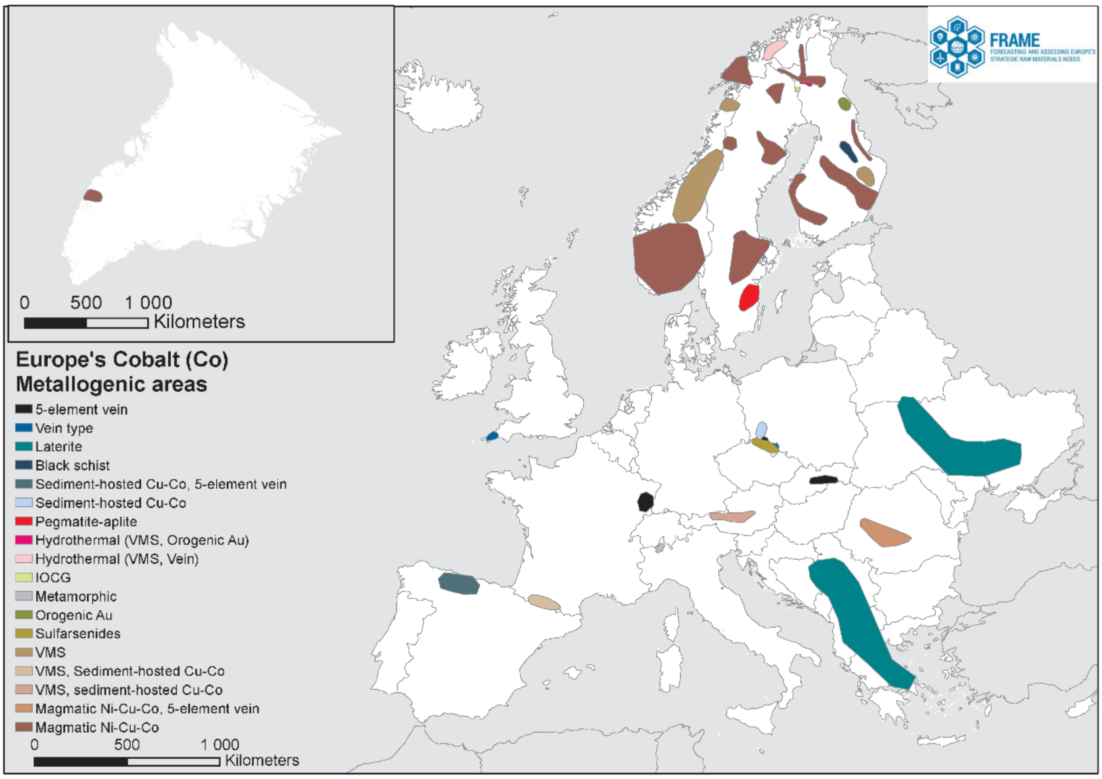

Figure 43. Genetic types of cobalt occurrences and the main metallogenetic provinces of cobalt in Europe.

Elsewhere in the Europe, small, mostly historic Co deposits and occurrences can be found related to variscan and Alpine orogenies, extending from Cantabrian mountains in NW Spain, trhough Pyrenees and France, northern Italy, Austria, Slovakina and Romania in the east. A cluster of Co-deposits also occur in the SW Poland. They represent a diverse suite of deposit types with sediment-hosted Cu-Co, 5-element vein type, VMS (to SEDEX) deposit and Co-sulfarsenide (vein) type being the most prominent types. In addition, magmatic Ni-Cu-Co deposits occur in Romania and lateritic Ni-Co deposits in SW Poland.

This project has received funding from the European Union's Horizon 2020 research and innovation programme under grant agreement No 731166

5 Seafloor mineral deposits in pan-European and their associated CRM cobalt and phosphorous

5.1 Introduction

Covering more than 70% of the planet, oceans represent a potentially promising new frontier for the exploration of mineral resources. Security of mineral supply has been identified by the European Commission as a priority challenge facing the raw materials sector. The 2020 list of Critical Raw Materials (CRM) now reflects societies growing demand for an ever-increasing number and quantity of elements and minerals that supply the green energy and technology sectors (European Commission, 2020). The global demand for cobalt, phosphorous, rare earth elements, tellurium, nickel, lithium, copper, and other rare and critical metals, concurrent with the rapidly diminishing quality and quantity of land-based mined deposits, has situated the seafloor as a promising new frontier for the exploration of mineral resources. Studies dedicated to understanding the genesis, distribution, and resource potential of deep-sea minerals began in the late 1970s to early 1980s (Hein et al., 2013). Spanning a large diversity of environments and resource style, including high and low temperature hydrothermal deposits (seafloor massive sulphides-SMS, sedimentary exhalative deposits-SEDEX), phosphorites, cobalt-rich ferromanganese crusts, manganese nodules and rare earth elements-rich muds, deep-sea deposits are particularly attractive for their polymetallic nature with high contents of transition, rare and critical elements. Moreover, shallow-water resources, like marine placer deposits, represent another source for many critical metals and gems. The seabed mineral resources host the largest reserves on Earth for some important metals like cobalt, lithium, tellurium, manganese, and the rare earth elements, critical for Industry.

5.2 From exploration to mining the seabed mineral deposits

The first deep-sea discoveries comprised: 1) extensive polymetallic nodule fields in Clarion–Clipperton Zone (CCZ) (Mero, 1962); 2) hydrothermal systems and associated metalliferous sediments, sulfide chimneys and mounds in the Red Sea and Pacific Ocean (Bäcker and Schoell, 1972; Corliss et al., 1979; MacDonald et al., 1980); and 3) Fe-Mn crusts rich in cobalt on seamounts from the Atlantic and Pacific Ocean (Halbach et al., 1982). These findings were the base for the research and exploratory works during the last five decades. Recent discoveries of white smokers associated with ultra-mafic hosted serpentinization (Lost City; Kelley et al., 2001) and rare earth elements-rich muds from the Pacific Ocean (Kato et al., 2011) have contributed to increased our knowledge on the diversity of mineralization styles, and the complex interactions between geosphere, biosphere and hydrosphere to form all these types of mineral deposits. Among the deep-

This project has received funding from the European Union's Horizon 2020 research and innovation programme under grant agreement No 731166

sea deposits, the most interesting for their cobalt and phosphorous concentrations are the ferromanganese crusts and phosphorites respectively, with a smaller impact of polymetallic nodules (Hein et al., 1997; Hein et al., 2016).

Mining of nodules anticipated to begin in the late 1970s to early 1980s did not take place. The abrupt fall in the price of base metals in the beginning of 1980s caused many of the onshore mining operations to cease, and the interest in the exploitation of marine minerals decreased. In the beginning, the commercial interest was based on base and noble metals (e.g., Mn, Cu, Zn, Au, Ag). Rare metals (e.g., Co, Te, Nb, Pt) and REEs beneficiation as by-products of mining of the major metals have centered the research undertaken in the last decade (Hein et al., 2013). Vast areas of deep-ocean floor have been contracted for exploration, and more contracts are taken out every year. The International Seabed Authority (ISA) is finishing the exploitation regulations that will permit State parties, State enterprises or natural or juridical persons or consortia of entities to extract minerals in areas beyond national jurisdictions, the so-called "Area" (Figure 40). In 2000, 2010 and 2012, the Council and Assembly of the ISA passed regulations for the exploration for polymetallic nodules, polymetallic sulfides and cobalt-rich ferromanganese crusts respectively (ISA, 2020). Thirty contractors have entered into 15-year contracts with ISA for exploration for polymetallic nodules, polymetallic sulphides, and cobalt-rich ferromanganese crusts on the deep seabed of the Atlantic, Pacific, and Indian oceans (ISA, 2020). Over the 15 years these exploration areas will be subject of relinquishment and will be smaller by the end of the contract (not more than 2500 km^2 in the case of polymetallic sulphides and not more than 1000 km^2 in the case of cobalt-rich ferromanganese crusts). Now, various deep-ocean small mines are scheduled to start operations in the Red Sea, Southeast Atlantic and Southwest Pacific Ocean within the next years in national jurisdictions (Figure 44).

This project has received funding from the European Union's Horizon 2020 research and innovation programme under grant agreement No 731166

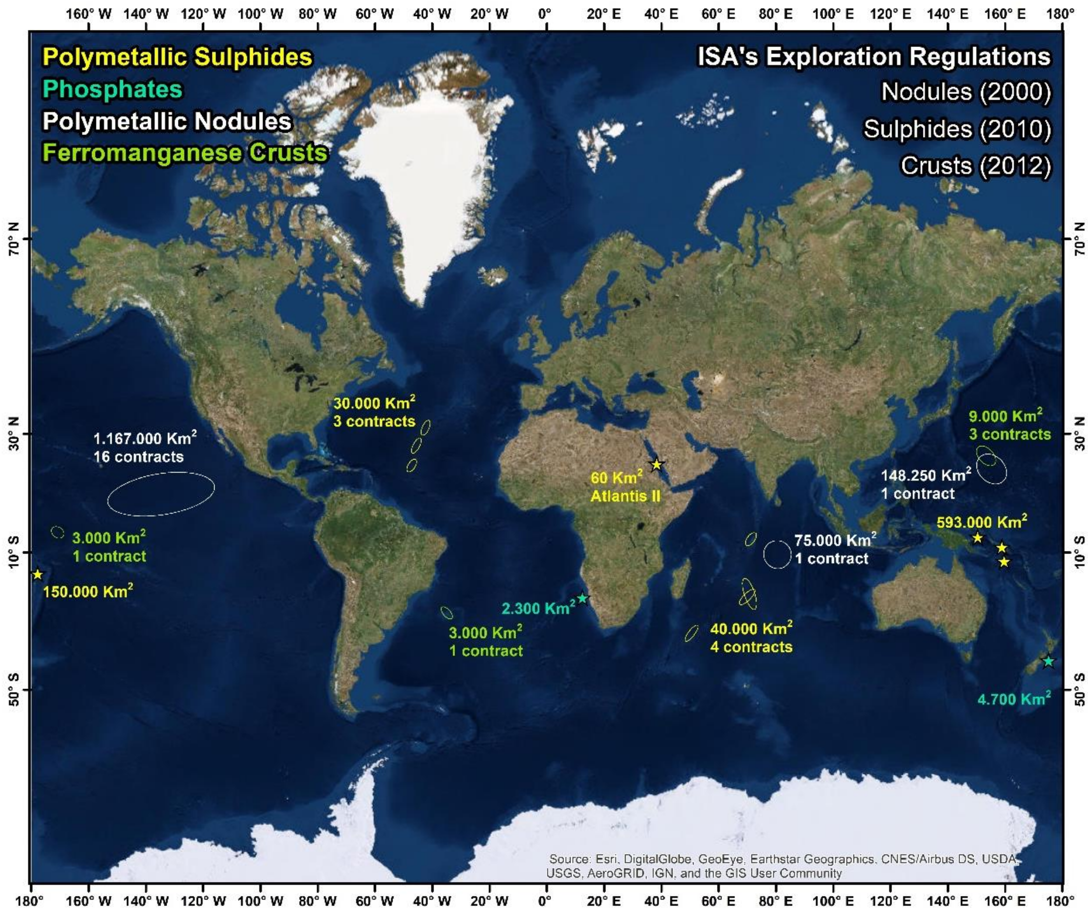

Figure 44. Global map of seabed minerals exploration present status. The stars represent areas under national jurisdictions. Modified from Hein et al. (2013).

5.3 Cobalt mineralization types in pan-European seas.

Ferromanganese (Fe-Mn) deposits are represented essentially by hydrogenetic Fe-Mn crusts, diagenetic polymetallic (or manganese) nodules and hydrothermal sediments and crusts. These deposits can be found in all the oceans covering both abyssal planes (nodules and metalliferous sediments) or hard surfaces on seamounts, banks, ridges and plateaus (Fe-Mn crusts). The main mineral deposit for cobalt is represented by Fe-Mn crusts. These deposits can be usually found covering sedimentary and basaltic substrates at water depths from about 400 to 7000 m, although thicker crusts can be found between 1500 and 2500 m (Hein et al., 2000; 2009; 2014). Several studies on Fe-Mn crusts show that they concentrate important contents of Co, but also, depending on the genetic

This project has received funding from the European Union's Horizon 2020 research and innovation programme under grant agreement No 731166

process and mineralogy, valuable contents of several other CRMs like Te, Li, REY, etc. In pan-European seas these deposits are localized essentially in the Macaronesia and Iberian continental margins (Spain and Portugal) and in the Arctic Ocean (Norway, Iceland, Greenland and Russia) (Baturin et al., 2014; González et al., 2016; 2018; Marino et al., 2017; Hein et al., 2017; Konstantinova et al., 2017; EMODNET, 2020; MINDeSEA, 2020) (Figure 45). These crusts form thin layered deposits of Fe and Mn oxyhydroxides that grow essentially by hydrogenesis, caused by the slow precipitation of oxide floccules from the cold seawater on the seamount substrates. The main mineralogy is represented by hydrogenetic vernadite (δMnO2) and goethite (α-Fe3+O(OH)), with small amounts of diagenetic Mn oxides (asbolane, buserite and todorokite) or hydrothermal minerals (essentially neo-formed goethite). Cobalt is concentrated especially in hydrogenetic Fe-Mn crusts with contents varying from 0.1 to 1 % and with an average contents of 0.4 %. Hydrogenetic Fe-Mn crusts also concentrate significant contents of other interesting metals like Mn, Ni, Cu (respectively in average 10, 0.2 and 0.08 %) and several CRMs as Mo, Te and REY (360, 40 and 2000 µg/g) that can be considered as byproduct of the main extraction. The hydrogenetic precipitation of Fe-Mn oxyhydroxides on hard surfaces with very slow growth rates (<1 to 10 mm/Ma), allow the enrichment in all the elements listed. This is why hydrogenetic Fe-Mn crusts show ages up to 90 Ma, and the oldest identified in pan-European seas can be found on the Canary Islands seamounts (Marino et al., 2017; 2018; 2019).

This project has received funding from the European Union's Horizon 2020
research and innovation programme under grant agreement No 731166

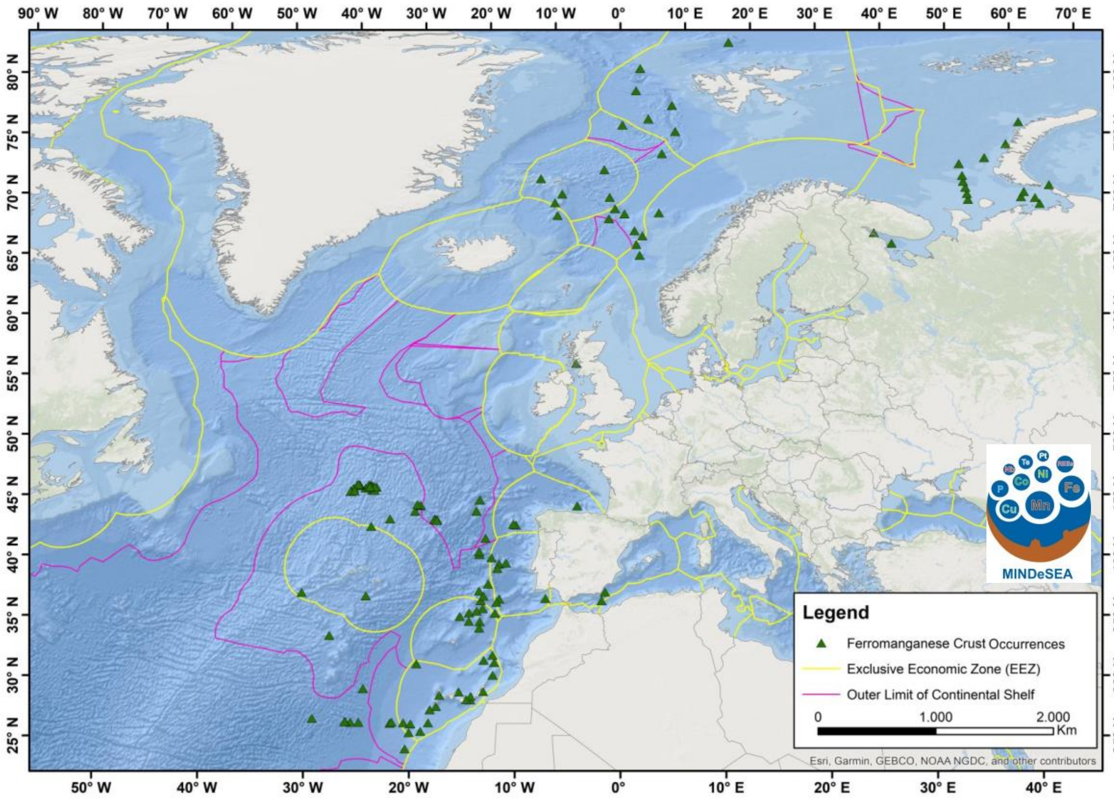

Figure 45. Simplified spatial distribution of Co occurrences in European seas.

5.4 Phosphorous mineralization types in pan-European seas.

Phosphorous can be found in different contents in all the submarine ferromanganese deposits but in general these contents are not interesting for its mining. The only deposit that shows great contents of P is represented by marine phosphorites. Phosphorites are formed during diagenetic processes in different oceanic settings as lagoon/insular areas, continental margins and seamounts (McArthur et al., 1984; Hein et al., 2016). In pan-European seas can be found on old seamounts in the Macaronesia and brans from the Iberian continental margins (Gaspar, 1981; Gonzalez et al., 2016; Marino et al., 2017; EMODNET, 2020; MINDeSEA, 2020) (Figure 46). This type of mineralization seems to have occurred during two main Cenozoic episodes of phosphatization: the Eocene-Oligocene (39– 34 Ma) and Oligocene-Miocene (27–21 Ma) with potentially other minor phosphogenic events, especially the middle Miocene, about 15 Ma ago (Hein et al., 1993). Phosphorites are formed essentially by carbonate fluor-apatite with small quantities of

This project has received funding from the European Union's Horizon 2020 research and innovation programme under grant agreement No 731166

detrital (e.g., quartz) and/or authigenic minerals (eg., calcite). Phosphorites show contents of P varying from 7.5 to 27 % and an average of 11 %, with low concentrations of all the other major elements except for Ca that vary from 17 to 35 %. Phosphorites and Fe-Mn crusts many times occur in association as occur in the Pacific and the Atlantic oceans (Hein et al., 2016; González et al., 2016; Benites et al., 2020), being the seamounts with substrates of phosphorites covered by Fe-Mn crusts as potential mine locations both for Co and P. Phosphorites also concentrate interesting contents of other elements as F (from 0.5 to 2.5 %) and especially REY (from 500 to 2000 µg/g with an average content of 1000 µg/g), with particular interesting contents of all the HREE and specially Y (MINDeSEA, 2020).

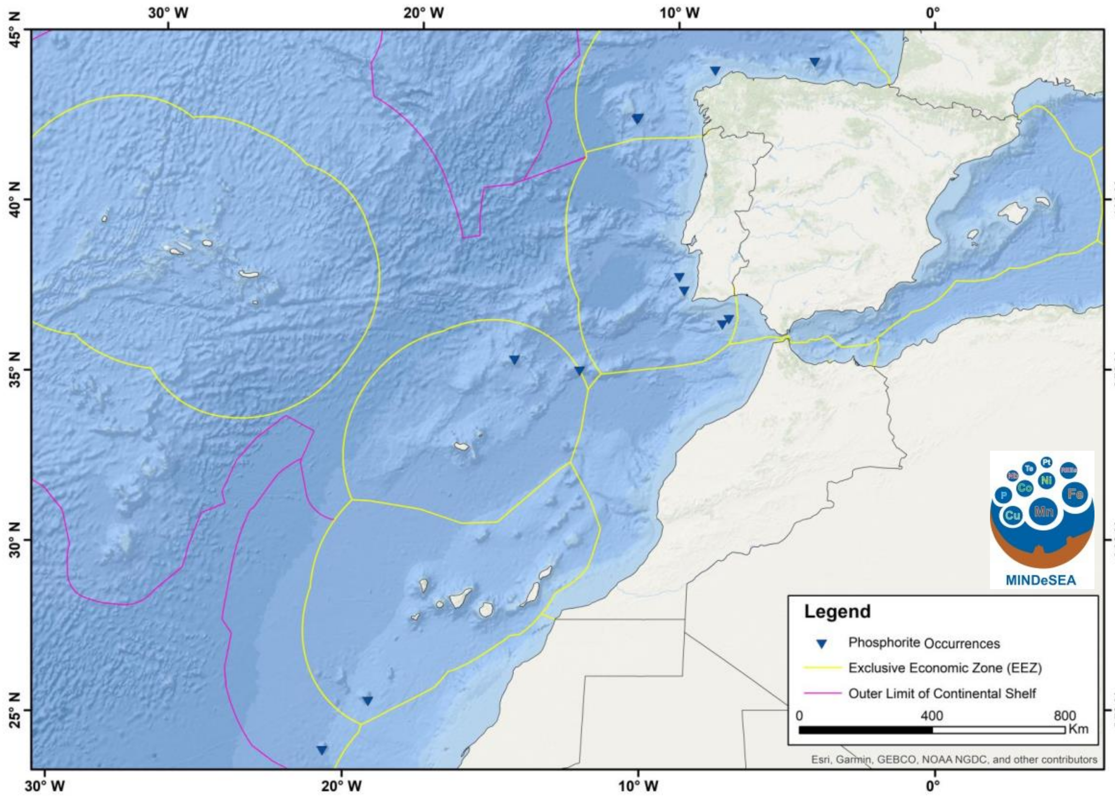

Figure 46. Simplified spatial distribution of P occurrences in European seas.

5.5 Co and P metallogenic areas in European seas

The MINDeSEA dataset contains a compilation of 141 ferromanganese crusts occurrences and 12 occurrences for phosphorites in pan-European seas (MINDeSEA, 2020). The metallogenetic areas definition, maps and reports are based on these records. Two

This project has received funding from the European Union's Horizon 2020 research and innovation programme under grant agreement No 731166

simplified maps with approximate spatial distribution of Co and P metallogenic areas on the base of previous research papers and projects are showed in Figs 47 and 48 (González et al., 2016; 2018; Marino, 2020; MINDeSEA, 2020).

5.5.1 Metallogenic areas for Co associated with Fe-Mn crusts

Three main areas can be separated in pan-European seas: 1) the Macaronesia and Iberian Margins, 2) the north Atlantic and Arctic oceans, 3) the Kara and Barents seas. In these areas can be found several marine seafloor elevations (knolls, seamounts, guyots, banks, plateaus) covered by Fe-Mn crusts with different Co concentrations.

Iberian margins and Macaronesia - All around the Iberian Margin have been recovered Fe-Mn crust samples covering the seamounts located at the south (Alboran Sea and Gulf of Cadiz) and in the north (essentially Galicia and Le Danois banks). Galicia Bank represents a huge plateau located 150 km at the west of the Spanish coasts. This plateau rises from a maximum depth of 5000 to 600 m with an area of 30,000 Km2. In this area have been recovered several Fe-Mn deposits (both crusts and nodules) but also numerous samples of phosphorites (González et al., 2016; MINDeSEA, 2020). The studies made on the Fe-Mn crusts show high contents of Co (up to 0.85 %) with remarkable contents of Mn (20 %) and Ni (0.65 %) but with lower contents of REY (0.1 %) compared with CISP. This difference is due essentially on the genetic processes that occurred in the formation of these crusts that are essentially diagenesis with a low participation of hydrothermalism (geothermal fluids).

In the Macaronesia area have been recognized hundreds of knolls and seamounts with significant Fe-Mn crust pavements. These seamounts are located in the south west of the Iberian Margin but also around the three archipelagos formed by Azores, Madeira and Canary Islands and on the Mid Atlantic Ridge. In this area have been recovered several Fe-Mn crusts with average contents of Co of 0.35 % and up to 0.79% (Muiños, 2015; Merle et al. 2018). The Canary Island Seamounts Province (CISP) represents a singular case with high economic potential in Macaronesia. The area encloses more than a hundred of seamounts and submarine hills in the Spanish EEZ that are considered an ancient “hot-spot” track in the Atlantic Ocean (Figure 47). These old seamounts (Jurassic and Cretaceous age i.e. Tropic, Las Hijas and The Paps) from the Central Atlantic (van den Bogaard, 2013) cover a summarized an area of 24,000 Km2 and are covered with extensive pavements of thick Fe-Mn crusts (up to 25 cm) (i.e. Marino et al., 2017; 2018; 2019; MINDeSEA, 2020). Co contents in this area show an average of 0.4 % and highest contents of 0.8 %, the main mineralogy is represented by vernadite that in spot analyses

This project has received funding from the European Union's Horizon 2020 research and innovation programme under grant agreement No 731166

concentrate up to 1.7 % of Co but also the highest contents of REY (0.5 %). Preliminary mining studies show that one square kilometer on the top of the Tropic Sm. could provide a minimum of 220 Mt of Co but also 9,000 Mt of Mn, 84 Mt of Ni and 170 Mt of REY (Marino, 2020).

North Atlantic and Arctic oceans - In this area have been recovered several Fe-Mn crusts associated at the presence of plateaus (420,000 Km2) and ridges (107,000 Km2) distributed from 63°N to 78°N in Norway, Iceland and Greenland (Figure 47). These crusts show a lower average Co contents respect to the CISP of 0.2 % and a maximum of 0.36 %. REY contents are also interesting with an average of 0.3 % (MINDeSEA, 2020).

Barents Sea and Kara Sea - The area represents shallow seas from Russia above the continental shelf with maximum depths of 450 m and an average of 250 m (Figure 47). In the area have been recovered several Fe-Mn crusts usually linked to the presence of large shelf areas. Fe-Mn crusts recovered here show a completely different, respect to the deep-sea deposits, mineralogy (dominated by goethite) and geochemistry (up to 20 % Fe and 18 % Si). Preliminary geochemical studies also show low contents of Co (0.01%) and very low REY (Ingri, 1985).

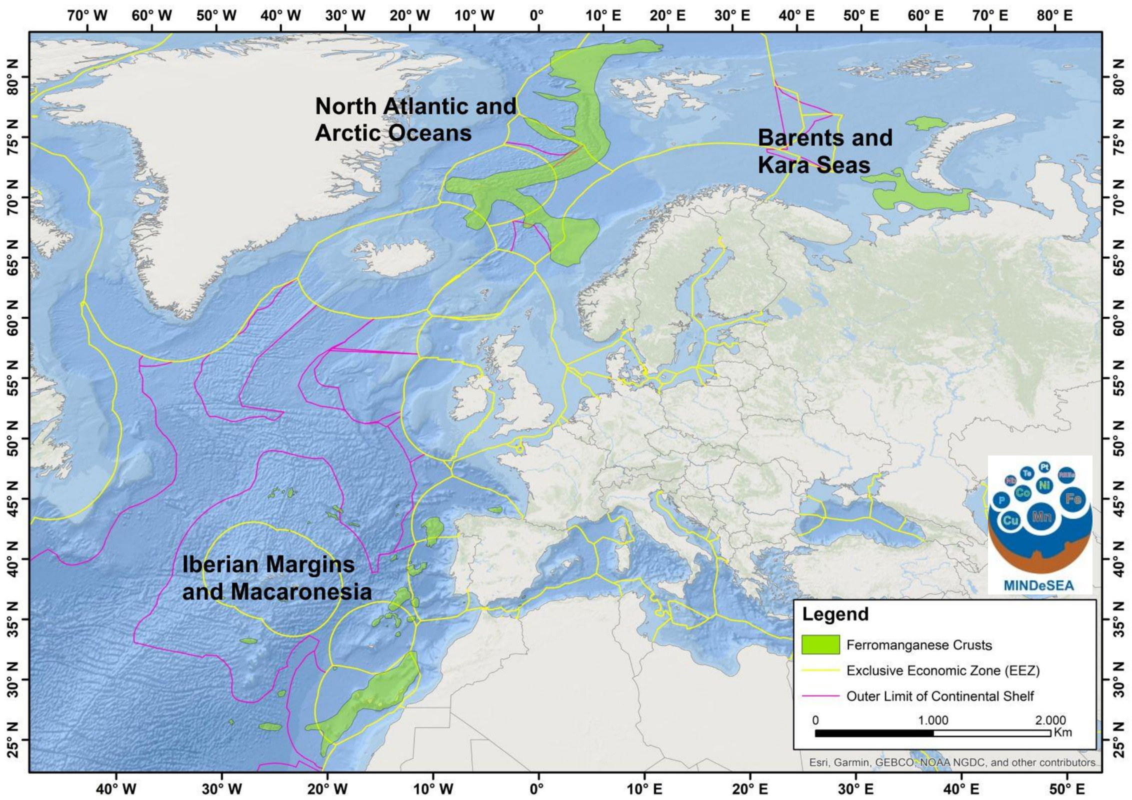

This project has received funding from the European Union's Horizon 2020 research and innovation programme under grant agreement No 731166

Figure 47. Overview map of pan-European seas showing the approximate extent of the key Co metallogenic areas related to ferromanganese crusts.

5.5.2 Metallogenic areas for P associated to phosphorites

Actually, the only known phosphorites deposits in the pan-European seas are located in the Macaronesia and Iberian Margin. Studied samples have been recovered in the north of Spain (Galicia) but also in the southwest of Portugal and Spain (Gulf of Cadiz) and are essentially linked to the continental shelf (Figure 48). The presence of phosphorites has been also detected in several seamounts of the area, sometimes at the base of thick Fe-Mn crusts.

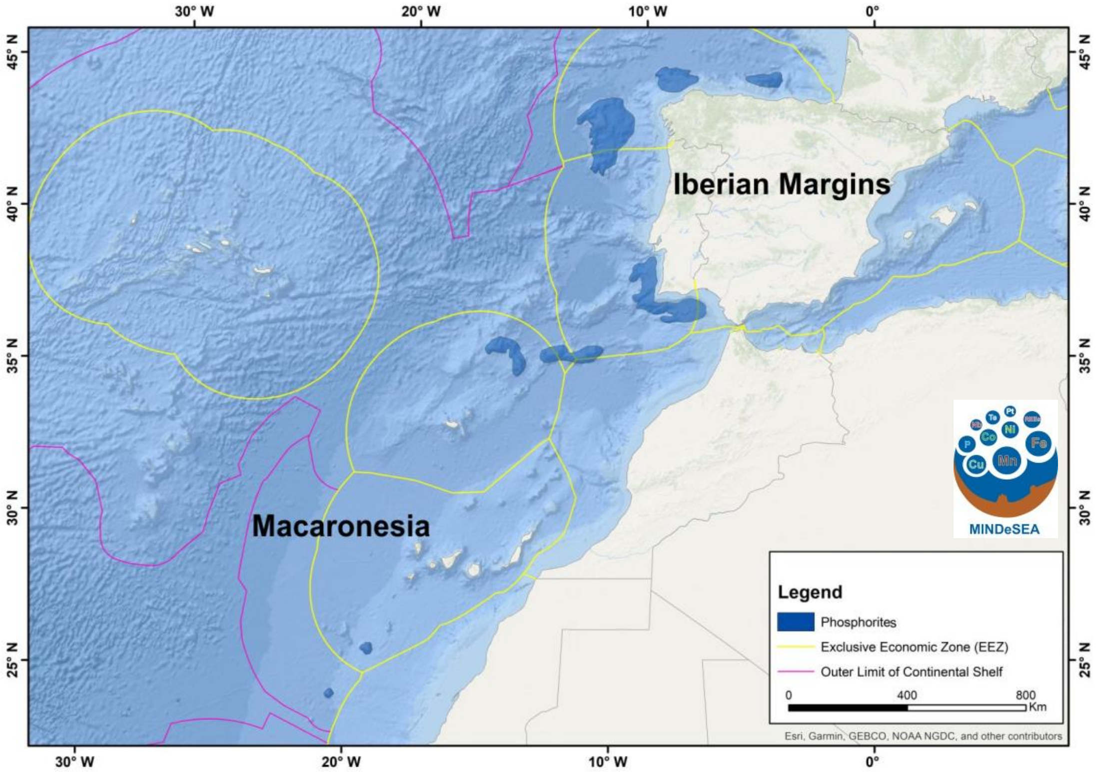

Figure 48. Overview map of pan-European seas showing the approximate extent of the key P metallogenic areas related to phosphorites.

Bay of Biscay - The occurrences of phosphorites deposits in this area are associated with the Sancho seamount, Ortegal Terrace, Le Danois Bank and especially Galicia Bank (Figure 48). Phosphorites recovered on Galicia Bank show the highest P contents with an average of 13 % and maximum up to 20 % but also high contents of REY with an average of 0.1 %

This project has received funding from the European Union's Horizon 2020 research and innovation programme under grant agreement No 731166

and up to 0.2 %. These samples have been dated as the Late Oligocene-Early Miocene period and formed during three main phosphorites events (González et al., 2016). Extensive deposits of phosphorites, with abundant detrital grains of quartz, feldspar and clay minerals, frequently encrusted by Fe-Mn oxy-hydroxides, and ferrous glauconites were discovered in the Ortegal Terrace and on Le Danois Bank (Lamboy, 1976; Lucas et al., 1978; Lamboy and Lucas, 1979). The phosphatization process was discontinuous in the space and time since the Miocene to Quaternary times in Cape Ortegal and Le Danois Bank and was driven in all the locations by the diagenetic replacement of carbonate by CFA.

Gulf of Cadiz. In this area phosphorites are located on the continental shelf covering small seamounts and terraces recognized on the seafloor (Figure 48). Several phosphorites have been recovered and analyzed showing an average P content of 6.5 % with maximum of 9.4 % (Baturin and Bezrukov, 1971; Baturin, 1982; Gaspar, 1981; 1982; 1986; 2000; Rona, 2008; MINDeSEA, 2020). They are forming part of the East Atlantic Phosphorite Province (Baturin and Bezrukov, 1971).

Macaronesia. Phosphorites can be found covering seamounts in the Macaronesia area (Portugal and Spain) (Figure 48). Occurrence of these deposits have been found on the Lion and Ampére seamounts, located in the area of south Portugal and Madeira Islands. Other Deposits have been found and studied in the CISP area, at the base of Fe-Mn crusts on the Tropic and Echo seamounts. Studies made on these deposits show higher contents of P respect to the continental shelf samples with an average of 9.8 and up to 11.6 %. In this area several other elements have been analyzed between which REY shows an average of 0.08 % with maximum of 0.15 % (Vázquez et al., 2011; Murton et al., 2017; MINDeSEA, 2020).

This project has received funding from the European Union's Horizon 2020 research and innovation programme under grant agreement No 731166

6 Conclusion remarks

The EU's Green deal policy recognizes that Europe needs a new growth strategy that transforms the Union into a model, resource-efficient and competitive economy. Many critical minerals and metals may be collected through recycling of mining related waste materials. However, there is a very strong argument for the extraction of primary raw material (*see Raw material Scoreboard, 2018- "Recycling rates for some metals are relatively high. However, recycling at end-of-life is not yet sufficient to meet the EU's current demands for various*") , even with the important contribution from recycling, to secure resource efficient supply. it will still be necessary to extract primary mineral deposits, focusing on applying new technologies for deep exploration and mining, turning low- grade ores to exploitable resources and reducing generation of mining wastes and large tailings by converting them into exploitable resources and solving environmental footprint and land-use challenges. To meet this strategy EU needs to increase the consumption of raw material necessary for the society. One of the GeoERA's RM projects is FRAME which is structured to carry out much needed research into strategic and critical minerals.

WP 3 (Critical and Strategic Minerals Map) is contributing in to collecting and producing maps on Critical Raw Materials and also of the strategic raw materials for Europe, which is the backbone of the project with links to the other WP's. WP 3 is acting as a focal point that all data on CRM collected either by this WP or the other WP's in the FRAME project. In this report, the metallogenic areas in Europeans land and sea are presented and the most important CRM and STRM in each metallogenic area is described. The methodology used for prospectivity mapping and examples have been shown and presented. Comparing the prospectivity mapping with the metallogenic area reveal that there are addition to present potential , there are additional areas in Europe that may be on considered for future investigation, focus in gathering fundamental geological, economic geology, geochemical and geophysical data and better understanding the mineral system knowledge on how the mineral deposits are formed in each specific area. WP3 in link with other WP 2 will act as a source of mineral information data that will support the continuous work going on in the DG-Grow, Raw material supply Group an the Ad Hoc Working Group on Criticality of the EU Commission.

This project has received funding from the European Union's Horizon 2020 research and innovation programme under grant agreement No 731166

7 References

Agterberg, F.P., Bonham-Carter, G.F., Wright, D.F. (1990). Statistical pattern integration for mineral exploration. In: Gaal, G., Merriam, D.F. (Eds.), Computer Applications in Resource Estimation, Pergamon Press, Oxford, pp. 1–21

Ahokas, K., 2015. Finland's phosphorus resources are more important than ever. Geofoorumi 2, 10-12

Alfonso, P., Hamid, S.A., García-Valles, M., Llorens, T., López-Moro, F.J., Tomasa, O., Calvo, D., Guasch, E., Anticoi, H., Oliva, J., Parcerisa, D., García Polonio, F., 2018. Textural and mineral-chemistry constraints regarding the columbite-group minerals in the Penouta deposit: evidences of magmatic and fluid-related processes. Mineralogical Magazine, 82(S1), S199-S222.

Allen, R.L., Weihed, P., Svenson, S.-Å., 1996a. Setting of Zn-Cu-Au-Ag massive sulfide deposits in the evolution and facies architecture of a 1.9 Ga marine volcanic arc, Skellefte district, Sweden. Economic Geology 91, 1022–1053.

Alves, R., Leal Gomes, C., 2015. Património Mineiro da Serra de Arga - Minho. Geonovas 28, 147 - 182.

Alves, R., Valente, T., Leal Gomes, C., 2010. A model for the characterization and promotion of forsaken mining sites – The case of Lagares do Estanho, Vila Nova de Paiva. GEOTIC – Sociedade Geológica de Portugal VIII Congresso Nacional de Geologia, Volume 18 – nº 19. e -Terra. http://e-terra.geopor.pt. ISSN 1645-0388

Andersson SS, Wagner T, Jonsson E et al., 2019. Apatite as a tracer of the source, chemistry and evolution of ore-forming fluids: The case of the Olserum-Djupedal REE-phosphate mineralisation, SE Sweden. Geochim Cosmochim Acta 255, 163-187

Andersen, T., 1986. Compositional variation of some rare earth minerals from the fen complex (Telemark, SE Norway): implications for the mobility of rare earths in a carbonatite system. Mineral. Mag. 50, 503–509.

Andersson, U. B. (ed.), 2004. The Bastnäs-type REE mineralisations in north-western Bergslagen, Sweden. Sveriges geologiska undersökning. Rapporter and Meddelanden 119, 34 pp.

Arribas, A., Gonzalo, F., Iglesias, M., 1982. Génesis de una mineralización asociada a una cúpula granítica: el yacimiento de estaño de Golpejas (Salamanca). Cuad. Lab. Xeol. Laxe, 3, 563-592.

Arvanitidis, N., Gautneb, H., Jonsson, E., Lynch, E., Reginiussen, H., Sadeghi, M., 2019. Producing a report describing the methodology used for the identification and selection process of the CRM to be included in the metallogenetic map. FRAME Deliverable 3.1

Arvanitidis N., 2010. New metallogenetic concepts and sustainability perspectives for non-energy metallic minerals in Greece - 12th International Congress Of The Geological Society Of Greece Bulletin Of The Geological Society Of Greece Volume XLIII. No 5. 2010.

Arvanitidis N.D., Michael C., Christidis C., Cassard D., Perantonis G., Bertrand G., Kaja J., Ballas D. Bakalis V., 2012. GIS-based datasets of mineral deposits and man-made resources as valuable exploration tools for discovering potential ore deposits in Greece. 7th EUREGEO- Bologna 2012.

Arvanitidis N.D., Michael C., Perantonis G., Bakalis V., Ballas D., Christidis C., 2012. Using 3D/4D modeling tools in exploration of gold-polymetallic potential areas in Greece. 7th EUREGEO- Bologna 2012.

Arvanitidis, N., 1993. Regional ore geologic studies setting controls and distribution of Metallic ore deposit types in the Serbo-Macedonian and Western Rhodope zone. I.G.M.E. technical report.

Arvanitidis, N., C. Michael, C. Christidis, G. Perantonis, V. Bakalis, D. Ballas, 2015. 3D- and 4D-Modelling of the Hellenic Belt, Greece. In "3D, 4D modelling Mineral belts in Europe Predictive resource modelling", ed. Pär Weihed, p. 299-331, Springer

Arlt, T., Diamond, L.W., 1998. Composition of tetrahedrite-tennantite and 'schwazite' in the Schwaz silver mines, North Tyrol, Austria. Mineral. mag. 62, 801–820. https://doi.org/10.1180/002646198548188

Arthur, M.A., Jenkyns, H.C., 1981. Phosphorites and paleoceanography. Ocean Acta, Special issue, https://archimer.ifremer.fr/doc/00245/35660/34169.pdf

This project has received funding from the European Union's Horizon 2020 research and innovation programme under grant agreement No 731166

Azim Zadeh, A.M., Ebner, F., Jiang, S.-Y., 2015. Mineralogical, geochemical, fluid inclusion and isotope study of Hohentauern/Sunk sparry magnesite deposit (Eastern Alps/Austria): implications for a metasomatic genetic model. Miner Petrol 109, 555–575. https://doi.org/10.1007/s00710-015-0386-2

Bäcker, H., Schoell, M., 1972. New deeps with brines and metalliferous sediments in the Red Sea. Nat. Phys. Sci. 240, 153–158.

Bardossy, G., Panto, G., and Varhegy, G., 1976. Rare metals of Hungarian bauxites and conditions of their utilisation.Travaux, ICSOBA, 13, 221-231.

Bárdossy, G., 1982. Karst Bauxites (Bauxite deposits on carbonate rocks). Budapest, Hungary.

Barros, R. F., 2017. Petrogenesis of the Leinster LCT (Li-Cs-Ta) pegmatite belt in southeast Ireland. Ph.D Thesis. University college Dublin.

Barros, R. and Menuge, J. 2016. The origin of spodumene pegmatites associated with the leinster granite in southeast Ireland. Canadian Mineralogist 54(4), pp. 847–862. doi: 10.3749/canmin.1600027.

Baturin, G.N., 1982. Phosphorites on the Sea Floor. Elsevier. 343 pp.

Baturin, G. N. & Bezrukov, P. L. 1971. Phosphorites on the sea floor and their origin. Mar. Geol. 31, 317–332.

Baturin, G.N., Dubinchuk, V.T., Ivanov, G.I., Siraev, A.I., 2014. A specific type of Fe-Mn mineralization on the Arctic seafloor. Dokl. Earth Sci. 458 (2), 1191–1196

Benites, M., Hein, J.R., Mizell, K., Blackburn, T., Jovane, L., 2020. Genesis and Evolution of Ferromanganese Crusts from the Summit of Rio Grande Rise, Southwest Atlantic Ocean. Minerals 10, 349.

Bergman, S., Kübler, L. & Martinsson, O., 2001. Description of regional geological and geophysical maps of northern Norrbotten County (east of the Caledonian orogen). Sveriges Geologiska Undersökning Ba 56, 110 pp.

Bergman, S., Persson, P.-O., Kubler, L., 2002. U-Pb titanite and zircon ages of the Lina granite at the type locality NWof Gällivare, northern Sweden. In: Bergman, S. (Ed.), 2002, Radiometric dating results 5. Geol. Surv. Sweden C Vol. 834, pp. 12–17.

Bergman Weihed, J., Bergström, U., Billström, K., Weihed, P., 1996. Geology and tectonic evolution of the Paleoproterozoic Boliden Au-Cu-As deposit, Skellefte district, northern Sweden. Economic Geology 91, 1073–1097.

Bergman, S.&Weihed, P. 2020. Archean (>2.6 Ga) and Paleoproterozoic (2.5−1.8 Ga), pre- and syn-orogenic magmatism, sedimentation and mineralization in the Norrbotten and Överkalix lithotectonic units, Svecokarelian orogen. In: STEPHENS, M.B. & BERGMAN WEIHED, J. (eds) 2020. Sweden: Lithotectonic Framework, Tectonic Evolution and Mineral Resources. Geological Society, London, Memoirs, 50, 27–81, https://doi.org/10.1144/M50-2016-29

Bergstøl, S., Svinndal, S., 1960. The carbonatite and per-alkaline rocks of the Fen area - petrology. Norges Geologiske Undersøkelse, Rapport 208, 99-105.

Bertrand G., Cassard D., Billa M., Angel J.M., Tertre F. & Tourlière B., 2017. Prédictive assessment of rare earth occurrences in Europe using the Database Querying method. ERES 2017, 2nd European Rare Earth Resources Conference, Santorini, Greece, 28-31 May 2017, extended abstract.

Bertrand G., Cassard D., Arvanitidis N., Stanley G., Solar S., de Oliveira D. and the EuroGeoSurveys Mineral Resources Expert Group (2018). New map of critical raw material deposits in Europe, based on the 2017 EU CRM list. RFG 2018, Resources for Future Generations, June 16-21 2018, Vancouver, Canada

Bertrand G., Tourlière B., Gloaguen E., Sadeghi M., Gautneb H., Törmänen T. and de Oliveira D.,2020.. Mineral prospectivity mapping for energy critical elements in Europe: the Cell Based Association approach. EAGE Mineral Exploration Symposium, 17-18 Sept. 2020, online event.

Beyssac, O. and Rumble, D. 2014. Graphitic carbon: a ubiquitous, diverse, and useful geomaterial. Elements, 10, 415-420, https://doi.org/https://doi.org/10.2113/gselements.10.6.415.

Berza, T., Constantinescu, E. & Vlad, S.N., 1998. Upper Cretaceous magmatic series and associated mineralisation in the Carpatho-Balkan Orogen. Res. Geol., 48, 291-306.

This project has received funding from the European Union's Horizon 2020 research and innovation programme under grant agreement No 731166

Billa M., Cassard D., Deschamps Y., and Salpeteur I., 2008. Europe's Mineral Resources GIS. In: International Geological Congress, August 6-14th 2008, Oslo, Norway.

Bonham-Carter, G.F., Agterberg, F.P., Wright, D.F. (1988). Integration of geological datasets for gold exploration in Nova Scotia. Photogrammetric Engineering and Remote Sensing, 54, 1585–1592.

Bonham-Carter, G.F., Agterberg, F.P., Wright, D.F. (1989). Weights of evidence modelling: a new approach to mapping mineral potential. In: Agterberg, F.P., Bonham-Carter, G.F. (Eds.), Statistical Applications in the Earth Sciences, Paper 89-9. Geological Survey of Canada, pp. 171–183.

Borcoş, M., Krautner, H.G., Udubaşa, G., Săndulescu, M., Năstăseanu, S., Biţoianu, C., 1984. Explanatory book of the Map of the useful raw materials in Romania, scale 1:1,000,000. Ministry of Geology. Bucharest.

Brady, A.E. and Moore, K.R. 2012. A mantle-derived dolomite silicocarbonatite from the southwest coast of Ireland. Mineralogical Magazine 76(2), pp. 357–376. doi: 10.1180/minmag.2012.076.2.06.

Brotzen, O., 1959. Mineral association in granitic pegmatites. A statistical study. Geologiska Föreningens i Stockholm Förhandlingar 81, 231–296.

Burchfiel, B.C., 1980. Eastern European Alpine system and the Carpathian orocline as an example of collision tectonics. Tectonophysics 63, 31– 61.

Burg, J.P., Ivanov, Z., Ricou, L.E., Dimor, D., Klain, L., 1990. Implications of shear-sense criteria for the tectonic evolution of the Central Rhodope Massif, southern Bulgaria. Geology 18, 451– 454.

Burg, J.-P., Ricou, L.-E., Ivanov, Z., Godfriaux, I., Dimov, D., Klain, L., 1996. Syn-metamorphic nappe complex in the Rhodope Massif. Structure and kinematics. Terra Nova 8, 6 – 15.

Burg, J-P., Godfriaux, I., Ricou, L.E., 1995. Extension of the Mesozoic Rhodope thrust units in the Vertiskos–Kerdyllion Massifs (northern Greece). Comptes Rendus de l'Academie des Science Paris 320, Serie IIa, 889– 896.

Buseck, P.R. and Beyssac, O. 2014. From Organic Matter to Graphite: Graphitization. Elements, 10, 421-426, https://doi.org/10.2113/gselements.10.6.421.

Bylund, G. & Patchett, P. J., 1977. Palaeomagnetic and Rb-Sr isotope evidence for the age of the Särna alkaline complex, western central Swede. Lithos, 10, 73-79

Canosa, F., Martín, A., Fuertes, M., 2012. Evolved granitic systems as a source of rare-element deposits: The Ponte Segade case (Galicia, NW Spain), Lithos, 153, 165-176.

Carranza, E.J.M., 2017. Natural Resources Research Publications on Geochemical Anomaly and Mineral Potential Mapping, and Introduction to the Special Issue of Papers in These Fields. Natural Resources Research, 26, 379–410.

Carranza, E. J. M., & Sadeghi, M., 2010. Predictive mapping of prospectivity and quantitative estimation of undiscovered VMS deposits in Skellefte district (Sweden). Ore Geology Reviews, 38(3), 219–241. http://doi.org/10.1016/j.oregeorev.2010.02.003

Carranza, E.J.M., Sadeghi, M 2014. Post-VMS mineralization deformations (1880–1820 Ma) of the Skellefte district (Sweden): insights from the spatial pattern of VMS occurrences. Front. Earth Sci. 8, 319–324 (2014). https://doi.org/10.1007/s11707-014-0466-3

Ciobanu, C. L.; Cook, N. J.; Stein, H., 2002. Regional setting and geochronology of the Late Cretaceous Banatitic Magmatic and Metallogenic Belt. Mineralium Deposita, 37, 541-567.

Ciobanu, C.L. and Cook, N.J., 2004. Skarn textures and a case study: the Ocna de Fier-Dognecea orefield, Banat, Romania. Ore Geology Reviews, 24, 315-370.

Chakhmouradian, A.R., Zaitsev, A.N., 2012. Rare earth mineralization in igneous rocks:
sources and processes. Elements 8, 347–353.

Charoy, B., Noronha, F., 1996. Multistage growth of a rare-element, volatile-rich microgranite at Argemela (Portugal). Journal of Petrology, 37, 73-94.

Chew, D.M. and Stillman, C.J., 2009. Late Caledonian orogeny and magmatism. In: The Geology of Ireland., pp. 143–174.

This project has received funding from the European Union's Horizon 2020 research and innovation programme under grant agreement No 731166

Chou, S.Y., Chang, Y.H., Shen, C.Y., 2008. A fuzzy simple additive weighting system under group decision-making for facility location selection with objective/subjective attributes. Eur. J. Oper. Res., 189 (1), 132-145.

Cook, N.J. and Ciobanu, C.L., 2001. Paragenesis of Cu-Fe ores from Ocna de Fier-Dognecea (Romania), typifying fluid plume mineralization in a proximal skarn setting. Mineralogical Magazine, 65: 351-372.

Cook, N.J, Ciobanu C.L., Spry, P.G., Vordouris, P., & the participants of IGCP-486., 2009. Understanding gold-(sylver)-telluride-(selenide) mineral deposits. Episodes 32, 4, 249-263.

Cook, P.J., Shergold, J.H., (Eds) 1986. Phosphate deposits of the world. Volume 1: Proterozoic and Cambrian phosphorites. Cambridge University Press

Corliss, J.B., Dymond, J., Gordon, L.I., Edmond, J.M., von Herzen, R.P., Ballard, R.D., Green, K., Williams, D., Bainbridge, A., Crane, K., van Andel, T.H., 1979. Submarine thermal springs on the Galápagos Rift. Science 203, 1073–1083.

Cultrone, G., Anfuso, G., Sebastián. E., 2010. Mineralogy of Miocene phosphatic nodules in SE Sicily (Italy). Geol Quarterly 52, 61-70

Dahlgren, S., Nordagutu, 2004. bedrock geology map 1713 IV, scale 1 : 50,000. Norges Geologiske Undersøkelse.

Dallmeyer, D., Krautner, H.-G. & Neubauer, F. 1997. Middle-late Triassic 40Ar/39Ar hornblende ages for early intrusions within the Ditrau alkaline massif, Romania: implications for Alpine rifting in the Carpathian orogen. Geologica Carpathica 48, 347-352.Gallego Garrido, M. 1992: Las mineralizaciones de litio asociadas a magmatismo ácido en Extremadura y su encuadre en la zona Centro-Ibérica. Tesis Doctoral, UCM, 323p.

Deady, E., Mouchos, E., Goodenough, K.M., Williamson, B., Wall, F., 2014. Rare earth elements in karst-bauxites: a novel untapped European resource? ERES2014: 1st Conference on European Rare Earth Resources, Milos, Greece

Demaiffe, D., Wisniewska, J., Krzeminska, E., Williams, I. S., Stein, H., Brassinnes, S., Ohnenstetter, D. & Deloule, E., 2013. A hidden alkaline and carbonatite province of early Carboniferous age in northeast Poland: zircon U-Pb and pyrrhotite Re-Os geochronology. Journal of Geology 121, 91-104.

Dinter, D.A., Royden, L., 1993. Late Cenozoic extension in northeastern Greece: Strimon valley detachment and Rhodope metamorphic core complex. Geology 21, 45–48.

Dolenec, T., Kušej, J., Pezdič, J., 1983. The Isotopic Composition of Oxygen and Carbon in Lead and Zinc Deposits from Northern Karavanke. In: Schneider, H.J. (edt.): Mineral Deposits of the Alps and the Alpine Epoch in Europe. Springer-Verlag, Berlin, Heidelberg, 1983.

Donnot, M., Guigues, J., Lulzac, Y., Magnien, A., Parfenoff, A., Picot, P., 1973. Un nouveau type de gisement d'europium : la monazite grise à europium en nodules dans les schistes paléozoïques de Bretagne. Mineralium Deposita (in French), 8, 7-18.

EMODnet-Geology, 2020. Available online: https://www.emodnet-geology.eu/

European Commission. 2020. Available online: https://ec.europa.eu/docsroom/documents/42849

European Commission., 2020. Study on the EU's list of Critical Raw Materials (2020), Factsheets on Critical Raw Materials. European Commission.

European Commission., 2015.Report on Critical Raw Materials for the EU. Critical Raw Materials Profiles. http://ec.europa.eu/DocsRoom/documents/11911/attachments/1/translations. Accessed 9 December 2016

European Commission., 2017. Study on the review of the list of Critical Raw Materials, Critical Raw Materials factsheets. https://publications.europa.eu/en/publication-detail/-/publication/7345e3e8-98fc-11e7-b92d-01aa75ed71a1/language-en

European Commission, 2017. Communication from the Commission to the European Parliament, the Council, the European Economic and Social Committee and the Committee of the Regions on the 2017 list of Critical Raw Materials for the EU. Brussels, COM (2017) 490 final.

This project has received funding from the European Union's Horizon 2020 research and innovation programme under grant agreement No 731166

Eurosun Mining, 2020. The Rovina Valley Project, Romania. Romania's Next Gold and Copper mine. http://eurosunmining.com/_resources/presentations/corporate-presentation.pdf. Accessed on 08.08.2020.
Eilu, P., Ahtola, T., Äikäs, O., Halkoaho, T., Heikura, P., Hulkki, H., … Västi, K., 2012. Metallogenic areas in Finland. Special Paper of the Geological Survey of Finland, 2012(53), 207–342.
Eilu, P. (ed.), 2012. Mineral deposits and metallogeny of Fennoscandia. Special Paper 53.
Eliopoulos D, Economou-Eliopoulos M, 1991. Platinum-Group Element and Gold Contents in the Skouries Porphyry Copper Deposit, Chalkidiki Peninsula, Northern Greece. Economic Geology. Vol. 86, 1991, pp. 740-749.
Eliopoulos, D., Economou, G., Tzifas, I., Papatrechas, C., 2014. The potential of rare earth elements in Greece. ERES2014: First European Rare Earth Resources Conference, Milos, Greece.Eliopoulos, D.G. and Economou-Eliopoulos, 2000. Geochemical and mineralogical characteristics Fe-Ni and bauxitic-laterite deposits of Greece. Ore Geology Reviews 16, 41-58.
Economou-Eliopoulos, M., Eliopoulos, D.G., Apostolikas, A., and Maglaras, K., 1997. Precious and rare earth element distribution in Ni-laterite deposits Lokris area, Central Greece. Proceedigs of the 4th Biennial SGA Meeting, Turku, Finland, 411-413.
Frei R., 1995. Evolution of Mineralizing Fluid in the porphyry copper system of the Skouries deposit, Northeast Chalkidiki (Greece) - Evidence from combined Pb-Sr and stable isotope data Economic Geology, vol 90, 1995, pp 746-762 Kalogeropoulos, S. I., Economou, G.S.
Fitikas M.; Giuliani O.; Innocenti F.; Manetti P.; Mazzuoli R.; Peccerillo A.; Villari, 1980. Neogene volcanism of the northern and central Aegean region. Ann.Geol.Pays Hell. 30(1) 1980.
Földessy, J., Németh; N., Gerges, A., Bodorés, S., Kasó, A., 2014. in Fehér B. (Ed.): Studies Attracting minerals. Studies in honor of the 60-year-old Sándor Szakáll. Herman Ottó Museum and Hungarian Minerofil Associaton. Miskolc, pp. 75–83.
Gaspar, L.C. 1981. Alguns aspectos geoquimicos sobre fosforites da margem continental Portugues, Diss., Univ. de Aveiro.
Gaspar, L.C. 1982. Fosforites da Margem Continental Portuguesa. Alguns Aspectos Geoquímicos. Boletim da Sociedade Geológica de Portugal, XXIII, 79-90 (in Portuguese).
Gaspar, L.C. 1986. Alguns Aspectos Geoquímicos sobre Fosforites da Margem Continental Portuguesa. Master, Departamento de Geociências, Aveiro, Portugal: Universidade de Aveiro, (in Portuguese).
Gaspar, L.C. and Halbach, P. 1999. Caracterização mineralógica e geoquímica de fosforites da montanha submarina de Lion, ZEE da Madeira, Portugal.
Gaspar, L.C. 2000. Comparative study of the phosphorites from the continental margin and seamounts in the Atlantic North off Portugal. 31st International Geological Congress. Rio de Janeiro. Brazil (poster and abstract).
Gautneb, H., Rønning, J.S. et al. 2020. The Graphite Occurrences of Northern Norway, a Review of Geology, Geophysics, and Resources. Minerals, 10, 626.
Gautneb H., Knežević J., Gloaguen E., Melleton J., Gourcerol B., Törmänen T., 2019. Occurrences of energy critical elements; Lithium – Cobalt and Graphite in Europe, a preliminary overview. 15th SGA biennial meeting, 20-23 August 2019, Glasgow, UK. Proceedings, vol. 4:1784-1787.
Gautneb, H. 2015. Natural Graphite in Norway. In: Graphite & Graphene Conference. London
Garate-Olave, I., Müller, A., Roda-Robles, E., Gil-Crespo, P.P., Pesquera, A., 2017. Extreme fractionation in a granite-pegamtite system documented by quartz chemistry: The case study of Tres Arroyos (Central Iberian Zone, Spain). Lithos, 286-287, 162-164.
García Guinea, J., Martínez Frías, J., (1992): Recursos minerales de España. CSIC, Madrid, 1448 pp.
Geijer P., 1961. The geological significance of the cerium mineral occurrences of the Bastnäs type in central Sweden. Arkiv för Mineralogi och Geologi 3, 99-105

This project has received funding from the European Union's Horizon 2020 research and innovation programme under grant agreement No 731166

Ghiţulescu T.P., 1935. Distribution de la mineralisation dans les gisements d'age tertiaire de Transylvanie. Buletinul Societăţii Române de Geologie 2, 56-97. Bucharest.

Goodenough, K. M., Schilling, J., Jonsson, E., Kalvig, P., Charles, N., Tuduri, J., Sadeghi, M., … Keulen, N., 2016. Europe's rare earth element resource potential: An overview of REE metallogenetic provinces and their geodynamic setting. Ore Geology Reviews, 72. https://doi.org/10.1016/j.oregeorev.2015.09.019

González, F.J., Somoza, L., Hein, J.R., Medialdea, T., León, R., Urgorri, V., Reyes, J., Martín-Rubí, J.A., 2016. Phosphorites, Co-rich Mn nodules, and Fe-Mn crusts from Galicia Bank, NE Atlantic: reflections of Cenozoic tectonics and paleoceanography. Geochem. Geophys. Geosyst. 17.http://dx.doi.org/10.1002/2015GC005861.

González, F.J., Blasco, I., Blanco, L., Marino, E., Somoza, L., Medialdea, T., Ferreira, P., Magalhaes, V. 2018. First compilation map of "energy-critical elements" in pan-European seas: ferromanganese deposits. https://69ef338c-adbf-4a98-94a6-1e32d03179fa.filesusr.com/ugd/e60895_12f36311663d480cbb852fc40c9ec7f0.pdf

Gourcerol, B., Gloaguen, E., Melleton, J., Tuduri, J., Galiegue, X., 2019. Re-assessing the European lithium resource potential – A review of hard-rock resources and metallogeny. Ore Geology Reviews 109, 494–519. https://doi.org/10.1016/j.oregeorev.2019.04.015

Göd, R., 1989. The spodumene deposit at "Weinebene", Koralpe, Austria. Mineralium Deposita vol. 24, pages 270-278.

Grad, M., Brückl, E., Majdański, M., Behm, M., Guterch, A., CELEBRATION 2000 and ALP 2002 Working Groups, 2009. Crustal structure of the Eastern Alps and their foreland: seismic model beneath the CEL10/Alp04 profile and tectonic implications. Geophysical Journal International 177, 279–295. https://doi.org/10.1111/j.1365-246X.2008.04074.x

Grancea, L., Bailly, L., Leroy, J., Banks, D., Marcoux, E.,Milési, J.P., Cuney, M., André, A.S., Istvan, D., Fabre, C., 2002. Fluid evolution in the Baia Mare epithermal gold/polymetallic district, Inner Carpathians, Romania. Mineralium Deposita 37, 630–647.

Grenne, T. et al., 1999. Scandinavian Caledonide metallogeny in a plate tectonic perspective. Mineralium Deposita 34(5–6), pp. 422–471. doi: 10.1007/s001260050215.

Grecula, P.; Chovan, M.; Rojkovič, I.; Slavkay, M., 1996. The Variscan metallogeny of the Western Carpathians. – In: Grecula, P. (ed.): Variscan metallogeny in the Alpine orogenic belt. Mineralia Slovaca, Monography, Bratislava, pp. 191–238.

Gumiel, P., Arribas, A., 1990. Part IV. Central-Iberian Zone. 2.5. Metallogeny, In: Pre-mesozoic geology of Iberia (Dallmeyer, R.D., Martínez García E., Eds.). Heidelberg, Germany, Springer Verlag, 212–219.

Gustafsson, B., 1992. Sällsynta jordartsmetaller. Regional fältkontroll 1991 av arkivuppslag. Sveriges Geologiska AB PRAP 91047. Unpublished prospecting report. 22 pp. (in Swedish)

Halbach, P., Manheim, F.T., Otten, P., 1982. Co-rich ferromanganese deposits in the marginal seamount regions of the Central Pacific Basin—results of the Midpac'81. Erzmetall 35, 447–453.

Hallberg, A., Bergman, T., Gonzalez, J., Larsson, D., Morris, G. A., Perdahl, J. A., Ripa, M., Niiranen, T. & Eilu, P. 2012. Metallogenic areas in Sweden. Geological Survey of Finland, Special Paper 53, 139–206.

Hallberg A, Bergman T, Gonzalez J et. Al., 2016 Chapter 7 – Sweden. In: Boyd R, Bjerkgård T, Nordah B et al (eds) Mineral Resources in the Arctic. Geological Survey of Norway Special Publication, http://www.ngu.no/upload/Aktuelt/CircumArtic/7_Sweden.pdf

Hallberg, A., Albrecht, L., Jonsson, E., Olsson, A., 2006. The Grängesberg apatite-iron deposit — biggest in Bergslagen, Sweden. Bulletin of the Geological Society of Finland, Special issue 1, 45.

Hallberg, A., 2012. S011 Riddarhyttan REE-Fe. In: Eilu, P. (ed.), Geological Survey of Finland, Special Paper 53, 162–163.

This project has received funding from the European Union's Horizon 2020 research and innovation programme under grant agreement No 731166

Hofbauer, R. 1995. 36 Jahre Grafitabbau der Firma Industrie & Bergbaugesellschaft Pryssok & Co. KG im Niederösterreichischen Waldvierte. Zeitschrift des Montanhistorischen Vereins für Österreich, 11, 28-31.

Hanski, E., 2015. Synthesis of the geological evolution and metallogeny of Finland. In: Maier,W.D., Lahtinen, R., O'Brien, H. (Eds.), Mineral Deposits of Finland. Elsevier, Oxford, pp. 39–71.

Hanski, E., Huhma, H., Vaasjoki, M., 2001. Geochronology of northern Finland: a summary and discussion. In: Vaasjoki, M. (Ed.), Radiometric Age Determinations from Finnish Lapland and Their Bearing on the Timing of Precambrian Volcano-Sedimentary Sequences. Geological Survey of Finland, Special Paper 33, 255–279.

Hanski, E., Huhma, H., 2005. Central Lapland Greenstone Belt. In: Lehtinen, M., Nurmi, P.A., Rämö, O.T. (Eds.), Precambrian Geology of Finland—Key to Evolution of the Fennoscandian Shield. Elsevier, Amsterdam, pp. 139–194.

Harangi, Sz; Lukács, R., 2019. The Neogene to Quaternary volcanism and its geodynamic relations in the Carpathian–Pannonian Region. Bull. of Hung. Geol. Soc. 149, pp. 197-232.

Hartai, E., Németh, N., Földessy, J., 2016. EGS-relevant review of metallogenesis CHPM2030 Deliverable D1.1, Published by the CHPM2030 project, 2016 University of Miskolc, H-3515 Miskolc-Egyetemváros, Hungary. 58 p.

Harlov, D.E., Andersson, U.-B., Foerster, H., Nyström, J.-O., Dulski, P., Broman, C., 2002. Apatite-monazite relations in the Kiirunavaara magnetite-apatite ore, northern Sweden. Chem. Geol. 191, 47–72.

Hein, J.R., Koschinsky, A., Halbach, P., Manheim, F.T., Bau, M., Kang, J.-K., Lubick, N., 1997. Iron and manganese oxide mineralization in the Pacific. In: Nicholson, K., Hein, J.R., Buhn, B., Dasgupta, S. (Eds.), Manganese Mineralization: Geochemistry and Mineralogy of Terrestrial and Marine Deposits: Special Publication Geological Society of London, London, vol. 119, pp. 123–138.

Hein, J.R., Koschinsky, A., Bau, M., Manheim, F.T., Kang, J.-K., Roberts, L., 2000. Cobalt-rich ferromanganese crusts in the Pacific. In: Cronan, D.S. (Ed.), Handbook of Marine Mineral Deposits. CRC Press, Boca Raton, Florida, pp. 239–279.

Hein, J.R., Conrad, T.A., Dunham, R.E., 2009. Seamount characteristics and mine-site model applied to exploration- and mining-lease-block selection for cobalt-rich ferromanganese crusts. Mar. Georesour. Geotechnol. 27, 160–176.

Hein, J.R., 2012. Prospects for rare earth elements from marine minerals. Briefing Paper 02/12, International Seabed Authority. (4 pp.).

Hein, J.R., Mizell, K., Koschinsky, A., Conrad, T.A., 2013. Deep-ocean mineral deposits as a source of critical metals for high- and green-technology applications: comparison with land-based resources. Ore Geol. Rev. 51:1–14. http://dx.doi.org/10.1016/j.oregeorev.2012.12.001

Hein, J. R., Spinardi, F., Okamoto, N., Mizell, K., Thorburn, D., Tawake, A., 2015. Critical metals in manganese nodules from the Cook Islands EEZ, abundances and distributions, Ore Geol. Rev., 68, 97–116.

Hein, J.; Koschinsky, A.; Mikesell, M.; Mizell, K.; Glenn, C.; Wood, R., 2016. Marine Phosphorites as Potential Resources for Heavy Rare Earth Elements and Yttrium. Minerals 6, 88.

Hein, J.R., Konstantinova, N., Mikesell, M., Mizell, K., Fitzsimmons, J.N., Lam, P.J., Jensen, L.T., Xiang, Y., Gartman, A., Cherkashov, G., Hutchinson, D.R., Till, C. P. 2017. Arctic Deep Water Ferromanganese-Oxide Deposits Reflect the Unique Characteristics of the Arctic Ocean. Geochemistry, Geophysics, Geosystems, 18(11), 3771–3800. doi:10.1002/ 2017gc007186.

Herlec, U., Spangenberg, J.E., Lavrič, J.V., 2010. Sulfur isotope variations from orebody to hand-specimen scale at the Mežica lead–zinc deposit, Slovenia: a predominantly biogenic pattern. Miner Deposita 45, 531–547. https://doi.org/10.1007/s00126-010-0290-y

Hitzman, M.W., Oreskes, N., Einaudi, M.T., 1992. Geological characteristics and tectonic setting of Proterozoic iron oxide (Cu-U-Au-REE) deposits. Precambrian Res. 58, 241–287.

This project has received funding from the European Union's Horizon 2020 research and innovation programme under grant agreement No 731166

Hitzman, M.W., 1995. Mineralization in the Irish Zn-Pb-(Ba-Ag) orefield. In: Society of Economic Geologists Guidebook Series. Society of Economic Geologists

Hollis, S.P. et al., 2014. Petrochemistry and hydrothermal alteration within the Tyrone Igneous Petrochemistry and hydrothermal alteration within the Tyrone Igneous Complex , Northern Ireland : implications for VMS mineralization in the British and Irish Caledonides. Mineralium Deposita (January). doi: 10.1007/s00126-013-0508-x.

Holtstam D, Andersson UB., 2007. The REE minerals of the Bastnäs-type deposits, south-central Sweden. Can. Mineral. 45: 1073-1114

Holzer, H. 1964. Die Flinzgraphitvorkommen im außeralpinen Grundgebirge Ober- und Niederösterreichs. Verhandlungen der Geologischen Bundesanstalt, 1964, 360-371.

Holzer, H. F., Stumpfl E. F., 1980. Mineral deposits of the Eastern Alps (An excursion guide). International geological congress, 26th session, excursion 080 C, Vienna, pages 172-195.

Horn, S., Gunn, G., Petavratzi, E., Shaw, R., Eilu, P., Törmänen, T., Jonsson, E., Bjerkgård, T., Sandstad, J.V., Kountourelis, S. and Wall, F. 2020. Cobalt resources in Europe and the potential for new discoveries. Ore Geol. Rev. (Submitted).

Ingri, J., 1985. Geochemistry of ferromanganese concretions in the Barents Sea. Mar. Geol., 67: 101--119.

Ihlen, P.M., Schiellerup, H., Gautneb, H., Skar, O., 2014. Characterization of apatite re-sources in Norway and their REE potential — a review. Ore Geol. Rev. 58, 126–147.

Inverno, C. et al., 2015. Introduction and geological setting of the Iberian Pyrite Belt. In: 3D, 4D, and predictive modelling of major mineral belts in Europe (P.Weihed, ed.). Mineral Resources Reviews, 191-208.

IRIS – Interaktives Rohstoff Informations System. Geologishe Bundesanstalt, Vienna. Available on:http://geolba.maps.arcgis.com/apps/webappviewer/index.html?id=ef8095943a714d7893d41f02ec9c156d (accessed: 19.07.2020)

ISA, International Seabed Authority, 2020. http://www.isa.org.jm

James, W. et al., 1993. Geology and K/Ar chronology of the Malvika scheelite skarns, Central Norwegian Caledonides. Bulletin - Norges geologiske undersokelse 424, pp. 65–74.

Jarvis, I., 1992. Sedimentology, geochemistry and origin of phosphatic chalks: the Upper Cretaceous deposits of NW Europe. Sediment 39, 55-97

Johnston, J.D. et al., 1996. Basement structural controls on Carboniferous-hosted base metal mineral deposits in Ireland. Geological Society Special Publication 107(107), pp. 1–21. doi: 10.1144/GSL.SP.1996.107.01.02.

Jones, C.E., Tarney, J., Baker, J.H., Gerouki, F., 1992. Tertiary granitoids of Rhodope, northern Greece: magmatism related to extensional collapse of the Hellenic orogen? Tectonophysics 210, 295– 314.

Jonsson, E., Högdahl, K., Sahlström, F., Nysten, P., Sadeghi, M., 2014. The Palaeoproterozoic skarn-hosted REE mineralisations of Bastnäs-type: overview and mineralogical-geological character. In: ERES2014: 1st European Rare Earth Resources Conference, Milos, 382–390.

Jonsson, E., Nysten, P., Bergman, T., Sadeghi, M., Söderhielm, J., Claeson, D., 2019. REE mineralisation in Sweden. In Sadeghi, M. (eds.) 2019: Rare earth elements distribution, mineralisation and exploration potential in Sweden. Sveriges geologiska undersökning, Rapporter och meddelanden 146, 184 pp.

Jonsson, E.(ed.), 2013. The Norra Kärr REE-Zr project and the birthplace of the light REEs. SGA excursion guidebook SWE3, SWE6 & SWE7. 36-51.

Julivert, M., Fontbote, J.M., Ribeiro, A., Conde, L. 1974. Mapa tectónico de la península Ibérica y Baleares, Escala 1/1000000. Instituto Geológico Minero de España.

Kaeter, D. & Menuge, J., 2017a. Rare-element mineralization and metasomatism in LCT pegmatites from Leinster, SE Ireland

This project has received funding from the European Union's Horizon 2020 research and innovation programme under grant agreement No 731166

Kaeter, D. & Menuge, J., 2017b.: Nb–Ta–Sn mineralisation in spodumene pegmatites of southeast Ireland. Applied Earth Science, DOI:10.1080/03717453.2017.1306264
Kalogeropoulos S I. Kilias S P. Bitzios D C., 1989. Genesis of the Olympias Carbonate-hosted Pb-Zn(Au -Ag) Sulfide ore deposit, eastern Chalkidiki Peninsula, northern Greece - Econ. Geol vS4 pp 1210-1234.
Kathol, B., Weihed, P. (eds.), 2005. Description of regional geological and geophysical maps of the Skellefte District and surrounding areas. Sveriges geologiska undersökning Ba 57, 197 pp.
Kato, Y., Fujinaga, K., Nakamura, K., Takaya, Y., Kitamura, K., Ohta, J., Toda, R., Nakashima, T., Iwamori, H., 2011. Deep-sea mud in the Pacific Ocean as a potential resource for rare-earth elements. Nature Geoscience 4, 535-539
Karup-Møller, S. & Rose-Hansen, J., 2013. New data on eudialyte decomposition minerals from kakortokites and associated pegmatites of the Ilímaussaq complex, South Greenland. Bulletin of the geological Society of Denmark 61, 47-70
Kelley, D. S., Karson, J. A., Blackman, D. K., Früh-Green, G. L., Butterfield, D. A., Lilley, M. D., Olson, E. J., Schrenk, M. O., Roe, K. K., Lebon, G. T., Rivizzigno, P., 2001. An off-axis hydrothermal vent field near the mid-atlantic ridge at 30° n. Nature, 412(6843), 145-149. https://doi.org/10.1038/35084000
Knudsen, C. & Buchardt, B., 1991. Carbon and oxygen isotope composition of carbonates from the Qaqarssuk Carbonatite Complex, southern West Greenland. Chemical Geology , 86, 263-274
Kolb, J. et al. 2016. Metallogeny of Greenland. Ore Geology Reviews 78, pp. 493–555. Available at: http://dx.doi.org/10.1016/j.oregeorev.2016.03.006.
Konstantinova, N., Cherkashov, G., Hein, J.R., Mirão, J., Dias, L., Madureira, P., Kuznetsov, V., Maksimov, F. 2017. Composition and characteristics of the ferromanganese crusts from the western arctic ocean. ore geol. rev., 87, 88–99
Kouzmanov, K., L. Bailly, C. Tămaş, P. Ivăşcanu, 2005. Epithermal Pb–Zn–Cu(–Au) deposits in the Baia Mare district, Eastern Carpathians, Romania, Ore Geology reviews, p. 48-49, Elsevier, 2005.
Kouzmanov, K., Ivascanu P., O'Connor G., 2005. Porphyry Cu-Au and epithermal Au-Ag deposits in the southern Apuseni Mountains, Romania. South Apuseni Mountains district: Lat. 46 degrees 03' N, Long. 22 degrees 58' E. Ore Geology Reviews 27: 46-47.
Kresten, P., Ahman, E., & Brunfelt, A. O., 1981. Alkaline ultramafic lamprophyres and associated carbonatite dykes from the Kalix area, Northern Sweden. Geol. Rundschau, 70, 1215-31.
Kärenlampi, K., Kontinen, A., Hanski, E., Huhma, H., Lahaye, Y. Krause, J. & Heinig, T., 2020. Age and origin of the Nb-Zr-REE mineralization in the Paleoproterozoic A1-type granitoids at Otanmäki, central Finland. Bulletin of the Geological Society of Finland 92, 39-71.
Kärkkäinen, N., Appelqvist, H., 1999. Genesis of a low-grade apatite-ilmenite-magnetite deposit in the Kauhajärvi gabbro, western Finland. Miner dep 34, 754-769
Kärki, A., Laajoki, K., Luukas, J., 1993. Major Palaeoproterozoic shear zones of the central Fennoscandian Shield. Precambrian Research 64, 207–223.
Lacomme, A., Hottin, A.M., Laval M., 1993. La monazite grise du massif de l'Arize (Pyrénées françaises). Report BRGM R 37041 GEO-SGN 93 (in French), 48 pp.
Lahtinen, R., 2012. Main geological features of Fennoscandia. In Eilu, P. (ed.). Mineral deposits and metallogeny of Fennoscandia. Geological Survey of Finland, Special Paper 53.
Lahtinen, R., Hallberg, A., Korsakova, M., Sandstad, J.S., Eilu, P., 2012. Main metallogenic events in Fennoscandia summary. Geol. Surv. Finland Spec. Pap. 53, 397–401.
Laine E. et al., 2015. The Vihanti-Pyhäsalmi Area. In: Weihed P. (eds) 3D, 4D and Predictive Modelling of Major Mineral Belts in Europe. Mineral Resource Reviews. Springer, Cham
Lamboy, M. 1976. Géologie marine et sous-marine du plateau continental au nord-ouest de l'Espagne : genèse des glauconies et des phosphorites, thèse Sciences, Rouen, 285 p.
Lamboy, M., Lucas, J. 1979. Les phosphorites de la marge nord de l'Espagne. Etude géologique et pétrographique. Oceanol. Acta, 2, 3, (à paraître).

This project has received funding from the European Union's Horizon 2020
research and innovation programme under grant agreement No 731166

Lang, B., 1979. The base metals–gold hydrothermal ore deposits of Baia Mare, Romania. Economic Geology 74, 1336–1351
Larsen, M., Piasecki, S. & Surlyk, F., 2003. Stratigraphy and sedimentology of a basement-onlapping shallow marine sandstone succession, the Charcot Bugt Formation, Middle-Upper Jurassic, East Greenland. Geological Survey of Denmark and Greenland Bulletin , 1, 893-930.
Laskou, M., and Andreou, G., 2003. Rare earth element distribution and REE-minerals from the Parnassos-Ghiona bauxite deposits, Greece. Proceedings of the 7th Biennial SGA Meeting, Athens, Greece V 1, 89-92.
Korpás, L., Hofstra, A.H., Odor, L., Horváth, I., Haas, J., & Leventhal,J.S., 1999. Carlin gold in Hungary. THE CARLIN GOLD PROJECT IN HUNGARY (1995-1998). Geologica Hungarica Series Geologica (1999), Tomus 24: 151-167.
Leal Gomes, C. 2016. Mineralizações e Recursos de Tântalo no Norte de Portugal - análise paragenética. Geonovas, 29, 3-42.
Lehtonen, M., Airo, M.-L., Eilu, P., et al., 1998. The stratigraphy, petrology and geochemistry of the Kittilä greenstone area, northern Finland. A report of the Lapland Volcanite Project. Geological Survey of Finland, Report of Investigation 140, p. 144 (in Finnish with summary in English).
Le Maitre, R.W., 2002. Igneous Rocks: A Classification and Glossary of Terms. International Union of Geological Sciences. Subcommission on the Systematics of Igneous Rocks. Cambridge University Press, Cambridge. 236 pp.
Lescuyer, J. L. , Bailly, D., Cassard, A. L. W. Lips & Piantone, P. Mc. Alister, M. 2003. Sediment - hosted gold in south - eastern Europe : the epithermal deposit of Perama, Thrace, Greece. Mineral Exploration and Sustainable Development et. al. (eds).
Lie, A., Østergaard, K., 2011a. The Fen carbonatite complex Ulefoss, South Norway. Results and conclusions from preliminary microscope and microprobe studies. 21st North Report (http://www.reemineral.no/no/OM-OSS/Geologirapporter).
Lie, A., Østergaard, K., 2011b. The Fen carbonatite complex Ulefoss, South Norway. Summary of historic work and data. 21st North Report (http://www.reemineral.no/no/OM-OSS/GeologirapporterLundqvist 1997
Lips, A.L.W., White, S.H., Wijbrans, J.R., 2000. Middle–Late Alpine thermotectonic evolution of the southern Rhodope Massif, Greece. Geodinamica Acta 13, 281–292.
López Moro, F.J., García Polonio, F., Llorens González, T., Sans Contreras, J.L., Fernández-Fernández, A., Moro Benito, M.C. 2017. Ta and Sn concentration by muscovite fractionation and degassing in a lens-like granite body: The case study of the Penouta rare-metal albite granite (NW Spain). Ore Geology Reviews, 82, 10-30.
Llorens, T., 2011. Las mineralizaciones magmático-hidrotermales de Sn-W-(Nb-Ta) del distrito de Navasfrías (SO Salamanca). Tesis doctoral. Univ Salamanca. 355 p.
Llorens González, T., García Polonio, F., López Moro, F.J., Fernández-Fernández, A., Sans Contreras, J.L., Moro Benito, M.C. 2017. Tin-tantalum niobium mineralization in the Penouta deposit (NW Spain): Textural features and mineral chemistry to unravel the genesis and evolution of cassiterite and columbite group minerals in a peraluminous system. Ore Geology Reviews, 81, 79-95.
Lucas, J., Prévôt, L., Lamboy, M. 1978. Les phosphorites de la marge nord de l'Espagne. Chimie, minéralogie, genèse. Oceanol. Acta, 1, 1, p. 55 - 72
Luque, C., Martínez-García, E., Ruíz, F., 1990. Part II. Cantabrian and Palentian Zones. 5. Metallogenesis, In: Pre-mesozoic geology of Iberia (Dallmeyer, R.D., Martínez-García E., Eds.). Heidelberg, Germany, Springer Verlag, 80-87.
Luque, C., Ruiz, F., 1990. Part III. West Asturian-Leonese Zone. 6. Metallogenetic characteristics, In: Pre-mesozoic geology of Iberia (Dallmeyer, R.D., Martínez García E., Eds.). Heidelberg, Germany, Springer Verlag, 134-139.

This project has received funding from the European Union's Horizon 2020 research and innovation programme under grant agreement No 731166

Lynch, E., P., Hellström, F.A. and Huhma, H. 2016. The Nunasvaara graphite deposit, northern Sweden: New geochemical and U-Pb zircon age results for the host greenstones. presented at the Conference abstract, Nordic Geological Winter Meeting, 13–15 January 2016, Helsinki.

Lynch, E.P., Hellström, F.A., Huhma, H., Jönberger , J., Persson, P.-O. and Morris, G.A. 2018. Geology, lithostratigraphy and petrogenesis of c. 2.14 Ga greenstones in the Nunasvaara and Masugnsbyn areas, northernmost Sweden. In: Bergan, S. (ed.) Geology of the Northern Norrbotten ore province, northern Sweden. Rapporter og medelande, Geological survey of Sweden, Stockholm, 19-70.

MacDonald, K.C., Becker, K., Spiess, F.N., Ballard, R.D., 1980. Hydrothermal heat flux of the "black smoker" vents on the East Pacific Rise. Earth Planet. Sci. Lett. 48, 1–7.

McArthur, J.M., Walsh, J.N., 1984. Rare-earth geochemistry of phosphorites. Chem. Geol. 47, 191–220.

Magnusson, N. H., 1923. The alkaline rocks of Siksjöberget and Ekorråsen in Särna. Geol. Fören. Stockh. Förh, 45, 295-334.

Marchev, P., Jelev, D., Hasson, S., 2005. Ada Tepe sedimentary-hosted, low-sulphidation epithermal Au deposit, SE Bulgaria. Ore Geology Reviews 27, 92–93.

Marien, C. et al., 2017. The hydrothermal alteration of carbonatite in the Fen Complex , Norway : Mineralogy , geochemistry , and implications for rare-earth element resource The hydrothermal alteration of carbonatite in the Fen Complex , Norway : mineralogy , geochemistry , and. Mineralogical Magazine 82(August), pp. 115–131. doi: 10.1180/minmag.2017.081.070.

Marignac, C., Cuney, M. 1999. Ore deposits of the French Massif Central: insight into the metallogenesis of the Variscan collision belt. Mineralium Deposita, 34: 472-504.

Martínez Catalán, J.R., Rubio Pascual, F.J., Díez-Montes, A., Díez-Fernández, R., Gómez-Barreiro, J., Dias da silva, I., González-Clavijo, E., Ayarza, P., Alcock, J.E., 2014. The late Variscan HT/LP metamorphic event in NW and Central Iberia: relationships to crustal thickening, extension, orocline development and crustal evolution. In: The Variscan Orogeny: Extent, Timescale and the Formation of the European Crust (Schulmann, K., Martínez Catalan, J.R., Lardeaux, J.M. Janousek, V., Oggiano, G. Eds.). Geol. Soc. London. Sp. Pub., 405: 225-247.

Martínez García, E., Antona, J.F., García-Sánchez, A., Quiroga de la Vega, J.L., 2004. Tectonic and metallogenic significance of sedimentary manganese deposits in the Eastern Cantabrian Domain, Asturias, Northwestern Spain. International Geology Review, 46: 273-288.

Marino, E., González, F.J., Somoza, L., Lunar, R., Ortega, L., Vázquez, J.T., Reyes, J., Bellido, E., 2017. Strategic and rare elements in CretaceousCenozoic cobalt-rich ferromanganese crusts from seamounts in the Canary Island Seamount Province (northeastern tropical Atlantic), Ore Geology Reviews, doi:10.1016/j.oregeorev.2016.10.00.

Marino, E., González, F.J., Lunar, R., Reyes, J., Medialdea, T., Castillo-Carrión, M., Bellido, E., Somoza, L., 2018. High-Resolution Analysis of Critical Minerals and Elements in Fe–Mn Crusts from the Canary Island Seamount Province (Atlantic Ocean). Minerals, 8(7), 285. doi:10.3390/min8070285.

Marino, E., González, F.J., Kuhn, T., Madureira, P., Wegorzewski, A.V., Mirao, J., Medialdea, T., Oeser, M., Miguel, C., Reyes, J., Somoza, L., Lunar, R. 2019. Hydrogenetic, Diagenetic and Hydrothermal Processes Forming Ferromanganese Crusts in the Canary Island Seamounts and Their Influence in the Metal Recovery Rate with Hydrometallurgical Methods. Minerals, 9(7), 439. doi:10.3390/min9070439.

Marino, E. 2020. Costras de Ferromanganeso ricas en cobalto de los Montes Submarinos al Suroeste de las Islas Canarias: Mineralogía y Geoquímica de Elementos Estratégicos y Críticos. Tesis Doctoral, 502 p.

Martinsson, O., Billström, K., Broman, C., Weihed, P., & Wanhainen, C., 2016. Metallogeny of the Northern Norrbotten Ore Province, northern Fennoscandian Shield with emphasis on IOCG and apatite-iron ore deposits. Ore Geology Reviews, 78, 447–492. http://doi.org/10.1016/j.oregeorev.2016.02.011

Matte, P., 1991. Accretionary history and crustal evolution of the Variscan belt in Western Europe. Tectonophysics, 196: 309-337.

This project has received funding from the European Union's Horizon 2020 research and innovation programme under grant agreement No 731166

Matte, P., 2002. Variscides between the Appalachians and the Urals: similarities and differences between Paleozoic subduction and collision belts. In: Variscan-Appalachian dynamics: The building of the late Paleozoic basement (J.R. Martínez Catalán, R.D. Hatcher, R. Arenas, F. Díaz García, Eds.). Geol. Soc. Amer. Sp. Paper, 364: 239-251.

McNamara, A.K. et al., 2001. West African proximity of the Avalon terrane in the latest Precambrian. Bulletin of the Geological Society of America 113(9), pp. 1161–1170. doi: 10.1130/0016-7606(2001)113<1161:WAPOTA>2.0.CO;2.

Melcher, F., Reichl, C., 2017: Economic Geology of the Eastern and South-eastern European (ESEE) Region. Berg Huettenmaenn Monatsh, 162, pp. 238–244. https://doi.org/10.1007/s00501-017-0625-4

Merle, R., Jourdan, F., Girardeau, J. 2018. Geochronology of the Tore-Madeira Rise seamounts and surrounding areas: a review, Australian Journal of Earth Sciences, 65:5, 591-605, DOI: 10.1080/08120099.2018.1471005

Mero, J. L., 1962. Ocean-floor manganese nodules. Economic Geology 57, 747–767

Michaud, J., 2019. Les granites a metaux rares: origine, mise en place et mecanismos de la transition magmatique-hydrothermale. Thèse Univ d'Orléans., 365 p.

Michael C., Papadopoulos P., Evangelou E., Marantos I., 1989. Epithermal gold mineralization at Konos area. In: 2nd Hellenic-Bulgarian symposium on the Geological and Physicogeographical problems of the massif. Abstract volume. Arist. Univ. of Thes., Sch of Geol., Greece.

Michael C., 1995. Conceptual model of Konos epithermal system. Geol. Soc. Greece, sp. Publ. 4/2.

Michael C., 2005. Mineralogical and Geochemical characteristics of Sappes epithermal system in western Thrace (Northern Greece). Comptes rendus de l'Academie Bulgare des Sciences, vol. 58, N6. Geologie, cites metalliferes.

MIDAS, 2020. Available online: http://eu-midas.net/

MINDeSEA. 2020. Available online: https://geoeramindesea.wixsite.com/mindesea

Mladenova V., Kerestedjian T., Dimitrova D., 2004. The Balkan Mountains Paleozoic Gold Deposits. Bulletin of the Geological Society of Greece, vol. XXXVI, 424-433.

Monchiardini, C., 1989. The Senonian (Cretaceous) phosphatic chalks of the Paris Basin, France. In: Notholt AJG, Sheldon RP, Davidson D (eds) Phosphate deposits of the world: volume 2, phosphate rock resources, Cambridge University Press, Cambridge, pp 407-410

Molnár, F., Jung, P., Kupi, L., Pogány, A., Vágó, E., Viktorik. O., Pécskay Z., 2008. Epithermal zones of the porphyry-skarn-epithermal ore complex at Recsk. – In: Földessy, J., Hartai, É. (eds): Recsk and Lahóca. Geology of the Paleogene ore complex, Publ. Univ. Miskolc, Ser. A, Mining, 73, pp. 99-128.

Moritz, R., Jacquat, S., Chambefort, I., Fontignie, D., Petrunov, R., Georgieva, S., von Quadt, A., 2003. Controls on ore formation at the high-sulphidation Au–Cu Chelopech deposit, Bulgaria: evidence from infrared fluid inclusion microthermometry of enargite and isotope systematics of barite. In: Eliopoulos, D., et al., (Eds.), Mineral Exploration and Sustainable Development. Millpress, Rotterdam, pp. 1209–1212.

Morteani, G., Möller, P., Schiley, F., 1982. The Rare Earth Element Contents and the Origin of the Sparry Magnesite Mineralizations of Tux-Lanersbach, Entachen Aim, Spiessn Sgel, and Hochfilzen, Austria, and the Lacustrine Magnesite Deposits of Aiani-Kozani, Greece, and Bela Stena, Yugoslavia. Economic Geology vol 77. Pages 617-631.

Muiños, S.B. 2015. Ferromanganese crusts from the seamounts north of the Madeira Island: composition, origin and paleoceanographic conditions. Tesis Doctoral, Univ. de Kiel (CAU), 170 p.

Murton, B.J. et al. 2017. MarineE-Tech Project. To Map the cobalt-rich Ferromanganese crusts of Tropic Seamount, NE Atlantic Ocean. https://www.bodc.ac.uk/resources/inventories/cruise_inventory/report/16292/

This project has received funding from the European Union's Horizon 2020 research and innovation programme under grant agreement No 731166

Müller, N., Boschi, M., Melcher, F., Rantish, G., Tscharf, A., Prochaska, W. and Meisel, T. 2016. The graphite mine of Zettlitz, Drosendorf (Bohemian Massif, Austria). GeoTirol 2016. Deutsche Geologische Gesellschaft – Geologische Vereinigung (DGGV), 25-28 September, Innsbruck, Austria, 227.

Neubauer, F., Lips, A. Kouzmanov, K., Lexa, J., IVĂŞCANU, P., 2005: Subduction, slab detachment and mineralisation: The Neogene in the Apuseni Mountains and Carpathians. – Ore Geology Reviews 27, 13–44.

Niegisch, M., Kamradt, A. & Borg, G., 2020. Geochemical and mineralogical characterization of the REE-mineralisation in the upper zone of the Storkwitz Carbonatite Complex from drill core SES-1/2012. Geoprofil des LfULG, Heft 15/2020.

Niiranen, T., Lahti, I., Nykänen, V., 2015. The orogenic gold potential of the central Lappland greenstone belt, northern Fennoscandian Shield, Mineral Deposits of Finland.733-752. http://dx.doi.org/10.1016/B978-0-12-410438-9.00028-5

North American Nickel Inc., 2015. Maniitsoq Overview. Accessed: 19/10/2020. Available at: https://www.northamericannickel.com/English/projects/greenland/maniitsoq/default.aspx.

Notholt, A.J.G., Highley, D.E., 1981. Investigation of the phosphate potential of the Loch Borralan Complex, north-west Highlands, Scotland. Open File Report, Institute of Geological Sciences (now BGS)

Notholt, A.J.G., Brasier, M.D., 1986. Proterozoic and Cambrian phosphorites-regional review: Europe. In: Cook PJ, Shergold JH (eds) Phosphate deposits of the world: volume 1, Proterozoic and Cambrian phosphorites, Cambridge University Press, Cambridge

Notholt, A.J.G., Highley, D.E, Slansky, M.,1979. Raw Materials Research and Development IV. Dossier on Phosphate, Commission of the European Communities, Brussels.

Notholt, A.J.G., Sheldon, R.P., Davidson, D., 1989. Europe-Introduction. In: Notholt AJG, Sheldon RP, Davidson D (eds) Phosphate deposits of the world: volume 2, phosphate rock resources, Cambridge University Press, Cambridge

O'Brien, H., Hyvönen, E., 2015. The Sokli carbonatite complex. In: Mineral Deposits of Finland, Elsevier, pp 305-325

O'Brien, H., Heilimo, E., Heino, P., 2015. The Archean Siilinjärvi carbonatite complex. In: Mineral Deposits of Finland, Elsevier, pp 327-343

Özlü, N., 1983. Trace-element content of "karst bauxites" and their parent rocks in the Mediterranean belt. Mineral. Deposita 18, 469–476.

Palosaari, J., Latonen, R.M., Smått, J.H., Raunio, S. and Eklund, O., 2020. The flake graphite prospect of Piippumäki—an example of a high-quality graphite occurrence in a retrograde metamorphic terrain in Finland. Mineralium Deposita, https://doi.org/10.1007/s00126-020-00971-z.

Parak, T., 1975. Kiruna iron ores are not "intrusive-magmatic ores of the Kiruna type". Economic Geology,70, 1242-1258.

Pereira, M., Leal Gomes, C., 2014. Contrasting paragenesis in Arga pegmatite field (NW of Portugal), diversity and equilibrium. Comunicações Geológicas 2014: 101, Especial I, 181-185 IX CNG/2º CoGePLiP, Porto 2014 ISSN: 0873-948X; e-ISSN: 1647-581X

Pohl, W., Belocky, R., 1999. Metamorphism and metallogeny in the Eastern Alps. Mineralium Deposita 34, 614–629. https://doi.org/10.1007/s001260050223

Pomoni-Papaioannou F., Papadopoulos P., 1986. Dolomitization of carbonate rocks of metasedimentary series of Makri unit, Southeast Rhodope. Bulletin Of The Geological Society Of Greece. 1988, XX/2, p. 429-447.

Porwal, A., Carranza, E. J. M., & Hale, M., 2003. Knowledge driven and data-driven fuzzy models for predictive mineral potential mapping Nat. Resour. Res., 12 (1) (2003), pp. 1-25.

Porwal, A., Carranza, E. J. M., & Hale, M., 2006. A hybrid fuzzy weights-of-evidence model for mineral potential mapping. Natural Resources Research, 15(1), 1–14. http://doi.org/10.1007/s11053-006-9012-7

This project has received funding from the European Union's Horizon 2020 research and innovation programme under grant agreement No 731166

Prochaska, W., 2016. Genetic concepts on the formation of the Austrian magnesite and siderite mineralizations in the Eastern Alps of Austria. Geol Cro 69, 31–38. https://doi.org/10.4154/GC.2016.03

Quesada, C., 1991. Geological constraint on the Paleozoic tectonic evolution of tectonostratigraphic terranes in Iberian Massif. Tectonophysics, 185: 225-245.

Raith, J.G., Schmidt, S., 2010. Tungsten deposit Felbertal, Salzburg, Austria. Acta Mineralogica-Petrographica, Field Guide Series 3, 1–24.

Ramos, F., 2010. Principais recursos minerais dos Concelhos de Chaves, Montalegre e Boticas in Mineração e povoamento na antiguidade no alto trás-os Montes Ocidental, Carla Maria Braz Martins (coord.), Edições Afrontamento, Porto, p. 27-45. ISBN 978-989-8351-03-6

Rantitsch, G., Grogger, W. et al. 2004. Conversion of carbonaceous material to graphite within the Greywacke Zone of the Eastern Alps. International Journal of Earth Sciences, 93, 959-973, https://doi.org/10.1007/s00531-004-0436-1.

Rasilainen, K., Eilu, P., Halkoaho, T., Heino, T., Huovinen, I., Iljina, M., Juopperi, H., Karinen, T., Kärkkäinen, N., Karvinen, A., Kontinen, A., Kontoniemi, O., Kousa, J., Lauri, L.S., Lepistö, K., Luukas, J., Makkonen, H., Manninen, T., Niiranen, T., Nikander, J., Pietikäinen, K., Räsänen, J., Sipilä, P., Sorjonen-Ward, P., Tiainen, M., Tontti, M. Törmänen, T., Västi, K.,2017. Assessment of undiscovered metal resources in Finland, Ore Geology Reviews, Volume 86, 2017, Pages 896-923, ISSN 0169-1368, https://doi.org/10.1016/j.oregeorev.2016.09.031

Raudsep, R., 1997. Phosphorite. In: Raukas A and Teedumäe A (eds) Geology and mineral resources of Estonia, Estonian Academy Publishers, 436 p

Reichl, C. and Schatz, M., 2019. World Mining Data 2019. Federal Ministry of Sustainability and Tourism, Vienna.

Rice, C.M. et al., 2016. Age and geologic setting of quartz vein-hosted gold mineralization at Curraghinalt, Northern Ireland: Implications for genesis and classification. Economic Geology 111(1), pp. 127–150. doi: 10.2113/econgeo.111.1.127.

Ricou, L.-E., Burg, J.-P., Godfriaux, I., Ivanov, Z., 1998. Rhodope and Vardar: the metamorphic and the olistostromic paired belts related to the Cretaceous subduction under Europe. Geodinamica Acta 11, 1 –25

Robaszynski, F., 1989. The phosphatic chalk of the Mons Basin, Belgium. In: Notholt AJG, Sheldon RP, Davidson D (eds) Phosphate deposits of the world: volume 2, phosphate rock resources, Cambridge University Press, Cambridge, pp 370-375

Rojkovič, I., Soták, J., Konečný, P. Čech, P., 2008. Stratiform manganese mineralisation in the Paleogene and Jurassic shale formations of the Western Carpathians: Mineralogy, geochemistry and ore-forming processes. – Geologica Carpathica, 59/6, pp. 503–514.

Roberts, D., 2003. The Scandinavian Caledonides: Event chronology, palaeogeographic settings and likely modern analogues. Tectonophysics 365(1–4), pp. 283–299. doi: 10.1016/S0040-1951(03)00026-X.

Roda, E., Pesquera, A., Gil-Crespo, P.P., Vieira, R., Lima, A., Garate-Olave, I., Martins, T., Torres-Ruiz, J., 2016. Geology and mineralogy of Li mineralization in the Central Iberian Zone (Spain and Portugal). Mineralogical Magazine, 2016, Vol. 80(1), p. 103–126.

Roda-Robles, E., Pesquera, A., de Madinabeitia, S.G., Ibarguchi, J. I. G., Nizamoff, J., Simmons, W., Falster, A. Galliski, M.A., 2014. On the geochemical character of primary Fe-Mn phosphates belonging to the triphylite-lithiophilite, graftonite-beusite, and triplite-zwieselite series: First results and implications for pegmatite petrogenesis. The Canadian Mineralogist, 52, 321-335.

Rodas, M., Luque, F.J., Barrenechea, J.F., Fernández-Caliani, J.C., Miras, A. and Fernández-Rodríguez, C. 2000. Graphite occurrences in the low-pressure/high-temperature metamorphic belt of the Sierra de Aracena (southern Iberian Massif). Mineralogical Magazine, 64, 801-814, https://doi.org/10.1180/002646100549805.

This project has received funding from the European Union's Horizon 2020 research and innovation programme under grant agreement No 731166

Romer, R. L. & Smeds, S.-A., 1997. U-Pb columbite chronology of post-kinematic Palaeoproterozoic pegmatites in Sweden. Precambrian Research 82, 1, 85-99.

Romer, R.L. & Smeds, S.-A., 1994. Implications of U-Pb ages of columbite-tantalites from granitic pegmatites for the Palaeoproterozoic accretion of 1.90-1.85 Ga magmatic arcs to the Baltic Shield. Precambrian Research 67, 141-158.

Romer, R. L. & Smeds, S.-A., 1996. U-Pb columbite ages of pegmatites from Sveconorwegian terranes in southwestern Sweden. Precambrian Research 76, 15-30.

Romer, R.L. & Smeds, S.-A., 1997. U-Pb columbite chronology of post-kinematic Palaeoproterozoic pegmatites in Sweden. Precambrian Research 82, 85-99.

Rona, P. A. 2008. The changing vision of marine minerals, Ore Geol. Rev., 33, 618– 666.

Roşu E., Szakacs A., Downes H., Seghedi I., Peckskay Z. (2004) Timing of Miocene-Quaternary magmatism and metallogeny in the South Apuseni Mountains, Romania. Romanian Journal of Mineral Deposits 81: 33-38.

Rukhlov, A. S. & Bell, K., 2010. Geochronology of carbonatites from the Canadian and Baltic shileds, and the Canadian cordillera: clues to mantle evolution. Mineralogy and Petrology 98, 11-54.

Sadeghi, M. (ed.) 2019. Rare earth elements distribution, mineralisation and exploration potential in Sweden. Sveriges geologiska undersökning, Rapporter och meddelanden 146, 184 pp.

Sadeghi, M., Bertrand, G., de Oliveira, D.P.S., Arvanitidis, N., Decrée, S.Gautneb, H., Gloaguen, E., Törmänen, T., Reginiussen, H., Sievers, H., Quental, L., Ferreira, M.J., Wittenberg, A., 2020a. Prospectivity mapping of critical raw material at the continental scale -State of the Art: a part of the FRAME project . EAGE Mineral Exploration Symposium, 17-18 Sept. 2020, online event

Sadeghi, M., Bertrand, Guillaume., Reginiussen, Helge., Arvanitidis, Nikolaos., Jonsson, E., and de Oliveira, Daniel., 2020b. EGU2020-7931. https://doi.org/10.5194/egusphere-egu2020-7931

Sadeghi, M., Arvanitidis, N., Ladenberger, A., 2020c. Geochemistry of Rare Earth Elements in Bedrock and Till, Applied in the Context of Mineral Potential in Sweden. Minerals 2020, 10, 365.

Sandstad, J. S., Bjerkgård, T., Boyd, R., Ihlen, P., Korneliussen A., Nilsson, L. P., Often, M., Eilu, P. & Hallberg, A. 2012. Metallogenic areas in Norway. Geological Survey of Finland, Special Paper 53, 35–138.

Sarapää, O., Ani, A.T., Seppo, I., Lauri, L., Sarala, P., Torppa, A., Kontinen, A., 2013. Rare earth exploration potential in Finland. Journal of Geochemical Exploration, 133, 25-41

Schatzlmaier, P., Schöllnberger, W. & Thomassen, B., 1973. Untersuchung des Vorkommens am Zirkon und seltenen Erden auf Kote 800 Milneland. Intemal Nordisk Mineselskab report 4/72, 91 pp. (GEUS report file no. 20669)

Schedl, A., Benold, C., Neinavaie, H., Lipiarski, P. and Hobiger, G. 2016. Rohstoffpotenzialen für kritische Rohstoffe: SEE-Potenziale ausgewählter Kaolin-, Ton-, Leukophyllit- und Grafitvorkommen in Niederösterreich und Oberösterreich.

Schuster, R., Pestal, G. and Reitner, J. 2006. Erläuterungen zur Geologischen Karte der Republik Österreich 1 : 50.000 Blatt 182 Spittal an der Drau.

Schmid, S.M., Fügenschuh, B., Kissling, E., Schuster, R., 2004. Tectonic map and overall architecture of the Alpine orogen. Eclogae Geologicae Helvetiae 97, 93–117. https://doi.org/10.1007/s00015-004-1113-x

Schmid, S.M., Fügenschuh, B., Kounov, A., Maţenco, L., Nievergelt, P., Oberhänsli, R., Pleuger, J., Schefer, S., Schuster, R., Tomljenović, B., Ustaszewski, K., van Hinsbergen, D.J.J., 2020. Tectonic units of the Alpine collision zone between Eastern Alps and western Turkey. Gondwana Research 78, 308–374. https://doi.org/10.1016/j.gr.2019.07.005

Schmid, S.M., Scharf, A., Handy, M.R., Rosenberg, C.L., 2013. The Tauern Window (Eastern Alps, Austria): a new tectonic map, with cross-sections and a tectonometamorphic synthesis. Swiss Journal of Geosciences 106, 1–32. https://doi.org/10.1007/s00015-013-0123-y

Schleicher H., Baumann A., Keller J. 1991: Pb isotopic systematics of alkaline volcanic rocks and carbonatites from the Kaiserstuhl, upper Rhine rift valley, FRG. Chemical Geology 93, 231–243.

This project has received funding from the European Union's Horizon 2020 research and innovation programme under grant agreement No 731166

Schuster, R., Kurz, W., Krenn, K., Fritz, H., 2013. Introduction to the Geology of the Eastern Alps. 11th Workshop on Alpine Geological Studies ˛7th IFAA 14.

Schroll, E., Pak, E. 1983. Sulphur Isotope Investigations of Ore Mineralizations of the Eastern Alps. In: Schneider, H.J. (edt.): Mineral Deposits of the Alps and the Alpine Epoch in Europe. Springer-Verlag, Berlin, Heidelberg, 1983

Secher, K. & Larsen, L.M., 1980. Geology and mineralogy of the Sarfartåq complex, southern West Greenland. Lithos 13, 199-212.

SIORMINP 2002. Sistema de Informação de Ocorrências e Recursos Minerais Portugueses (coords., A. Parra and A. Filipe), LNEG. http://geoportal.lneg.pt/geoportal/egeo/bds/siorminp/

Skyttä, P., Weihed, P., Högdahl, K., Bergman, S.& Stephenes,M.B. 2020. Paleoproterozoic (2.0–1.8 Ga), syn-orogenic sedimentation, magmatism and mineralization in the Bothnia–Skellefteå lithotectonic unit, Svecokarelian orogen. In: STEPHENS, M.B. & BERGMAN WEIHED, J. (eds) 2020. Sweden: Lithotectonic Framework, Tectonic Evolution and Mineral Resources. Geological Society, London, Memoirs, 50, 83–130, https://doi.org/10.1144/M50-2017-10

Skyttä, P., Bauer, T.E., Tavakoli, S., Hermansson, T., Andersson, J. & Weihed, P. 2012. Pre-1.87 Ga development of crustal domains overprinted by 1.87 Ga transpression in the Palaeoproterozoic Skellefte district, Sweden. Precambrian Research, 206–207, 109–136, https://doi.org/10.1016/j.precamres.2012.02.022

Skyttä, P., Bauer, T. et al., 2013. Crustal 3-D geometry of the Kristineberg area (Sweden) with implications on VMS deposits. Solid Earth, 4, 387–404, https://doi.org/10.5194/se-4-387-2013

Smeds, S.-A. 1990. Regional trends in mineral assemblages of Swedish Proterozoic granitic pegmatites and their geological significance. GFF 112, 227-242.

Standish, C.D. et al. 2014. The genesis of gold mineralisation hosted by orogenic belts: a lead isotope investigation of Irish gold deposits. Chemical Geology (378–379), pp. 40–51.

Steenfelt, A., Schj0th, F., Sand, K.K., Secher, K., Tappe, S., Moberg, E. & Tukiainen, T., 2007. Initial assessment of the geology and economic potential of the Tikiusaaq carbonatite camplex and ultrarnatic lamprophyre dykes. Mineral resource assessment of the Achaean eraton (66° to 63°30'N) SW Greenland Contributian no. 3, Danmarks og Grönlands Geologiske Undersögelse Rapport 2007/64, 53 pp. + 1 DVD.

Stendal, H. and Frei, R. 2008. Mineral occurrences in central East Greenland (70°N-75°N) and their relation to the Caledonian orogeny- A Sr-Nd-Pb isotopic study of scheelite. Memoir of the Geological Society of America 202(12), pp. 293–306. doi: 10.1130/2008.1202(12).

Stensgaard, B.M., Stendal, H., Kalvig, P. & Hanghøj, K., 2016. Review of potential resources for critical minerals in Greenland. MiMa rapport 2016/3.

Stensgaard, B.M., Stendal, H., Kalvig, P. and Hanghøj, K. 2017. Review of potential resources for critical minerals in Greenland. Videncenter for Mineralske Råstoffer og Materialer. Ucik, F.H. 1992. Graphit in Kärnten.

Stephens, M. B. & Bergman Weihed, J. (eds) 2020. Sweden: Lithotectonic Framework, Tectonic Evolution and Mineral Resources. Geological Society, London, Memoirs, 50, 27–81, https://doi.org/10.1144/M50-2016-29

Stephnes, M.B., 2020a. Outboard-migrating accretionary orogeny at 1.9–1.8 Ga (Svecokarelian) along a margin to the continent Fennoscandia. In: STEPHENS, M.B. & BERGMAN WEIHED, J. (eds) 2020. Sweden: Lithotectonic Framework, Tectonic Evolution and Mineral Resources. Geological Society, London, Memoirs, 50, 237–250, https://doi.org/10.1144/M50-2019-18

Stephnes, M.B., 2020b. Upper and uppermost thrust sheets in the Caledonide orogen, Sweden: outboard oceanic and exotic continental terranes. In: STEPHENS, M.B. & BERGMAN WEIHED, J. (eds) 2020. Sweden: Lithotectonic Framework, Tectonic Evolution and Mineral Resources. Geological Society, London, Memoirs, 50, 549–575, https://doi.org/10.1144/M50-2019-12

This project has received funding from the European Union's Horizon 2020 research and innovation programme under grant agreement No 731166

Stephenes, M.B. & Bergman, S. 2020. Regional context and lithotectonic framework of the 2.0–1.8 Ga Svecokarelian orogen, eastern Sweden. In: STEPHENS, M.B. & BERGMAN WEIHED, J. (eds) 2020. Sweden: Lithotectonic Framework, Tectonic Evolution and Mineral Resources. Geological Society, London, Memoirs, 50, 19–26, https://doi.org/10.1144/M50-2017-2

Stephenes, M.B. & Jansson, N.F. 2020. Paleoproterozoic (1.9–1.8 Ga) syn-orogenic magmatism, sedimentation and mineralization in the Bergslagen lithotectonic unit, Svecokarelian orogen. In: STEPHENS, M.B. & BERGMAN WEIHED, J. (eds) 2020. Sweden: Lithotectonic Framework, Tectonic Evolution and Mineral Resources. Geological Society, London, Memoirs, 50, 155– 206, https://doi.org/10.1144/M50-2017-40

Stoppa, F., Pirajno, F, Schiazza, M., Vladykin, N.V., 2016. State of the art: Italian carbonatites and their potential for critical-metal deposits. Gondwana Res 37, 152-171

Sundius, N., 1951. Kvarts, fältspat och glimmer samt förekomster därav i Sverige. SGU Serie C 520, 231 pp.

Sutphin, D.M., Hammarstrom, J.M., Drew, L.J., Large, D.E., Berger, B.B., Dicken, C.L., and DeMarr, M.W., with contributions from Billa, M., Briskey, J.A., Cassard, D., Lips, A., Pertold, Z., and Roşu, E., 2013, Porphyry copper assessment of Europe, exclusive of the Fennoscandian Shield, U.S. Geological Survey, Scientific Investigations Report, 2010–5090–K, 197 p., and GIS data.

Sørensen, H., Bailey, J.C., Rose-Hansen, J., 2011. The emplacement and crystallization of the U–Th–REE rich agpaitic and hyperagpaitic lujavrites at kvanefjeld, ilímaussaq alkaline complex, south Greenland. Bull. Geol. Soc. Den. 59, 69–92.

Svinndal, S., 1970. Undersøkelser etter sjeldne jordartselementer (RE) i Fensfeltet, Ulefoss. Norges Geologiske Undersøkelse. Rapport 966, 18 pp. (in Norwegian)

Szantner, F., Knauer, J., Mindszenty, A. 1986: Bauxite exploration, Veszprémi Akadémiai Bizottság, Veszprém, p. 472 (in Hungarian).

Tappe, S., Steenfelt, A., Heaman, L.M. & Simonetti, A., 2009. The newly discovered Jurassic Tikiusaaq carbonatite-aillikite occurrence, West Greenland, and some remarks on carbonatite-kimberlite relationships. Lithos 112, 385-399.

Tămaş, C.G., Andrii, M.P., 2020. Mineralogy of Skarn Ores from Bait,a-Bihor, Northern Apuseni Mountains, Romania: A Case Study of Cu-, Bi-, and Sn-minerals. Minerals, 10, 436.

Takács, Á., Molnár, F., Turi, J. Mogessie, A., Menzies JC., 2017. Ore mineralogy and fluid inclusion constraints on the temporal and spatial evolution of a high-sulfidation epithermal Cu-Au-Ag deposit in the Recsk Ore Complex, Hungary. Economic Geology,. 112, pp. 1461-1481.

Thrane, K., Kalvig, P. & Keulen, N., 2014: REE deposits and occurrences in Greenland. ERES2014: 1st European Rare Earth Resource Conference, Milos, Greece.

Torbica, S., Lapčević, V., 2012. Concept of underground mining of phosphate deposits in Lisina near Bosilegrad. Podzemni radovi, 23-29

Tornos, F., Inverno, C.M.C., Casquet, C., Mateus, A., Ortiz, G. And Oliveira, V. 2004. The metallogenic evolution of the Ossa-Morena Zone. Journal of Iberain Geology, 30: 143-181.

Tornos, F. 2006. Environment of formation and styles of volcanogenic massive sulfides: The Iberian Pyrite Belt. Ore Geology Reviews, 28: 259-307.

Tourlière, B., Pakyuz-Charrier, E., Cassard, D., Barbanson, L., & Gumiaux, C., 2015. Cell Based Associations: A procedure for considering scarce and mixed mineral occurrences in predictive mapping. Computers and Geosciences, 78, 53–62. http://doi.org/10.1016/j.cageo.2015.01.012

Tukiainen, T., 1988. Niobium-tantalum mineralisation in the Motzfledt Centre of the Igaliko Nepheline Syenite Complex, South Greenland. In Boisonnas, J. & Omenetto, P. (ed.) Mineral Deposits within the European Community. Springer Verlag Berlin & Heidelberg, 230-246.

Tzifas, I.T., Godelitsas, A., Magganas, A., et al 2014. Uranium-bearing phosphatized limestones of NW Greece. J Geochem Explor 143, 62-73

This project has received funding from the European Union's Horizon 2020 research and innovation programme under grant agreement No 731166

Uher, P., Žitňan, P. 2007: Pegmatitic Nb-Ta oxide minerals in alluvial placers from Limbach, Bratislava Massif, Western Carpathians, Slovakia: compositional variations and evolutionary trend. Journal of GEOsciences 52, 133–141. https://doi.org/10.3190/jgeosci.007

Uher, P., Chudík, P., Bačík, P., Vaculovič, T., Galliová, M., 2010. Beryl composition and evolution trends: an example from granitic pegmatites of the beryl-columbite subtype, Western Carpathians, Slovakia. Journal of Geosciences 55, 69–80.

USGS 2020: Mineral commodity summaries 2020: U.S. Geological Survey, 200 p., https://pubs.usgs.gov/periodicals/mcs2020/mcs2020.pdf

Upton, B.G., Emeleus, C.H., Heaman, L.M., Goodenough, K.M. & Finch, A.A., 2003. Magmatism of the mid-Proterozoic Gardar Province, South Greenland: chronology, petrogenesis and geological setting. Lithos 68, 43-65.

van den Bogaard, P. 2013. The origin of the Canary Island Seamount Province-New ages of old seamounts. Sci. Rep., 3, 2107.

Vast Resources PLC, 2020. Mamaila polymetallic mine. https://www.vastplc.com/operations/manaila-polymetallic-mine/. Accessed on 12 Aug. 2020.

Vázquez, J.T., Somoza, L., Rengel, J.A., Medialdea, T., Millán, A., Alcalá, C., González, F.J., Jiménez, P., León, R., López-González, N., Palomino, D., López, F.J., García Muñoz, M., Martín, D., Sánchez-Guillamón, O., Correa, A., Martínez, J.C., Corbalán, A., Cruces, M., García, J.M., García, M. 2011. Informe científico-técnico de la campaña oceanográfica DRAGO0511. Ampliación de la plataforma continental de España al oeste de las islas Canarias (273 pp.). http://www.repositorio.ieo.es/e-ieo/handle/10508/451

Venturelli, G., Capedri, S., Barbieri, M. et al., 1991. The Jumilla lamproite revisited: a petrological oddity. Europ J Miner, 123-146

Velinov I., Kunov A., Petrounov R., Michael C., 1999. Mineralogy and zoning of hydrothermal alterations with examples from Bulgaria, Greece and Turkey. Metallogenesis of Bulgaria, International symposium, 22-24 Nov. 1999, Sofia.

Vieira, R., 2010. Aplitopegmatitos com elementos raros da região entre Almendra (V. N. de Foz Côa) e Barca DÁlva (Figueira de Castelo Rodrigo). Campo aplitopegmatítico da Fregeneda-Almendra. Tese de Doutoramento, Universidade do Porto, 275 p.

Vindel E, Chicharro E, Villaseca C et al., 2014. Hydrothermal phosphate vein-type ores from the southern Central Iberian Zone, Spain: Evidence for their relationship to granites and Neoproterozoic metasedimentary rocks. Ore Geol Rev 62, 143-155

Vodă, A. 2002. Geologic-structural and metallogenetic map of the Crystalline-Mesozoic Zone of the Eastern Carpathians, scale 1:200 000. S.C. Prospecţiuni S.A. Bucharest.

Walter, B.F., Parsapoor, A., Braunger, S., Marks, M.A.W., Wenzel, T., Martin, M. & Markl, G. 2018. Pyrochlore as a monitor for magmatic and hydrothermal processes in carbonatites from the Kaiserstuhl volcanic complex (SW Germany). Chemical Geology, 498, 1–16.

Walters. A.S., Goodenough, K.M., Hughes, H.S. et al., 2013. Enrichment of Rare Earth Elements during magmatic and post-magmatic processes: a case study from the Loch Loyal Syenite Complex, northern Scotland. Contrib Miner Pet 166(4), 1177-1202

Weber, L. 1983. The Stratiform Lead-Zinc Mineralization of the »Paleozoic of Graz« (Styria, Austria). In: Schneider, H.J. (edt.): Mineral Deposits of the Alps and the Alpine Epoch in Europe. Springer-Verlag, Berlin, Heidelberg, 1983

Weber, L. (eds.), 1997. Archiv für Lagerstätten Forschung 1997, Band 19: Handbuch der Lagerstätten der Erze, Industrieminerale und Energierohstoffe Österiches. Geologishe Bundesanstalt, Vienna, 607 pages.

Wilberg R., 1989. Data for malmsonering for Bordvedåga-forekomsten, analyser fra Be-mineraliseringer og regional geologi i Høgtuva-området. Norges Geologiske Undersøkelse rapport 89.097, 67 p.

Wilberg R., Lindahl I., 1991. Bordvedåga beryllium-forekomst, Rana kommune, Nordland. Norges Geologiske Undersøkelse rapport 91.180, 38 p.

This project has received funding from the European Union's Horizon 2020 research and innovation programme under grant agreement No 731166

Wilson, M., Downes, H., 2006. Tertiary-Quaternary intra-plate magmatism in Europe and its relationship to mantle dynamics. Geological Society London Memoir, 32, 147–166.

Weihed, P., Arndt, N., Billström, C., Duchesne, J.C., Eilu, P., Martinsson, O., Papunen, H., Lahtinen, R., 2005. Precambrian geodynamics and ore formation: the Fennoscandian Shield. Ore Geol. Rev. 27, 273–32

8 Acknowledgment

The Authors would like to thank the mineral resource expert group (MREG) and MINDeSEA -GEOERA team for their contribution in the data and information related to mineral resources in Europe and the mineral resources in European seas.

This project has received funding from the European Union's Horizon 2020 research and innovation programme under grant agreement No 731166